Durham University

Durham E-Theses

The generation and continued existence of overpressure in the Delaware Basin, Texas

Thomas Daniel Sinclair

How to cite:

Sinclair, Thomas Daniel (2007) The generation and continued existence of overpressure in the Delaware Basin, Texas. Doctoral thesis, Durham University.

Use policy

The full-text may be used and/or reproduced, and given to third parties in any format or medium, without prior permission or charge, for personal research or study, educational, or not-for-profit purposes provided that:

- a full bibliographic reference is made to the original source
- a https://etheses.durham.ac.uk/id/eprint/2289/ is made to the metadata record in Durham E-Theses
- the full-text is not changed in any way

The full-text must not be sold in any format or medium without the formal permission of the copyright holders.

Please consult the full Durham E-Theses policy for further details.

Academic Support Office, The Palatine Centre, Durham University, Stockton Road, Durham, DH1 3LE
e-mail: e-theses.admin@durham.ac.uk Tel: +44 0191 334 6107
https://etheses.durham.ac.uk

University of Durham

The Generation and Continued Existence of Overpressure in the Delaware Basin, Texas

Thomas Daniel Sinclair. BSc. MSc.

August 2007

Thesis submitted for the degree of Doctor of Philosophy

The copyright of this thesis rests with the author or the university to which it was submitted. No quotation from it, or information derived from it may be published without the prior written consent of the author or university, and any information derived from it should be acknowledged.

17 OCT 2007

Department of Earth Sciences

Declaration

I declare that no part of this thesis has been previously submitted for a degree at Durham University, or any other university, and is entirely the result of my own independent research, except where otherwise stated.

Signed

Thomas Daniel Sinclair

August 2007

The copyright of this thesis rests with the author. No quotation from it should be published in any form, including electronic and the Internet, without the author's prior written consent. All information derived from this thesis must be acknowledged appropriately.

Abstract

'Generation and Continued Existence of Overpressure in the Delaware Basin, Texas.'

Tom Sinclair

The Delaware Basin, part of the larger Permian Basin, contains important hydrocarbon plays. Permian strata contain 71% of in-place oil and 53% of in-place gas, with the remainder hosted in the Lower Palaeozoic. Excessive pore fluid pressures (up to ~ 8000 psi above hydrostatic) are found within Early Permian and Pennsylvanian strata, which account for 30-35% of the hydrocarbon producing zones. This study has utilised an array of basin analysis techniques to analyse the pressure history of the Delaware basin.

To fully appreciate the geopressure history in the Delaware Basin, a rigorous quantitative approach has been applied using advanced thermochronology techniques. This has enabled for the first time an accurate burial history curve to be established for the basin. The results show that maximum burial occurred in the basin at 55 Ma as a consequence of an additional 6890 ft of Mesozoic and Cenozoic sediment. The basin then underwent two major tectonic uplift events during the Cenozoic. The Laramide orogeny (55-50 Ma) uplifted and eroded off 3890 ft of sediment, then during the Eocene and Oligocene the basin subsided and accumulated a further 600 ft of sediment. The Basin and Range event (25-10 Ma) then uplifted and tilted the basin further, eroding off 3600 ft of sediment from the centre of the basin. The new burial history curve has been integrated with wireline logs and basin modelling software to evaluate the mechanism of overpressure generation and its maintenance through geological time.

This study has shown that the main mechanism for overpressure generation in the Delaware Basin was disequilibrium compaction. Analysis of the sonic log using the Equivalent Depth Method and the Eaton Ratio Method, combined with velocity / density cross-plots, indicate that compaction is driven by vertical loading, and undercompaction seen in the basin is a consequence of the sediments' inability to dewater. Basin modelling shows that it was the rapid deposition of the Permian sediments that enabled disequilibrium compaction to generate overpressure. These techniques have also shown that a secondary cause of overpressure due to unloading mechanisms (e.g. gas generation or expansion with uplift, lateral transfer and hydrocarbon buoyancy) may be occurring within localised horizons below the Wolfcampian Series.

Overpressure has been maintained within the basin for more than 250 Myr. Basin modelling and wireline logs have shown that numerous intercalated tight limestones (Mississippian to Late Permian) acted as pressure seals to maintain overpressure. In addition, low permeability mudstones (10^{-6}mD) have contributed to the inability of the Delaware Basin to reach pressure equilibrium.

Contents

	Page
Abstract	iii
Contents	iv
Acknowledgements	ix
Chapter1: Introduction and Methods	1
1.1 Introduction	2
1.2 Context of study	3
1.3 Aims	4
1.4 Methods	4
1.5 Layout of thesis	5
Chapter 2: Geological History of the Delaware Basin	8
2.1 Introduction	9
2.2 Geological history of the Delaware Basin	12
2.2.1 Tobosa Basin phase	12
2.2.1.1 Precambrian basement	12
2.2.1.2 Tobosa Basin formation	14
2.2.2 Permian Basin phase	21
2.2.2.1 Tectonic overview	21
2.2.2.2 Sedimentation and tectonics	25
2.2.3 Stable Platform phase	32
2.2.4 Cenozoic tectonic uplift phase	33
2.2.4.1 Laramide orogeny	34
2.2.4.2 Basin and Range uplift	34
2.2.4.3 Cenozoic deposition	35

Chapter 3: Pore pressure 36
3.1 Introduction 37
3.2 Introduction to the pore pressure system 38
3.2.1 Hydrostatic pressure 38
3.2.2 Lithostatic pressure 39
3.2.3 Effective stress 40
3.2.4 Formation pressure measurement 41
3.2.5 Overpressure 42
3.2.5.1 Generating mechanisms of overpressure 43
3.2.6 Underpressure 52
3.3 Overpressure in the Delaware Basin 53
3.3.1 Summary of results 61
3.4 Literature review 62
3.4.1 Luo et al (1994) 62
3.4.2 Lee and Williams (2000) and Hansom and Lee (2005) 65
3.4.3 Anadarko Basin 66
3.5 Conclusions 69

Chapter 4: Mesozoic and Cenozoic tectonic history of the Delaware Basin 70
4.1 Introduction 71
4.1.1 The Mesozoic: Subsidence and sediment fill 71
4.1.2 The Cenozoic: Uplift and erosion 73
4.1.3 Aims 77
4.2 Burial history of the Delaware Basin 78
4.2.1 Apatite fission track analysis (AFTA) 78
4.2.1.1 Delaware Basin sampling 79
4.2.1.2 Basic principle of AFTA 83
4.2.1.3 Temperature 85
4.2.1.4 How AFTA results are displayed 88
4.2.1.5 Determining the amount of section removed 90

4.2.1.6 AFTA results for the JE Haley 24-1 well 91
4.2.1.7 AFTA results from outcrop samples 94
4.2.1.8 AFTA summary 98
4.2.2 Vitrinite reflectance (VR) 101
4.2.2.1 Delaware Basin sampling 104
4.2.2.2 Results 105
4.2.2.3 Summary of vitrinite data 108
4.2.3 Integration of AFTA, VR, and T-max data 111
4.2.4 Shale compaction curves 114
4.2.4.1 Results from shale compaction curves 119
4.2.5 Summary analysis techniques 123
4.3 Discussion 126
4.3.1 Determining the palaeogeothermal gradient 127
4.3.1.1 Alton Brown (2004) 127
4.3.1.2 Barker and Pawlewicz (1987) 130
4.3.1.3 Palaeogeothermal gradient discussion 130
4.3.2 Constraining an accurate burial and tectonic history 136
4.3.2.1 Triassic 138
4.3.2.2 Jurassic 140
4.3.2.3 Lower Cretaceous 140
4.3.2.4 Upper Cretaceous 140
4.3.2.5 Palaeocene 141
4.3.2.6 Upper Cretaceous continued 141
4.3.3 When was the basin tilted? 146
4.4 Conclusions 150

Chapter 5: Wireline data and its signatures 151
5.1 Introduction 152
5.1.1 Data 153
5.1.1.1 Controls on data quality 155
5.2 Pore pressure prediction from wireline logs 157
5.2.1 Factors affecting pore pressure prediction 161

5.2.1.1 Normal compaction 161
5.2.1.2 Non-mechanical compaction 164
5.2.1.3 Other parameters 164
5.2.2 Results of pore pressure prediction 165
5.3 Mechanism for overpressure generation 170
5.3.1 Methodology behind velocity / density cross plots 170
5.3.2 Results of velocity / density cross plots 173
5.4 Discussion: Application of sonic logs in pore pressure analysis 178
5.4.1 Evidence for pore pressure dewatering 178
5.5 Conclusions 181
5.5.1 Pore pressure prediction 181
5.5.2 Mechanism of generation 182
5.5.3 Dynamic or a static pressure system 182

Chapter 6: Basin Modelling of the Delaware Basin 183
6.1 Introduction 184
6.1.1 Aims of basin modelling 185
6.2 Data input and methodology 186
6.2.1 Basin subsidence and compaction 189
6.2.2 Fluid flow 189
6.2.3 Thermal history 192
6.2.3.1 Heat flow history 192
6.2.4 Hydrocarbon generation and expulsion 194
6.2.5 Sensitivity of basin modelling 198
6.3 Results of 1D and 2D modelling 202
6.3.1 Mechanism behind overpressure generation in the basin 202
6.3.1.1 Disequilibrium compaction 202
6.3.1.2 Non-stress related 208
6.3.2 Modelling the retention of overpressure in the basin 222
6.3.2.1 Late Permian evaporites 222
6.3.2.2 Late Permian evaporites modelled as being

permeable on the edge of the basin 226
6.3.2.3 Tight laterally extensive carbonates 232
6.4 Discussion: A sensitivity analysis 240
6.4.1 Impact of different shale compaction curves on pore pressure modelling 240
6.5 Conclusions of basin modelling 243

Chapter 7: Synthesis and discussions 245
7.1 Introduction to the discussions 246
7.2 Mechanisms of overpressure generation 246
7.2.1 An overview 246
7.2.2 Disequilibrium compaction 250
7.2.3 Non-stress related 255
7.3 Maintenance of overpressure in the Delaware Basin 259
7.3.1 Gas capillary seals 260
7.3.2 Pressure seals 261
7.4 A summary 263

Chapter 8: Conclusions 264
8.1 Key Findings 266
8.1.1 Origins of overpressure 266
8.1.2 Maintenance of overpressure 267
8.1.3 Techniques 268
8.2 Summary comments 268
8.3 Further work 269

References **271**

Acknowledgements

Well, where do I begin? Since starting this PhD in October of 2002, I think I have experienced every single emotion there is during the course of completing this thesis: Joy, excitement, worry, glee, anger, frustration, confusion, happiness and the final emotions which I've just experienced are relief and pride!

Without the help and assistance from numerous people, or the love and encouragement from others, this thesis would not have been possible, and my final emotion may well have been one of failure instead of pride.

Firstly, I'd like to thank the various sources that supplied funding to this project. The Natural Environmental Research Council (NERC) have been the main sponsors for this PhD, and without the funding and support of NERC, I would not have been able to undertake a PhD, so I am entirely grateful for this funding.

BP were 'case sponsors' for this project, and provided invaluable funding. Without their help, I would not have been able to visit my study area in west Texas, or the BP offices of Houston and Sunbury, or go to international conferences where I was able to present my research. So once again I am entirely grateful for their help.

For this research, numerous research techniques have been utilised, which were applied to countless data sets. Therefore I would like to add my gratitude to numerous people and companies for their support. I would like to thank BP for supplying me with numerous well data sets, and for the basin modelling training. Beicip Franlab, and Zhiyong He for providing me with the basin modelling software 'Temis2D' and 'Genesis' respectively. Newcastle University for undertaking mercury porosimetry analysis on my samples.

Special thank you's, are reserved for Ian Duddy of Geotrack, and Rick Webster of Anadarko. Ian Duddy and Geotrack, analysed my samples using apatite fission track analysis (AFTA), and this was done with no charge. This technique would have otherwise cost thousands and would never have been possible. Consequently, the results from AFTA were significant in the final research results. Anadarko, were never originally part of this study, however the company came aboard and provided me with a quality data set, and invaluable assistance of which I am entirely grateful, especially Rick Webster, who I more or less adopted as another supervisor during this project.

I would now like to thank personally the supervisors who have helped me through this study. Stuart Jones of the Earth Sciences department in Durham became invaluable while I was writing up, constantly at hand and willing to advise me with my research and his constant marking of my chapters. His support is truly appreciated, and during the last 6 months totally invaluable. I'd also like to thank Richard Swarbrick of Geopressure technology for his technical input and support, and without him, this project would never have started.

James Iliffe of BP and Phil Heppard of Conoco (previously of BP), were also invaluable to this study. Their technical input, and advise on my research were second to none, and I sincerely hope that during my future within the oil and gas

industry, I will meet them again. Well as long as its not in competition with Shell for a new discovery!

All staff within the Department of Earth Sciences here at Durham University deserve a collective mention. The list would be too large if I mentioned everyone and how they've helped me. So just trust me in the knowledge that everyone has helped me at some point, even if it was just providing proper coffee to the tea room!!

I've been so lucky during my time at Durham to make the friends I have, and I feel privileged to call them friends, and I am sure in 10 or 20 years time my opinion would not have changed in the slightest. So here's to Phil, Adam, Tom, Mike, Jen, Nicola, Chris, Jim, Matt, Leanne, Sarah, Tim, Ehab, Dougal, Gary, Fabio, Steve, Wonkey, Monks, mini L, and mini T. You all are truly great people.

Well finally, but most importantly of all, I'd like to thank those that gave me support and love during times when it was so much needed. Mum and Dad were always there, as parents always seem to be, and you never appreciate them until you sit back and think about what they've done for you. Finally Anna, well words can't actually describe how much it meant having you in my life while I was finishing this PhD. You brought sanity back to my life, you gave me encouragement, and support, and you made me realise the important aspects of life. So thank you.

Chapter 1:

Introduction and Methods

1.1 Introduction

A geological map of West Texas, a stratigraphic column and a cross section through the Delaware Basin, are included at the end of this chapter for reference throughout the thesis (Fig's 1.1 and 1.2)

The Delaware Basin is a Palaeozoic foreland basin located in West Texas in the United States of America (Figs 1.1 and 1.2). Over 23,000 ft (7 km) of Phanerozoic sediments have been deposited in the basin, with the majority of deposition occurring during the Palaeozoic. The Mesozoic was a time of relative stability in the basin, while the Cenozoic was associated with phases of substantial uplift and erosion in the basin. The Delaware Basin is part of the larger Permian Basin, which is an important hydrocarbon producing province, accounting for 17% of United States production (327 million bbl) in 2002. Within the Delaware Basin, the majority of hydrocarbons are found within Permian strata, where 71% of in-place oil and 53% of in-place gas is being produced from the Permian strata. The remainder (predominantly gas) is produced from Pennsylvanian or Lower Palaeozoic strata.

The basin is overpressured in the deep section, where the overpressured section is isolated. The pore pressures in the Lower Permian Wolfcampian Series and the Pennsylvanian System are up to 8000 psi above hydrostatic, but sediments above and below this section are hydrostatically pressured. The existence of overpressure within clastic dominated basins has been known for several decades. In oil and gas exploration, predicting the depth and magnitude of an overpressured reservoir before and while drilling could potentially save the costs of a blow out, kicks, stuck pipe and other problems associated with overpressured rocks.

This chapter introduces the reasons for studying overpressure in the Delaware Basin, the aims of the study, the way the research was carried out, and how the results are presented in this thesis.

1.2 Context of study

The occurrence of fluid pressures above the hydrostatic pressure gradient is common in many sedimentary basins and is termed overpressure (Spencer 1987; Hunt 1990; Osborne & Swarbrick 1997 and Swarbrick et al 2002). High fluid pressures in sedimentary basins can be attained by a variety of different geological processes and mechanisms. These include the rapid deposition of low-permeability sediments (disequilibrium compaction), the generation of hydrocarbons, mineral transformation, aquathermal pressuring, hydraulic head and osmosis (Swarbrick et al 2002). Disequilibrium compaction is often the cause of overpressure in young Tertiary deltaic systems (e.g. Mississippi delta, Gulf of Mexico; Niger delta, West Africa and Mahakam delta, SE Asia), where clastics are deposited rapidly on top of low permeability mudstones. If pore fluids cannot escape at a rate quick enough to allow pore pressure to equilibrate in the system, then overpressure will develop.

What has not been understood is how overpressure can exist in older basins that have not undergone active subsidence for tens or even hundreds of millions of years. In many 'old' Palaeozoic basins, areas can be found with extensive overpressuring and this is particularly the case for many basins within the United States (e.g. Delaware Basin west Texas, and the Anadarko basin Oklahoma). A near zero permeability seal (less than nanoDarcy scale $< 10^{-6}$mD) is needed to maintain any overpressure in the system for tens to hundreds of millions of years, given that overpressure developed through disequilibrium compaction during the basin's formation. For this reason, alternative mechanisms for overpressure generation are often proposed to explain overpressure in Palaeozoic basins. Mechanisms such as gas generation might have occurred later on in the basin's geological history, helping to explain the occurrence of overpressure at present day.

Numerous authors, (Luo *et al* 1994; Lee & Williams 2000; and Hansom & Lee 2005) have studied overpressure in the Delaware Basin, with both disequilibrium compaction and later fluid expansion mechanisms being proposed to explain the presence of the overpressure. This study aims to achieve a more accurate understanding of the overpressure in the Delaware Basin, with emphasis on the maintenance as well as the mechanism behind generation.

1.3 Aims of study

The aims of this study may be summarised as:

- In the current literature on the Delaware Basin (Hills 1984; Horak 1985; Barker & Pawlewicz 1987; Frenzel et al 1988; Luo et al 1994 and Hill 1996) there are numerous variations on the burial history of the basin. This study aims to accurately deduce the true burial history of the basin.
- There is limited published literature concerning the pore pressure history of the Delaware basin (Luo et al 1994; Lee & Williams 2000 and Hansom & Lee 2005). This study aims to conduct a more detailed analysis on how overpressure was generated in the basin, using techniques not used previously in other studies.
- The overpressure system in any basin is one of a dynamic rather than a static nature. Excess pore pressures will attempt to reach pressure equilibrium over time. Therefore this study aims to understand how overpressure is maintained in the Delaware Basin, which is just as important as how it is generated.

1.4 Methods

This section will briefly describe the methods used in obtaining the results, which are presented in this thesis. More detail regarding the methods is given in the Introduction of the respective chapter.

The burial history of the Delaware Basin is analysed in Chapter 4. The results were based on apatite fission track analysis, vitrinite reflectance analysis, and shale compaction curve analysis. Chapter 5 deals with wireline logs and how they can be used to predict pore pressure, and how the generation and maintenance of overpressure can also be analysed. The use of 1D and 2D modelling to assess the basin's pore pressure history through geological time is described in Chapter 6.

1.5 Layout of thesis

The thesis has been divided into eight chapters, and aims to take the reader logically through an understanding of the basin initially, before three results chapters, and then the discussions and conclusions.

- **Chapter 2: Geological history**. A review of the geological history of the Delaware Basin, and its surrounding area.
- **Chapter 3: Formation and development of overpressure in the Delaware Basin.** Detailed analysis and a literature review of the pore pressure system in the Delaware Basin.
- **Chapter 4: Mesozoic and Cenozoic tectonic history of the Delaware Basin.** A comprehensive review of the depositional and tectonic uplift history of the basin.
- **Chapter 5: Wireline analysis of pore pressure.** The use of wireline logs in interpreting the pore pressure history of the Delaware Basin.
- **Chapter 6: Basin Modelling of the Delaware Basin.** Using 1D and 2D basin models to analyse the pore poressure and petroleum system history of the basin.
- **Chapter 7: Synthesis and discussions.** Integrating the previous results with published work to answer fundamental questions regarding the pore pressure history of the Delaware Basin.
- **Chapter 8: Conclusions.**

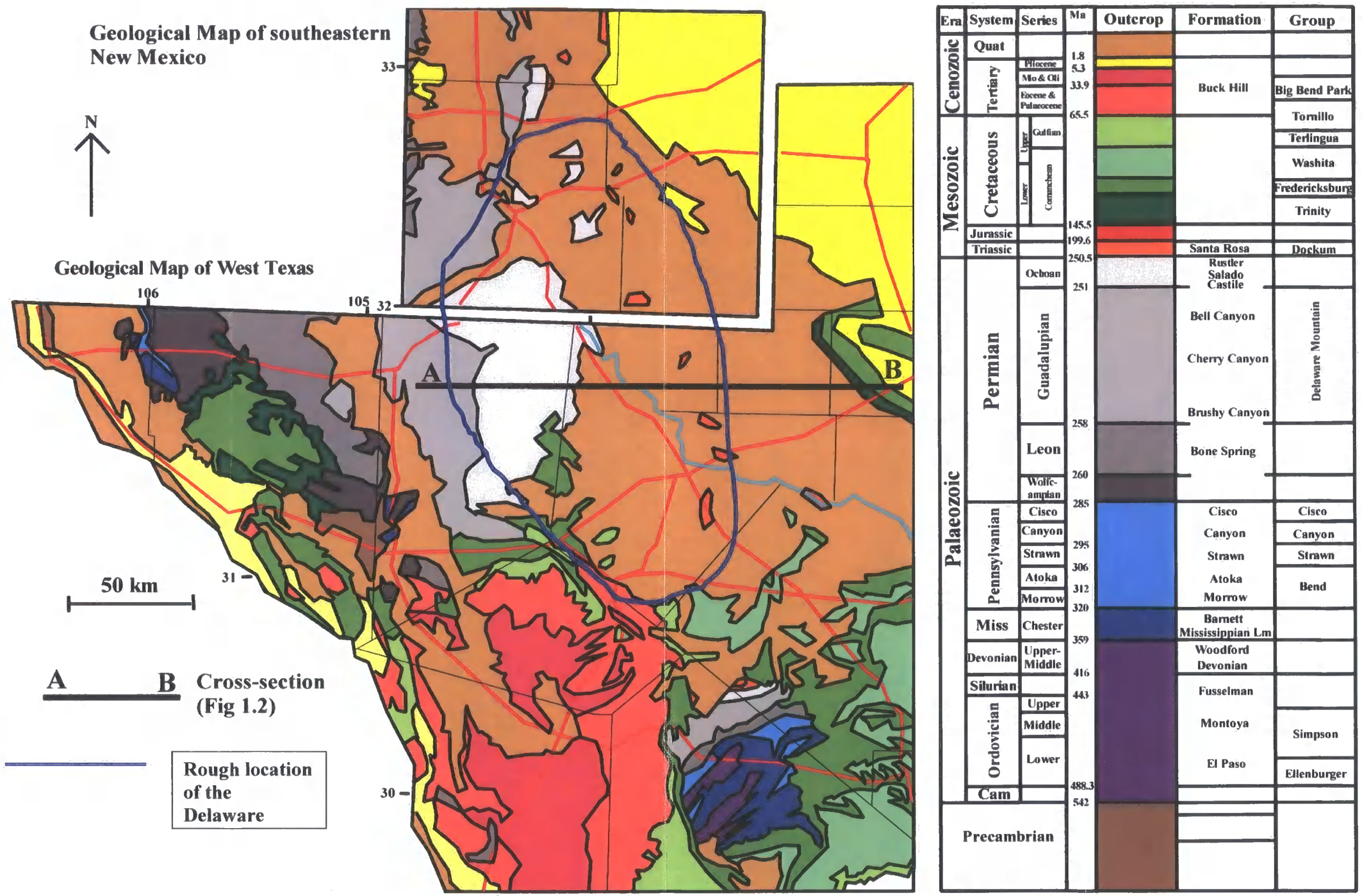

Fig 1.1. Geological map of west Texas, highlighting the rough location of the Delaware Basin, and its associated stratigraphic column.

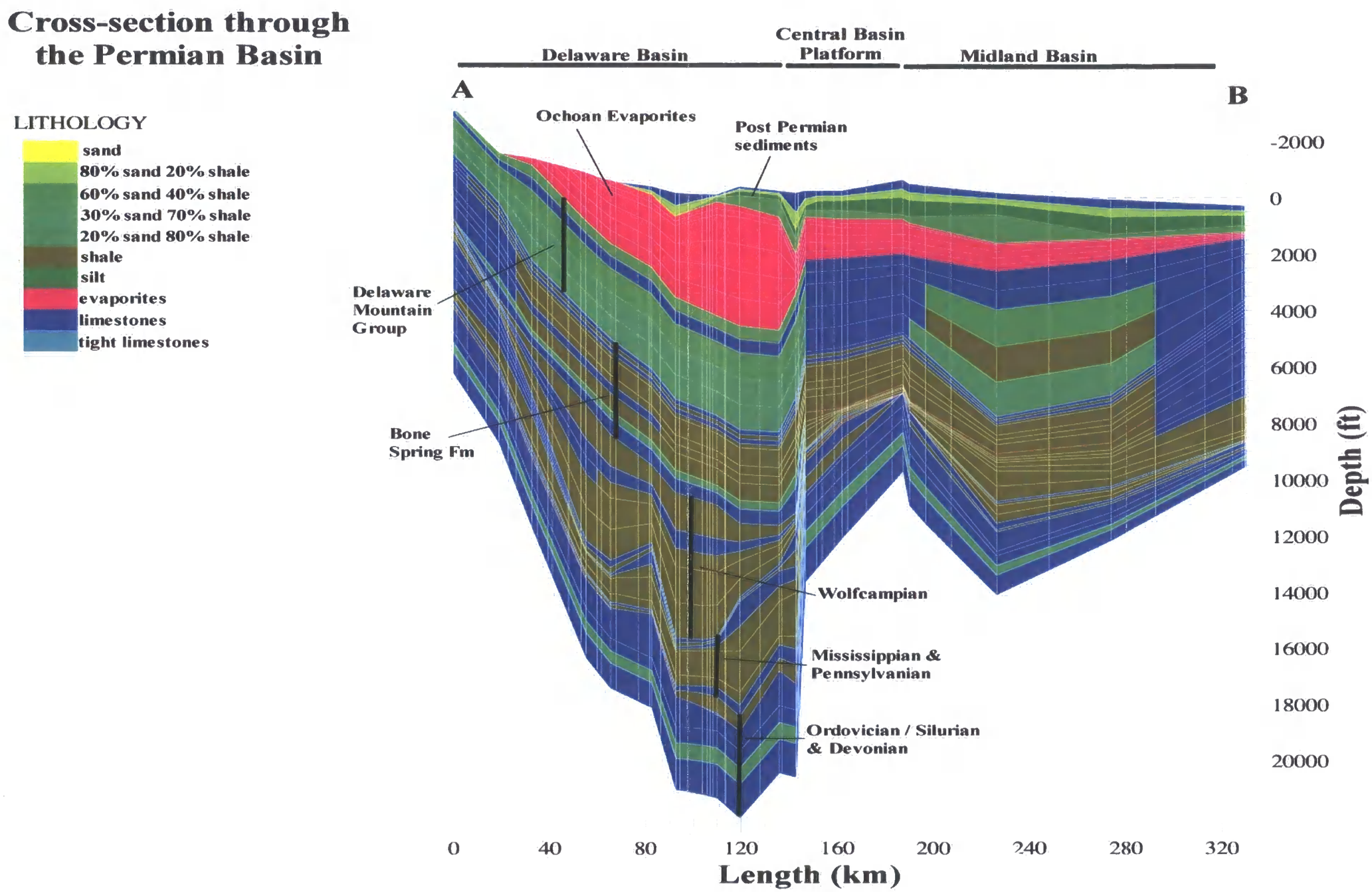

Fig 1.2. Cross section through the Delaware Basin, Central Basin Platform, and the Midland Basin (A-B on the Fig 1.1).

Chapter 2:

Structural and Stratigraphic History of the Delaware Basin

2.1 Introduction

This chapter will present an overview of the structural and stratigraphic history of the Delaware Basin, and the surrounding basins and highs, from the Precambrian (c. 1300 Ma) basement through to present day. The stratigraphic column (Fig 1.1) and the present day cross-section (Fig 1.2) will be useful aids to this chapter.

The study area of this thesis is the Delaware Basin of southeastern New Mexico and West Texas. It is an irregular NNW-SSE trending inverted pear-shaped depression, about 250 km long and 180 km wide, covering an area of more than 33,500 km^2. It is filled to a maximum depth of 24,000 ft (7.3km) with Phanerozoic sedimentary rocks having an estimated volume of 170,000 km^3, making the Delaware basin one of North America's deepest intercratonic basins with over 1 billion years of rock record in the basin.

The Delaware Basin is the major western subdivision of a larger framework of structural highs and lows in the southwestern part of the mid-continent craton of North America known as the Permian Basin (Fig 2.1). The Midland Basin, Val Verde Basin and the Central Basin Platform along with the Delaware Basin make up the Permian Basin.

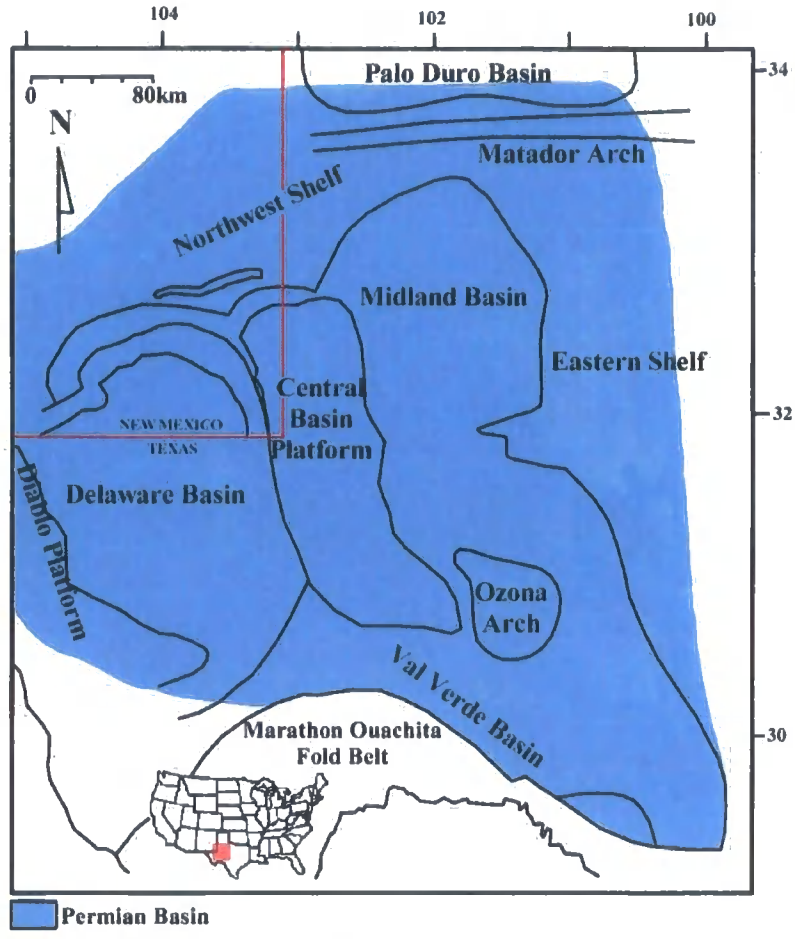

Fig 2.1. Map of west Texas and New Mexico highlighting the Permian Basin and its separate entities.

The Permian Basin's history as separate structural entities dates from the Pennsylvanian, but an ancestral basin, known as the Tobosa Basin (Galley 1958), existed between the Late Precambrian and the Pennsylvanian. The divisions of the Tobosa Basin into the separate basins was influenced by Proterozoic lines of weakness (Hills 1984). It was movement along these lines of weakness during the Pennsylvanian that culminated in the formation of the Delaware and other Permian basins and highs in the Early Permian. Deposition of sediments into the basin continued through the Palaeozoic and into the Mesozoic, with tectonic activity being experienced later on in the Cenozoic. This evolution of the Delaware Basin was subdivided by Hill (1996) into eight phases.

- Precambrian phase (c. 1300-850 Ma).
- Passive margin phase (c. 810-310 Ma).
- Collision phase – Division of the Tobosa Basin (c.310-265 Ma).
- Permian Basin phase – Subsidence of the Delaware Basin due to sedimentation (c. 265-230 Ma).
- Stable platform phase (c. 230-80 Ma).
- Laramide phase – Late Cretaceous to Eocene uplift (c. 80-40 Ma).
- Volcanism phase (c. 40-30).
- Basin and Range phase – Late Oligocene to present uplift (c. 30-0 Ma).

Based on the above classification by Hill (1996), this study has sub-divided the basin's geological history into just four phases representing the major tectonic events of the basin, as shown by a published burial curve of the basin (Barker & Pawlewicz 1987) (Fig 2.2).

- Tobosa Basin phase.
    - Initial basin subsidence in a passive margin setting from Late Precambrian to Late Mississippian (c. 810-310 Ma).
- Permian Basin phase.
    - Division of the Tobosa Basin due to tectonic plate collision, and rapid basin subsidence from beginning of the Pennsylvanian through to the beginning of the Mesozoic (c. 265-230 Ma).
- Stable platform phase.
    - Little subsidence or uplift from Triassic to Early Cretaceous (c. 230-80).
- Cenozoic tectonic uplift phase (c. 80-0 Ma).

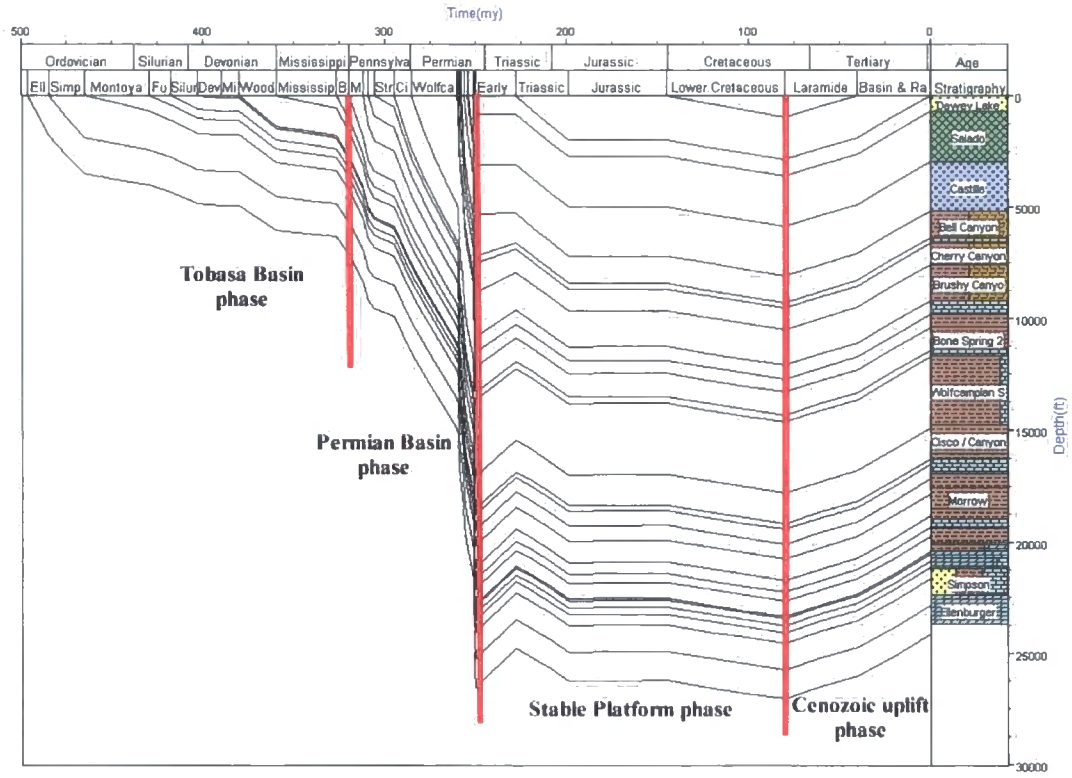

Fig 2.2. A burial history curve of the Delaware Basin as suggested by Barker and Pawlewicz (1987). Four phases of the basin's burial and tectonic history can be identified. (Adapted from Barker & Pawlewicz 1987).

2.2 Geological History of the Delaware Basin

2.2.1 Tobosa Basin phase

2.2.1.1 Precambrian Basement

The development of the Delaware Basin began during the Precambrian phase of tectonism (c.1300-850 Ma). It was the Grenville orogeny (c. 1000 Ma) that caused high angle faulting of basement rock. This led to regional lineaments of weakness that were to be reactivated by later deformational events.

During the Proterozoic, the Delaware Basin was on the southwest edge of the North American craton. However little information exists on the Proterozoic history of the region. For example, from over 600 wells studied as part of this research, only 3 were drilled to a depth where the granitic basement was hit. Despite a few wells actually penetrating the basement, the problem is that they only penetrated a few tens of feet. Flawn (1956) studied the cuttings from some wells that had been drilled in the basin at this time, and conclude that the majority of the Delaware Basin is underlain by granitic rocks of the North American craton. To the North of the Permian Basin, where metamorphic rocks are exposed in the peripheral basement highs, they indicate that the cratonic crystalline rocks had been intruded into Palaeozoic sediments. These metamorphic rocks have been dated in the peripheral highs in central New Mexico, where they correspond with the Grenville orogeny about 1 – 1.3 Ga (Hill 1996).

The Grenville orogeny (c. 1-1.3 Ga) was a widespread tectonic event that affected the supercontinent of Rodinia into which the North American craton was embedded during the Late Proterozoic. Plate convergence created crustal shortening and thrust faulting (e.g. the Carrizo Mountain Thrust, west of the study area). The orogeny appears to have had a NW-SE trend (Hills 1984).

The late Precambrian (c. 850 Ma), was characterised by fragmentation and rifting that extended all the through the North American craton. Associated with this were a number of high angle NW-SE trending faults with right lateral displacement. The basement beneath the Permian Basin was affected by this tectonism, and a number of Precambrian faults have been mapped in the area (Fig 2.3) (Hills 1984). The map shows the configuration of the Precambrian basement, and the deepest section is seen to the west of the main Precambrian fault zone. The strong NW lineation of the Precambrian faults is prominent, especially the large fault zone that runs from the Frontal Zone to SE corner of New Mexico. This Precambrian fault zone lies almost exactly in the position of the Central Basin Platform that separates the Delaware Basin from the Midland Basin at present day. These lines of weakness were reactivated later to compartmentalise the Tobosa Basin.

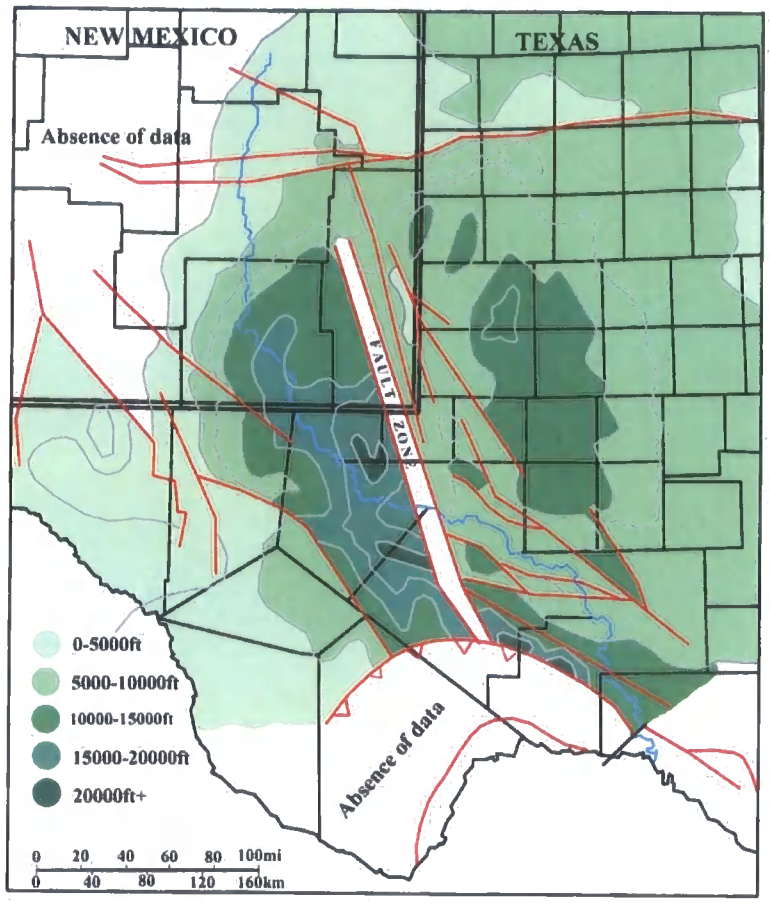

Fig 2.3. Depth to basement of the Precambrian surface, and lines of weakness (Adapted from Hills 1984).

2.2.1.2 Tobosa Basin Formation (810 – 310 Ma)

2.2.1.2.1 Tectonic Overview

By the end of the Precambrian, all activity along the fault zones had ceased and the region was welded onto the southwestern part of the North American craton, where passive margin conditions existed. Inland, rifting of a continental block during the Cambrian (Dickinson 1981) enabled the ancestral Permian Basin (Tobosa Basin) to form (Figs 2.4 & 2.5). Accommodation space was generated through this period by sagging and warping in an intracratonic setting. A shallow sea advanced over the

area of southeastern New Mexico and West Texas, enabling almost continuous deposition of thin platform sediments for 300 Myr in a 'layer cake fashion' (Horak 1985). This long period of passive sedimentation without any phases of tectonism is referred to as the "passive margin phase" by Horak (1985), the "sedimentation phase" by Hills (1985), and the "Permian Basin phase" by Hill (1996).

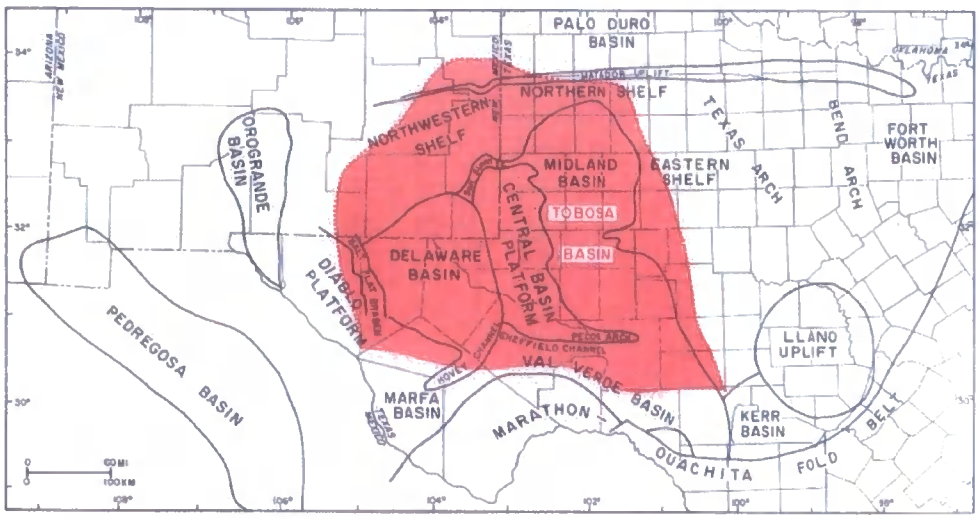

Fig 2.4. Present day geological divisions of Central, W Texas and SE New Mexico. Location of the ancestral Tobosa Basin is shown in red (Frenzel et al 1988).

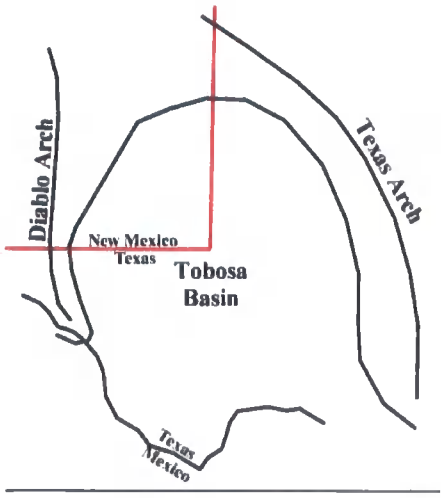

Fig 2.5. Sketch of the Tobosa Basin and its bounding uplifted arches from the Ordovician to the Pennsylvanian (Hill 1996).

2.2.1.2.2 Sedimentation and Tectonism

Cambrian to Ordovician

From the time of the Late Proterozoic intrusions and metamorphism, through to the Late Cambrian, the area was probably above sea level, because there is no record of Early and Middle Cambrian strata. The Late Cambrian saw the deposition of the Hickory Sandstone Member of the Riley Formation, which were deposits of a transgressive sea whose shoreline moved northwards. The amount of accumulation was dependent on the underlying eroded Precambrian surface, where thicknesses of up to 300 m are recorded near the Llano uplift in topographic depressions. Very limited Cambrian strata have been recorded in wells from the Delaware Basin.

The Early Ordovician saw minor tectonism, where weak extension produced block faulting (Kyle 1990). The depositional style of the Early Ordovician strata was that of a transgressive character, with the Ellenburger Formation deposited under broad shelf sea conditions (Fig 2.6). The formation pinches out in southeastern New Mexico due to the Pedernal Massif topographic high. The thickest section of Ellenburger most likely indicates the position of the incipient Tobosa Basin, with the boundary of the Diablo Arch developing on the western edge (Fig 2.5).

The Ellenburger Formation consists of light grey to grey, medium-grained crystalline, mostly siliceous dolomite. A slightly sandier dolomite is more common towards the top of the section (Hill 1996). The Ellenburger Formation was initially deposited in a restricted open shelf environment depositing over 500m of mud dominated carbonates, recording the initial transgression, and subsequent progradation and aggradation of the Ordovician sea. Within the mid-upper Ellenburger Formation, a diverse range of facies indicated a change to more tidal deposition. The sea regressed during the deposition of the Upper Ellenburger Formation, where dissolution and karstification of the exposed surface was common.

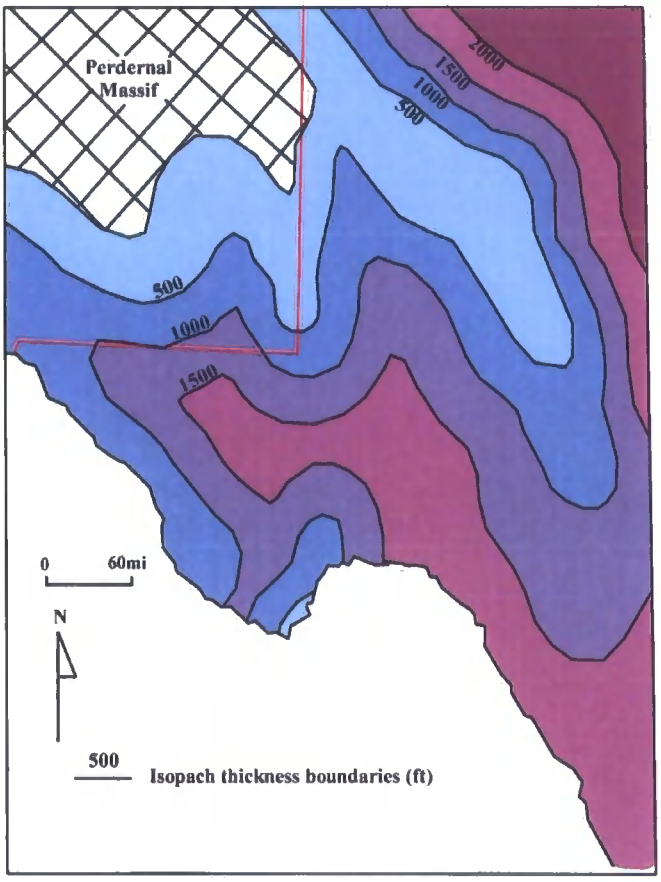

Fig 2.6. Isopach map of the Ellenburger Formation in the Early Ordovician.

The Middle Ordovician saw the deposition of the Simpson Group, as an unconformable layer on top of the Ellenburger Formation. The restricted distribution of the Simpson Group (Fig 2.7) represents the fully developed area of the Tobosa Basin. Simpson Group strata filled the basin to a depth of more than 600 m as the basin continued to subside. The Simpson Group has been described (Hayes 1964) as a black shale interbedded with limestone, and coarse to fine grained sands. It contains abundant fossils such as ostracods, graptolites and trilobites. The Simpson Group contains the following Formations: Joins, Oil Creek, McLish, Tulip Creek, and Bromide.

The Late Ordovician Montoya Formation overlies the Simpson Group. It consists of cherts and finely crystalline carbonates, both dolomitic and calcitic. At the depocentre of the Tobosa Basin the Montoya Group would have reached a thickness of around 150 m coincident with the depocentre of the Simpson Group.

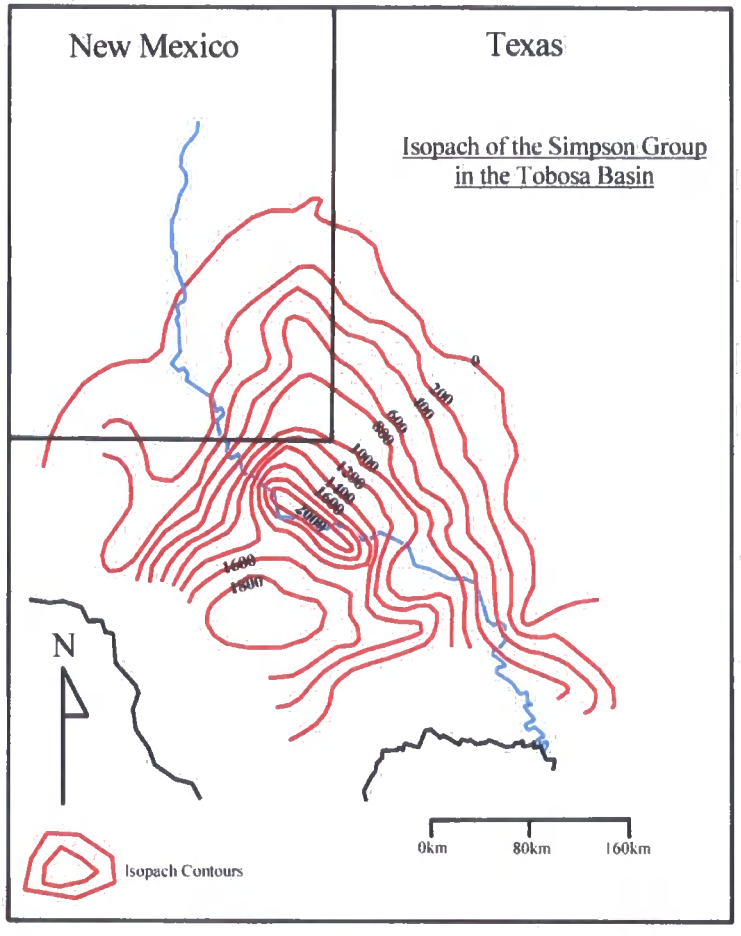

Fig 2.7. Isopach map of the Simpson Group in the Tobosa Basin (adapted from Frenzel et al 1988).

Silurian and Devonian

During the early Silurian there was a relative rise in sea level and the carbonate sequence of the Fusselman Formation was laid down in a highstand systems tract. The Fusselman Formation is mainly dolomitic in the northern and western parts of the Tobosa Basin, and calcitic towards the southeast. Up to 300 m of massive white limestones were deposited unconformably over the Montoya Formation. This unconformity is a prominent lithological break, where the light grey, coarse to medium grained crystalline dolomites of the Fusselman contrast sharply to the underlying darker finer grained Montoya (Hill 1996). The top of the Fusselman is described as an irregular eroded surface, which has undergone karstification. The

widespread occurrence of this karstified surface suggests a platform-wide drop in sea level (Hill 1996).

The unconformably overlying Wristen Formation of the Upper Silurian is a mud and shale rich rock dominated by dolomite. At present day, it is thickest in the northeastern part of the Delaware Basin, but thins northwards onto the Northwest Shelf, and eastwards onto the Central Basin Platform. Following on from the post Fusselman lowstand, a major transgression occurred during the Early Wristen time, which was followed by a significant sea level fall in the Late Wristen, and then another highstand.

At the end of the Silurian and the into the Early Devonian during this late highstand, shelf carbonates were deposited at the shallower margins of the Tobosa Basin, while dense limestones, cherts and black shales accumulated in the deeper water. The Devonian Formation was one such carbonate to be deposited during the Early and Mid Devonian. Since the deposition of the Simpson Group, the basin has not changed much in its geometry. The only significant change in geometry is that the depocentre for the basin has shifted northwards through time (Fig 2.8).

Since the onset of deposition of the Montoya Formation in the Late Ordovician through to and including the Devonian Formation in the Early Devonian, a sequence of carbonates was laid down. The carbonates were deposited without any major structural interference, and record a continuous period of carbonate sedimentation.

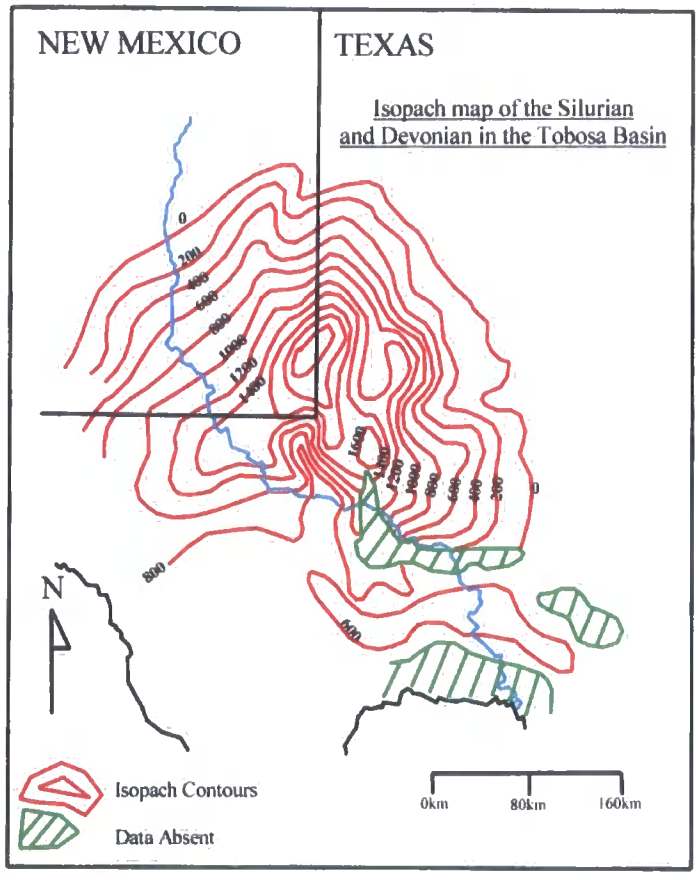

Fig 2.8. Isopach map of the Silurian and the Devonian in the Tobosa Basin (adapted from Frenzel et al 1988).

Late Devonian and Early Mississippian

In the Late Devonian there was a phase of uplift and the Tobosa Basin was tilted to the east, allowing up to 500 m of sediment to accumulate (Hills 1985). A western compressive stress at this time also produced a broad arching over most of New Mexico and northern Texas such as the Texas Arch that is seen today (Figs 2.4 and 2.5). During this time, a transgressive sea flooded the basin that brought about a distinct change in the depositional environment of the basin as well as for the rest of the North American craton. The amount of carbonate deposition decreased as dark shales unconformably covered the earlier sediments.

In the Tobosa Basin, the Late Devonian shale is known as the Woodford Formation. It is highly organic, which makes it a world class source rock, as well as being highly radioactive, which makes it a good marker bed on gamma ray logs. It is fine grained, dark brown to black, and rich in spores and microfossils such as

conodonts. Its thickness in the basin varies between 30 m and 200 m, with the thickest deposits being seen in Winkler County.

The Woodford Formation's origin is an area of slight controversy. Conant and Swanson (1961) believe that the shale was deposited in shallow water of less than 10 m, under a slow transgressing sea environment. There was abundant algal mat growth with stagnant bottom conditions under anaerobic conditions. They also believe there is a lack of evidence to suggest any agitation of the water. Hill (1996) suggested that the Late Devonian sea was substantially deeper, around 350 m, where there was poor circulation and low oxygen levels in a restricted environment, a modern day example would be the Black Sea.

The Early and Mid Mississippian sedimentation was much like that of the Early Ordovician, a transgressive sequence of clastics in the south of the Tobosa Basin grading into carbonates in the north, with thick carbonates eventually covering the whole of the basin. Deposition of the green-grey Kinderhook Formation was followed by thick southward thinning deposits of the Mississippian Limestone Formation. This Formation is a fine crystalline non porous calcitic limestone, ranging from being more argillaceous in some places to more siliceous and cherty in others.

2.2.2 Permian Basin phase (310-255 Ma)

2.2.2.1 Tectonic overview

This was a significant phase in the evolution of the Delaware Basin when a major tectonic episode split the Tobosa Basin into separate tectonic highs and lows, giving rise to the Permian Basin that is seen today (Delaware Basin, Midland Basin, Central Basin Platform, and Val Verde Basin). As can be seen from the burial history curve of Barker and Pawlewicz (1987) (Fig 2.2), this was also a time of rapid basin subsidence, creation of accommodation space, and subsequent sediment deposition.

Up to a maximum of 5.5 km of sediment was deposited in the Delaware Basin during this phase.

Before the major phase of tectonism, the Mississippian (360-320 Ma) was regarded as a transitional period between two very different tectonic styles in the evolution of the Permian Basin. From the Cambrian through to the Mid-Mississippian, the ancestral Permian Basin (Tobosa) was a stable part of the North American craton, where all tectonism was epeirogenic. However from the Late Mississippian, tectonism became more aggressive. Old fault lines and lines of weakness from the Precambrian were exploited to cause significant uplift and form depressions. A change in deposition also occurred with widespread masses of limestone being succeeded by dominantly shale, with later coarser grained and thicker clastic units.

This major tectonic episode was a consequence of the collision of the continents of Laurasia and Gondwanaland to form the supercontinent of Pangaea at the start of the Pennsylvanian (c.310 Ma) (Figs 2.9 & 2.10). This collision affected the central and eastern edge of the North American craton, creating a number of orogenies with thrust movement to the northwest. The Appalachian orogeny was responsible for the formation of the folded and faulted mountain belt that extends down from southern New York southward into Alabama.

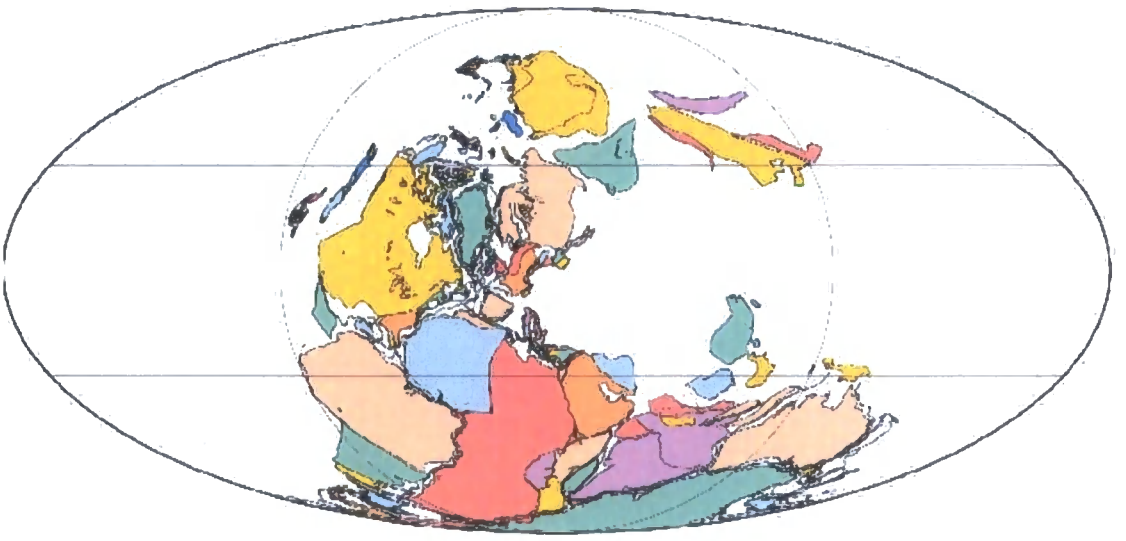

Fig 2.9. 310 Ma – Collision of Gondwana and Laurasia to form Pangaea (Dalziel 2002).

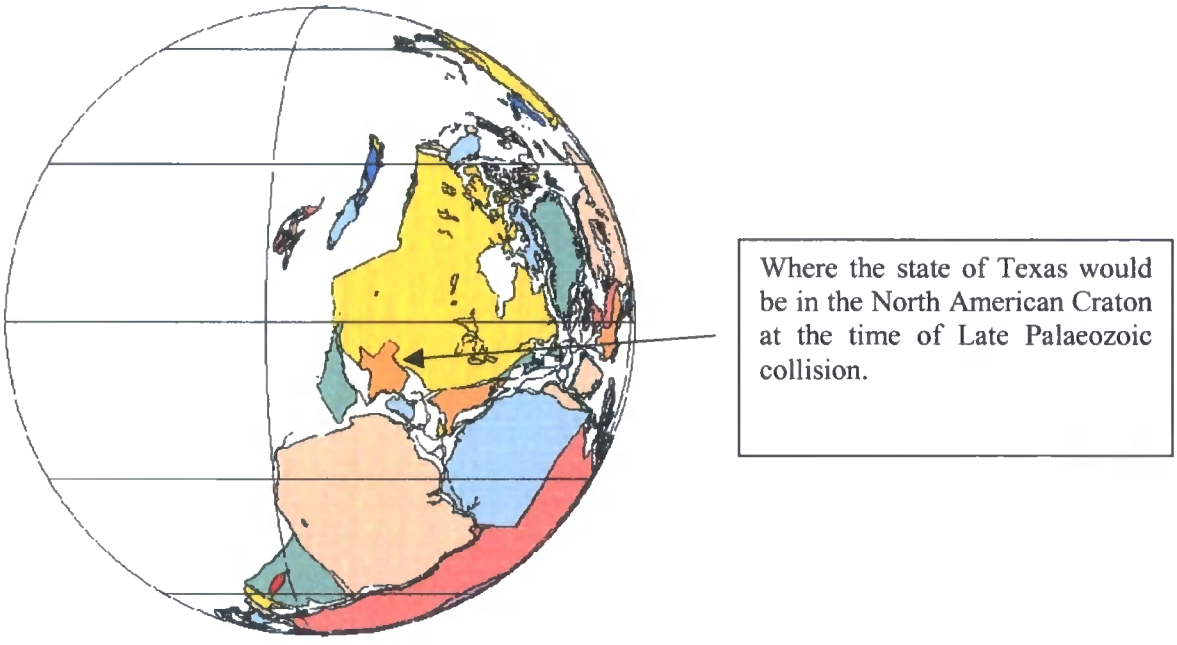

Fig 2.10. 310 Ma – Super continent of Pangaea, highlighting the state of Texas within the North American craton (Dalziel 2002).

The Ouachita orogeny (Fig 2.11) was responsible for the thrust zone seen in the study area, which affected the Tobosa Basin. The consequence of the Ouachita orogeny was that the predominant stress (σ^1) was orientated WNW-ESE due to the major compressive stress component exerted along the entire Ouachita thrust front. This stress was transmitted into the foreland and caused reactivation of Precambrian basement block faulting. This caused some blocks to uplift, such as the Central Basin Platform and the Pedernal Uplift, while others were downfaulted forming the Delaware Basin, Midland Basin and Val Verde Basin. The intermediate principal stress σ^2 was orientated vertically, due in part to the loading by the thick sedimentary cover. σ^3 was orientated horizontally in a NNE-SSW direction. This stress system resulted in the formation of predominantly strike slip faulting, where two types are recognised. Faults that are orientated NW have a sinistral displacement whereas

dextral displacement is seen on faults that trend to the NE-SW. Also the stress system caused folding, with the fold axis trending NE-SW.

The continental collision was also a time of high heat flow in the Delaware Basin, and thermal doming of the lithosphere occurred during the Pennsylvanian (c. 310-300 Ma), which caused anticlines to develop in the strata. Today these Pennsylvanian topographic features are essential structures for hydrocarbon exploration.

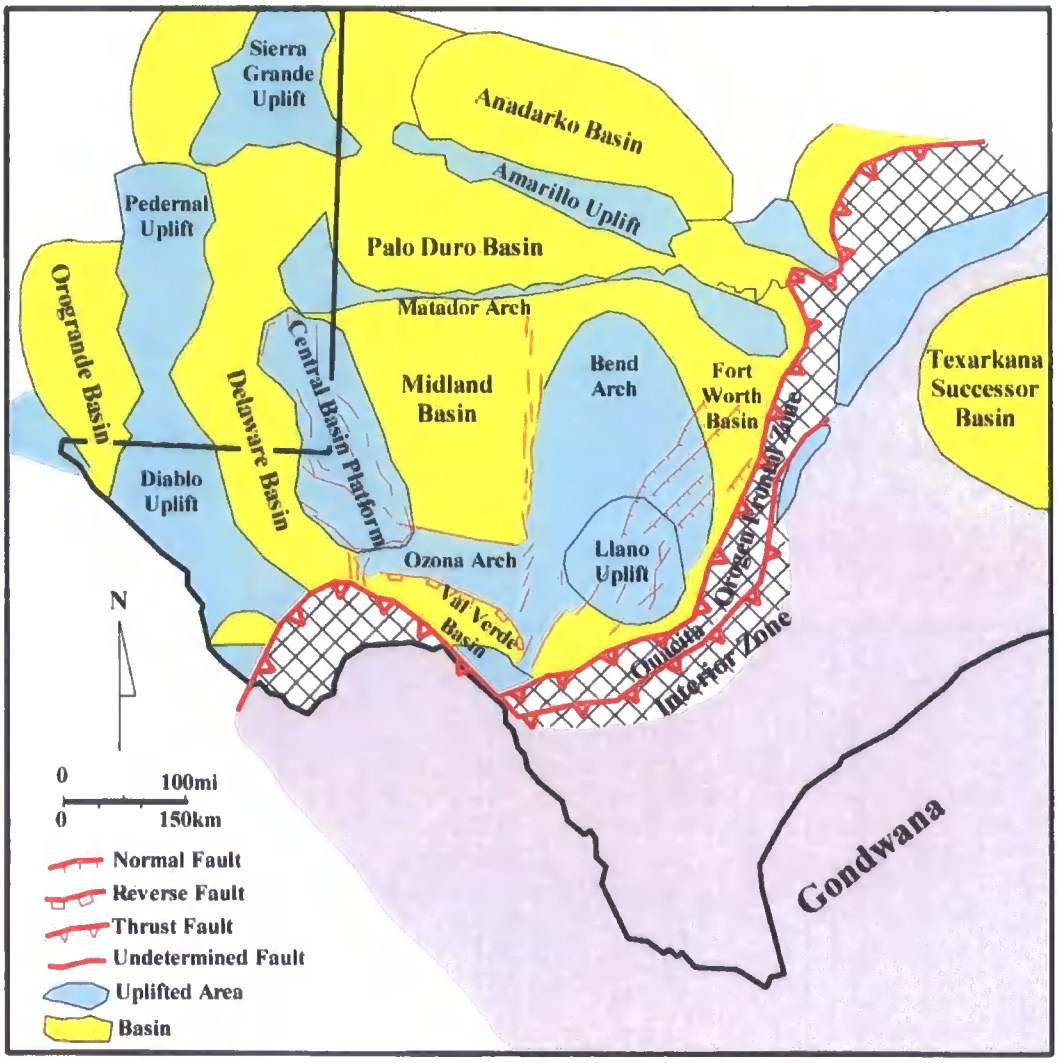

Fig 2.11. Location of Late Palaeozoic structural features, highlighting the Ouachita Orogenic fault zone.

2.2.2.2 Sedimentation and Tectonics

Late Mississippian

The Barnett shale is the result of tectonic movement at the onset of the Ouachita orogeny. It is a hard siliceous grey to dark grey shale, which is organic and very pyritic. The Barnett shale is an extensive deposit covering not only the whole of the Tobosa Basin but also the entire Texas Arch, where it lies unconformably over Ellenburger dolomites.

Pennsylvanian

The Pennsylvanian strata of the Permian Basin are extremely variable in distribution, thickness and lithology (Fig 2.12). The variability stems from the continuation of Late Mississippian Ouachita tectonism in the basin, which caused non-deposition and erosion on the structural highs. The influx of sediment into the separate basins would have come from the exposed and eroded uplifted areas, with deposition of mudstones, carbonates and sandstones. Because of the rapid and complex lateral and vertical facies changes, the Pennsylvanian rocks are not divided up into lithological units. Instead they have been divided into five formations based upon fusulinid occurrences. From the oldest they are the Morrow, Atoka, Strawn, Canyon and Cisco.

In the Late Pennsylvanian, the Delaware Basin subsided rapidly due to increased compression of the Ouachita orogenic front. This is recorded in the Late Pennsylvanian strata of the Strawn Canyon Formation in the Glass Mountains, which borders the Delaware Basin on its southern margin where a major unconformity is seen. Conditions were stable for the rest of the Pennsylvanian with shelf edge sands and carbonates being deposited on the margins of the basin.

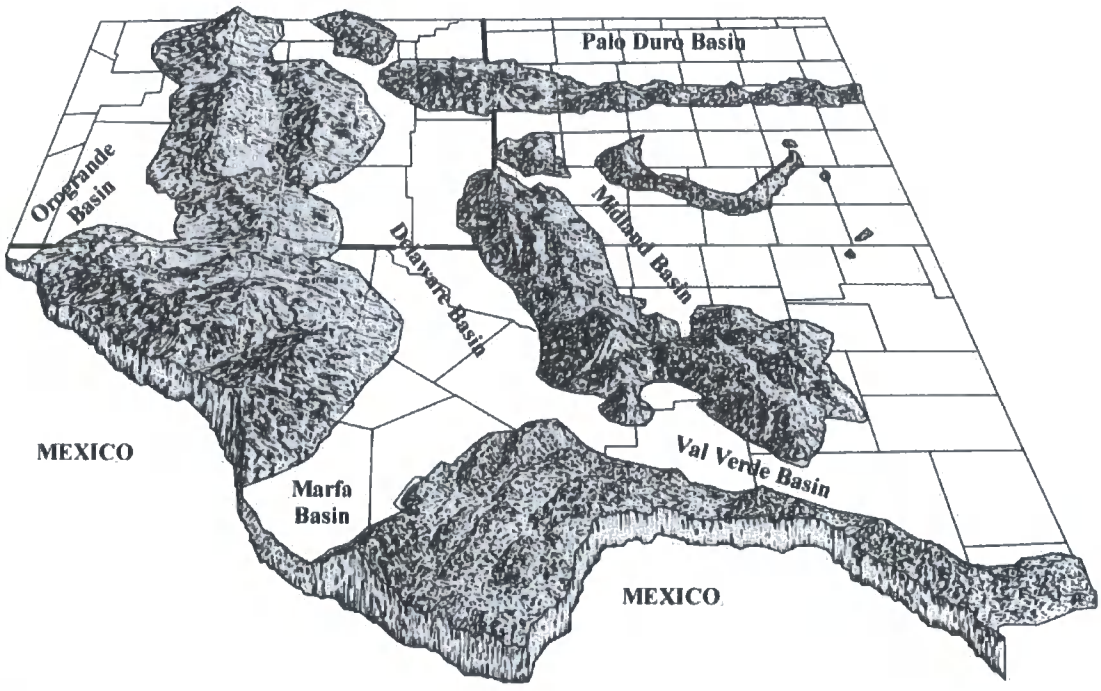

Fig 2.12. Palaeogeography of the Permian Basin in the Late Pennsylvanian (Wright 1979).

Permian (c. 302 – 251ma)

During the Permian, the Delaware Basin was located on the western edge of Pangea at about a latitude of 5-10° N. It was predominantly a time of tectonic stability with high rates of basin subsidence due to flexure. Enough accommodation space was generated for up to 4.8 km of Permian sediments to be deposited in the basin depocentre and 1.9 km on the shelf. The subsidence was at a rate that allowed the shelf of the basin to remain at shallow water depths all throughout, allowing carbonate banks to form.

Adams (1939) was the first to divide up the Permian strata in the Delaware Basin into four series: the Wolfcampian, Leonardian, Guadalupian and Ochoan. The divisions were based on fossil content as well as lithology. The type section for the whole of the Permian is seen in the Glass Mountains, where a complete and continuous 1.9 km section of strata ranges from the base of the Wolfcampian through to the top of the Guadalupian. The fossil record here was used to set up the divisions of the Delaware Basin as well as other Permian stratigraphy in North America.

In the Wolfcampian period, seas covered the whole of west Texas and New Mexico (Fig 2.13). The only structural highs that were exposed were the Pedernal Uplift to the NW, the Ouachita Orogen Front to the south and a small section of the Central Basin Platform. It was only in the Late Wolfcampian that the Central Basin Platform became sub-aerially exposed. The majority of sediment was eroded off the Ouachita Mountains and thick deposits accumulated in the southern part of the Delaware Basin. The Wolfcampian strata progressively thin from about 1.9 km of dark coloured shale and limestone in the south to about 300 m of carbonate reefs and limestone banks on the shelf margins to the north and west (Fig 2.14). Pockets of silts and coarse sands are also found in the deep basin. The only period of tectonic activity in the Permian was during the Mid Wolfcampian times (c.290 Ma). This is represented in the section by a major unconformity, which is seen in the Glass Mountains at present day, and corresponds to a time of major folding and thrust faulting in the basin. After this Mid Wolfcampian tectonic activity, the basin was tectonically quiet and nowhere in the Permian Basin do the faults or folds in the older strata propagate through into the later younger Permian strata.

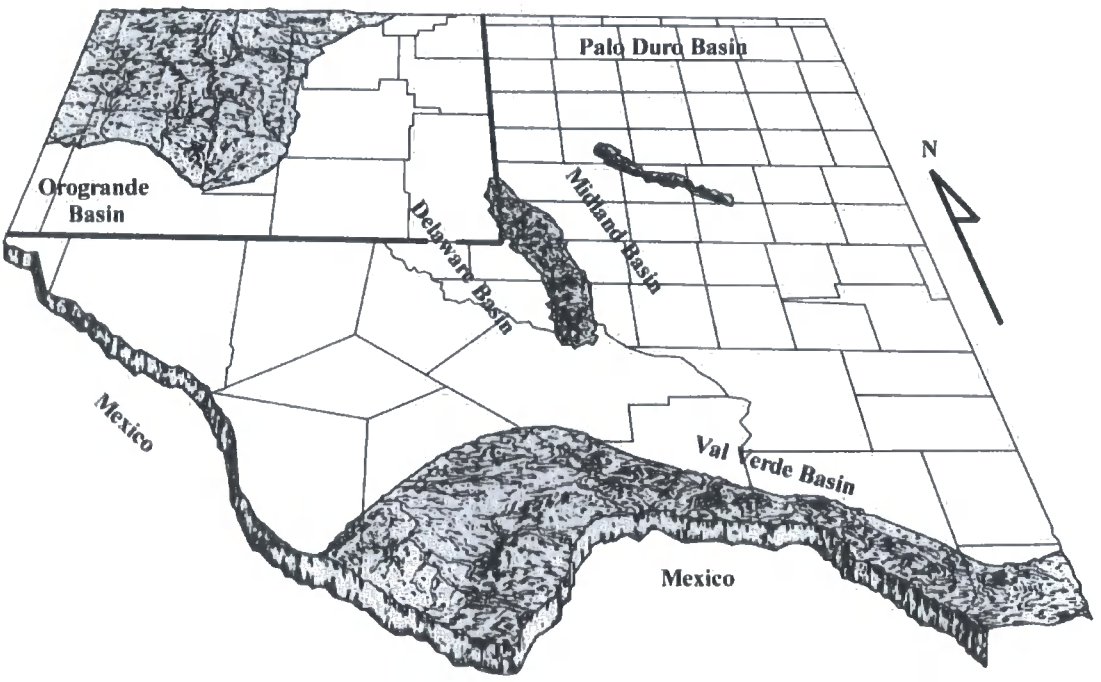

Fig 2.13. Palaeogeography of the Permian Basin in the Early Permian (Wright 1979).

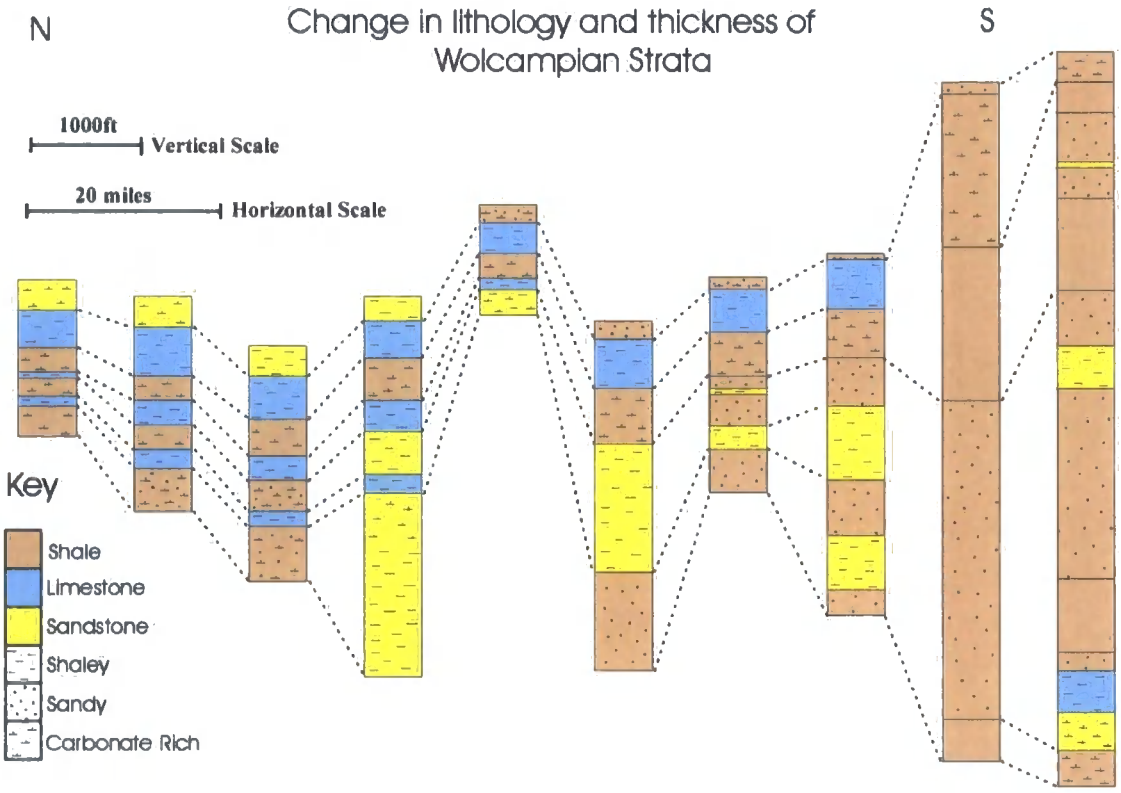

Fig 2.14. Log of the Wolfcampian Series through the Delaware Basin from north to south

During the Leonardian, the Delaware Basin continued to subside, although not as rapidly as in the Wolfcampian because shelf to basin depositional relief had decreased. The basin remained as a deep marine environment with the Upper Wolfcampian Series grading conformably into the Lower Leonardian Series. The Leonardian Series consists of the Bone Spring Formation, a dark grey deep marine shale, which grades upwards into interbedded shales with quartzose sands and black limestones. In the basin, the Bone Spring Formation varies in thickness of between 700 m and 1000 m and is typified by alternating cycles of clastic and carbonate beds in both large scale and small scale cycles (Sarg 1991). The three large-scale cycles are referred to as the 1st, 2nd and 3rd Bone Spring sands, which are separated by three carbonate sequences. According to Friedman et al (1986), the sands were deposited during times of low sea level as debris flows or turbidites. The black limestones are bituminous rich, and suggest that at the bottom of the Bone Spring Sea, during deposition, there was little circulation and a lack of oxygen, making the Bone Spring

limestones characteristic of a deep euxinic basinal origin. Because of this, the Bone Spring is an important source rock in the area.

Along the shelf margins of the basin, banks of carbonate sand or patch reefs were developing, and it was during the Leonardian that the general sequence of backreef-reef basin facies were being established in the Delaware Basin. Fossils can be found on the shelf, including gastropods, brachiopods, trilobites, sponges and conodonts. The conodont 'Neogondolella idahoensis' is found in the Upper Bone Spring Formation, and has been used as a chronological marker (Behnken 1975).

During the Guadalupian, a thick unit of siliciclastics was deposited conformably over the Bone Spring Formation. Over the 9 Myr of deposition, the basin continued to subside; however, its aerial extent was continually decreasing. The Series comprises the Brushy Canyon, Cherry Canyon and Bell Canyon formations in ascending order. Previously, the Bone Spring Formation had been deposited across the whole of the Permian Basin; however, beginning in the Early Guadalupian with the Brushy Canyon Formation, deposition was restricted to the Delaware Basin.

The Guadalupian Series reaches a maximum thickness of nearly 1500 m in the centre of the Delaware Basin. The Group is nicely exposed on the western edge of the Delaware Basin near the Guadalupe Mountains (Fig 2.15), which the Guadalupian Series is named after. These mountains are where one of the most extensive outcrops of Guadalupian aged rocks in the world can be found. They are predominantly made up of light grey fine grained sandstones and siltstones interbedded with shales, with reef complexes forming on the edge of the basin. The environment was a time when the Permian Sea had regressed to the limits of the Delaware Basin, enabling the large reef complexes to build on the shelf edges. The siliciclastics of the Guadalupian Series are interpreted to have originated from a sedimentary source from the Pedernal Uplift to the northwest, and were transported into the Delaware Basin by fluvial and aeolian mechanisms to a back reef environment; then turbidite and density currents transported the sands via erosional channels into the deep marine environment of the Delaware Basin (Cromwell 1984). The sands of the Guadalupian Series make very good reservoirs for exploration, with

most oil production coming from stratigraphic traps in the Bell Canyon Formation sand.

Fig 2.15. Outcrop of the Brushy Canyon Formation Sand on the western edge of the Delaware Basin

The Ochoan Series deposited in the Late Permian represents a significant change in the Delaware Basin. After the deposition of back reef and basinal deposits in the Guadalupian Series, the basin became characterised by thick deposits of evaporites and thin red beds. This signified the final stages of the Permian Sea, with the closing of the Delaware Basin to marine waters and the start of a continental regime. During the Ochoan age, the West Texas and New Mexico area was an interior continental desert within Pangea. The Delaware Basin lay at a latitude of 15° N, and had an inlet along the western edge of the supercontinent to allow deposition of evaporites over 500,000-600,000 years. The deposition of evaporites in the Late

Permian was a worldwide occurrence in other basins, and signified the end of some invertebrates (Late Permian extinction).

The Ochoan Series consists of the Castille, Salado, Rustler and the Dewey Lake Formation. They had a combined thickness of over 1 km, and extended across the whole of the Delaware Basin, the Midland Basin and the Central Basin Platform, with the exception that the Castille Formation is seen only in the Delaware Basin. The extent of the Ochoan Series today is limited due to Tertiary erosion and uplift, where they are absent on the western edge of the Delaware Basin. The Castille Formation is predominantly composed of anhydrite, and sections of the Castille appear to have a cyclic nature with muddy laminations interbedded with the anhydrite, indicating annual varves (fig 2.16). The Salado is composed of halite, the Rustler of dolomite, and the Dewey Lake is a continental red bed.

Fig 2.16. Anhydrite of the Castille formation showing rhythmites.

2.2.3. Stable Platform phase (c. 230-80 Ma)

At the boundary between the Permian and Triassic (c.250 Ma), a distinct change was seen in the Permian Basin area. After being a marine basin for 300 Myr, the area had a positive relief during the Mesozoic, due to worldwide dramatic shifts in tectonics and sedimentation. Key elements of this global change were

- The final assemblage of Pangea before its break up into separate plates.
- A major marine regression, where marine basins changed into evaporitic basins (Ochoan Series), followed by continental environment.
- A major extinction event at the Permian Triassic boundary, when about 90% of all Late Permian invertebrate marine species and 70% of terrestrial vertebrate species died out.

In the Delaware Basin this shift was represented by uplift and replacement of marine conditions with deltaic, lacustrine and fluvial systems. The Delaware Basin was also tilted to the east, as seen by the angular unconformity between the overlying Mid-Late Triassic Chinile Group and the underlying the Dewey Lake Red Beds. The Mesozoic period is as shown in the burial history plot (Fig 2.2), where little deposition or subsidence occurred, and this phase is often referred to as the 'stable platform phase, (Hill 1996).

Mesozoic sedimentation did not begin in the Delaware Basin until the Mid-Late Triassic with the deposition of the Triassic Chinile Group. Erosion and dissolution predominated in the Early and Mid Triassic with up to 120 m of Late Permian sediment removed, before the fluvial and terrestrial deposits of the Chinile Group were laid down. These deposits are red coloured, heterogenous, poorly sorted conglomerates and coarse sands (Santa Rosa Formation), and floodplain mudstones (Dockum formation).

There was no deposition of Jurassic sediment in the Delaware Basin, as the Permian Basin continued to be emergent with extensive erosion and dissolution. An angular unconformity exists between underlying Triassic sediments and the overlying Cretaceous. The nearest exposures of Jurassic rocks to the Delaware Basin are found in northwest Texas at Malone Mountain. It is inferred that the Jurassic Sea

that deposited these sediments never reached as far east as the Delaware area. Despite little to no deposition, the Jurassic was a time of important plate tectonic movement. The opening of the Gulf of Mexico and the Tethys seaway (c.170 Ma) caused the northward drift of the North American craton from its equatorial Permian latitude. Evidence of Jurassic tectonism was seen on the North American craton, in northeastern Mexico, where a series of northwest trending highs and basins formed. Their formation is not fully understood, but could have resulted from strike slip faulting or extension associated with the opening of the Gulf of Mexico.

In the Early-Mid Cretaceous, the Comanchean epoch, weak subsidence of the area allowed the North American craton to be connected with the Gulf of Mexico seaway, and a shallow epicontinental sea transgressed across the area. The Diablo Platform and the Marathon Uplift were topographic highs at this time, and supplied sediment to the Delaware Basin. The full transgression of the Comanchean Sea reached to the far north of the Delaware Basin in the Mid-Late Cretaceous, although there were a number of minor transgressions and regressions (Richey 1985). Up to 500m of Cretaceous sediment is present in the southern counties of the Delaware Basin. Other Cretaceous sediment is limited to the mountains that border the basin. Sedimentation in the Comanchean consists of basal conglomerates, sandstones and limestones.

2.2.4 Cenozoic tectonic uplift phase (80-0 Ma)

Following on from the long period of quiescence in the Mesozoic, the stable platform phase was terminated by uplift and tilting by two separate events: The Laramide event during the Late Cretaceous and Early Tertiary, and the Basin and Range event from Late Oligocene to present.

2.2.4.1 Laramide orogeny (80 -40 Ma)

The Laramide orogeny was a consequence of the convergence of the Farallon and North American plates. This convergence produced low angle subduction and ENE-WSW compressive stresses, which forced the uplift of the whole Rocky Mountain region from New Mexico to Wyoming (Dickinson 1981). There are variable opinions (Hills 1984, Horak 1985, Barker and Pawlewicz 1987, and Hill 1996) as to the impact that the Laramide Orogeny may have had on the basin. Horak (1985) suggested that the basin may have been uplifted by up to 1.5 km, while others (Hills 1984, and Barker & Pawlewicz 1987) have suggested that the tilting of the basin is a consequence of the Laramide orogenic event.

The influence of the Laramide orogenic event on the Delaware basin is dealt with in more detail in chapter 4, which describes the use apatite fission track analysis in determing the uplift history of the basin.

2.2.4.2 Basin and Range uplift 30-0 Ma

The Basin and Range phase (30-0 Ma) is described as being a period of time characterised by regional crustal extension and thinning, high heat flow, rifting, low gravity values and low compressional velocities in the Upper Mantle (Horak 1985). Uplift during this time was a consequence of the thermal doming associated with the thinning of the lithosphere due to the extension (Hill 1996). The transition from a Laramide compressional phase to a Basin and Range extensional phase was complete by the Late Oligocene.

With Basin and Range lithosphere thinning, extension and normal faulting came a regime of higher heat flow in the Delaware Basin, where geothermal gradients are suggested to have reached up to 50°C/km (Barker & Pawlewicz 1987). Schneider and Hinojasa (1991) suggest an explanation for the high heat flows. Where the upper mantle and lower crust in the Basin and Range Rio Grande rift area, contains a thermal anomaly, which has both deep and shallow components. The deep anomaly produced the bulk of the isostatic uplift for the Basin and Range, but made

little contribution to the surface heat flow. The shallow anomaly was responsible for elevated heat flow but contributed little to uplift. The deeper anomaly was also responsible for the volcanism that is seen in the basin.

As with the Laramide orogeny, the effect that the Basin and Range event had on the Delaware Basin is not quantified in the literature. This study, however, uses apatite fission track analysis to quantify the uplift on the basin (chapter 4).

2.2.4.3 Cenozoic deposition

Deposition of Cenozoic sediment in the Delaware Basin was limited according to Hills (1984), and Hill (1996). By the Late Cretaceous, the Comanchean sea was withdrawing from the area in response to the Laramide Uplift which affected the whole of North America. The Laramide continued through to the Palaeocene, and by the Eocene, Laramide tectonism had ended and a period of quiescence prevailed on the North American craton. There is no rock record for the Palaeocene or the Eocene in the Delaware Basin.

The Late Eocene saw a change in the tectonics of the area, from a time of quiescence to a time of continental arc volcanism. By the Mid Oligocene, magmas were emplaced in the high crustal levels and within the space of 8 Myr, magmas vented to the surface forming the volcanic field of the southern Delaware Basin. A series of northward migrating intrusions were then emplaced, with the youngest intrusion (c. 30 Ma) in the northwest of the basin.

During the Miocene, the Basin and Range event uplifted the western edge of the Delaware Basin, exposing the underlying strata. The Gatuna Formation is seen along the drainage system of the Pecos river, and its deposition continued through to the Pleistocene. It is composed of poorly consolidated orange / red siltstone and sandstone.

The Pleistocene was a time of glacials and intraglacials, with alluvial deposits forming in the topographic lows of the basin. Further alluvium of Holocene age is located along the drainage system of the Pecos River.

Chapter 3:
Pore Pressure

3.1 Introduction

Pressure is the force per unit area acting on a surface. In porous sediments, every point within any sedimentary basin has a pore pressure associated with it, and its pressure can be classified as being hydrostatic, overpressured or underpressured (Fig 3.1).

If the pore pressure at a specific depth falls on the hydrostatic curve, then the rock is classed as being hydrostatically or normally pressured. If the measured pore pressure lies between the hydrostatic curve and the lithostatic curve, then the rock is classed as being overpressured. Underpressuring occurs where the pore pressure is less than the hydrostatic.

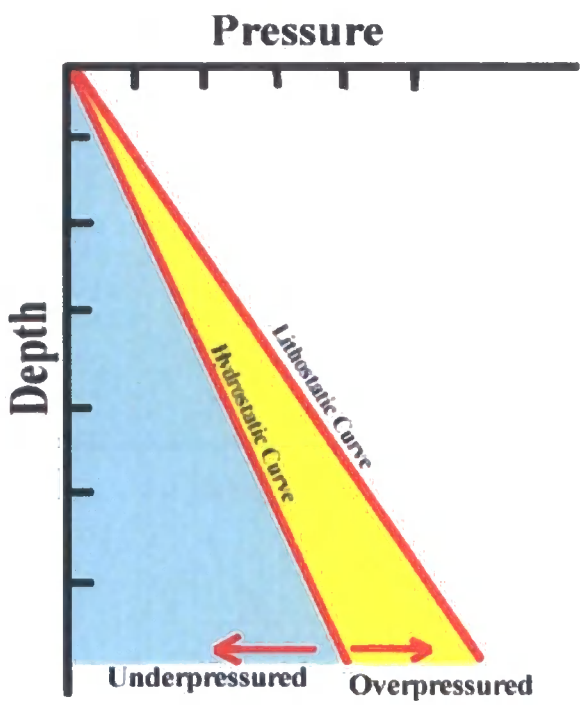

Fig 3.1. A pore pressure with depth curve highlighting the three classifications of pore pressure.

Section 3.2 introduces the pore pressure system and the terminologies used, and explains the mechanisms for generating abnormal pressures. A description of the pore pressure distribution in the Delaware Basin is given in section 3.3. Section 3.4 is a review of published literature on overpressure in the Delaware Basin and other

Palaeozoic basins in the US, and integrates this information with the overpressure distribution in the Delaware Basin described in the preceding section.

3.2 Introduction to the pore pressure system

3.2.1 Hydrostatic pressure

The definition of hydrostatic pressure is a "pressure exerted by the weight of a static column of fluid". Therefore, in a normally pressured reservoir the fluid within the pores is equivalent to the overlying water column extended vertically to the surface. The hydrostatic pressure is a function of the density of the pore fluid and depth. It can be expressed by the equation:

$$P = \rho.g.h \qquad (3.1)$$

where:
P = hydrostatic pressure,
ρ = fluid density,
g = acceleration due to gravity, and
h = vertical height of the fluid column measured from datum.

The reference datum for the hydrostatic curve is sea level, where atmospheric pressure is at 1Atm, or 14.7 psia (pounds per square inch absolute). The hydrostatic pressure increases with depth at a rate dependent on the density of the pore fluid. If the pore fluid is fresh water (1.00 g/cc), then the hydrostatic pressure increases by 0.433 psi/ft. This is also known as the pressure gradient. If the formation fluid is brackish, with a NaCl content of 20,300 ppm, then the hydrostatic pressure gradient is 0.4338 psi/ft. Typically, in a basin where salt is not part of the sedimentary

succession, a pressure gradient of 0.45 psi/ft is sufficient to use in a pore pressure study.

3.2.2 Lithostatic pressure

The lithostatic pressure is caused by the weight of the overlying rock, including the fluids in the pores. It is also known as the overburden stress (Sv). The lithostatic pressure is dependent on depth and the density of the overburden. It can be expressed by the following equation:

$$S = \rho_b . D \qquad (3.2)$$

where:
S = lithostatic pressure,
ρ_b = bulk density, and
D = vertical depth.

The bulk density is a function of the rock matrix, fluid density and the porosity:

$$\rho_b = \rho m (1-\Phi) + \rho f (\Phi) \qquad (3.3)$$

where:
ρm = density of the rock matrix,
ρf = density of the pore fluid, and
Φ = porosity.

Because sedimentary basins contain a mixture of lithologies that have undergone various degrees of compaction, an average bulk density of 2.31 g/cm^3 is commonly used for a thick sedimentary section. In the majority of sedimentary basins, the overburden typically increases at 1.0 psi/ft below 2 km. At shallow levels, the lithostatic pressure increases more slowly due to higher porosity of the sediments.

3.2.3 Effective stress

Effective stress is the grain-to-grain contact stress. At any given depth, some of the overburden stress (lithostatic pressure) is supported by the pore pressure, and the rest by the contact between the rock particles (effective stress). The relationship between effective stress and overburden stress is given by Terzaghi's equation:

$$\sigma = Sv - p \qquad (3.4)$$

where:
σ = effective stress,
Sv = overburden stress, and
p = pore pressure.

In a basin where the sediments are normally compacted for their depth of burial, the effective stress is likely to be the difference between the lithostatic pressure and the hydrostatic pressure. As effective stress increases, the grain-to-grain contact stress increases and the sediment compacts forcing out fluid. However, in an overpressured section the grain-to-grain contact stress is reduced, and so the overburden is supported less by the matrix of the rock than it would be if the pore pressure were hydrostatic (Fig 3.2).

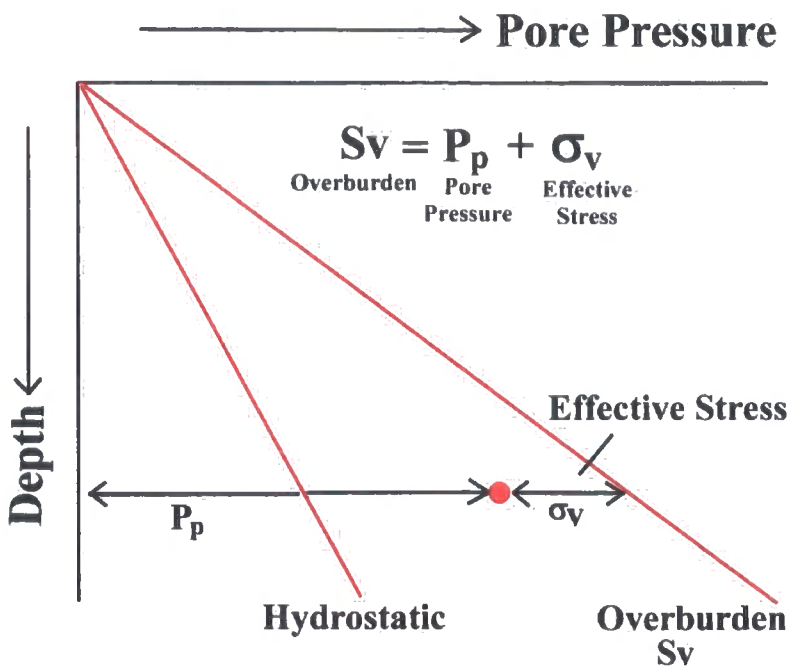

Fig 3.2. Diagram showing the relationship between depth and effective stress based on Terzaghi's equation (equation 3.4).

3.2.4 Formation pressure measurement

Formation pressures can be measured directly during drilling using wireline pressure tools, such as the RFT (repeat formation tester), or by a DST (drill stem test). The formation pressure can only be measured using these tools in permeable formations, and not impermeable layers such as muds, silts, shales, marls and chalk. A permeable layer is needed because the measurements require a flow of pore fluids from the formation.

It is often assumed that mudrocks in the section have pore pressures equal or similar to the reservoir section directly above or below the mudrock interval. In a clastic dominated basin, where mudrock intervals are sparse thin beds within thick coarse clastic units, measuring the pore pressures exclusively in the coarse clastic horizons would give an accurate reading of the basin's pressure profile. However, in a mudstone dominated basin, formation pressure readings in reservoir beds will not always accurately represent the pore pressure of a thick mudstone sequence and so caution needs to be applied.

Other methods of determining the formation pressures include inferring pore pressure from the mud weight that was used during drilling. Also pore pressure prediction methods which utilise the porosity logs (sonic, density, neutron or resistivity) from wireline data, can be used. The use of wireline logs for this purpose is explained in chapter 5.

3.2.5 Overpressure

As mentioned at the start of the chapter, a reservoir is overpressured if its pore pressure exceeds the hydrostatic pressure of a static column of water, or formation brine (Dickinson 1953).

Overpressured sequences in sedimentary basins are not uncommon. Hunt (1990) identified 180 basins worldwide where overpressured sections have been found. Overpressure is especially common in 'young' Tertiary basins, where there is a high sediment influx into the basin, such as the Gulf of Mexico. However, overpressured basins are seen throughout the whole of the Phanerozoic. The concept of overpressure has been known for over 50 years: Dickinson (1953) identified overpressure based on data from the Gulf of Mexico. He suggested that the high pore pressures seen in the clastic sequences were due to the inability of the sediments to dewater fully and reach equilibrium. Dickinson's (1953) concept of overpressure is still valid, but with more emphasis being placed on the question 'why can't the pore fluids de-water?' Swarbrick (2003) came up with a more complete definition:

"Overpressure results from the inability of pore fluids to escape at a rate which allows equilibration with a column of static water connected to the surface."

This definition takes into account that overpressure in sedimentary basins is more dynamic than static, and therefore the pore pressure that is measured, either directly or indirectly, is a function of both the generating mechanism and the dewatering through the formation where the primary control is permeability.

3.2.5.1 Generating mechanisms of overpressure

The question that needs to be answered is: how is overpressured generated? Several mechanisms have been suggested (Table 3.1) as being main causes, or significant causes of overpressure in basins throughout the world.

Various authors have grouped overpressure generation mechanisms into differing categories. Slavin & Smirnova (1998) grouped the mechanisms into synsedimentary processes and post-sedimentary processes. This compares to Lee and Demming (2002), who referred to two processes being responsible for overpressure generation, 'static' and a 'dynamic' process. By static, they meant that overpressure was generated as a result of the presence of pressure seals or barriers, where in the dynamic process overpressure resulted from the imbalance between pressure generation and pressure dissipation. In this scenario, the presence of a perfect seal is not needed. Hall (1993) attributed either internal or external processes to be the cause of overpressure.

For the rest of this sub-chapter, the categories suggested by Swarbrick & Osborne (1998) will be used to explain the different mechanisms. Three categories into which the mechanisms can be grouped were suggested, based on the processes that create them.

1. Stress related mechanisms
    - Disequilibrium compaction
    - Tectonic stress

2. Fluid volume increase as a mechanism
    - Temperature increase
    - Water release due to mineral transformation
    - Hydrocarbon generation
    - Cracking of oil to gas
    - Gas expansion with uplift

3. Fluid movement and buoyancy mechanisms
    - Hydraulic head
    - Osmosis
    - Buoyancy due to density contrasts
    - Lateral transfer

Author	Study Area	Notes
Disequilibrium Compaction		
Dickinson (1953)	Gulf Coast Louisiana	Disequilibrium compaction
Bredehoeft and Hanshaw (1968)	Gulf Coast	Disequilibrium compaction
Burrus, Schneider & Wolf (1994)	North Sea, Norway, Gulf Coast, 7 Mahakam Delta	Disequilibrium compaction
Yardley (1998)	Central Graben, North Sea	Disequilibrium compaction due to rapid Late Tertiary burial
Harold, Swarbrick & Goulty (1999)	Southeast Asia	Disequilibrium Compaction
Swarbrick et al (2000)	Judy Field, Central North Sea	Disequilibrium compaction
Luo et al (2003)	Yinggehai Basin, South China Sea	Disequilibrium compaction
Tectonic Lateral Stress		
Yassir & (Bell 1996)	Beaufort-Mackenzie Basin Canada	Lateral tectonic compression
Henning et al (1998)	Papua New Guinea	Tectonic Compression

Hydrocarbon Generation		
Meissner (1978)	Williston Basin, Montana USA	Kerogen transformation to oil and gas. A 25% increase with oil generation, and a 100% volume increase during dry gas production
Spencer (1987)	Williston Basin, Rocky Mountains, US	Hydrocarbon generation
Ungerer (1993)	Paris Basin, France	50% volume increase – but only at a late stage of maturation (Ro 2.0%)
Hunt et al (1994)	Gulf of Mexico	Oil to gas cracking – Strong coincidence between top of overpressure and peak gas generation
Burrus et al (1993)	Williston Basin, US	Overpressure seen within reservoirs of the mature Bakken shale source rock
Lee and Demming (2000)	Anadarko Basin, Oklahoma, US	Gas generation
Wilson et al (1998)	Piceance Basin, Colorado, US	Gas generation
Clay Diagenesis		
Bruce (1984)	Gulf of Mexico	Smectite to Illite
Lahann (2002)	Gulf Coast U.S	Smectite to Illite
Combination of Mechanisms		
Luo et al (1994)	Delaware Basin, West Texas, US	- Disequilibrium compaction - Hydrocarbon generation - Clay dehydration - Aquathermal expansion

Lee & Williams (2000)	Delaware Baisn West Texas, US	- Disequilibrium compaction - Hydrocarbon generation
Williamson (1995)	Sable Basin, offshore Nova Scotia	- Disequilibrium compaction - Gas generation

Table 4.1. Examples of overpressured basins around the world, indicating the mechanism for generation.

3.2.5.1.1 Stress-Related Mechanisms

When the rate of sediment supply to a basin is low, then the underlying sediments will be able to dewater and compact and hydrostatic pressure equilibrium will be reached. However if the rate of sediment supply increases, the underlying sediments cannot dewater fast enough, so compaction is halted and pore space is preserved with the sediments being overpressured. This process is known as disequilibrium compaction. Young Tertiary deltaic basins on continental margins are typical basinal environments where disequilibrium compaction is the cause of overpressure, due to the rapid rate of sediment input and distal low permeable muds / silts overlying the sequence.

The main controls on overpressure by disequilibrium compaction are sediment input rate, permeability, temperature and the compaction coefficient. These four variables determine the depth at which disequilibrium compaction commences. For example, taking the sedimentation rate as a constant parameter, overpressure is generated at a shallower depth in a basin if the sediment has a lower permeability and / or a more compressible sedimentary sequence. The depth at which pore pressure becomes greater than the hydrostatic is known as the fluid retention depth (FRD).

As mentioned previously, disequilibrium compaction is common in Tertiary basins with high sedimentation rates (e.g. Gulf of Mexico). Authors often dismiss disequilibrium compaction as a mechanism of overpressure generation for old

Palaeozoic basins, as any overpressure generated through burial might be expected to dewater back to hydrostatic over tens to hundreds of millions of years. However, the definition of overpressure by Swarbrick (2003), used at the start of chapter (section 3.2.5), suggests that the overpressure system is dynamic and depends on the rate at which fluids can reach equilibrium. Therefore disequilibrium compaction can still be a mechanism for overpressure generation in Palaeozoic basins if the permeability is low enough to maintain the overpressure. The question of whether disequilibrium compaction is responsible for the overpressure seen in the Palaeozoic Delaware Basin, is dealt with throughout this thesis in the results and discussion chapters.

The other stress related mechanism is tectonic compression. Where thrusting and folding in a basin will apply lateral stresses on the rock unit, as well as the vertical stress resulting from the burial. Examples of where overpressure is found in a compressional regime include the Barbados accretionary prism (Fisher & Zwart 1996), and Papua New Guinea (Henning et al 1998).

3.2.5.1.2 Fluid volume increase as a mechanism

Overpressure can also be created by an increase in the pore fluid volume, which can occur where there is: a) temperature increase (aquathermal expansion), b) mineral transformation, c) hydrocarbon generation and d) oil to gas cracking. The term 'unloading mechanisms' is often used to describe mechanisms by fluid volume increase (Bowers 2002).

Overpressure generated by fluid volume increase, will tend to occur in low permeability rocks, where an increase in the pore fluid volume does not increase porosity, but will decrease the effective stress. The rate of volume change is the controlling factor on the magnitude of overpressure generated.

a) Temperature Increase

An increase in temperature increases the volume occupied by a fixed mass of fluid due to thermal expansion, as water expands when heated above 4°C. However, Osborne & Swarbrick (1997) concluded that the amount of volume expansion due to

aquathermal processes is quite small, with a volume increase of 1.65% for a 40°C rise in temperature at constant pressure. To calculate the rate of expansion, the burial rate and the geothermal gradient are needed. Even with a high burial rate of 2000 m/Myr and a high geothermal gradient of 40 °C/km, Osborne & Swarbrick (1997) calculated that the rate of expansion is no more than 3.30 vol%/Myr.

b) Mineral Transformation

Some mineral transformations generate a volume increase due to water being expelled during a reaction. Common reactions include smectite dehydration and smectite – illite transformation.

When smectite dehydrates, there are three phases of dewatering, with each one causing a 1.3 % increase in volume (Osborne & Swarbrick 1997). The first two pulses occur at shallow depths, and due to high permeability at shallow depths, the increase in volume has little effect on pore pressure (Osborne & Swarbrick 1997). The last pulse happens around 3-5 km, and even with sediment composed entirely of smectite the amount of excess pressure generated would only have a magnitude of 100 psi (0.68 MPa). Therefore smectite dehydration is insignificant for generating the large overpressures that are recorded in basins, and would only be a secondary cause of overpressure generation.

The other mineral transformation is smectite to illite transformation, which tends to occur within the temperature range 70-150 °C. The maximum rate of volume change seen assuming 100% smectite is 0.2 vol%/Myr, producing no more than 112 psi (0.7 MPa) of overpressure (Swarbrick et al 2002). This is therefore an insignificant increase. However, in several mud-dominated basins, there is a general coincidence that at the stratigraphic horizon where overpressure is being recorded, smectite-illite transformation is also occurring.

c) Hydrocarbon Generation

Volume changes occur when kerogen transforms to oil and gas, with maturation typically occurring at depths of around of 2-4 km, and at temperatures in

the range of 70-120 °C. Meissner (1978) studied the Bakken shale type II source rock in the Williston Basin, Montana and North Dakota USA. He found there was a volume increase of 25 % due to oil generation, with a further increase when maturation proceeds to wet gas and later to dry gas (Figure 3.3). In contrast, Ungerer et al (1983) looked at volume increase during the maturation of kerogen, and found that a small decrease in volume is seen from kerogen maturation up to a vitrinite reflectance (Ro) of 1.3 %. However there was a volume increase of 50% during late maturation at Ro 2.0 %. Swarbrick et al (2002) concluded that volume change during oil generation is negligible, but that during gas generation there is a significant increase in volume, as shown by Meissner (1978) and Ungerer (1983).

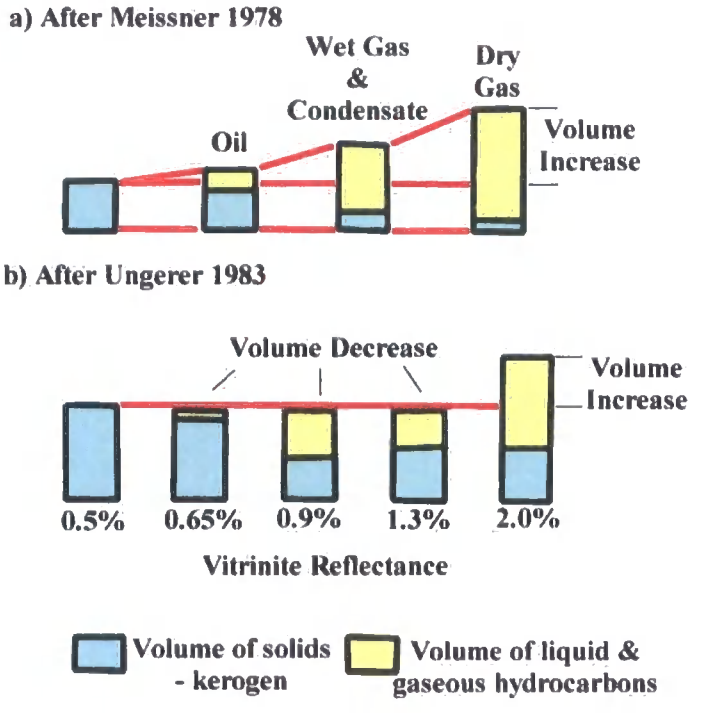

Fig 3.3 Diagram showing the estimation of volume change when Type II kerogen in the Bakken shale Williston Baisn matures to produce oil, then wet gas and condensate, and finally dry gas (Taken from Meissner 1978).

d) <u>Oil to Gas Cracking</u>

At temperatures around 120-140 °C, thermal cracking of hydrocarbons is initiated, with almost complete cracking to gas at around 180 °C (MacKenzie &

Quigley 1988). At standard temperatures and pressures, 1 volume of standard crude oil will crack to 534.3 volumes of gas (Barker 1990); therefore oil to gas cracking has the potential to produce a large pore volume increase in the source rock. Several basins have overpressured intervals in the deep parts of the basin, coinciding with depths where gas is cracking. For example, Hunt et al (1994) observed a strong coincidence between peak gas generation and the top of the overpressured zone in the Gulf of Mexico.

e) Gas expansion with uplift

When gas rises and decreases in temperature, the volume of the gas increases. If the gas is in a well sealed unit, then it is unable to expand because of the incompressibility of the surrounding fluid and consequently the pressure of the gas will increase (Swarbrick & Osborne 1998). The potential for this mechanism to create overpressure in an uplifted basin has not been fully evaluated in the literature and will depend upon the permeability, temperature and the compressibility of the fluids.

3.2.5.1.3 Fluid Movement & Buoyancy

a) Hydraulic Head

Overpressure can result from a hydraulic head in highland areas, where the water table is elevated. In order for this to occur, a seal is needed above the reservoir or aquifer. The magnitude of excess pressure generated by this process would only be negligible (Swarbrick et al 2002).

b) Osmosis

Large salinity contrasts in formation waters can induce a transfer of fluids that can induce overpressuring. Swarbrick & Osborne (1998) looked at osmotic pressure created in a typical North Sea shale, and even with a salinity contrast as high as 35 wt% NaCl, the amount of excess pressure would only amount to 435 psi (3 MPa). Therefore osmosis is not a significant overpressuring mechanism, and would be of more importance on a local scale.

c) Hydrocarbon Buoyancy

In a reservoir, where oil, gas and formation waters co-exist, the oil will lie on top of the formation water, and the gas on top of the oil, due their relative densities. A pressure differentiation will therefore exist in the column due to this density difference. The formation water at the base of the hydrocarbon column will be hydrostatically pressured. The overlying oil will have a lower density than the formation water below and so will have a lower pressure gradient. This will cause pore pressures to be greater than the hydrostatic at any depth in the oil column (Fig 3.4). The magnitude of overpressure is increased further once in the gas column. In order for this mechanism to work, a large hydrocarbon column height is needed, and even then, the excess pressure generated is negligible (Swarbrick et al 2002). For example in the North Sea the maximum overpressure generated by buoyancy is about 600psi (4.13 MPa) (Swarbrick & Osborne 1998).

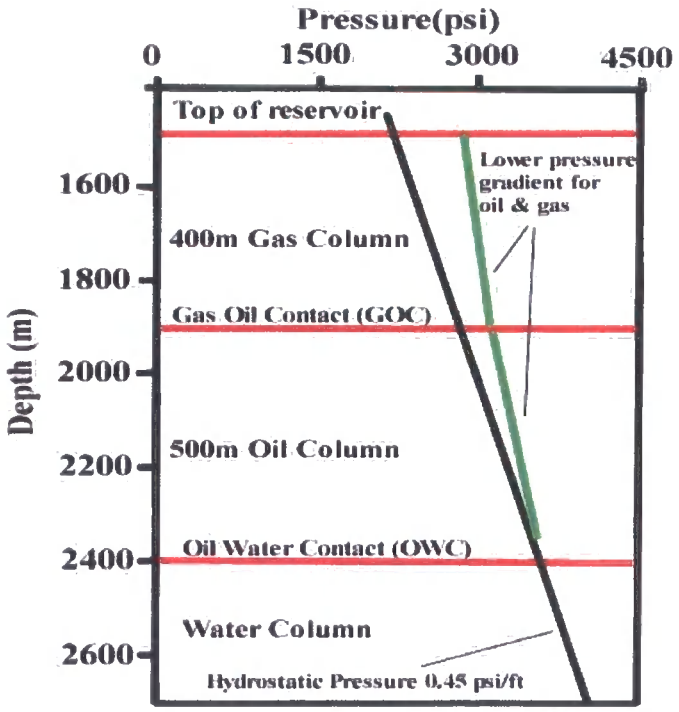

Fig 3.4. Figure showing hydrocarbon buoyancy due to the lower densities of light medium oils and gases relative to water will lead to overpressure (Taken from Swarbrick & Osborne 1998).

d) Lateral transfer

The lateral transfer of fluids from deep overpressured parts of the basin along laterally extensive inclined aquifers will enhance overpressure on the structural high (Yardley & Swarbrick 2000). Pressure differences up to 3000 psi have been recorded in the South Caspian Sea, believed to be a consequence of lateral transfer (Swarbrick 2003). High permeability reservoir units will be the most effective rocks in redistributing excess pore pressure.

3.2.5.2 Summary of overpressure generating mechanisms

In conclusion, the main overpressuring mechanisms that could generate a large magnitude of excess pore pressure are disequilibrium compaction and gas generation from source rock maturation or from oil to gas cracking. The other mechanisms are more likely to be additional contributors to the overpressure system.

Table 3.1 showed that gas generation has been suggested as a major mechanism for generating overpressures in basins throughout the United States, and especially in Palaeozoic Basins (e.g. Meissner 1978; Luo et al 1994; Wilson 1998; Lee & Demming 2000).

3.2.6 Underpressure

Underpressured rocks have been found within various basins around the world, particularly in Canada and the U.S, including West Canada Basin, Alberta (Gies 1984; Davies 1984), San Juan Basin, New Mexico and Colorado (Meissner 1978), and Green River Basin, Wyoming (Davies 1984). In each of the above cases, the basin has been uplifted and contains gas-bearing reservoirs. The following mechanisms can be used to create underpressure Swarbrick and Osborne 1998):

- Differential discharge
- Differential gas flow
- Rock dilatancy

- Osmosis
- Thermal effects

Although it is possible that the Delaware Basin may be experiencing underpressuring, this study has not seen any substantial evidence to suggest this. Therefore no more detail will be given. Further detail concerning underpressure can be found in Swarbrick and Osborne (1998) and Swarbrick et al (2002).

3.3 Overpressure in the Delaware Basin

This study has used over 500 DST data points from over 300 wells (Fig 3.5) throughout the Delaware Basin, in order to obtain a comprehensive pore pressure data set for the basin. The following units within the basin were found to be overpressured:

- Lower Permian Wolfcampian Series
- Pennsylvanian System
    - Cisco Canyon Formation
    - Strawn Formation
    - Atoka Formaiton
    - Morrow Formation
- Mississippian System
    - Mississippian Limestone Formation (Note however that only three wells recorded overpressure in this section, which is considered not enough evidence to suggest it is a main overpressured unit).
- Devonian System
    - Devonian Formation (12 wells have recorded overpressure)

The overlying and underlying units to this overpressured zone are hydrostatically pressured, giving evidence for an isolated zone of overpressure.

The following diagrams (Figs 3.6 to 3.11) are pressure maps displaying the distribution of excess pressure in the basin for each overpressured section (excluding the Mississippian Limestone Formation due to limited pressure data). The maps are

created using 'Oilfield Data Manager' version 3.2.36, developed by PGL Engineering Geoscience. It needs to be noted, that the maps are produced using an 'inverse distance' gridding method, which is a weighted average system. This means that the program will compute the inputted overpressure for each well and create a weighted average between the two wells to create a map. This has a disadvantage where wells become sparse, such as on the edges of the basin. The program extrapolates overpressure values beyond the boundary, because there is no well control saying the overpressure is zero. Therefore it is best to interpret the maps as a qualitative schematic representation of the overpressure distribution, where the data is more reliable with well control.

Key

Overpressure (Psi)			colour code
0.00	yes	———	
500.00	yes	———	
1000.00	yes	———	
1500.00	yes	———	
2000.00	yes	———	
2500.00	yes	———	
3000.00	yes	———	
3500.00	yes	———	
4000.00	yes	———	
4500.00	yes	———	
5000.00	yes	———	
5500.00	yes	———	
6000.00	yes	———	
6500.00	yes	———	
7000.00	yes	———	
7500.00	yes	———	
8000.00	yes	———	
8500.00	yes	———	

The line contours on the maps represent the depth (in feet) to top Ellenburger Formation, to illustrate the basin geometry.

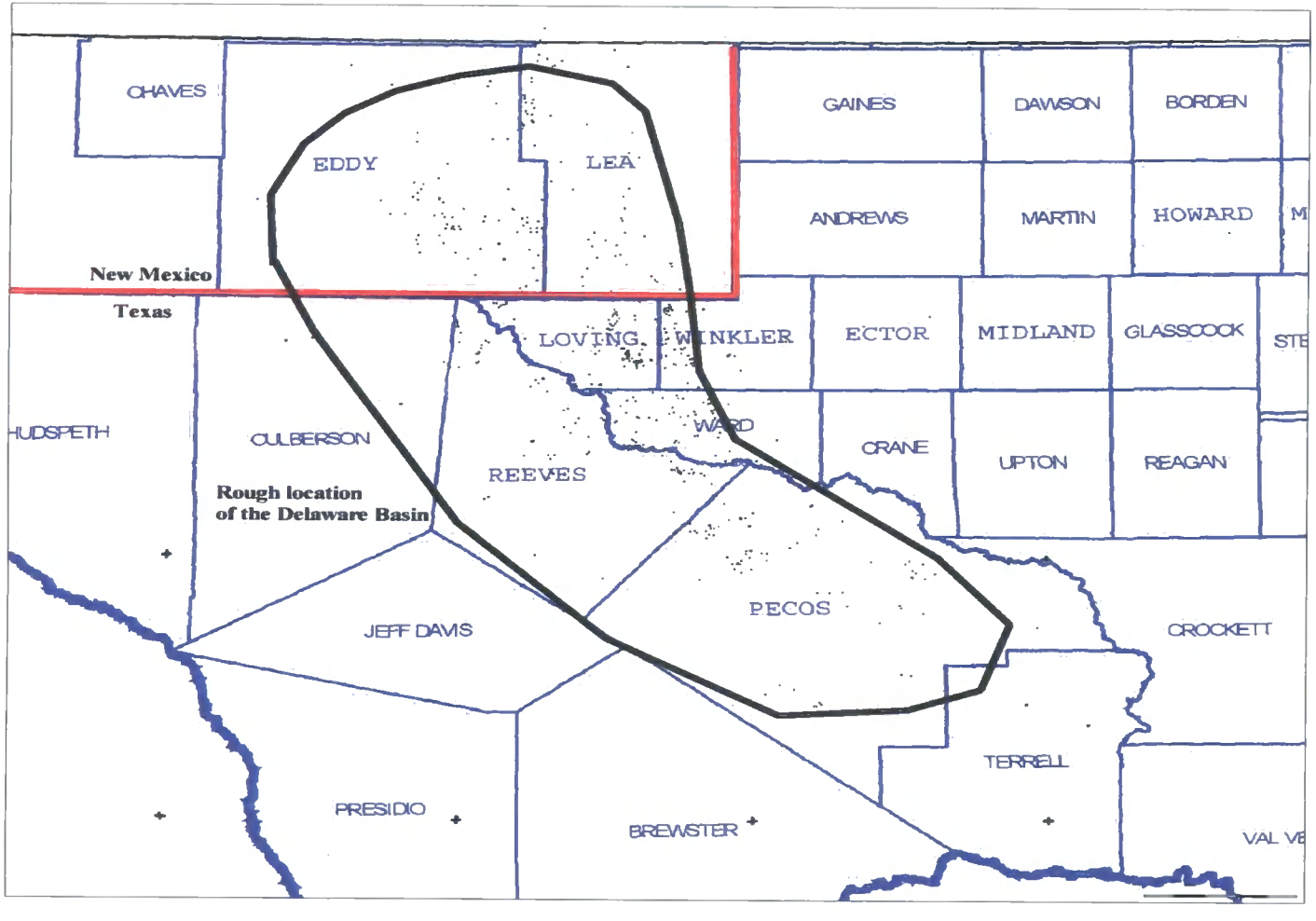

Fig 3.5. Map of west Texas and New Mexico, showing the rough location of the Delaware Basin, counties within the basin, and wells with DST pressure data (each dot on the map represents 1 well)

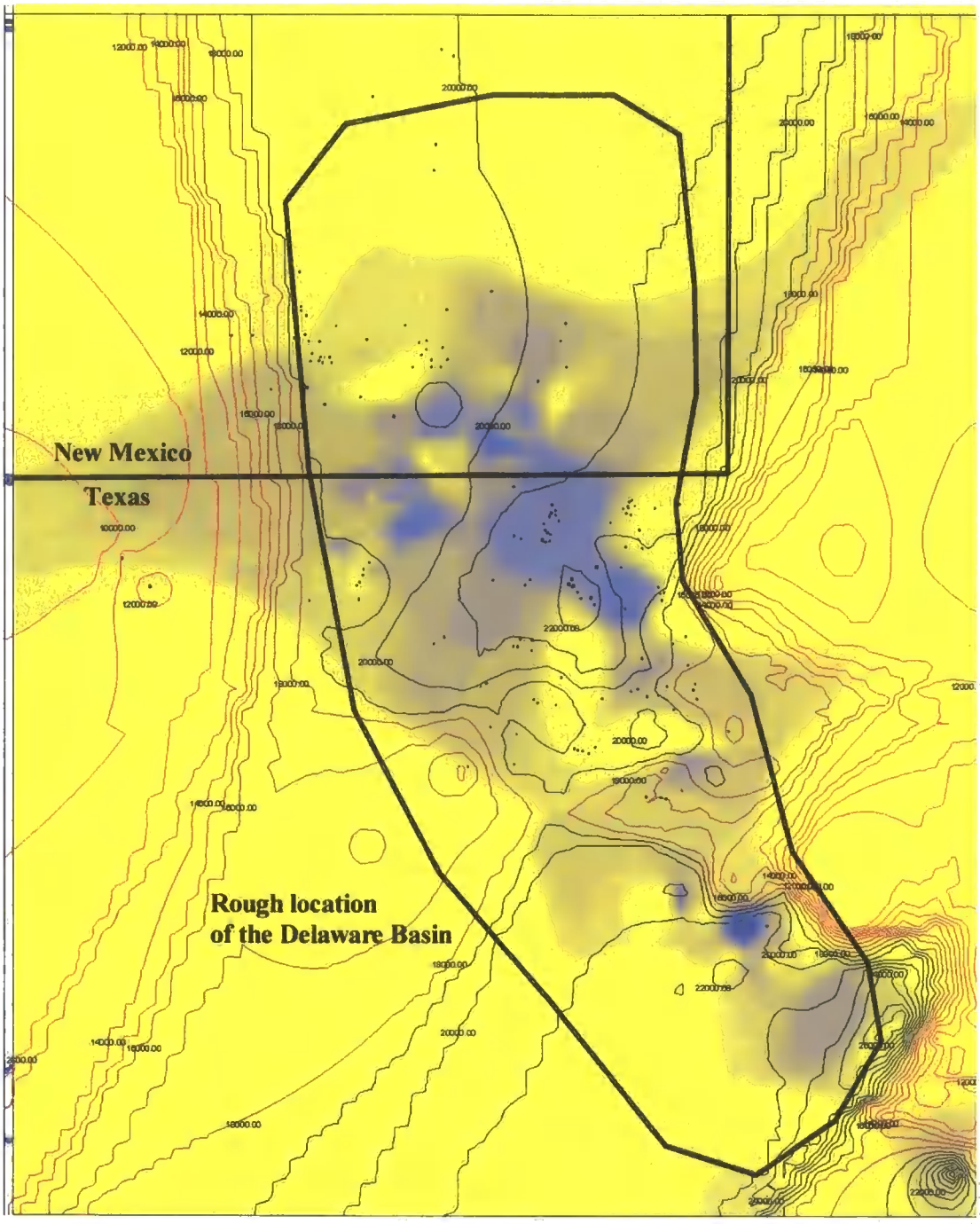

Fig 3.6. Map showing the distribution of excess pore pressures of the Wolfcampian Series in the Delaware Basin.

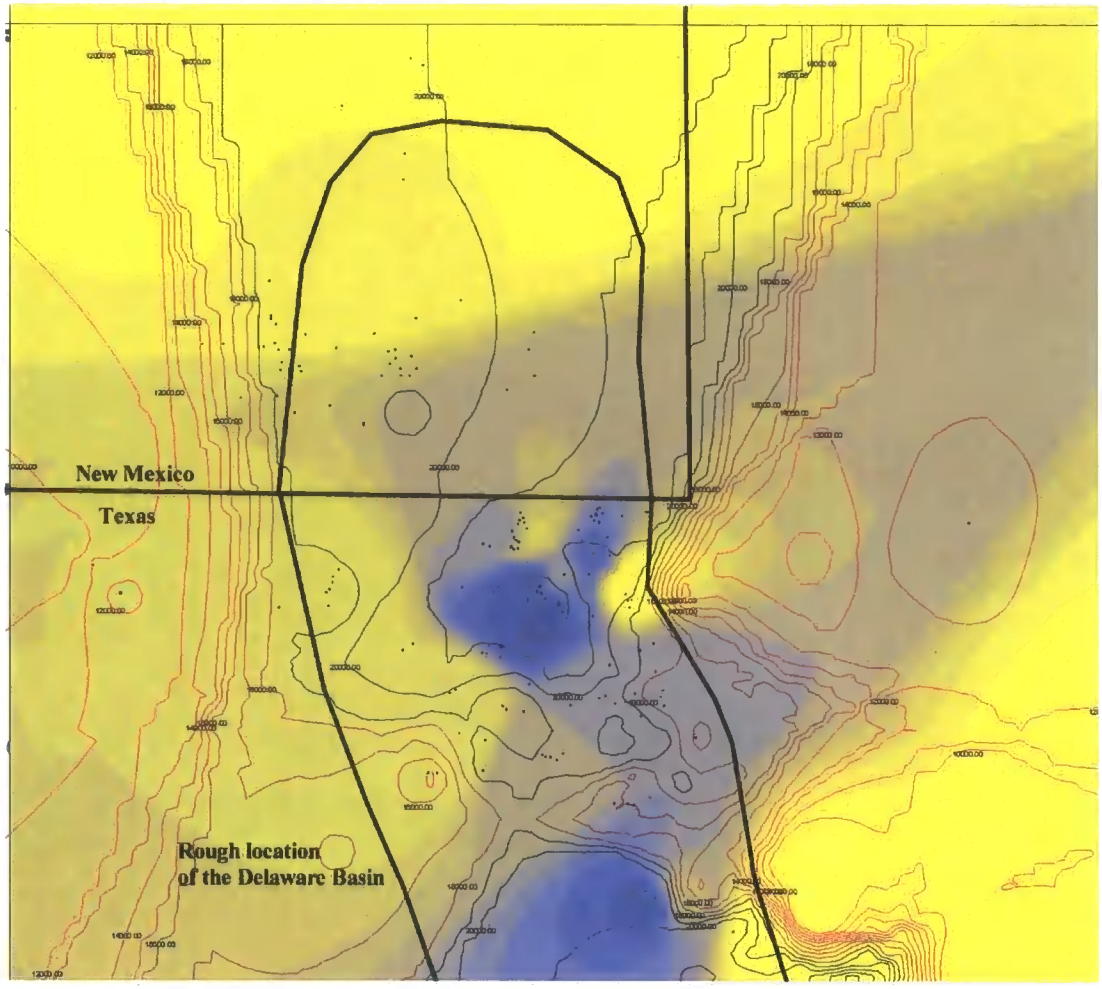

Fig 3.7. Map showing the distribution of excess pore pressures of the Cisco Formation in the Delaware Basin.

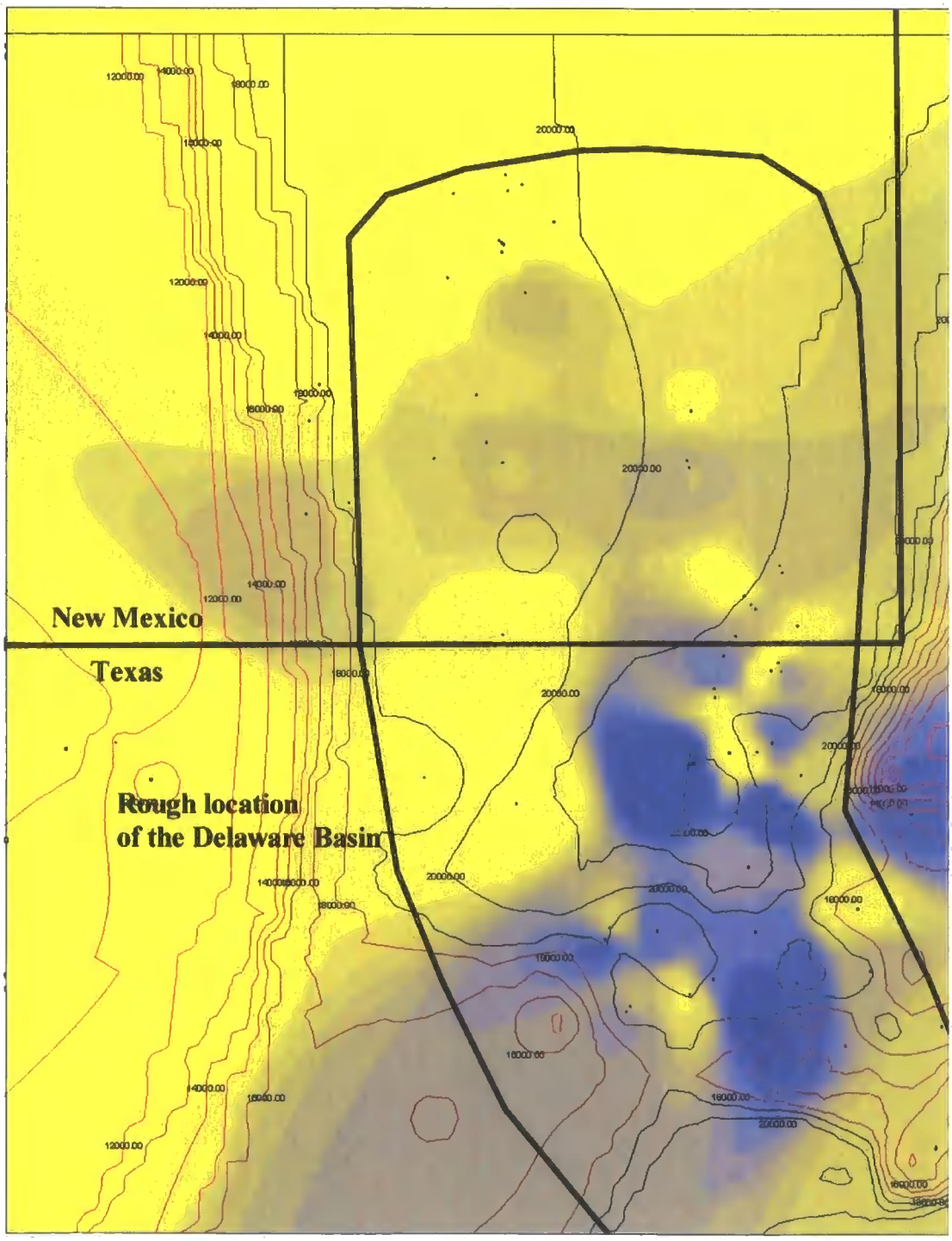

Fig 3.8. Map showing the distribution of excess pore pressures of the Strawn Formation in the Delaware Basin.

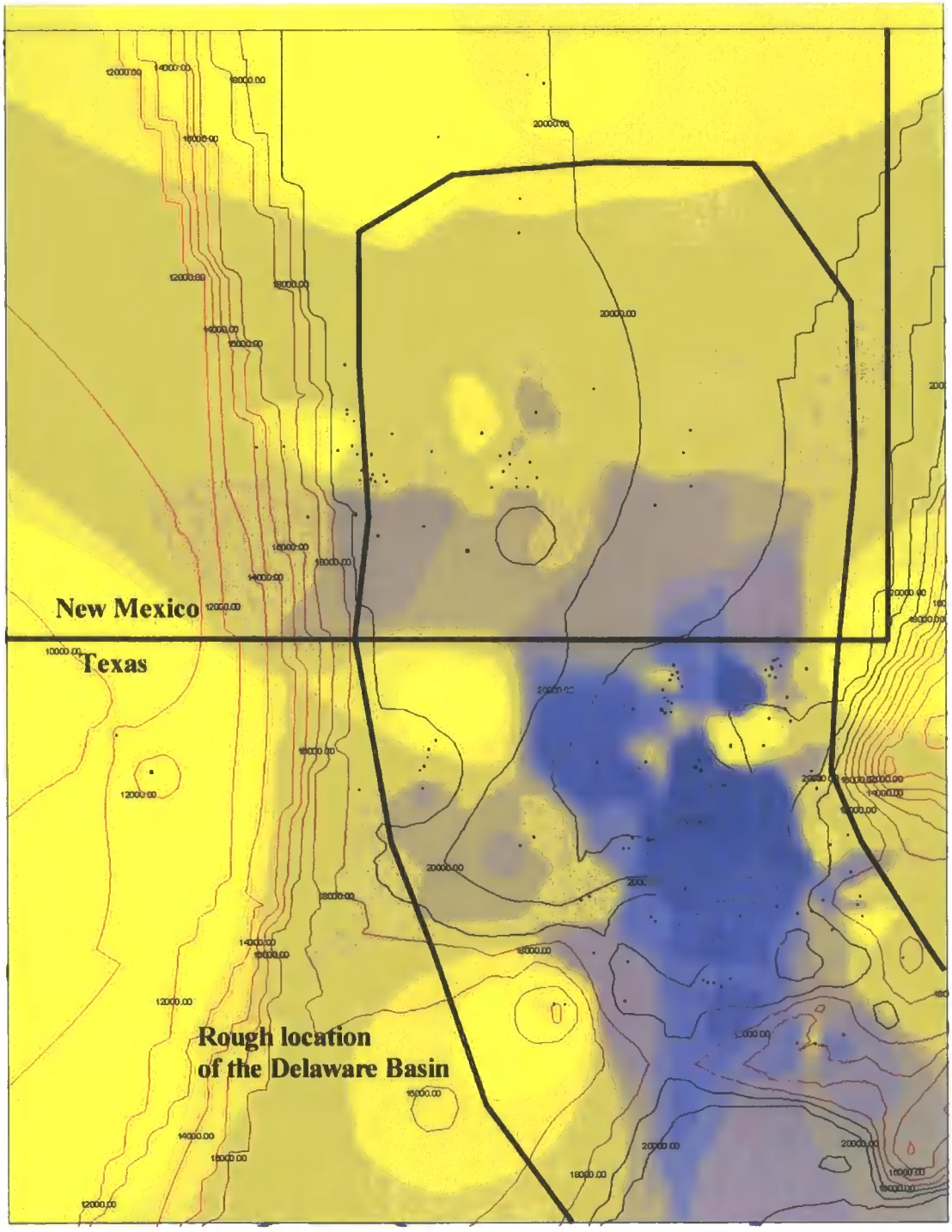

Fig 3.9. Map showing the distribution of excess pore pressures of the Atoka Formation in the Delaware Basin.

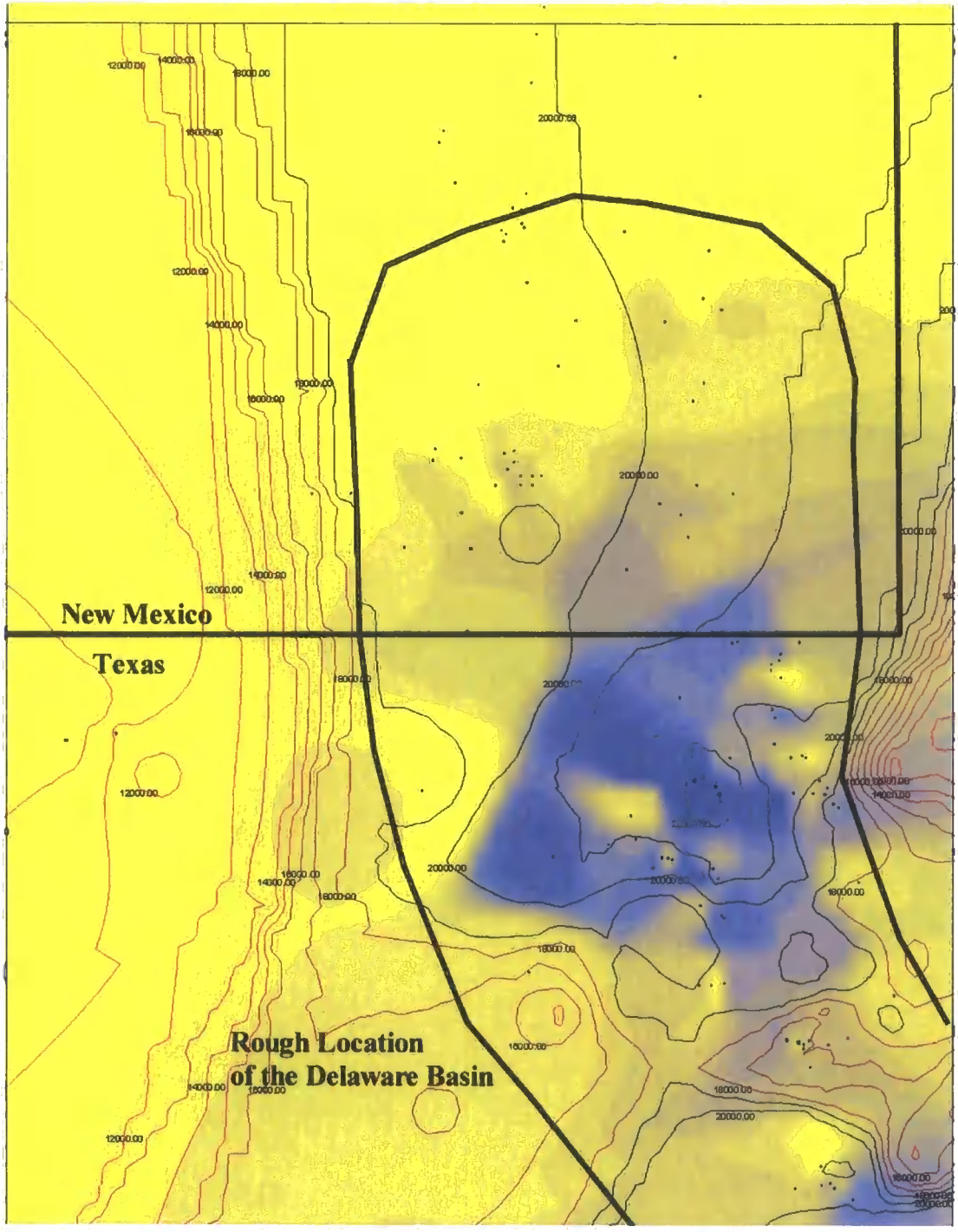

Fig 3.10. Map showing the distribution of excess pore pressures of the Morrow Formation in the Delaware Basin.

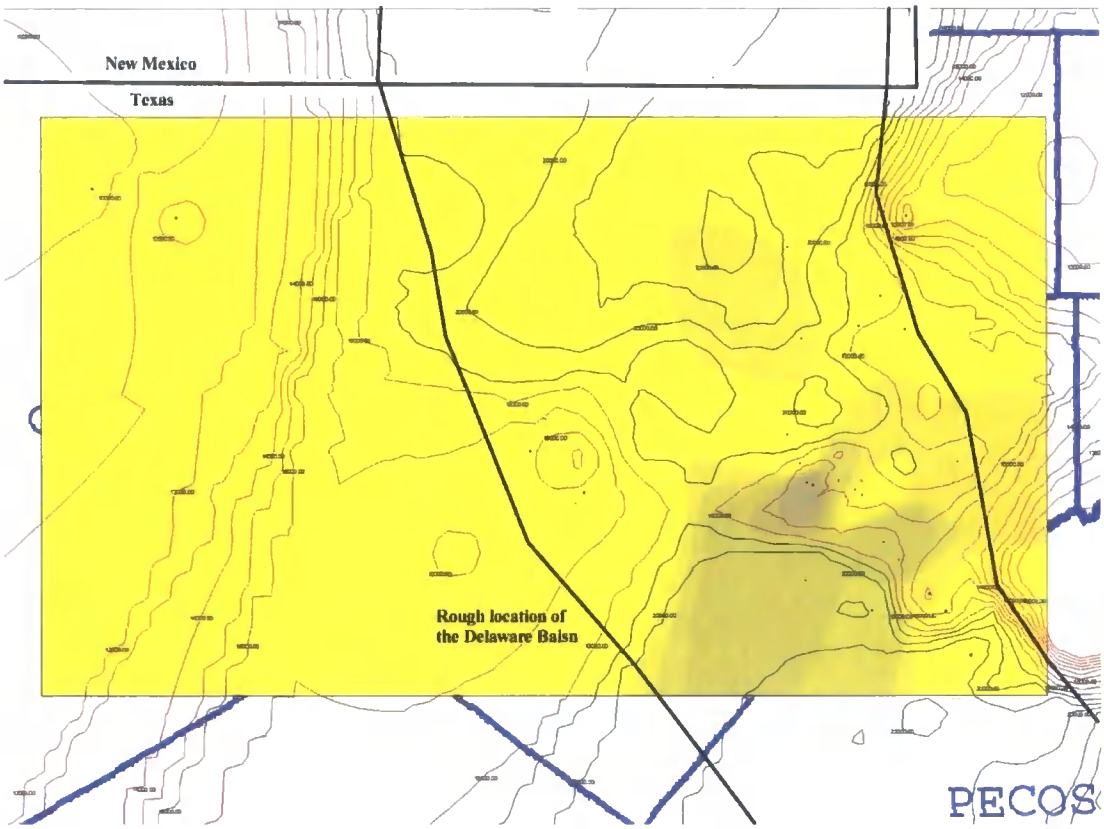

Fig 3.11. Map showing the distribution of excess pore pressures of the Devonian Formation in the Delaware Basin.

3.3.1 Summary of overpressure in the Delaware Basin

The excess pressure maps show that high overpressures are present in the Wolfcampian Series and all formations of the Pennsylvanian System, with pressures reaching up to 7500 psi (51 MPa) above hydrostatic. The overpressure is highest in the centre of the basin around Loving, Ward and East Reeves Counties (Fig 3.5). Also Pecos County has high overpressures, especially within the Wolfcampian Series and the Cisco Formation.

In comparison to the Wolfcampian Series and the Pennsylvanian System, the Devonian Formation does not have the same magnitude of overpressure. Excess pore pressures reach only 2000 psi (14 MPa) above hydrostatic, and is only found in the south of Reeves County and the north of Pecos County.

3.4 Literature review

This section provides a literature review on previous studies of pore pressure in the Delaware Baisn. To date only three papers have been published documenting the overpressure in the basin (Luo et al 1994; Lee & Williams 2000; Hansom & Lee 2005). A literature review is also given for the Anadarko Basin in Oklahoma US. It is an overpressured Palaeozoic basin, which can be use as an analogue to this study of the Delaware Basin.

3.4.1 Luo et al (1994)

In his research paper, "Distribution and Generation of the Overpressure System, Eastern Delaware Basin, Western Texas and Southern New Mexico", Luo et al (1994) used the initial hydrostatic or the final hydrostatic readings from DST data to compile pressure profiles for the Delaware Basin (Fig 3.12), whereas in this study the initial shut-in pressures from DST data were used to compile the pressure plots. By using the initial hydrostatic or final hydrostatic pressure, Luo et al (1994) are overestimating the overpressure in the basin, whereas the initial shut-in values will provide a more accurate representation of the pressure. This potential variation is seen in the results: Luo et al (1994) state overpressures up to 8800 psi (60 MPa) are recorded in the basin, whereas this study has found 8000 psi (55 MPa) of excess pore pressure to be the maximum recorded.

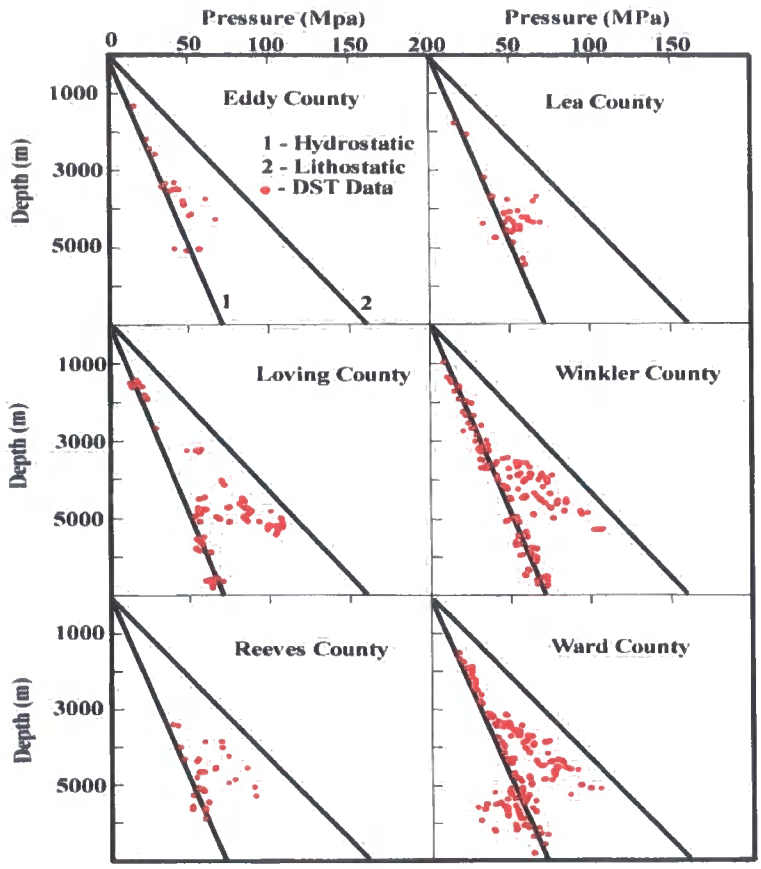

Fig 3.12. Plot of pressure vs. depth for six counties in the Delaware Basin. After Luo et al (1994).

Luo et al (1994) stated that three pressure regimes exist in the basin covering six counties in the states of New Mexico and Texas (Fig 3.12). An upper normally pressured section was recognised which coincided with clastics and evaporates of the Permian sequence. An overpressured middle section comprising the shales of the Mississippian, Pennsylvanian and the Early Permian Wolfcampian formation is recognised from 10,000 ft (3 km) to 17,400 ft (5.3 km). Then a lower normally pressured section consisting mainly of the basal Ordovician and Silurian carbonates is present. These findings by Luo et al (1994) are similar to the findings of this study; although this study suggests that overpressure is seen further south in the basin in the Pecos County, and there is little evidence that the Mississippian System is heavily overpressured (albeit three wells recorded overpressure in the Mississippian Formation). However, this research has also shown that the Devonian Formation is

overpressured in the south of the basin, but not to such a magnitude as the Wolfcampian Series or the Pennsylvanian System.

Luo et al (1994) suggested that the overpressured section is compartmentalised, with pressure seals on top of and below the overpressured compartment. They described the top of the compartment as being generally flat and coincident with the top of the Wolfcampian sequence. The base of the compartment varied, with the topography varying between 10,000 ft (3 km), in the East of the basin, up to 17,400 ft (5.3 km) in Loving County. This base may coincide with the Mississippian or the Woodford Formation but there was not enough evidence for Luo et al (1994) to make a definite match. The idea that the pressure compartment has a flat top is in agreement with Hunt's (1990) view on pressure compartments. Luo et al (1994) also stated that the greatest overpressures coincided with the depocentre of the Delaware Basin, as this is where the highest sedimentation rate had taken place, where the thickest section of low permeability sediments was deposited and where the maximum preservation of organic material would be. According to Luo et al (1994), the depocentre is found in Loving County. Some of the excess pressures recorded almost reached the lithostatic pressure gradient and a lot of the pore pressures would have caused lithologies to reach their fracture point, which is 0.64psi/ft (Hubbert & Willis 1957).

The suggestion by Luo et al (1994), that the overpressured section is isolated, and compartmentalised is in agreement to this study's initial analysis of the overpressure. A more detailed analysis concerning compartmentalisation will be dealt with in chapter 7 of this thesis.

Luo et al (1994) stated that the overpressures seen in the Delaware Basin could be attributed to four mechanisms: disequilibrium compaction, clay dehydration, hydrocarbon generation and aquathermal pressuring.

Disequilibrium Compaction

Luo et al (1994) stated that disequilibrium compaction can only have generated excess pore pressure in the Wolfcampian formation, as the sedimentation rate was as high as 300 ft/Myr. The excess pressures recorded in the Mississippian

and the Pennsylvanian cannot be attributed to disequilibrium compaction, as the sedimentation rate was no more than 100 ft/Myr.

Clay Mineral Dehydration

The transformation of smectite to illite may have occurred in the Delaware Basin because, according to Luo et al (1994), the shales of the overpressured section were all in the correct temperature window for the reaction to take place

Hydrocarbon Generation

The Delaware Basin has five main source rocks: the Upper Devonian Woodford black shales, the Upper Mississippian Barnett black shales, the Pennsylvanian black shales, the Lower Permian Wolfcampian shale and the Lower Bone Spring shales (Luo et al 1994). Based on the observations that four of these shales fall within the overpressured section and that, at present day the Wolfcampian Series is in the oil window and the Pennsylvanian, Barnett and Woodford source rocks are in the gas window, Luo et al (1994) concluded that hydrocarbon generation may contribute to overpressure generation within the basin.

Aquathermal Expansion

Luo et al (1994) also stated that because the overpressured zone is isolated, the pore fluids cannot dissipate, and so any rise in temperature would have caused the pore fluids to expand and hence generate overpressure.

3.4.2 Lee & Williams (2000) and Hansom & Lee (2005)

Lee & Williams (2000) and Hansom & Lee (2005), from the same research group, published papers that dealt with the modelling of overpressure in the Delaware Basin. The models were based on the burial history scenario suggested by Luo et al (1994).

The results show that excess pressure was generated by a combination of disequilibrium compaction and hydrocarbon generation. Their modelling also shows

that to preserve the overpressure, a top seal with a permeability of 10^{-11} mD is needed, suggesting that most mudstones are too permeable. Modelling also indicates that oil generation in the Wolfcampian reached its peak about 240 Ma, so therefore argues against Luo et al (1994) who suggested that oil generation in the Wolfcampian at the present day may contribute to the overpressure. However, Lee & Williams (2000) do state that their modelling shows that the Wolfcampian is currently generating natural gas; therefore gas generation could be a mechanism.

3.4.3 Anadarko Basin

The Anadarko Basin is considered to be one of the deepest foreland Palaeozoic Basins on the North American craton. It has a very similar geological history to that of the Delaware Basin (Chapter 2). Deposition began in the Cambrian, with rapid subsidence and deposition occurring from the Late Mississippian through to the Pennsylvanian, with up to 15000 ft (4.5 km) of sediment being deposited. In contrast to the Delaware Basin, the Permian sequence is not as thick (~3000 ft or 1km). The total sediment thickness in the deep basin exceeds 39,000 ft (12 km), and consists of sandstones, limestones and shales. It is a prolific hydrocarbon producer with over 50 major fields and hundreds of minor ones (Lee & Demming 2002). The major source rocks include shales of the Ordovician, Devonian-Mississippian and Pennsylvanian.

The overpressure system found in the basin is within a completely sealed overpressured compartment known as the megacompartment complex (MCC) (Fig 3.13). The top of the MCC is located between 7500 ft (2.2 km) and 10,000 ft (3 km), coinciding with the Upper Pennsylvanian. The bottom of the MCC coincides with the Woodford shale, at varying depth throughout the basin. Pressures have been recorded up to 7000 psi (48 MPa) in excess of the hydrostatic in the Morrow Formation of the Early Pennsylvanian (Al-Shaieb et al 1994).

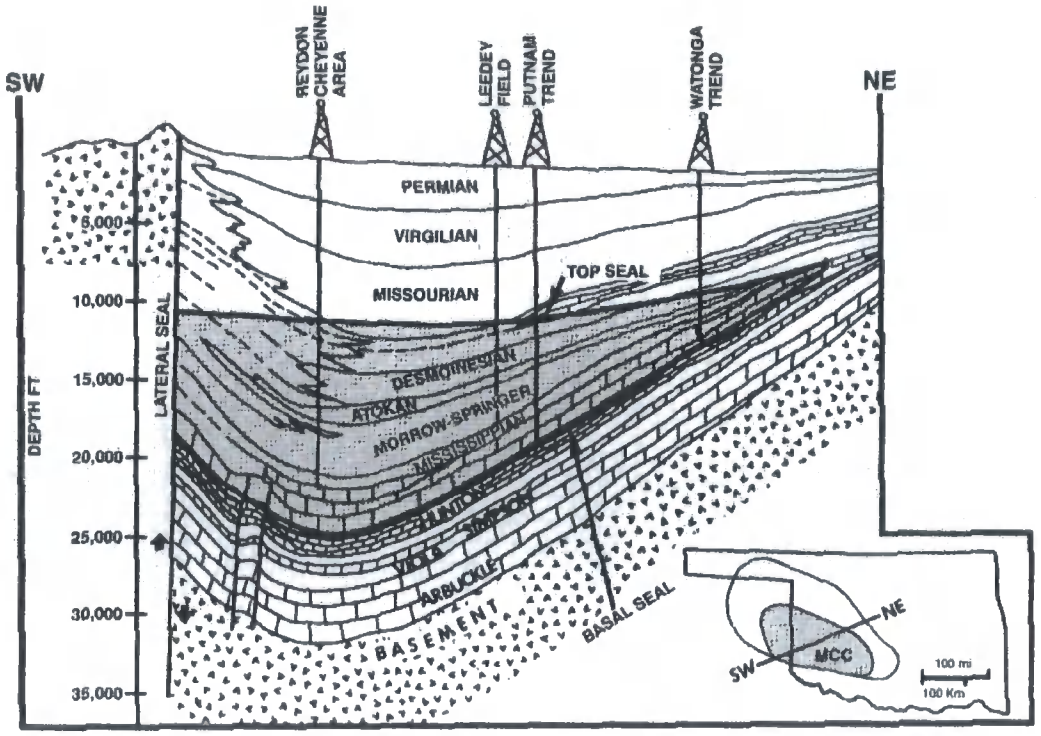

Fig 3.13. Anadarko Basin – showing the extent of the MCC (Al-Shaieb et al 1994).

Lee & Demming (2002) considered the two end members of disequilibrium compaction and hydrocarbon generation as potential mechanisms for the cause of the overpressure in the basin. Rapid burial of Palaeozoic sediment occurred 250-300 Ma. Therefore if overpressure was generated through disequilibrium compaction, then extremely low permeabilities are needed. Lee & Demming (2002) worked out that permeabilities on the order of 10^{-12} mD are needed to maintain the excess pressure. To put this into perspective, the lowest permeabilities ever recorded for sedimentary rocks are only of the order $10^{-7} - 10^{-8}$ mD (Swarbrick 2003).

Lee & Demming (2002) also looked at whether hydrocarbon generation could be a suitable mechanism for overpressure generation. In modelling this as a potential mechanism, the most critical variables are temperature and permeability. The present day geothermal gradient in the Anadarko Basin is around 21 °C/km, whereas the palaeo-geothermal gradient may have been up to 25 °C/km. Also the Anadarko Basin has undergone uplift and cooling, with anywhere between 1 km and 3 km of

denudation. Therefore Lee & Demming (2002) modelled two end member scenarios, a cold and a hot history. The cold thermal history assumes that the thermal gradient remained constant at 21 °C/km and there was only 1 km of Mesozoic sedimentation and subsequent erosion. If this was the case, then an average basin permeability of 10^{-6} mD is needed to explain the overpressuring. Also at depths between 14700 ft – 21300 ft (4.5–6.5 km), the Pennsylvanian shales would presently be producing hydrocarbons, which corresponds to the maximum overpressures seen today. The hot model assumes a geothermal gradient that cooled from 25 to 21°C/km, with 3 km of Mesozoic sedimentation and Tertiary erosion. In this scenario, a lower permeability of 10^{-8} mD is needed to contain the high pore fluid pressures caused by hydrocarbon generation.

In conclusion Lee & Demming (2002) stated that for disequilibrium compaction to be the main mechanism for overpressure generation in the Anadarko Basin, then permeabilities 1-2 orders of magnitude lower are required compared to scenarios where gas generation was the main mechanism. Although they state that if gas generation was the mechanism behind the excess pore pressure, then thin layers of zero permeability within the MCC are still needed to explain the excess pore pressures seen today. Therefore gas capillary seals could exist in the basin where formations consist of alternating layers of coarse and fine-grained sediment and capillary forces prevent gas from being expelled from the coarse-grained rock into the fine-grained lithology (Revil et al 1998).

Al-Shaieb et al (2002) believe that there is a hierarchy of pressure seals within the MCC, where first order seals separate the MCC, then second order seals separate stratigraphic intervals, and third order seals separate individual compartments. Fluid inclusion analysis of the seals enabled Al-Shaieb et al (2002) to get an insight into their genesis and burial history. The seals evolved with burial and confined the overpressures, which were caused by hydrocarbon generation and thermal expansion. Then once the seals were in place, overpressure increased further due to the generation of gas. These seals would have had a high sealing capacity and were able to confine the excess pressures through geological time.

Cranganu (2004) concluded that the origin of the overpressure in the Anadarko Basin was not due to a classic common cause such as disequilibrium

compaction or gas generation, but the capillary sealing mechanism itself. The movement of gas molecules from coarse-grained sediments into fine-grained rocks creates the capillary seal and the actual movement of the gas creates a capillary pressure drop across the gas-water interface. This pressure change could be enough to account for the magnitude of overpressure seen in the basin.

The general consensus concerning the overpressure in the Anadarko Basin is that, regardless of what the generating mechanism was, a super seal of near zero permeability is needed to maintain the excess pore pressure. Also the idea of disequilibrium compaction is dismissed as a potential generating mechanism, while gas generation is deemed the likely cause.

3.5 Conclusions

Overpressure (up to 8500 psi or 58.6 MPa above hydrostatic) is seen in the Delaware Basin, where it is isolated in the Early Permian Wolfcampian Series, the Pennsylvanian System and the Devonian Formation. The overlying and underlying units are hydrostatically pressured.

This study of overpressure in the Delaware Basin will use numerous basin analysis techniques to understand the pore pressure history of the basin with regard its generation and its maintenance. The results will be discussed in detail and integrated with the results of previously published papers in the discussions chapter (chapter 7).

Chapter 4:

Mesozoic and Cenozoic Tectonic History of the Delaware Basin

4.1 Introduction: Mesozoic and Cenozoic Tectonic Events of the Delaware Basin

The Earth's surface is continuously reshaped by the interaction of tectonic and surface processes. Where tectonic forces are acting on the lithosphere, it can lead to downward vertical motions or subsidence, the resulting depressions are usually filled with sediments that contain a record of these vertical motions over geological timescales. However, in actively uplifting regions, the surface response will mostly be erosional and contain no direct sedimentological record of past vertical motions. In such systems, thermochronology provides a useful technique to reconstruct the basinal history and vertical movements of the basin sediments (Braun *et al.* 2006). However, it should be stated that the sedimentological record is non-linear and is dependent upon many parameters that need to be understood in order to interpret thermochronological data meaningfully. These will be explored later in the chapter when the techniques used in this study are described.

This chapter provides the first detailed thermochronological study of the Delaware Basin during the Mesozoic and Cenozoic. The thermochronological data is treated in a rigorous and quantitative manner, to extract the data pertaining to the depositional and uplift history of the Delaware Basin. Such histories are of considerable importance for understanding the generation and maintenance of excessive pore pressures in the basin.

4.1.1 The Mesozoic: Subsidence and sediment fill

The area of uncertainty that surrounds the Mesozoic are the questions of how much deposition actually occurred during this time, and when during the Mesozoic was the basin at maximum burial?

As previously mentioned in chapter 2, the Delaware Basin was an area of positive relief in a stable platform setting during the Mesozoic, with little deposition. However, Triassic and Lower Cretaceous sediments of 500 ft (150 m) and 1250 ft

(381 m) thickness respectively, are found within the basin, and although the distribution is sporadic, it is accepted that these sediments once continuously covered the whole basin (Hills 1984). Numerous authors (Hills 1984; Horak 1985; Barker & Pawlewicz 1987; Frenzel *et al* 1988; Hill 1996) believe that this thickness of preserved Mesozoic sediments represents the total amount of deposition that occurred during the Mesozoic. This leads to burial history curves (Fig 4.1) similar to the one published by Luo et al (1994) being used in research papers associated with the Delaware Basin, where little to no deposition is associated with the Mesozoic. Previously Friedman *et al* (1986) had speculated that some 2000 ft (600 m) of sediments were deposited during the Cretaceous, which would have been an extra 750 ft (230 m) of sediment on top of what is preserved at present day.

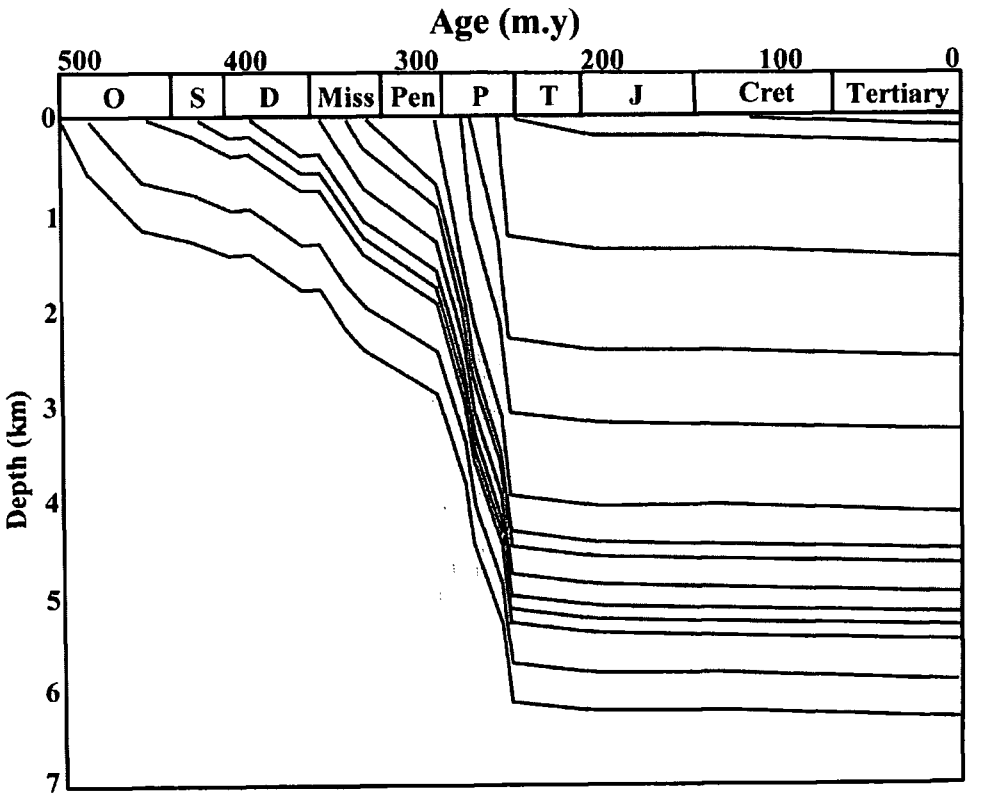

Fig 4.1. Burial history curve for the Delaware Basin as suggested by Luo et al (1994) and used by Lee and Williams (2000). The Mesozoic and Cenozoic burial history is interpreted solely from preserved strata in the basin.

There is a considerable degree of uncertainty regarding the deposition and burial histories during the Mesozoic, especially concerning the Jurassic and Late Cretaceous. There are two prominent hiatuses evident in the Mesozoic succession, at top Triassic and top Lower Cretaceous, with a complete absence of Jurassic and Upper Cretaceous strata. Hills (1984) has speculated that these may have been erosional hiatuses, indicating that Jurassic and Upper Cretaceous sediments were once deposited and since been eroded.

This chapter reports the use of apatite fission track analysis, vitrinite reflectance analysis and shale compaction curves to demonstrate for the first time that previous studies have grossly underestimated the thickness of sediment that was deposited in the basin since the end of the Triassic.

4.1.2 The Cenozoic: Uplift and erosion

Two major tectonic events affected the Delaware Basin during the Cenozoic: the Laramide Orogeny (80-40 Ma) and the Basin and Range extension with associated uplift (30-0 Ma). It can be assumed that both of these tectonic events had substantial effects upon sedimentation in the basin but perhaps the more important question to be asked is: how much uplift occurred and over what timescale?

Stratigraphic units within the basin all dip to the east, due to tilt and subsequent uplift of the western edge, causing Permian strata to be exposed in the west. The tilt has caused post-Wolfcampian beds on the western edge to be 7500 ft (2.2 km) higher up than their lateral equivalent in the depocentre of the basin. The tilt can be seen in both cross-section and outcrop (Figs 4.2 and 4.3).

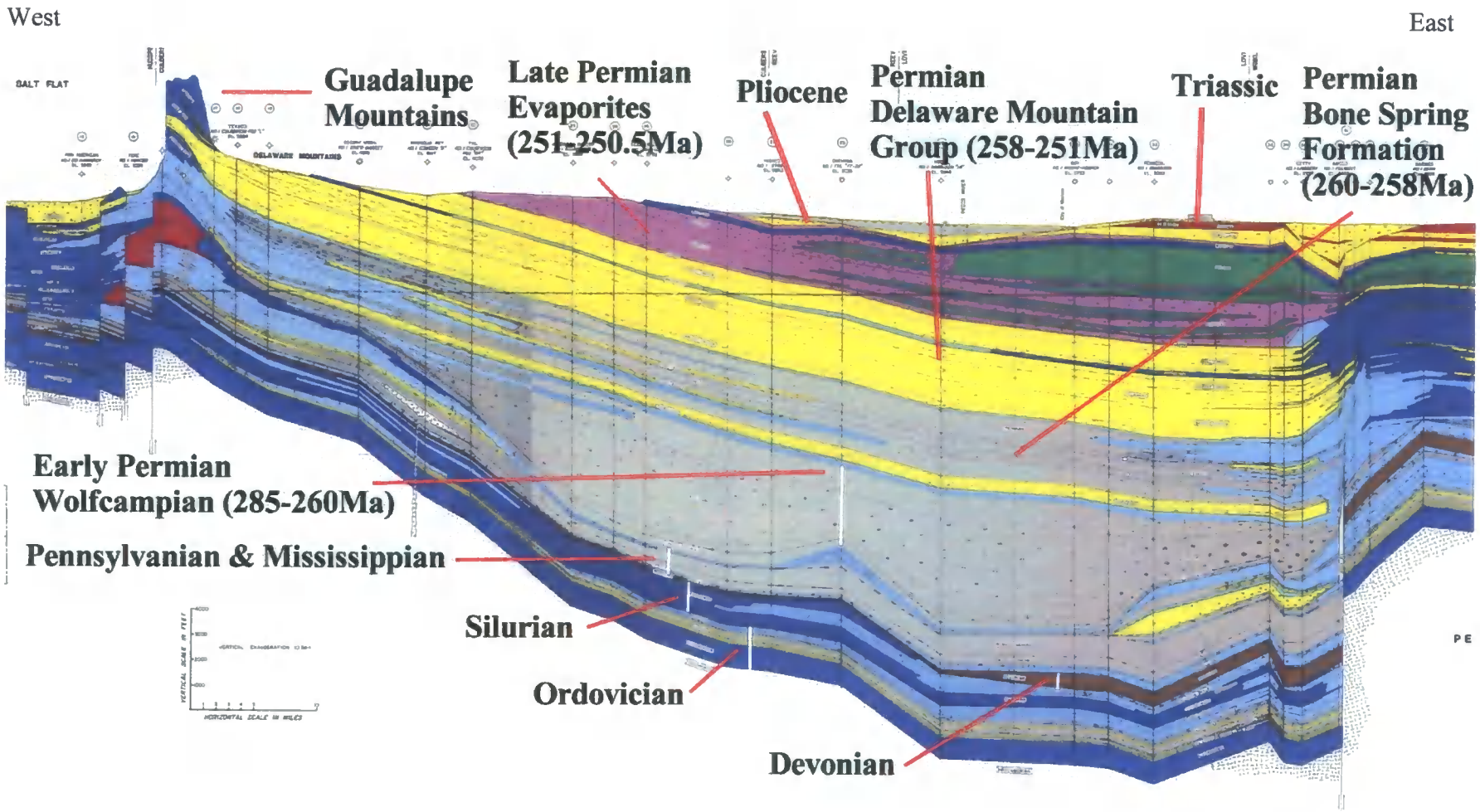

Fig 4.2. Cross-section trending east-west through the Delaware Basin. The basin is tilted to the east exposing the Permian Delaware Mountain Group, and Late Permian evaporites. Preserved Triassic is only seen at the far east of the basin. (Taken from the West Texas Geological Society Publication 84-79).

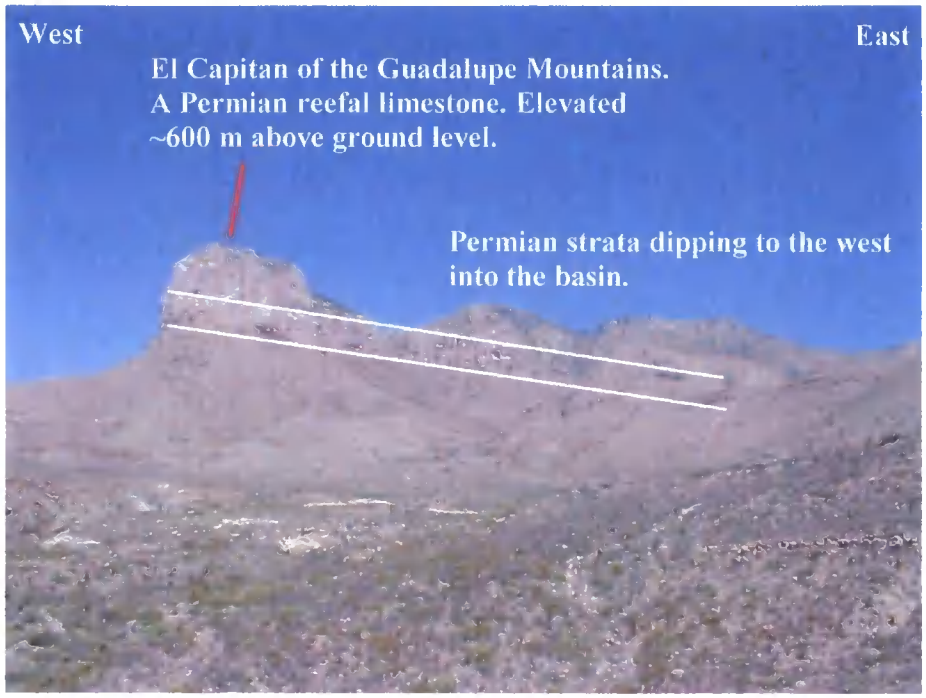

Fig 4.3. Looking north from the western edge of the Delaware Basin. The exposure of the Guadalupe Mountains is seen where the easterly tilt of the strata into the basin is clearly noticeable.

Hills (1984), Horak (1985), Barker & Pawlewicz (1987), Frenzel *et al* (1988) and Hill (1996) document that the tilting of the basin stratigraphy is a direct result of the two-stage basin uplift. However, there is considerable uncertainty as to which event contributed to the tilting the basin, or whether it was actually a consequence of both. It is summed up by Hill (1996) who has compiled the most detailed study of the basin to date:

"A problem which has rarely been discussed but which has important consequences is: how much uplift of the Delaware Basin occurred during the Laramide orogeny (first event 80-40 Ma) versus how much occurred during the Basin and Range (second event 30-0 Ma)?"

Gregory & Chase (1992) and Hill (1996) believe that all the tilt and subsequent uplift of the western edge is attributable to the Laramide compression, whereas Horak (1985) and Barker & Pawlewicz (1987) suggest that half of the 7500

ft (2.2 km) of overall flank uplift is due to Laramide compression and half is due to the Basin and Range event. At the other extreme, Elston (1984) and Sahagian (1987) suggested that isostatic uplift associated with the Basin and Range extension could be as much as 6500 ft (2 km).

Despite several researchers recognising that the Laramide orogeny and / or the Basin and Range event resulted in the uplift of the western edge of the basin, there has been no detailed study to suggest whether these uplift phases may have also affected the whole of the basin, let alone quantify the amount of Cenozoic uplift that may have taken place. A burial history curve (Fig 4.4) used by Barker and Pawlewicz (1987) representing the deep portion of the eastern Delaware Basin shows up to 3000 ft (900 m) of Cenozoic uplift, suggesting that these two tectonic phases did affect the rest of the basin and not jut the western flank. However, in the text they make no reference to this, and comment that the eastern portion has remained relatively stable since the Permian.

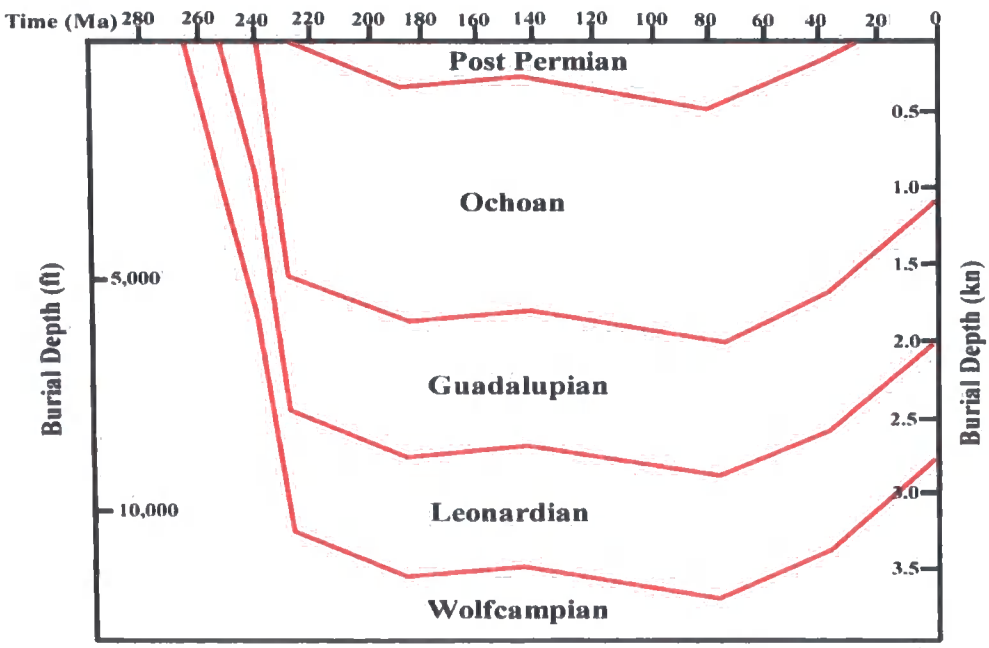

Fig 4.4. Burial history plot of the eastern Delaware Basin according to Barker & Pawlewicz (1987). It shows that during the Cenozoic the basin experienced around 3000ft (900m) of uplift (Taken from Barker and Pawlewicz 1987).

It highlights the uncertainty surrounding the uplift history of the basin, when two widely cited papers (Barker & Pawlewicz 1987; Luo et al 1994) document burial history curves that differ dramatically, with the former suggesting 3000 ft (900 m) of uplift and the later zero.

4.1.3 Aims: Tectonic controls on excess pore pressure in the Delaware Basin

The lack of quantitative data documenting the timing of burial and subsequent uplift of the Delaware basin is addressed through thermochrology and shale compaction curves, permitting the extraction of information about the thermal history of the sediments. This allows a new burial history curve to be assigned documenting the timing of key events in the basin history.

A revised burial history has fundamental implications for the study of overpressure in the Delaware Basin, because burial and temperature are key factors in the mechanisms that generate overpressure. It is also believed that uplift can cause a reduction in pore pressure. Hunt (1990) suggested that when a sedimentary system is uplifted and eroded, the rocks cool and the greater shrinkage of the pore fluids reduces the pore pressure. Neuzil & Pollock (1983) also suggested that when uplift occurs fine-grained siliciclastics will experience elastic rebound, where pore space increases, leading to a decrease in pore pressure. Therefore, having an accurate burial history will provide a better constraint on how pressure is generated, and how it has remained in the basin.

The results from this chapter also have implications for previous published results concerning pore pressure in the basin (Luo et al 1994; Lee & Williams 2000; Hansom & Lee 2005). Luo et al (1994) made assumptions about temperature and burial of sediments in the basin based on a very basic burial history curve (Fig 4.1) that suggested little Mesozoic deposition and no Cenozoic uplift. Therefore, a revised burial history must seriously compromise their results. A more detailed critical appraisal of these research papers will be dealt with in the discussions (Chapter 7).

4.2 Burial history of the Delaware Basin

To test the hypothesis that the Delaware Basin underwent greater burial in the Mesozoic greater uplift in the Cenozoic than have previously been proposed, a number of techniques have been applied:

1) Apatite Fission Track Analysis (AFTA)
2) Vitrinite Reflectance Analysis (VR)
3) Shale Compaction Curve Analysis

Each of these techniques and the results obtained from them are discussed in this section and then all the results are collated in section 4.3.

4.2.1 Apatite fission track analysis (AFTA)

Over the last 20 years, fission-track thermochronology has become an established technique for constraining the low-temperature thermal histories of rocks and for analysing the thermal and burial histories of sedimentary basins (e.g. Naeser et al 1989; Green et al 1989; Feinstein et al 1989; Brown et al. 1994; Wang et al 1994; Gallagher et al. 1998; Donelick et al 2005). The understanding of fission track behaviour in apatite grains during geological thermal events is based upon numerous laboratory studies. (e.g. Green et al 1986; Duddy et al 1998), while in-depth discussions of the theory can be found in Fleischer et al (1975) and Wagner & Van Den Haute (1992).

4.2.1.1 Delaware Basin Sampling

Five samples from the JE Haley 24-1 well in Loving County in the eastern Delaware Basin (Fig 4.5 & Fig 4.6) and five outcrop samples from the western Delaware Basin (Fig 4.5) were analysed by Geotrack in Western Australia for AFTA. The following standard technique was advised by Geotrack (Duddy *pers comm.*) and used for sampling of the Delaware Basin.

- Samples should come from sands or silts in any form, i.e. cuttings, core, or outcrop etc.
    - Four of the outcrop samples were from Late Permian sands that are exposed on the western edge of the basin (Fig 4.5 & 4.6, and Table 4.1). The last sample is a Triassic sand found 30 km to the north of the other four samples in New Mexico (Table 4.1).
    - Samples from the JE Haley 24-1 well came from cuttings and were picked from prominent sandstone formations within the Permian Leonardian and Guadalupian Series (Fig 4.6 & Table 4.2).
- Where samples have come from a well, each individual sample can be composited over a depth interval where the change in downhole temperature is no more than 5°C.
    - The modern day geothermal gradient is between 18-22°C/km (Mazzullo 1986; Barker & Pawlewicz; Luo et al 1994), therefore each sample from the JE Haley 24-1 well was composited over no more than 800 ft (250 m) (Table 4.2).
- Well samples should not come from depths where the downhole temperature is greater than 110 °C.
    - The deepest sample from the JE Haley 24-1 well is from the Bone Spring formation in the Permian Leonardian Series, where the present temperature is 98 °C (Table 4.2).
- The weight of the sample should be between 500-1000 g to enable a good enough frequency of apatite grains.
    - The samples from both the well and outcrop were nowhere near the suggested sampling weight. However 80% of the samples contained good

to excellent yields of apatite, meaning the weight was not an issue (Table 4.2).

- Individual samples from a well should not be composited across an unconformity.
    - All of the well samples came from the conformable Leonardian and Guadalupian Series.

Sample	Sample Type	Stratigraphic Position & Depth (ft)	Stratigraphic Age (Ma)	Present Temp (°C)	Weight (g) & Apatite Yield
GC 930-1	Cuttings	Bell Canyon 5200 - 6020	270 - 260	58	360 Excellent
GC 930-2	Cuttings	Cherry Canyon 6200 - 7020	270 - 260	65	440 Good
GC 930-3	Cuttings	Brushy Canyon (A) 7500 - 8300	270-260	72	230 Excellent
GC 930-4	Cuttings	Brushy Canyon (B) 8300 - 9120	270 – 260	78	310 Good
GC 930-5	Cuttings	Bone Spring 11500-12010	280 – 270	98	290 Fair

Table 4.1. Description of the five well samples from the JE Haley 24-1 well, Loving County in the Delaware Basin (Taken from Duddy 2006). Refer to Figs 4.5 and 4.6.

Sample	Sample Type	Stratigraphic Subdivision	Stratigraphic Age (Ma)	Weight (g) & Apatite Yield
GC 930-6	Outcrop	Brushy Canyon	270 – 260	190 and Excellent
GC 930-7	Outcrop	Cherry Canyon	270 – 260	320 and Excellent
GC 930-8	Outcrop	Bell Canyon (A)	270 – 260	110 and Excellent
GC 930-9	Outcrop	Bell Canyon (B)	270 – 260	80 and Excellent
GC 930-10	Outcrop	Triassic	245 – 208	150 and Excellent

Table 4.2. Description of the five outcrop samples from the exposed Late Permian and Triassic section in Western Delaware Basin (Taken from Duddy 2006). Refer to Figs 4.5 and 4.6.

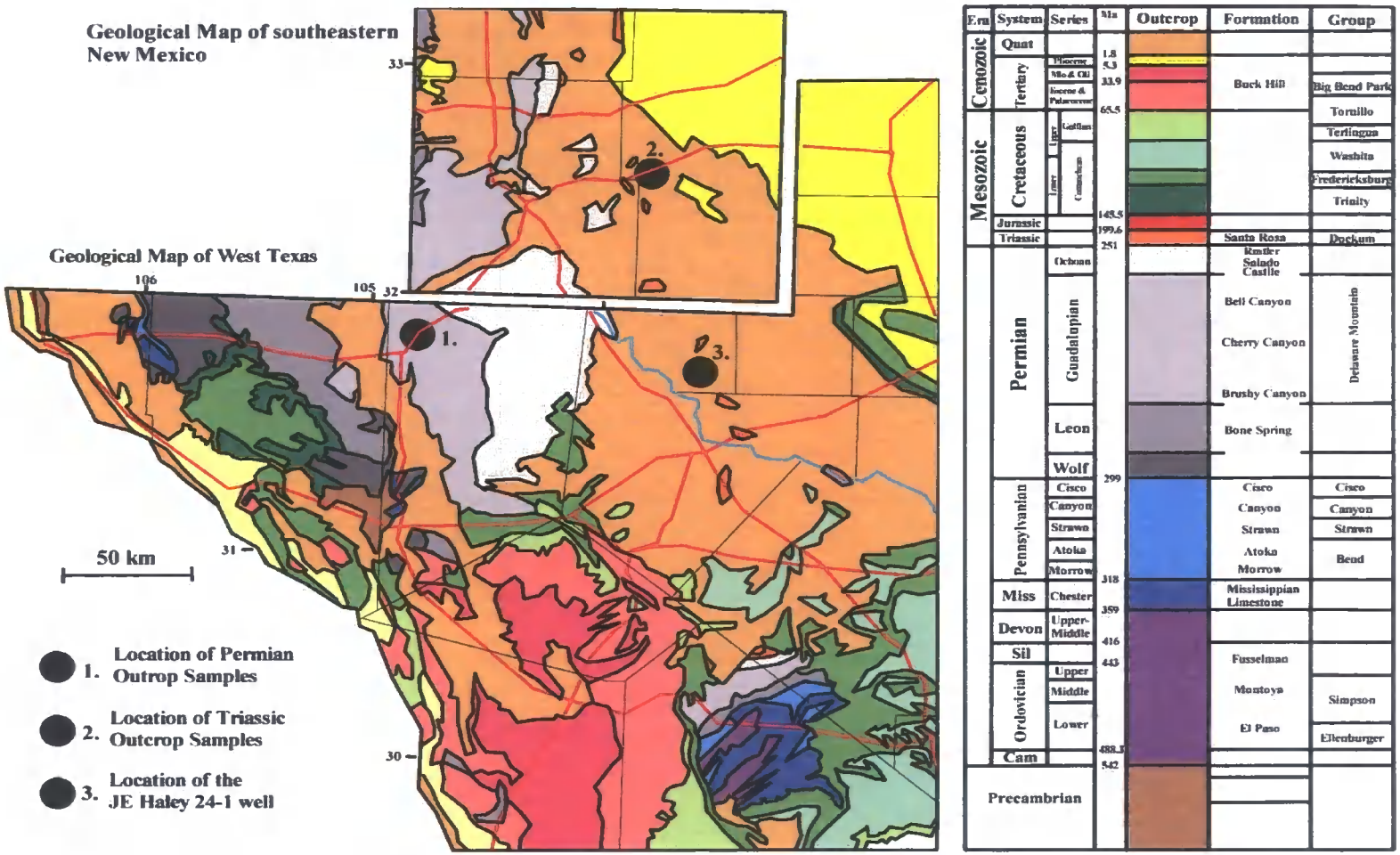

Fig 4.5. Geological map of west Texas, showing the location of the outcrop samples used for AFTA

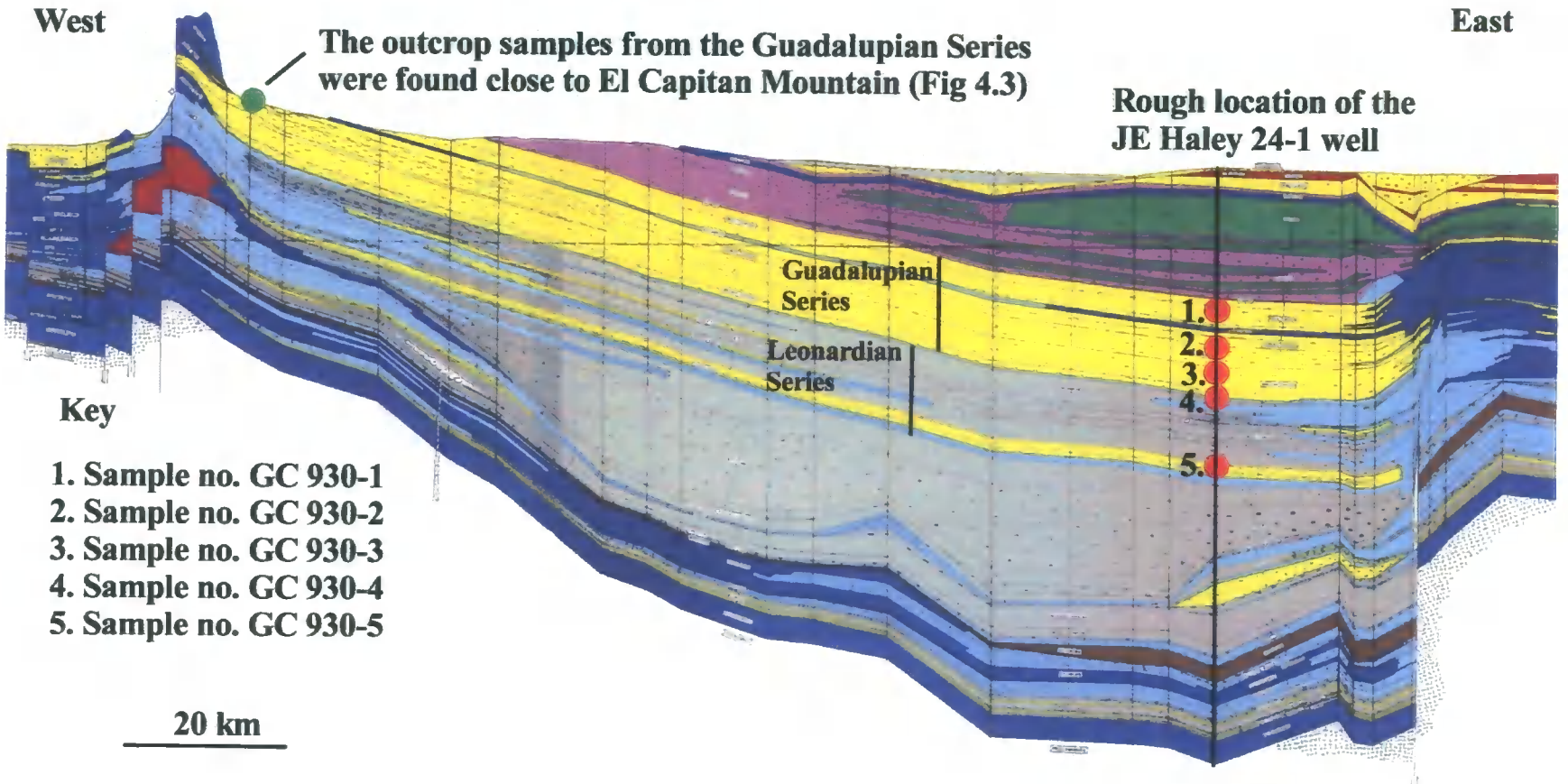

Fig. 4.6. Location of the samples on a cross section of the basin. The five well samples were taken from cuttings from the main sandstone beds within the Permian Guadalupian and Leonardian Series. Outcrop samples recovered near to El Capitan came from the exposed Guadalupian Series (Taken from West Texas Geological Society Publication 94-79).

4.2.1.2 Basic Principle of AFTA

By analysing the trail of radiation damage caused within an apatite grain when ^{238}Uranium (^{238}U) atoms fission, AFTA will essentially determine whether or not a sample has been hotter in the past. When ^{238}Uranium (^{238}U) atoms fission, it causes fission tracks (Fig 4.7) to be created. The number of tracks that are etched into the unit area of the surface of an apatite grain (spontaneous track density) will depend on three factors:

- The time over which the tracks have been accumulating.
- The uranium content of the apatite grain
- The distribution of track lengths in the grain.

Fig 4.7. Picture of an apatite grain showing numerous fission tracks. This grain has a moderate spontaneous track density.

In a sedimentary rock where temperatures have not exceeded more than 50 °C since deposition, apatite grains have a characteristic distribution of confined track lengths, with a mean length in the range of 14-15 μm, and a standard deviation of 1μm. In such samples, measurements of spontaneous track density and uranium content enable a fission track age to be calculated, which equals the time over which the tracks have been accumulated.

If the temperature of the sediment exceeds 50 °C, then the fission tracks will start to anneal. They become shorter by shrinking from each end due to the gradual

repair of the radiation damage. Numerous studies have been conducted where quantitative models were used to analyse how fission tracks anneal in sediments (Green et al 1986; Carlson 1990; Crowley 1991; Corrigan 1992). As temperature increases, all existing tracks will shorten to a length determined by the prevailing temperature regardless of when they formed. The mean track length falls progressively from ~14 μm at 50 °C to zero at 110-120 °C. A decrease in track length will also accompany a reduction in fission track age because of the reduced proportion of tracks that can intersect the polished surface.

If the sediment then decreases in temperature, all the tracks formed prior to the temperature maximum, will then freeze at the length attained and the length of each track will then be an indicator of the maximum palaeotemperatures the sediment experienced.

AFTA can be used to determine whether or not a sample has experienced greater temperatures in the past. This is achieved by determining whether the degree of annealing shown by the tracks in an apatite grain could have been produced if the sample has never been hotter than its present temperature at any time since deposition. A default thermal history profile is created using the burial history curve of the preserved sediments. If the data show a greater degree of annealing than calculated with the default thermal history, the sample must have been hotter in the past. The maximum palaeotemperature and timing of cooling are determined using a forward modelling approach based on the default thermal history and quantitative annealing techniques. The model works through successive thermal history scenarios in order to identify one that could account for the observed annealed tracks and then a range of values for maximum palaeotemperature and time of cooling are assigned using a maximum likelihood approach which has a 95% confidence limit. In the estimation of absolute palaeotemperatures there is an uncertainty of ~10 °C (Duddy 2006), which is a significant improvement on earlier approaches.

Most AFTA procedures are only sufficient to determine two episodes of heating and cooling. If a basin has undergone a complex series of heating and cooling episodes, then AFTA results will record the two events that were the most dominant, which tend to be the earliest and the latest (Duddy 2006; Braun et al. 2006).

4.2.1.3 Temperature

Temperature is an essential factor to interpreting AFTA data, as it is temperature that controls the amount of annealing the apatite grain experiences. Firstly, it is important to quantify what the present day temperature profile is for the well, since any estimation of maximum palaeotemperature will proceed from determining whether the mean track length is explained by the magnitude of present-day temperatures (Duddy 2006), and it forms a basic point of reference for track length data. For example, if the observed mean track length is shorter than the mean track length predicted from the default thermal history (based on the present-day geothermal gradient), then the sample must have been subjected to higher palaeotemperatures at some time after deposition. (This assumes that the measured tracks were not from grains inherited from the original sediment source).

A present day temperature profile was created for the Haley 24-1 well, in which four samples were analysed for AFTA (Fig 4.8). The temperature profile was created using five bottom hole temperature (BHT) readings from the well. The measured BHT readings were adjusted by a correction procedure, as the measured formation temperatures tend to be underestimated due to drilling effects. A present-day surface temperature of 20 °C is taken for the well location in West Texas USA. Coupled with the corrected BHT readings, an estimated linear geothermal gradient of 21.8 °C/km was derived. This is similar to the geothermal gradient of 20 °C/km and 18° – 21 °C/km suggested by Luo et al (1994) and Mazzullo (1986), respectively, for the Delaware Basin.

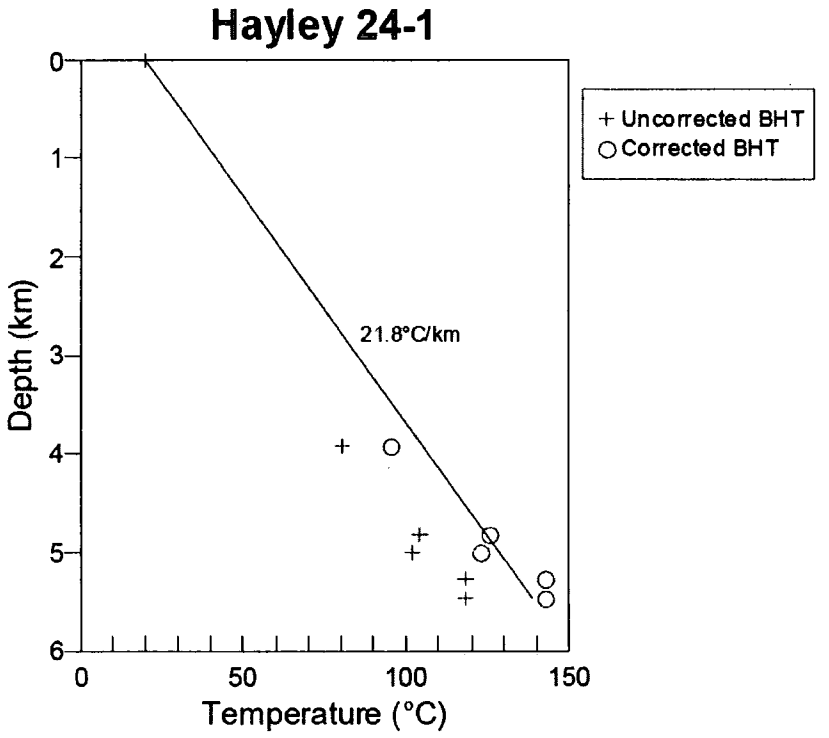

Fig 4.8. Present temperature profile created for the Haley 24-1 well. A surface temperature of 20°C is assumed. (Taken from Duddy 2006).

As well as the importance of knowing the present-day geothermal gradient, it is also important to determine the palaeogeothermal gradient. The shape of the palaeotemperature profile and the magnitude of the geothermal gradient will provide an insight into the heating and cooling history of the basin (Bray et al 1992). If the palaeotemperature profile is linear, this can be compared against the present-day temperature profile to gain an idea of the basin's thermal history (Fig 4.9). However if there are departures from the linear palaeogeothermal gradient (Fig 4.10), then this would indicate a departure from a constant temperature with depth. This could be due to either strong contrasts in thermal conductivities through the section, or a localised heating effects such as hot fluid movement or intrusive bodies.

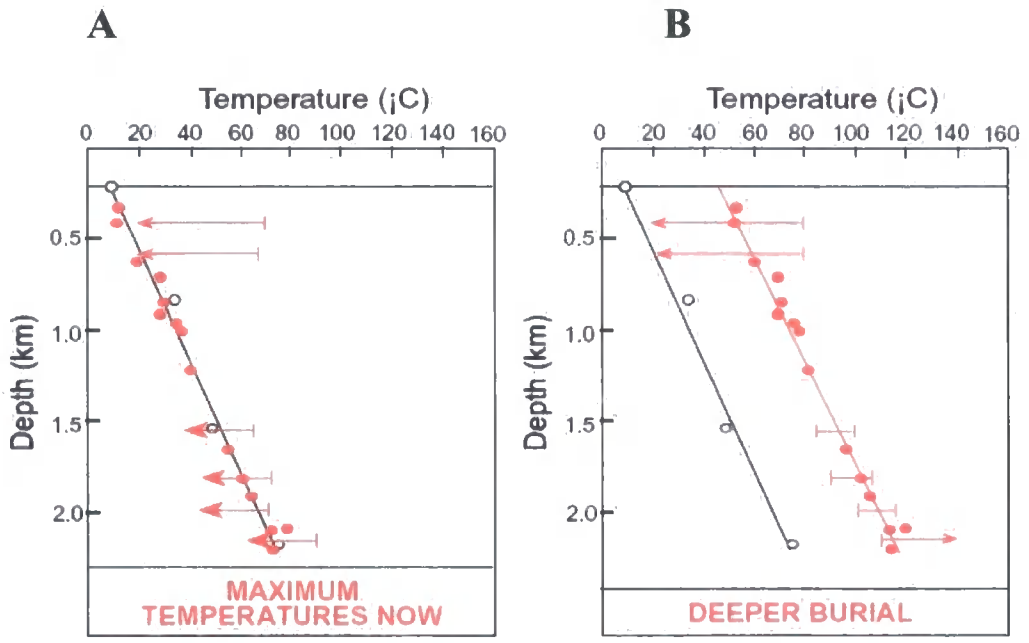

Fig 4.9. If the palaeotemperature profile is identical to the present-day temperature profile (A), then the section is experiencing maximum temperatures at present day. However if the palaeotemperature profile is higher than that at present (B), then it implies that the section has experienced greater burial and the cooling was due to uplift and erosion. However, it also needs to be noted that if the palaeotemperature profile is higher than at present, then it may be due to an elevated basal heat flow. (Taken from Duddy 2006).

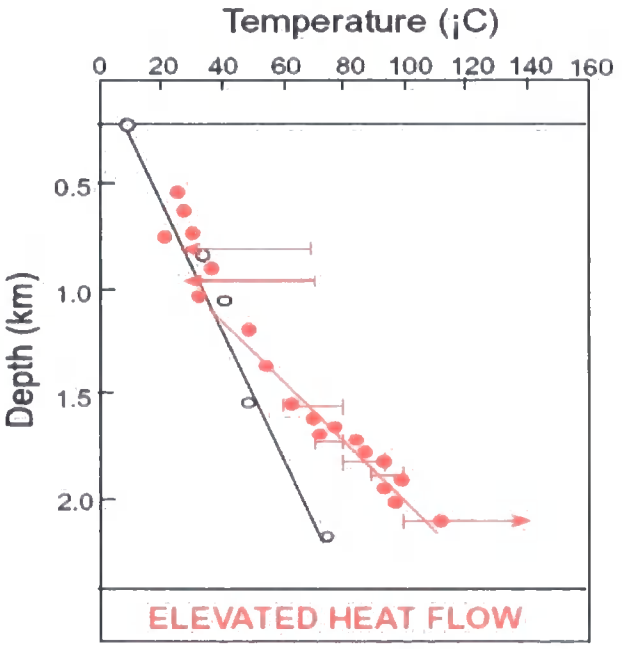

Fig 4.10. Example of well data, where the palaeogeothermal gradient is not linear. The departure may be due to localised heating effects (Taken from Duddy 2006).

The palaeogeothermal gradient prior to the onset of cooling can be determined using the maximum palaeotemperatures, which were derived from the AFTA results. However the accuracy of the value depends upon two factors. To achieve an accurate palaeogeothermal gradient, it is best to have samples that have been analysed over as large a depth range as possible. If the samples come from a narrow depth range (<1km), then the palaeogeothermal gradient will be very loosely constrained. Also it is important that the difference between the maximum palaeotemperature and the present temperature is greater than 10 °C, as this is the uncertainty range when palaeotemperatures are determined.

4.2.1.4 How AFTA results are displayed

AFTA results are generally shown as plots of fission track age against depth and mean track length against temperature. Figures 4.11 and 4.12 are an example of these plots, and demonstrate two possible scenarios. In Fig 4.11, deposition has been continuous since the Carboniferous to the present, and all samples are currently their maximum palaeotemperature. In Fig 4.12, the section experienced greater palaeotemperatures prior to cooling in the Early Tertiary.

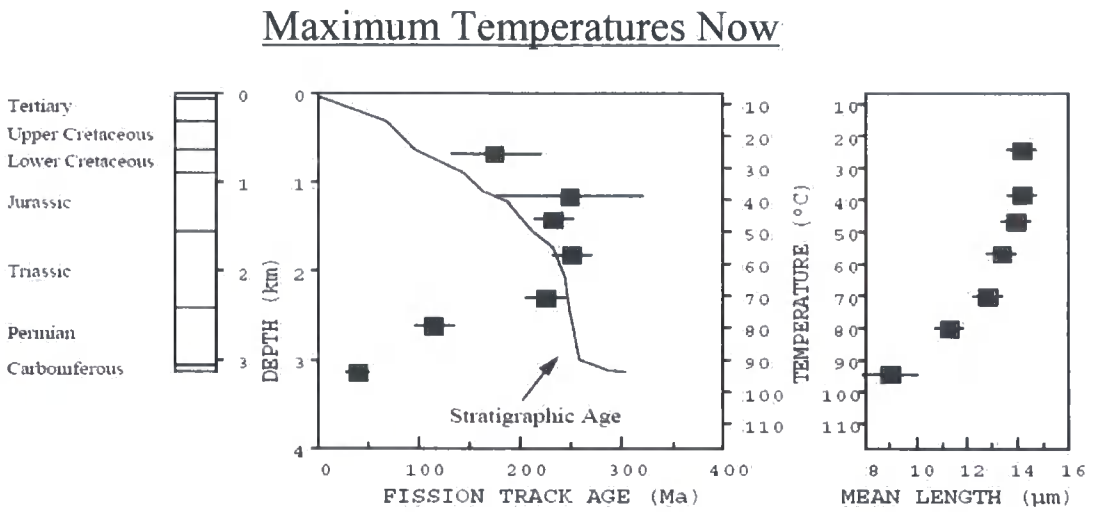

Fig 4.11. In this example, in the samples below 70°C, the fission track age is either just above or close to the stratigraphic age, and minimal amounts of annealing have taken place to decrease fission track age or track length. Above 70°C, the fission tracks are being annealed, and both the fission track age and the mean track length are reduced. This pattern is characteristic of a sequence, which is currently at maximum temperature. (Taken from Duddy 2006).

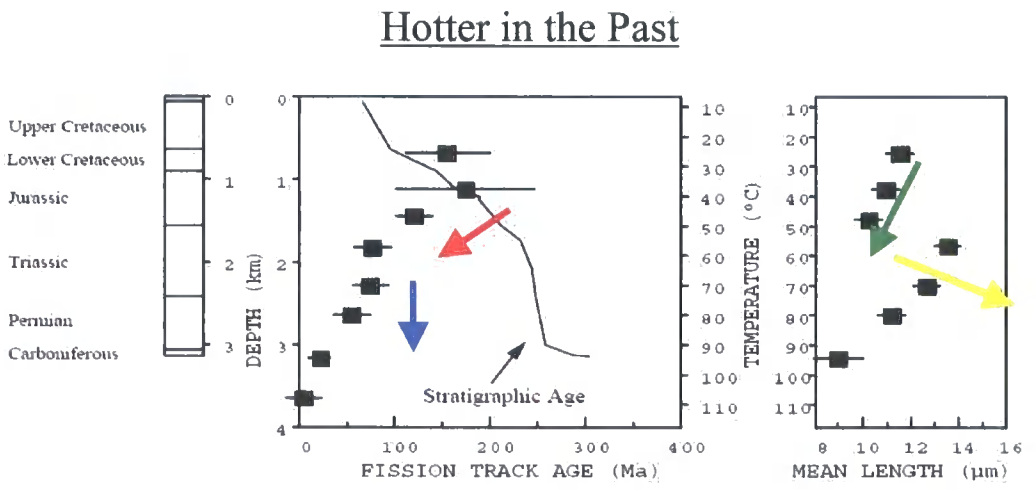

Fig 4.12. This data set shows a very different pattern to Fig 4.11. At 40-50°C, the fission track age decreases rapidly (red arrow), so that it is less than the stratigraphic age. This degree of age reduction is more than would be expected for these temperatures. The fission track age becomes consistent (blue arrow), which is diagnostic of the transition between partial and total annealing. The mean track length plot shows two distinct patterns. In the shallow section (green arrow), the mean length is a lot less then expected, indicating that these samples have experienced greater burial and temperatures and hence annealing. However between 50-60°C, the track length increases (yellow arrow) as tracks formed prior to maximum burial have been fully annealed, and are representative of tracks formed after cooling. (Taken from Duddy).

4.2.1.5 Determining amount of section removed

Once it has been determined that the samples have been hotter in the past due to greater burial, then the last important stage in the analysis, is to determine how much uplift the section has experienced. This is done by constraining the palaeogeothermal gradient before uplift and then extrapolating this profile to the estimated palaeosurface temperature (Fig 4.13). Obviously, a number of assumptions are made (Duddy 2006):

- The palaeotemperature profile through the preserved section is linear.
- The palaeogeothermal gradient can be extrapolated linearly through the missing section.
- The palaeosurface temperature is known.

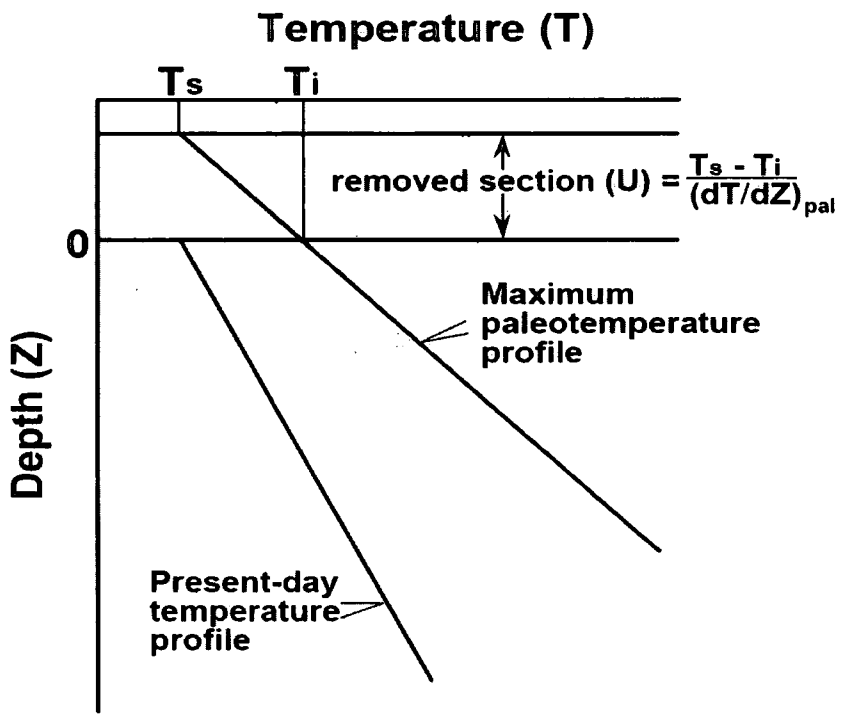

Fig 4.13. Diagram to illustrate how the amount of removed section is estimated. The net amount of section removed is calculated by dividing the difference between the palaeosurface temperature (Ts) and the intercept of the palaeotemperature profile at the present ground surface (Ti) by the estimated geothermal gradient. If there has been reburial, then the total amount of section removed is obtained by adding the net amount to the thickness of section redeposited above the unconformity. (Taken from Duddy 2006).

4.2.1.6 AFTA results for the JE Haley 24-1 well

Results of the AFTA analysis on the samples from the JE Haley 24-1 well, are summarised in Table 4.3 and displayed as a plot (Fig 4.14) where fission track age and mean track length are plotted against depth and present temperature. The temperature variables used to extract the thermal history information are a surface temperature of 20°C and a present day geothermal gradient of 21.8 °C/km (section 4.2.1.3). For the following results, the palaeogeothermal gradient is assumed to be identical to the present one. Variations on the palaeogeothermal gradient and the effect on the AFTA results will be dealt with in the discussions section of this chapter.

The four shallower samples (GC930-1 to –4) all showed clear evidence that they had been hotter in the past, because their determined fission track ages are lower than the fission track ages predicted from the default thermal history (Table 4.3). The deepest sample (GC930-5), however, shows a fission track age higher than predicted. This is because the sample is dominated by the present day thermal regime. Also this sample contained a number of apatite grains with very high chlorine content, which has been interpreted as evidence of possible down-hole contamination. For these two reasons, this sample cannot provide any constraints on the palaeo-thermal history (Table 4.3).

Sample number	Average depth (m)	Present temperature (°C)	Stratigraphic age (Ma)	Mean track length (μm)	Predicted mean track length (μm)	Fission track age (Ma)	Predicted fission track age (Ma)
GC930-1	1737	58	270-260	11.17 ± 0.30	12.4	103.9 ± 13.8	218
GC930-2	2088	65	270-260	12.27 ± 0.33	11.5	110.0 ± 13.9	206
GC930-3	2408	72	270-260	11.72 ± 0.42	11.2	37.3 ± 8.6	188
GC930-4	2667	78	270-260	12.11 ± 0.81	9.9	34.1 ± 7.6	150
GC930-5	3583	98	280-270	14.24 ± 0.58	10.3	51.1 ± 17.5	34

Table 4.3. Summary of apatite fission track data, and default thermal history predictions for samples from the JE Haley 24-1 well.

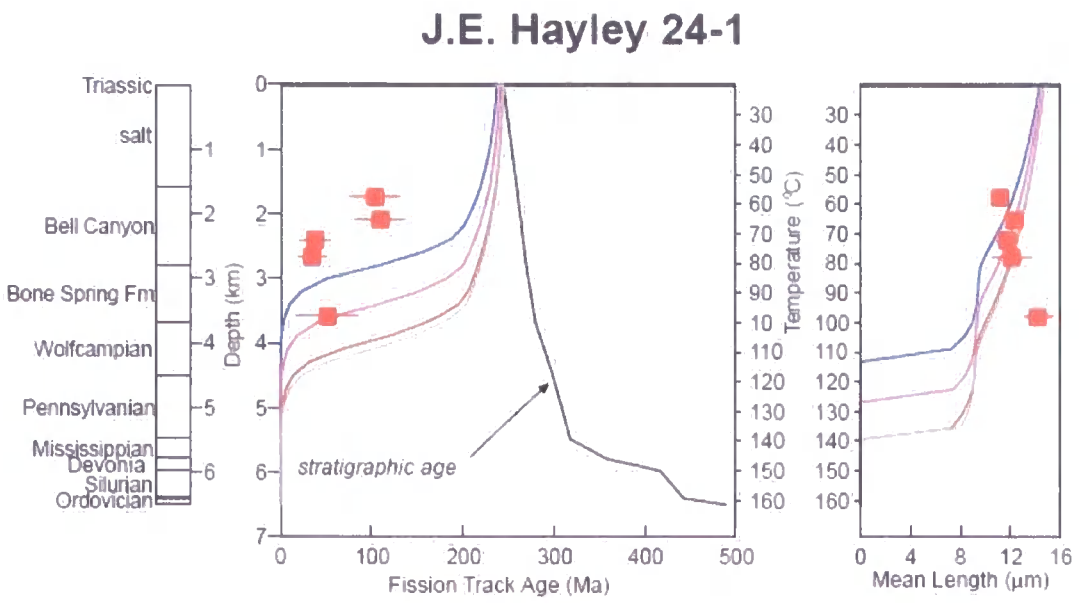

Fig 4.14. AFTA parameters plotted against sample depth and present temperature for samples from the JE Haley 24-1 well. Coloured lines show the pattern of fission track age and mean track length predicted from the default thermal history for apatites containing 0-0.1, 0.4-0.5, 0.9-1, and 1.5-1.6 wt% Cl, where the apatites from the Delaware Basin have a wt% Cl of between 0-0.5.

4.2.1.6.1 Palaeotemperature estimates

The apatite fission track data were then interpreted using forward modelling techniques (section 4.2.1.2) to determine the magnitude and timing of maximum palaeotemperatures. The thermal history solutions derived from the all the samples (Table 4.4) indicate that there were two discrete palaeo-thermal events. Two events are needed, as the earliest (maximum palaeotemperature) episode is required to explain the degree of fission track reduction and also the shortest tracks within the track length distribution, while the later event is required to account for the shortening of the main mode of track length distribution. Based on this interpretation, the following ages can be assigned for the onset of cooling, assuming that the onset for each episode was synchronous in all four of the shallow samples (Duddy 2006).

- **125 to 50 Ma (Early Cretaceous to Eocene)**
- **40 to 10 Ma (Late Eocene to Late Miocene)**

				Early event "E.Cret.-E. Eocene"		Later event "L. Eocene-L. Miocene"		
Geotrack sample number	Depth	Strati-graphic age	Present temperature	Maximum paleo-temperature	Onset of cooling	Peak paleo-emperature	Onset of cooling	Equivalent Vitrinite Reflectance
GC	(m)	(Ma)	(°C)			(°C)	(Ma)	(%)
930-1	1737	270-260	58	100-105	135 to 50	85-95	50 to 10	0.61-0.63
930-2	2088	270-260	65	>95	Dep^n to 40	<95	40 to 0	>0.57
930-3	2408	270-260	72	>110	125 to 45	90-110	50 to 10	>0.66
930-4	2667	270-260	78	>105	165 to 45	<105	45 to 0	>0.63
930-5	3583	280-270	98	No	constraint	-	-	>0.60
Integrated constraint	**AFTA (Ma)**	**timing**			**125 to 50**		**40 to 10**	

Table 4.4 Palaeotemperature analysis summary for the samples from the JE Haley 24-1 well.

4.2.1.6.2 Estimates of removed section

The amount of section removed at the times of cooling can now be worked out to explain the observed palaeotemperatures. A number of assumptions are assumed for this calculation. These are a surface temperature of 20 °C and a palaeogeothermal gradient of 21.8 °C/km, which is the same as the present day geothermal gradient. Also the palaeogeothermal gradient is assumed to be linear through the removed section. Variations on the palaeogeothermal gradient and its effect on the estimates of removed section will be dealt with in the discussions sub-chapter.

The results show that the amount of additional burial needed to explain palaeotemperatures prior to the onset of each cooling event is:

- **Early Cretaceous to Eocene (125-50 Ma) – 6890 ft (2100 m)**
- **Late Eocene to Late Miocene (40-10 Ma) – 3600 ft (1100 m)**

These estimates are quoted with a +/- 95% confidence limit (Duddy 2006). The above values will be quoted throughout the thesis, but it needs to be noted that there could be couple of hundred feet of difference in these estimates.

4.2.1.7. Results from the outcrop samples

The five outcrop samples from the western edge of the Delaware Basin were analysed by the same process as the well samples, and again a present day surface temperature of 20 °C is used. The measured fission track ages in the five samples are significantly younger than expected, and the mean track lengths are shorter than expected from the default thermal history (Table 4.5 and Fig 4.15). These results show clear evidence that the samples have cooled from maximum palaeotemperatures higher than the present outcrop temperature of 20 °C.

Sample number	Source No.	Present temperature (°C)	Stratigraphic age (Ma)	Mean track length (μm)	Predicted mean track length (μm)	Fission track age (Ma)	Predicted fission track age (Ma)
GC930-6	-	20	270-260	11.47 ± 0.35	14.39	67.6 ± 10.2	259
GC930-7	-	20	270-260	10.95 ± 0.53	14.37	169.4 ± 18.6	258
GC930-8	A	20	270-260	11.12 ± 0.40	14.36	106.4 ± 12.7	258
GC930-9	B	20	270-260	10.79 ± 0.46	14.35	121.2 ± 9.4	258
GC930-10	-	20	245-208	10.49 ± 1.02	14.44	145.8 ± 13.0	221

Table 4.5. Summary of apatite fission track data, and default thermal history predictions for outcrop samples from the western Delaware Basin. (Taken from Duddy 2006).

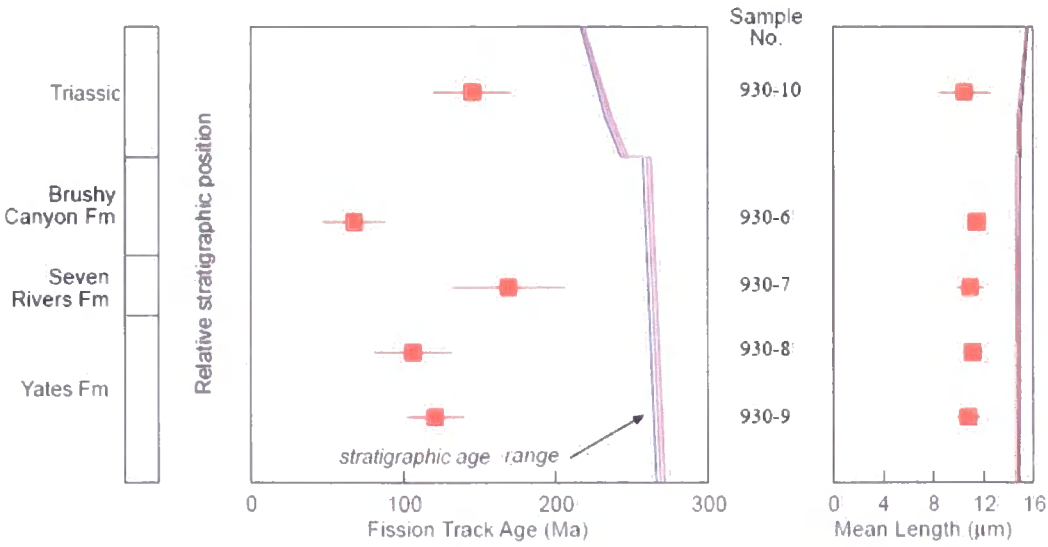

Fig 4.15. AFTA parameters plotted against relative stratigraphic position for Triassic and Permian outcrop samples from the Delaware Basin, where a present day temperature of 20°C is assumed. Coloured lines show the pattern of fission track age and mean track length predicted from the default thermal history for apatites containing 0-0.1, 0.4-0.5, 0.9-1, and 1.5-1.6 wt% Cl, where the apatites from the Delaware Basin have a wt% Cl of between 0-0.5.

4.2.1.7.1 Time of cooling from maximum palaeotemperatures

As with the well samples, the outcrop samples show two discrete palaeo-thermal events (Fig 4.16). All samples show a varying range of estimated palaeotemperatures, with two of the samples only recording one event. The Brushy Canyon 930-6 sample has the best constraint on timings of the thermal episodes, and a thermal history solution for this sample is illustrated in Figure 4.17. Taking into account the entire outcrop samples, the estimates for onset of cooling are:

- 55 to 45 Ma (Eocene)
- 25 to 0 Ma (Late Oligocene to present day)

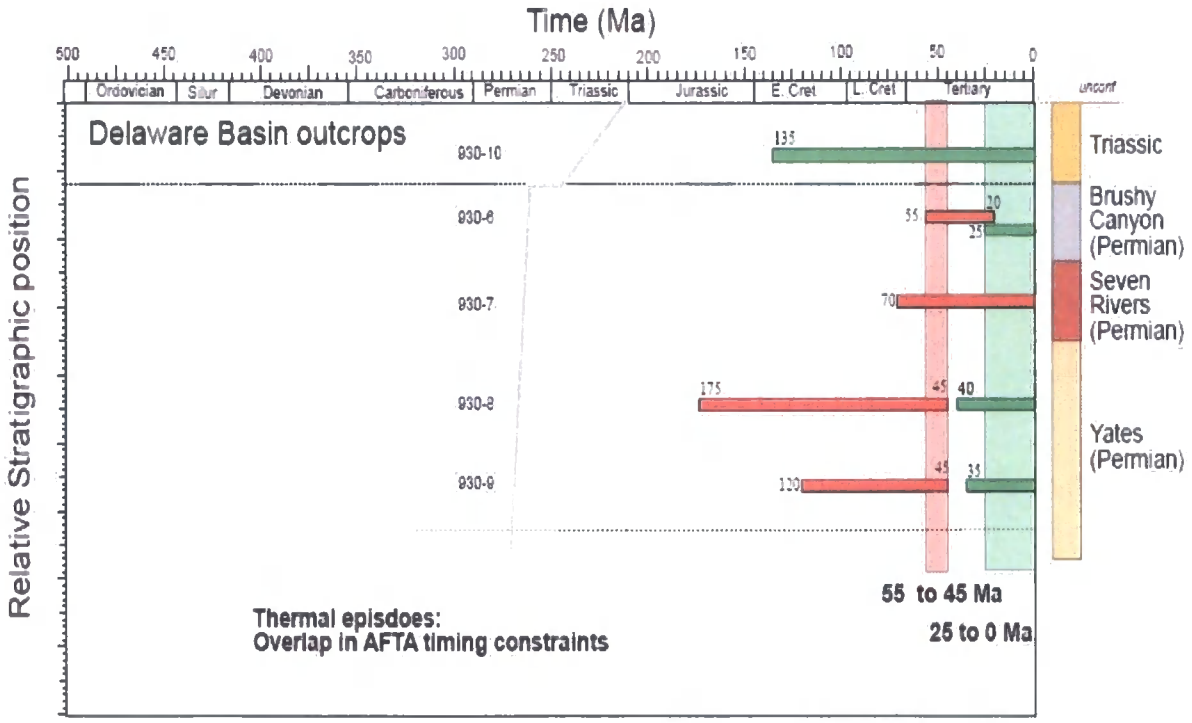

Fig 4.16. Constraints on the onset of cooling derived from AFTA from outcrop samples from the western Delaware Basin. The AFTA results define two post-depositional thermal episodes with cooling beginning at some time between 55-45 Ma, and 25 Ma to present day.

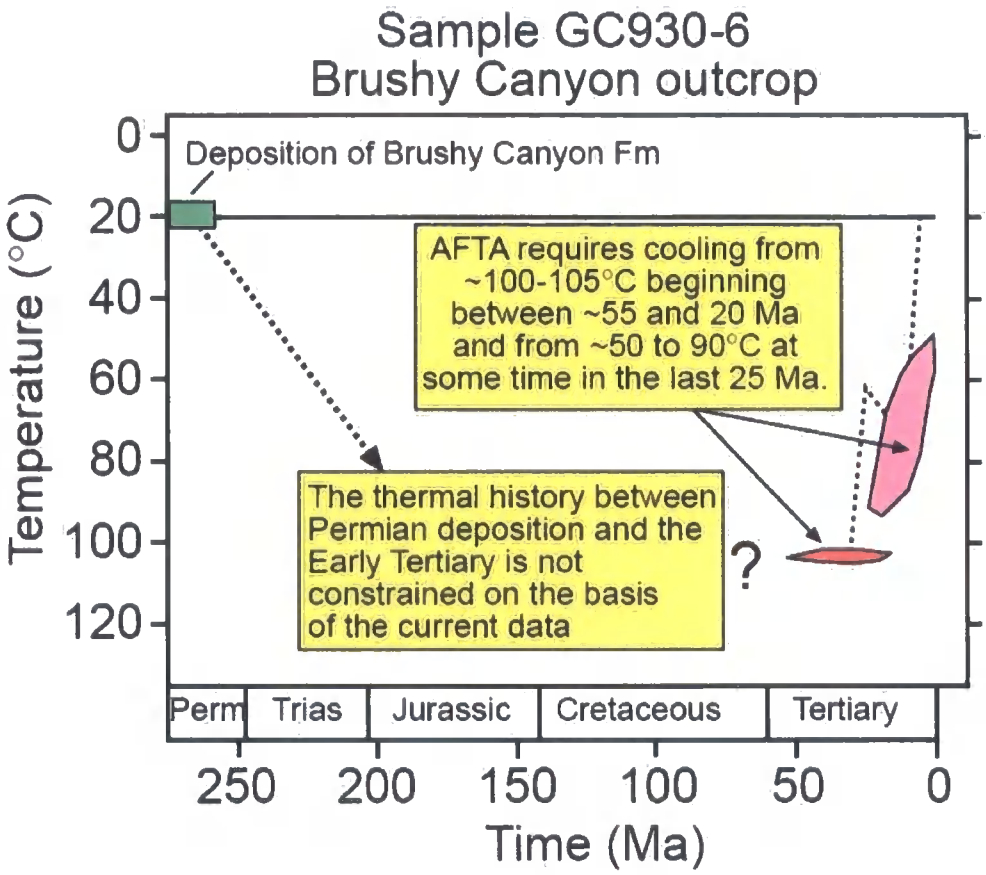

Fig 4.17. AFTA thermal history solution for the Brushy Canyon Formation outcrop sample (GC 930-6). The coloured fields show 95% confidence constraints on the time and temperature conditions required to explain the AFTA data. The results indicate two major thermal episodes with cooling through 100-105°C occurring between 55 –20 Ma, followed by cooling from 50 – 90°C beginning at some time in the last 25 Ma.

4.2.1.7.2 Estimation of removed section

Because the estimation of palaeogeothermal gradients is not possible for outcrop samples, as a vertical sequence of samples over reasonable depth range is needed, then the method of extrapolating the palaeogeothermal gradient to determine removed section is not possible.

However, from the AFTA results, it is clear that the samples experienced maximum palaeotemperatures greater than 90 °C, which cannot be achieved at ground surface, and so must have experienced greater burial. A very rough estimate

can be suggested for the outcrop based on palaeotemperature and an assumed palaeogeothermal gradient. For example, sample GC9301-1 experienced a maximum palaeotemperature of 100-105 °C between 55-20 Ma, and assuming a palaeogeothermal gradient of 25 °C/km, then 11000 ft (~3.3 km) of additional burial is required. Similar calculations can be made using different palaeotemperatures and palaeogeothermal gradients. However, it is clear that for the outcrop samples, it would require kilometre scale uplift and erosion in both cooling events to explain the maximum recorded palaeotemperatures seen.

4.2.1.8 AFTA summary

The AFTA results for both the well samples and the outcrop samples showed that the basin did experience greater burial, and AFTA suggested two thermal episodes of regional significance with associated phases of cooling:

For the JE Haley 24-1 well samples the phases of cooling are:

- Early event: 125-50 Ma Early Cretaceous-Eocene
- Later event: 40-10 Ma Late Eocene-Late Miocene

For the outcrop samples, the phases of cooling are:

- Early event: 55-45 Ma Early to Middle Eocene
- Later event: 25-0 Ma Latest Oligocene to recent

Combining the results from the well and outcrop samples, providing they represent two regionally synchronous cooling episodes, the following constraints can be made:

- Early event: 55-50 Ma Early Eocene
- Later event: 25-10 Ma Latest Oligocene to Late Miocene

Estimates of missing section were made for the JE Haley 24-1 well, where a surface temperature of 20 °C and a palaeogeothermal gradient of 21.8 °C/km were used.

- To explain observed maximum palaeotemperatures prior to the early uplift event. The section would need **6890 ft (2.1 km)** of additional burial.
- For the later exhumation event, **3600 ft (1.1 km)** was removed at some time between 25-10 Ma.

AFTA has therefore uniquely defined two episodes of the basin's burial history (Fig 4.18). Firstly, AFTA uniquely shows that the basin experienced maximum burial between 55-50 Ma as a consequence of 6890 ft (2.1 km) of additional burial. Secondly, AFTA also indicates that the last cooling episode (25-10 Ma) resulted in 3600 ft (1.1 km) of exhumation. In between these two events, the basin's tectonic history is not defined by AFTA, but could be one of three scenarios (Fig 4.18).

1. Maximum uplift and maximum subsidence (fig 4.18 - red lines).
    - The first uplift episode removed all the additional overburden of 6890 ft (2.1 km) recorded by the maximum palaeotemperatures. The basin then subsided and accumulated 3600 ft (1.1 km) of sediment during the Eocene and Oligocene prior to the second uplift event (25-10 Ma) which removed the 3600 ft (1.1 km) just added.
2. Period of quiescence (fig 4.18 – green lines).
    - Between the two uplift events there was no basinal subsidence and hence no further deposition of sediment. Consequently, as the final amount of uplift (3600 ft) is uniquely defined from AFTA, the first uplift event would have eroded off 3290 ft of sediment (1 km).
3. Intermediate (fig 4.18 – blue lines)
    - The first uplift episode eroded off anywhere between 6890 ft – 3290 ft, and then the necessary amount of subsidence occurred during the Eocene and Oligocene to allow for the final 3600 ft of uplift which explains the preserved strata seen today.

The question of which scenario best suits the Delaware Basin, will be analysed later in the discussion (sub-section 4.3) and the answer will enable an accurate burial history of the basin to be constructed.

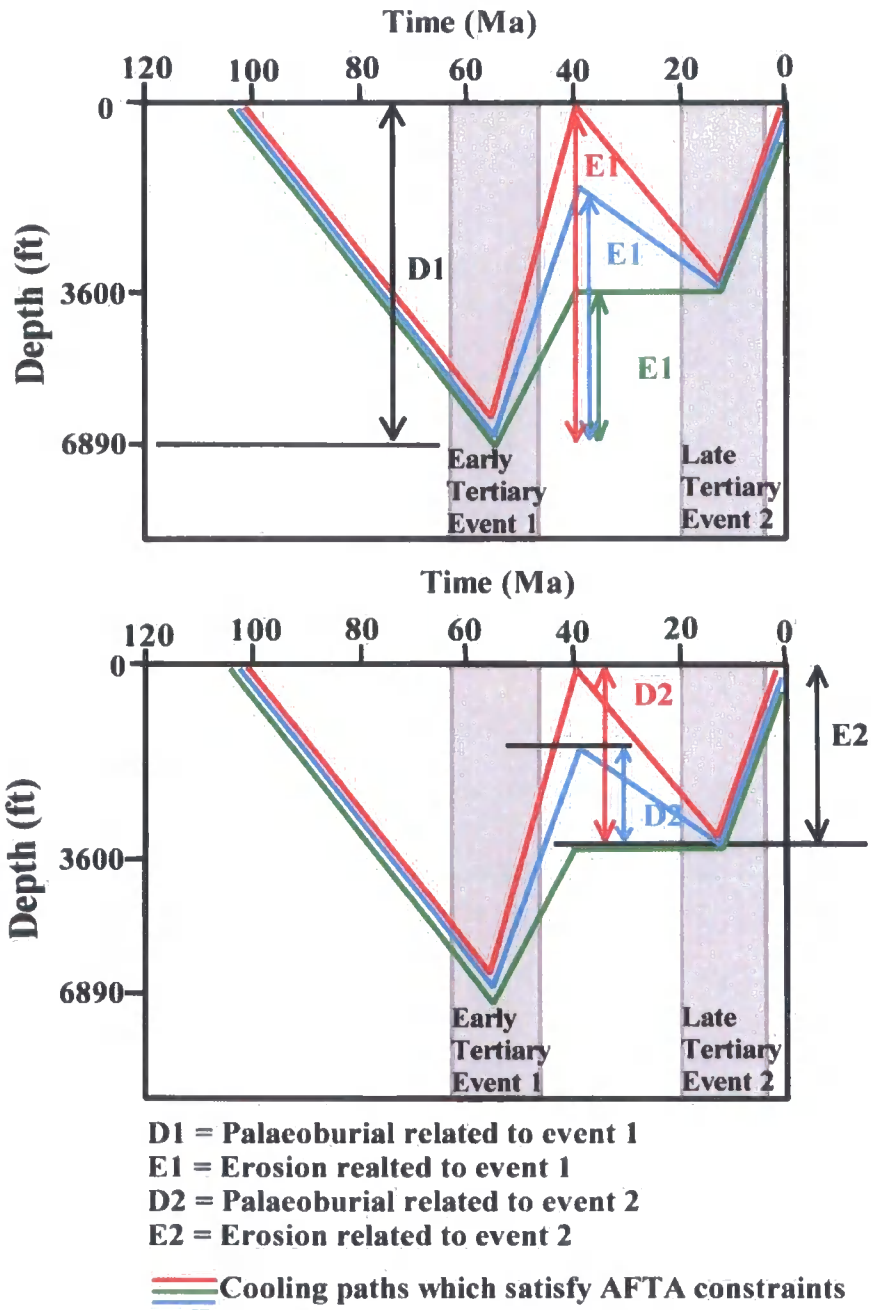

Fig 4.18. The constraints on defining amount of uplift from AFTA. In this example E2 is uniquely defined by the total amount of section removed during the later episode, while D1 is also uniquely defined as the amount of additional material needed to explain the palaeotemperatures in the earlier episode. But E1 and D2 are not uniquely defined.

4.2.2 Vitrinite reflectance

Vitrinite reflectance is the most widely used indicator for maturity of organic materials (Allen and Allen 1990). Vitrinite itself occurs as a dispersed component in the kerogen of source rocks in sedimentary basins; therefore to carry out vitrinite reflectance a basin needs to have organic rich source rocks within its stratigraphy. In the Delaware Basin, the shales of the Lower Permian Wolfcampian Series, and shales within the Pennsylvanian, Mississippian and Devonian strata are known to contain organic rich source rocks.

It is the reflectance of vitrinite in oil (Ro) that is measured. Generally, temperature increases with depth, and so does the reflectance of vitrinite as the sediment becomes more thermally mature (Gluyas and Swarbrick 2004). The measured vitrinite reflectance is plotted against depth, typically with reflectance values on a logarithmic scale with depth on a linear scale. In a basin showing continuous sedimentation which is at maximum burial at present day, and where there are no unconformities or intrusions, the Ro values should fall on a straight linear trend and can be extrapolated to 0.2% Ro at the surface (common % Ro of near surface sediments) (Fig 4.19). The actual rate of maturity increase with depth expressed by the Ro values, is not the same for each basin or source rock, but varies due to the type of kerogen, the age of the sample, and the palaeogeothermal gradient (Fig 4.20).

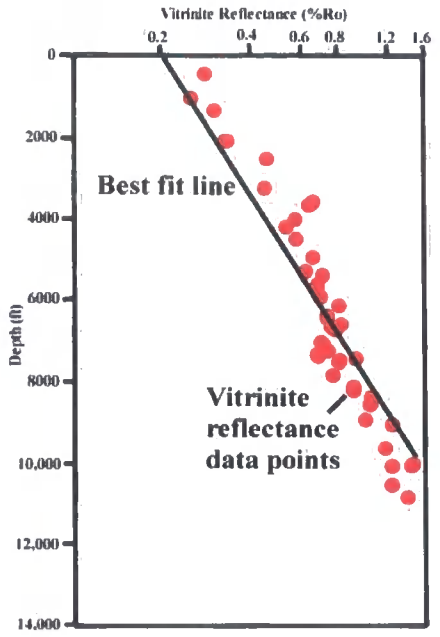

Fig 4.19. Vitrinite reflectance plotted against depth showing a linear trend of increasing maturity with depth. Vitrinite reflectance typically has a value of 0.2 %Ro at the surface. (Adapted from Gluyas and Swarbrick 2004).

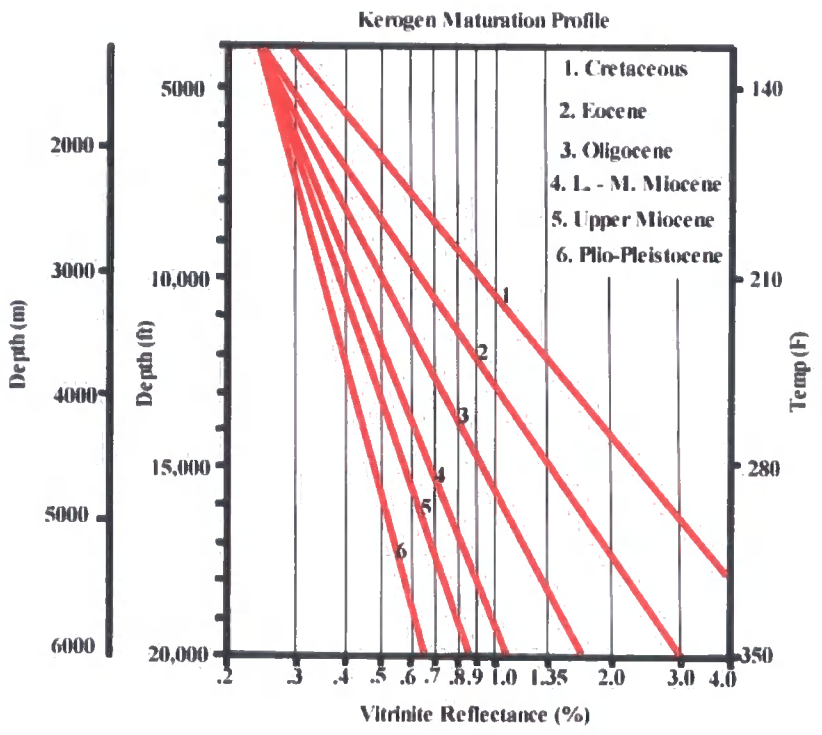

Fig 4.20. Plot of depth versus vitrinite reflectance for kerogens of different ages, where the older kerogens are significantly more mature. (Taken from Allen and Allen 1990).

There are two main uses of vitrinite reflectance data. Firstly, it is a good indicator of a source rock's maturity with regards hydrocarbon generation, where the following reflectance boundaries can be used:

<0.5% Ro	Immature (oil)
0.5 - 0.7% Ro	Early mature (oil)
0.7 - 1% Ro	Mid mature (oil)
1 - 1.3% Ro	Late mature (oil)
1.3 – 2.2% Ro	Peak mature (gas)
2.2 – 3% Ro	Late mature (dry gas)

Secondly, vitrinite reflectance data from within a well can indicate whether the section has been hotter in the past, and experienced later uplift. If the section has been hotter in the past, then the vitrinite reflectance will show a greater maturity for its present depth of burial; however, this could just indicate a higher palaeotemperature and not necessarily greater burial. Therefore it is the projection of the Ro data to the present surface that indicates whether the greater maturity is due to extra burial or just a higher heat flow. If the projected value at the surface is greater than 0.2% Ro, then it can be inferred that the section underwent exhumation. To estimate the amount of exhumation, the inferred Ro profile is extended beyond the surface until the value of Ro reaches 0.2 %, and then the difference between that elevation and the surface elevation is the amount of exhumation (Fig 4.21).

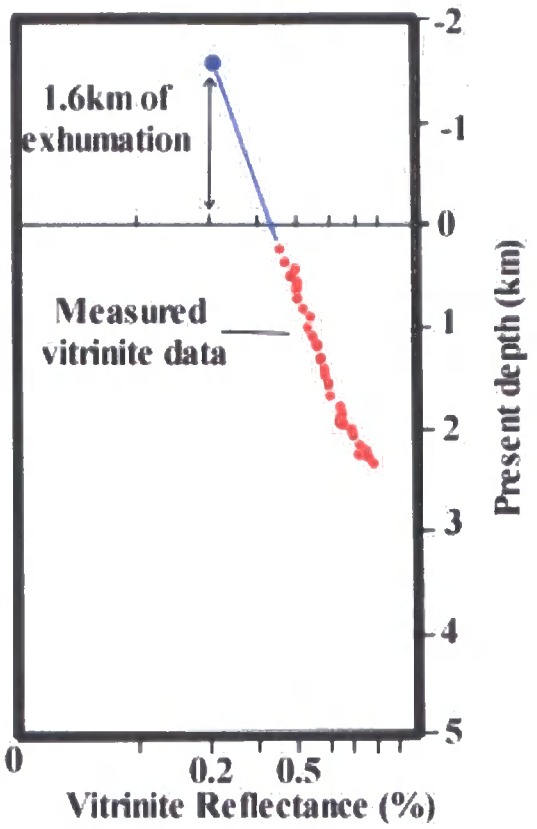

Fig 4.21. Vitrinite reflectance plot with depth where the section has been more deeply buried in the past. The amount of uplift can be calculated by extrapolating the measured vitrinite data to the depth where it intercepts 0.2% Ro. In this example the depth at which the extrapolated best fit line reaches 0.2% Ro is –1.6km, indicating that this was the amount of exhumation.

4.2.2.1 Delaware Basin sampling

In order to determine the uplift history of the Delaware Basin, thirteen wells from the Delaware Basin and one well from the Midland Basin (Fig 4.22) containing vitrinite reflectance data were analysed.

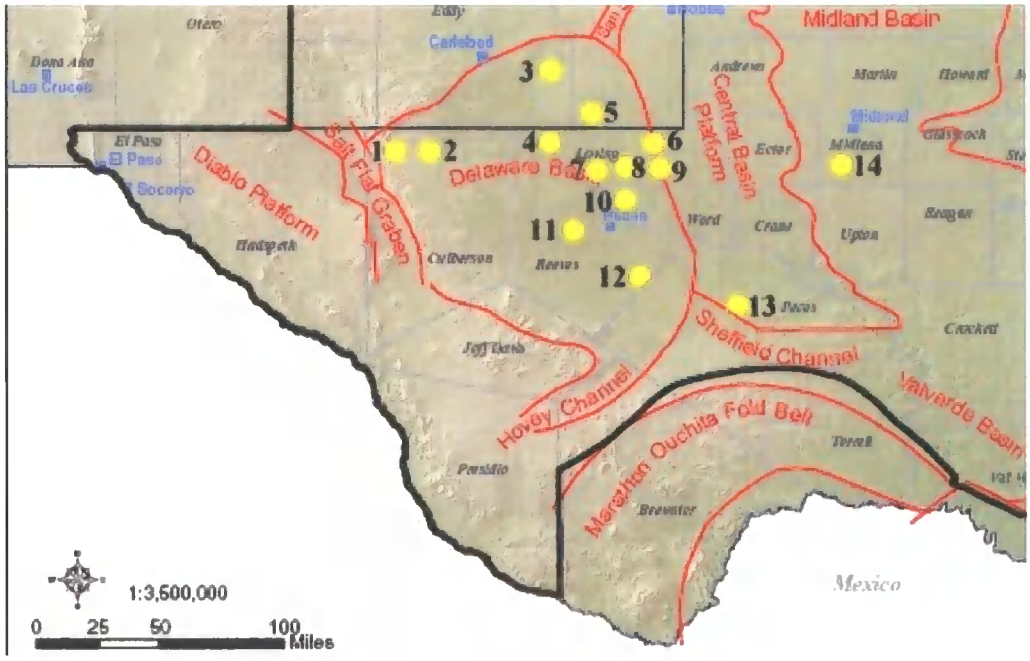

Fig 4.22. Map showing locations of wells containing vitrinite reflectance data. The wells are: **1)** Culberson Fee L-1; **2)** Homer Cowden A-1; **3)** James Ranch Unit; **4)** Lago Gas; **5)** Red Hills Unit 1; **6)** Lineberry Evelyn; **7)** Johnson 87-1; **8)** JE Haley 24-1; **9)** Roark; **10)** Greer McGinleas Unit; **11)** Mrs VL Shurtleff; **12)** Wapples Platter 1; **13)** Stroman W A/C; **14)** Braun Etal Unit. (Adapted from Pawlewicz et al 2005).

4.2.2.2 Results of the vitrinite reflectance analysis in the Delaware Basin

Vitrinite reflectance (VR) data from the JE Haley 24-1 well were plotted against depth using a 1D basin modelling program called "Genesis" developed by Zetaware. The first model (Fig 4.23) plotted VR data against depth of burial at present day with the assumption that the section is at maximum burial at present day. The plot shows that the vitrinite data indicate greater maturity than expected for present depths of burial, indicating the section may have experienced greater burial in the past.

The model was then adapted to take into account the AFTA results for the JE Haley 24-1 well, where maximum burial for the well was achieved around 55-50 Ma as a consequence of 6890ft (2.1km) of additional burial. The model was changed by adding 6890 ft (2.1 km) of Late Triassic, Cretaceous and Palaeocene sediments prior to 55 Ma, and then uplifting the section to remove the additional 6890 ft of overburden. The results (Fig 4.24) highlight that if the section did experience around 6890 ft (2.1km) of greater burial prior to uplift as suggested by AFTA, that is enough to explain the higher maturity shown by the vitrinite.

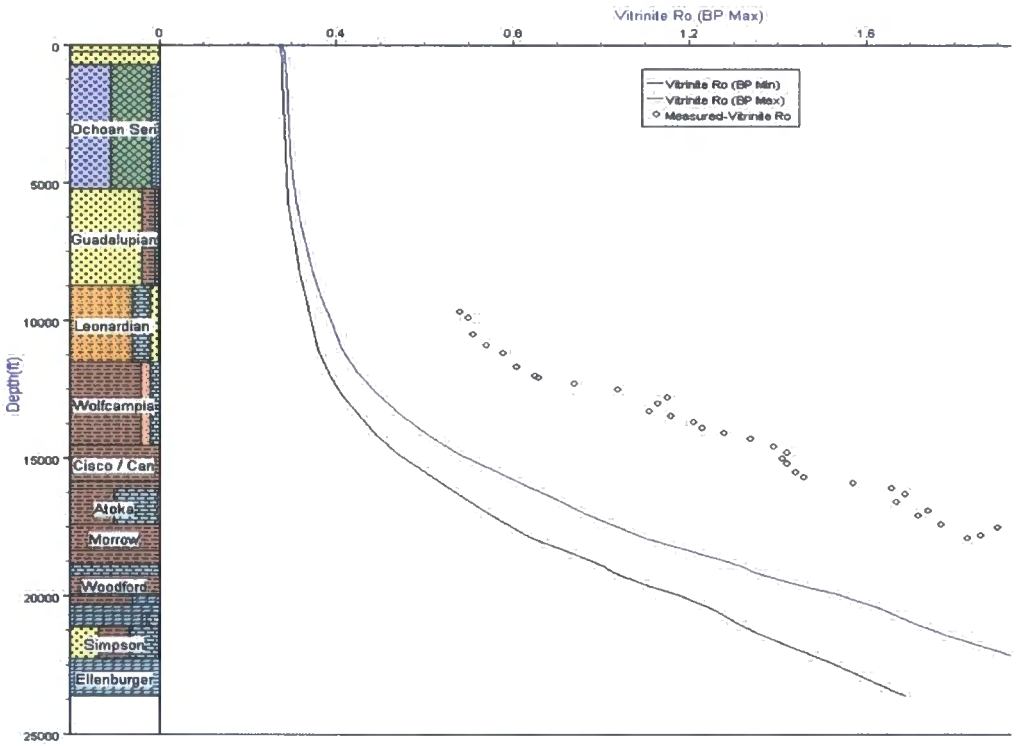

Fig. 4.23. A plot of vitrinite reflectance (VR) against depth for the JE Haley 24-1 well using a 1D model where all preserved strata are at their maximum burial at present day. The lines indicate the proposed maximum and minimum VR values for the depth of burial.

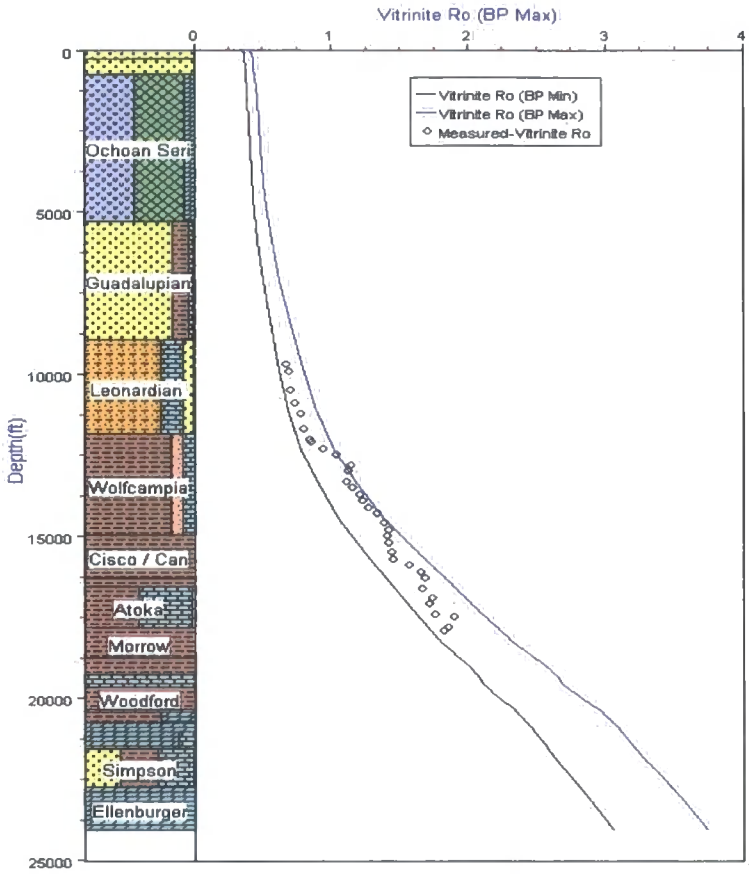

Fig. 4.24. Plot of vitrinite reflectance against depth for the JE Haley 24-1 well, where the section has been buried by a further 6890ft (2.1km), and subsequently uplifted. The extra burial is enough to explain the higher maturity recorded by the vitrinite.

Vitrinite reflectance analysis was also done on 12 other wells in the Delaware Basin and one other in the Midland Basin (sub-chapter 4.2.2.1. and Fig 4.22). The results (Fig 4.25) were plotted on a typical VR versus depth plot where VR is on a logarithmic scale. Extrapolating the best-fit linear line to the elevation where the VR value is 0.2 %Ro, and measuring the height difference between this elevation and the present day surface gives the amount of predicted uplift.

The results show two distinct linear best-fit lines through the data, where two wells (Homer Cowden A-1 and Culberson Fee L-1) are significantly more thermally mature for their depth of burial than the other wells. This is most likely because those two wells are located on the western edge of the basin which has been uplifted due to tilt more than the centre of the basin (Fig 4.26), and so for the equivalent depth of burial they appear more thermally mature than the other wells. All the wells,

however, show evidence of greater burial, with present day surface VR values of 0.25 %Ro and 0.5 %Ro, suggesting exhumation of 2000 ft (600 m) and 5500 ft (1.6 km) for the wells in the centre and the two wells on the edge respectively. This estimate of exhumation for the wells is highly dependent on how the best-fit line is interpreted, and therefore there is potential for large variations in the estimates.

4.2.2.3 Summary of vitrinite reflectance data

1D modelling of the vitrinite reflectance data from the JE Haley 24-1 well, clearly indicate that the sediments are more thermally mature than expected for their depth of burial. The high maturity can be explained if the basin experienced greater burial by an additional 6890 ft (2.1 km) of sediment.

Plots of the vitrinite reflectance data from all the wells also show that the basin is more thermally mature; however, estimates of removed section would be vague as each is dependent on the interpretation of a best-fit line. Consequently, these vitrinite reflectance results should be interpreted solely to demonstrate that sediments on the western edge of the basin appear to be more thermally mature for their depth of burial compared to sediments in the centre of the basin. This can be explained because the western edge has experienced greater uplift than the centre, and so the sediments on the western edge appear to be more thermally mature than the depth equivalent sediments in the centre of the basin because they have experienced greater burial.

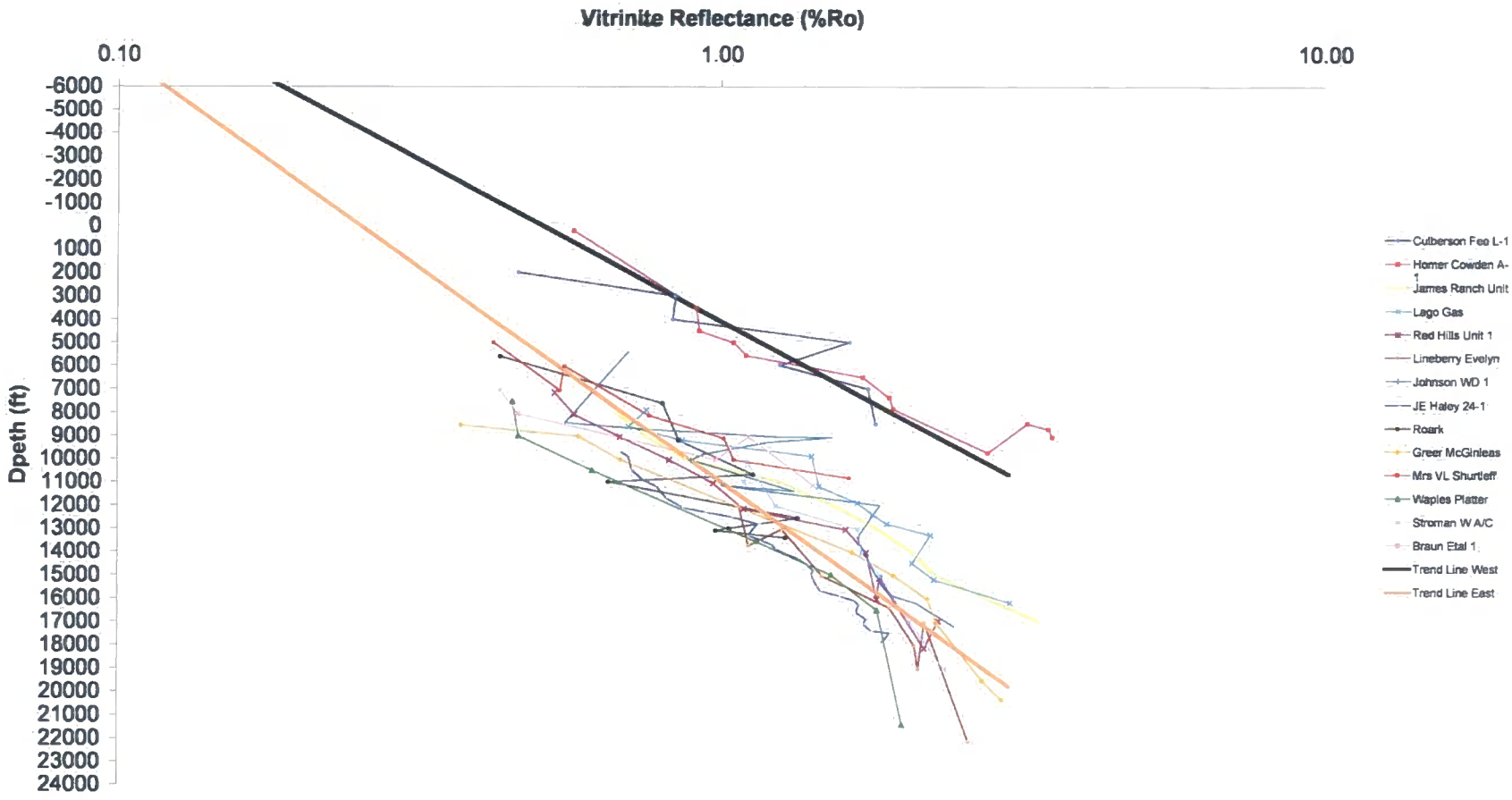

Fig 4.25. Vitrinite reflectance plots versus depth for 13 wells in the Delaware Basin, and 1 well (Braun Etal 1) in the Midland Basin (refer to Fig 4.22). Two distinct best-fit lines through the results can be identified. Each line is suggestive of greater burial in the past. The greater maturity seen in the wells Homer Cowden A-1 and Culberson Fee L-1 is because they have experienced greater uplift by being located on the western edge of the basin, in comparison to the centre of the basin for the other well.

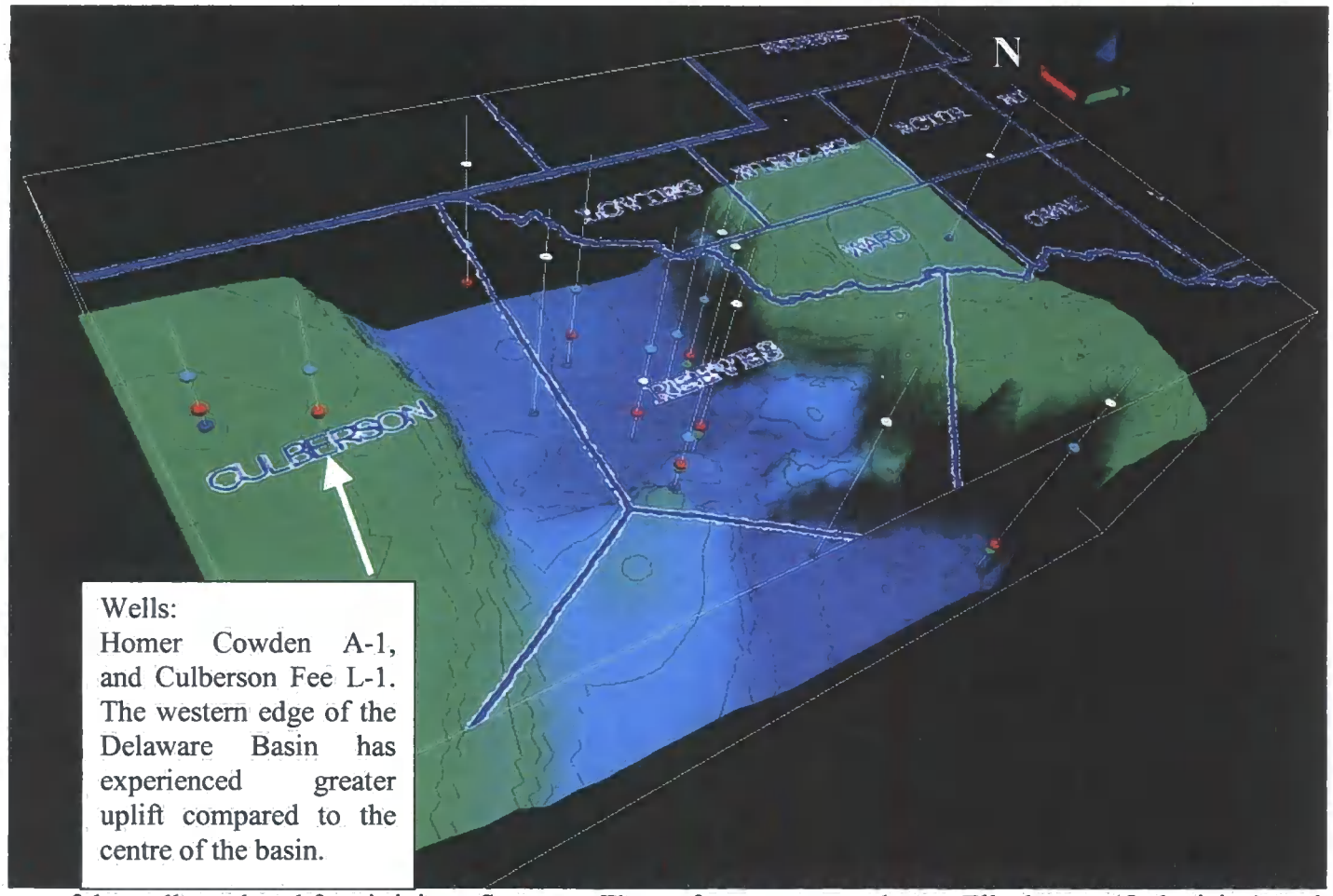

Fig 4.26. 3D map of the wells analysed for vitrinite reflectance. The surface represents the top Ellenburger (Ordovician) to show the geometry of the basin. The western edge of the basin is clearly significantly more uplifted due to tilt than the centre of the basin, hence the two wells Homer Cowden A-1 and Culberson Fee L-1 appear more thermally mature for the depth of burial than the other wells.

4.2.3 Integration of AFTA, vitrinite reflectance and rock-eval T-max data

As part of their analysis for this project, Geotrack also analysed vitrinite reflectance (VR) data and rock-eval T-max data from the JE Haley 24-1 well. This was done for correlation with the AFTA results to check that the estimation of maximum palaeotemperature from AFTA is in agreement with other thermal indicators. Also combining VR and rock-eval data with the AFTA results will give a greater spread of data through the well, because the AFTA samples were only from the shallow Delaware Group whereas VR and rock-eval data extend down to strata of Pennsylvanian age.

In sub-section 4.2.2.2 vitrinite reflectance data from the JE Haley 24-1 well were used in a 1-D modelling program to show that 6890ft of extra burial prior to the first uplift event (55 Ma) can explain the high thermal maturity shown by the vitrinite reflectance. Geotrack also interpreted the VR data from the JE Haley 24-1 well and came to the same conclusion. However, Geotrack noted that the VR data for the Bone Spring Formation plots on, or very close to, the default history vitrinite reflectance profile (Fig 4.27), so suggesting that the Bone Spring Formation is at maximum palaeotemperatures at present day. By plotting VR data derived from the AFTA results (especially sample GC930-1 where a definite value can be given) and rock-eval pyrolysis Tmax data, it can be seen that the VR data for the Bone Spring are anomalously low, and the true maturity trend is the same as the VR data for the Wolfcampian Series and the Pennsylvanian (Fig 4.27). The anomalous VR is thought to be caused by some form of geochemical suppression or misidentification of the vitrinite maceral (Duddy 2006). There are also anomalously low T-max data starting at around 4000 m, where the decline is explained due to contamination of the rock-eval samples by oil-based drilling mud that was introduced at 12856 ft (3918 m). Overall, the data show evidence that the section experienced greater palaeotemperatures in the past.

Maximum palaeotemperature estimates can also be determined from the rock-eval data in the Bone Spring Formation and the VR from the Early Permian Wolfcampian Series and the Pennsylvanian strata (Fig 4.28). The results are very

consistent with the AFTA results shown in sub-section 4.2.1.6.1, where maximum temperatures were reached at some time between 125-50 Ma.

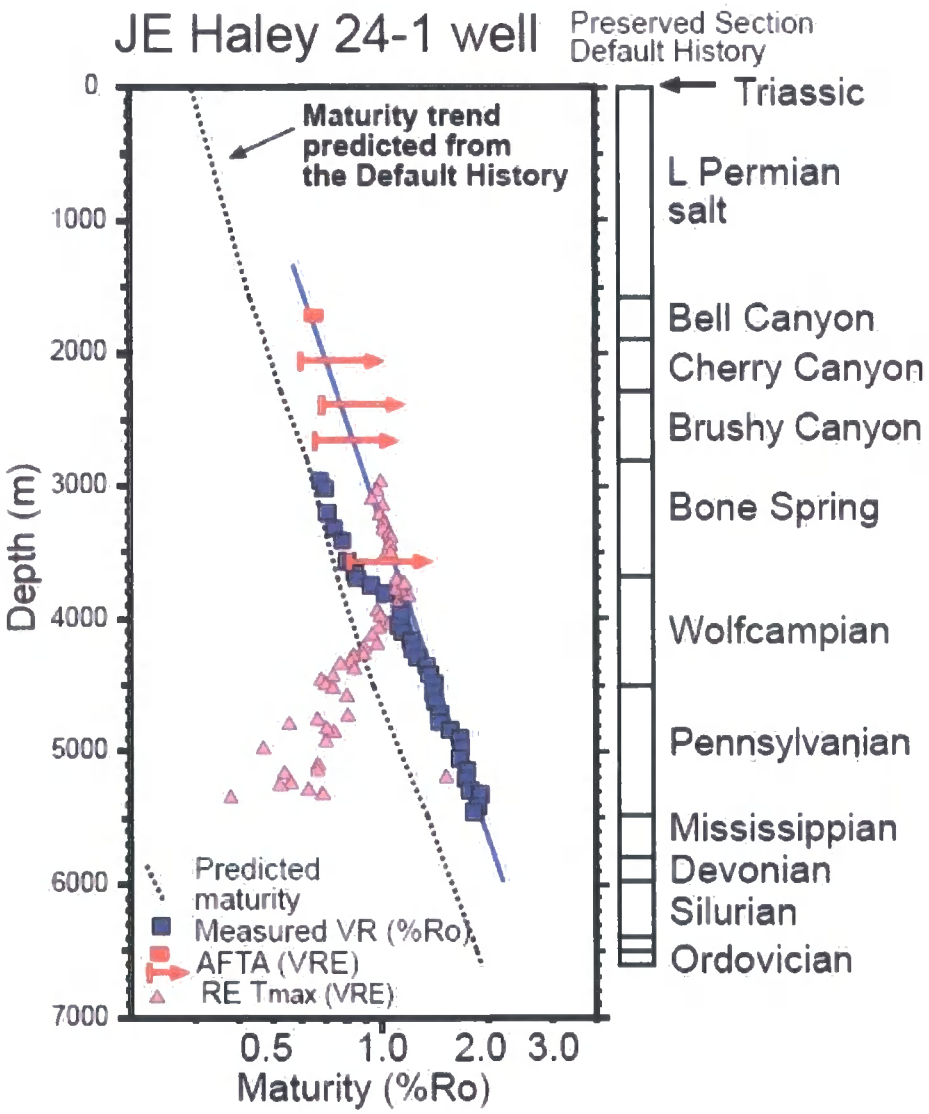

Fig 4.27. Thermal maturity plot of the JE Haley 24-1 well, using true vitrinite reflectance data from the well, vitrinite reflectance data derived from the AFTA results, and rock eval T-max data. The true maturity trend for the JE Haley 24-1 well is marked by the blue line based on the given maturity data. This maturity trend is higher than the predicted maturity trend, indicating that the section has experienced greater palaeotemperatures. The anomalous VR data for the Bone Spring may be explained by geochemical suppression or misidentification of the vitrinite maceral. The anomalous Tmax data coincides with where oil-based drilling mud was introduced in the well. (Taken from Duddy 2006).

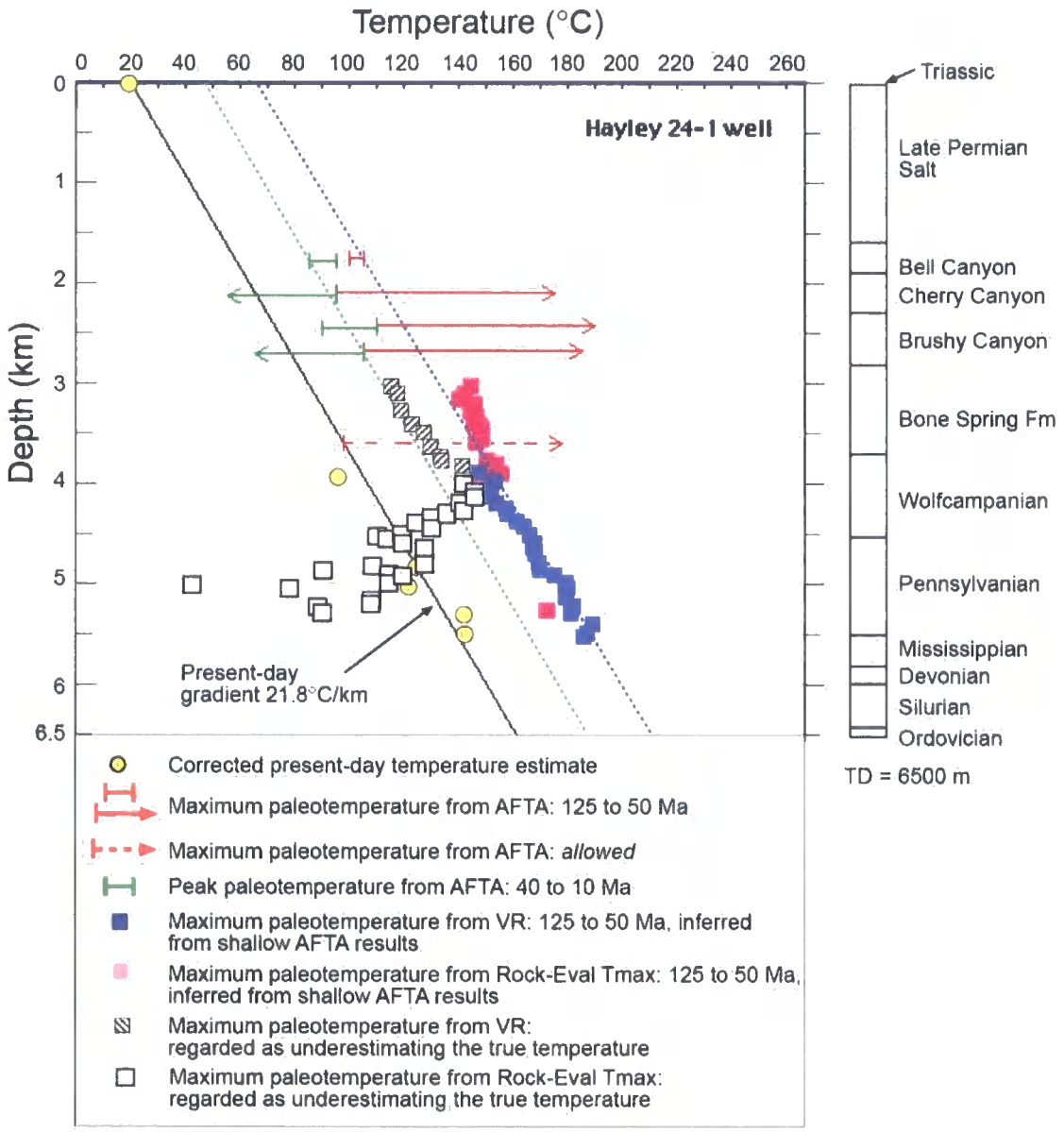

Fig 4.28. Palaeotemperature constraints derived from AFTA, VR and Rock-eval pyrolysis for the JE Haley 24-1 well. Maximum temperatures were reached some time around 125-50 Ma. (Taken from Duddy 2006).

4.2.4 Shale Compaction Curves

Another method for estimating palaeoburial is by using shale compaction curves. Progressive burial of a mudrock will result in an increase in vertical stress, resulting in compaction and a subsequent loss of porosity. Porosity-depth relationships for shales have been studied by numerous authors (e.g. Chilingarian 1974), and vary from one study area to the other (Fig 4.29). They are dependent on a number of factors: a) geological age, b) effective stress, c) lithology, d) mineralogy, e) tectonic stresses, f) speed of deposition, g) thickness of sedimentary formations, h) sorting, i) amount and nature of cement, j) chemistry of pore fluid (Dzevanshir *et al* 1986).

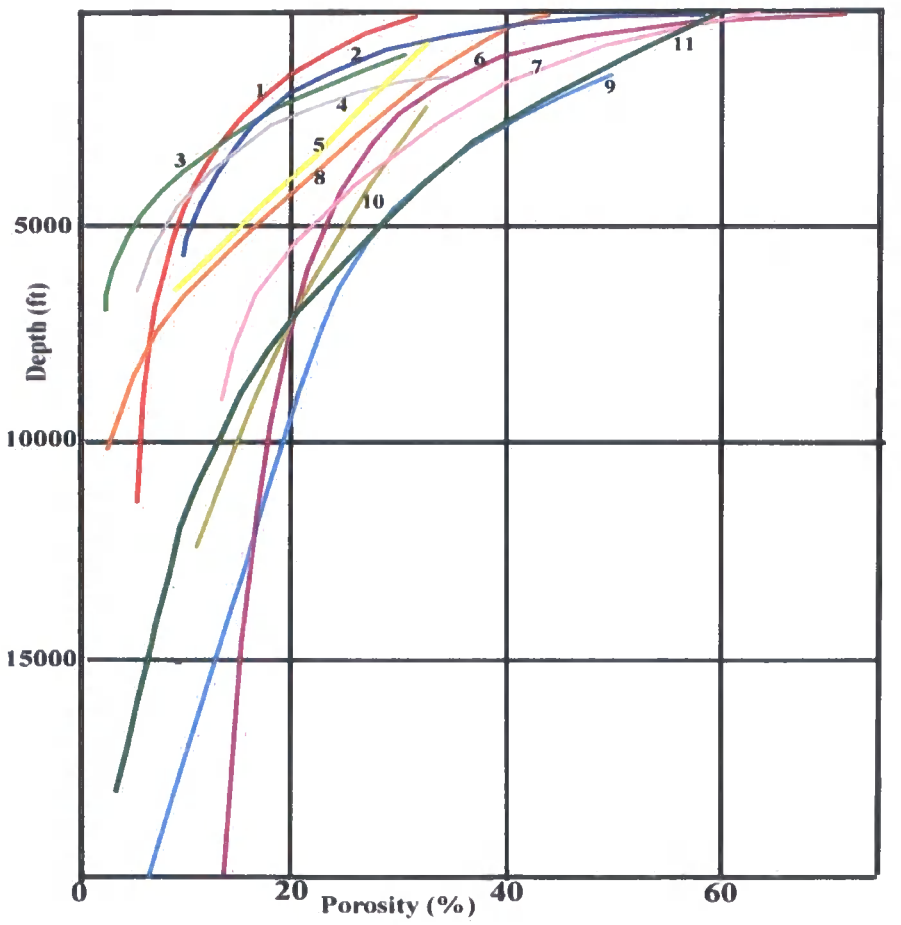

Fig 4.29. Relationship between porosity and depth of burial for shales. 1= Proshlyakov (1960); 2 = Meade (1966); 3= Athy (1930); 4 = Hosoi (1963); 5 = Hedburg (1936); 6 = Dickinson (1953); 7 = Magara (1968) ; 8 = Weller (1959); 9 = Ham (1966); 10 = Foster and Whalen (1966); 11= compaction curve used for this study. Taken from Dzevanshir, R.D., et al 1986.

The earliest compaction law was introduced by Athy (1930):

$$\Phi = \Phi o e^{-cz} \quad (4.1)$$

where:

Φ = porosity at depth z,

Φo = surface porosity,

c = compaction coefficient constant.

Hubbert and Rubey (1959) modified Athy's compaction law by substituting the depth (z) with vertical effective stress (σv) to reflect the changes of porosity due to loading stress rather than burial depth:

$$\Phi = \Phi o e^{-c\sigma v} \quad (4.2)$$

The pore pressure prediction software 'presgraf' is used in this study to analyse shale compaction in the Delaware Basin. The compaction curve used by 'Presgraf' is based on Hubbert and Rubey's porosity-depth relationship, but uses the mean effective stress instead of the vertical, which assumes that horizontal stresses also affect compaction not just vertical loading:

$$\Phi i = \Phi o e^{-c\sigma m} \quad (4.3)$$

where:

Φi = porosity at infinite stress,

Φo = surface porosity,

σm = mean effective stress, and

c = compaction coefficient constant.

The variables for this normal compaction curve are VClay (volume of clay), Φo (surface porosity) and the compaction coefficient. It needs to be noted that a

normal compaction curve will vary for every unit of sediment within a basin, due to differing clay fraction and cementation factors.

In order to utilise shale compaction curves to analyse the Delaware Basin's burial history, a shale compaction curve is first constructed using the sonic travel time values of shales through the JE Haley 24-1 well in Loving County using the pressure prediction software "presgraf" (Fig 4.30). The resulting plot shows three potential normal compaction curves through the well; the Delaware Group, Upper Bone Spring Formation and the Bone Spring 3rd Sand Unit. (Fig 4.30). Through well test pressure data, it is known that the Bone Spring 3rd Sand Unit is normally pressured at present day in the basin, and the first sign of overpressure is in the underlying Wolfcampian Series. Therefore for this study, it is taken that the assigned normal compaction curve for basin should run through the Bone Spring 3rd Sand Unit. Through the use of mercury injection porosimetry analysis on shales of the Bone Spring 3rd Sand Unit which was undertaken as part of this research, a porosity value of 10% can be assigned to these shales. Also assuming an initial starting porosity of 60%, a porosity-depth curve can be produced using the Hubbert & Rubey relationship (Equation 4.3) (Fig 4.29 and Fig 4.30).

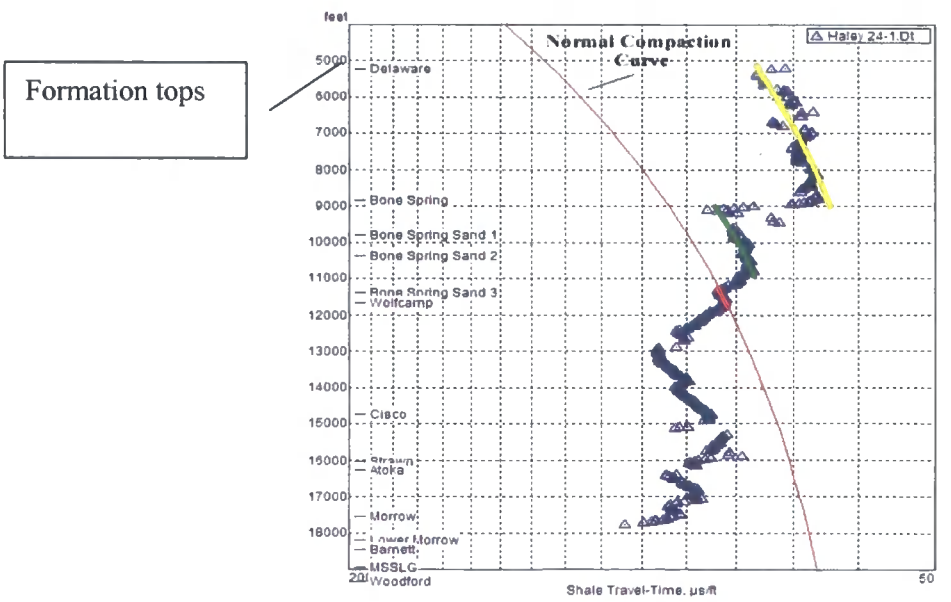

Fig 4.30. Shale compaction curve for the JE Haley 24-1 well. The presgraf assigned normal compaction curve (based on Hubbert and Rubey's (1959) compaction relationship), indicates that the shales of the Bone Spring 3rd Sand Unit are normally compacted at present day.

As can be observed from the compaction curve (Fig 4.30), the majority of the shales do not plot on the assigned normal compaction curve. For instance, the shales of the Wolfcampian Series plot to the left of the normal compaction trend. Three processes can explain these deviations. If the deviation is to the left of the normal compaction curve, then this could be due to excess pore pressure, where the shales have a higher porosity for their depth of burial. If the deviation is to the right of the normal compaction curve, that indicates the shales have low porosity for their present depth of burial. This could be due to either porosity loss through cementation, or it could indicate that the shale has been more deeply buried in the past and has experienced uplift (Fig 4.31). In the Delaware Basin, this is the case in both the Delaware Group and the Upper Bone Spring Formation where they have clear compaction trends but the trends are shifted to the right of the normal compaction curve (Fig 4.30 – yellow and green trend). The results (section 4.2.4.1) will analyse whether these trends could be palaeo-compaction trends from past maximum burial episodes.

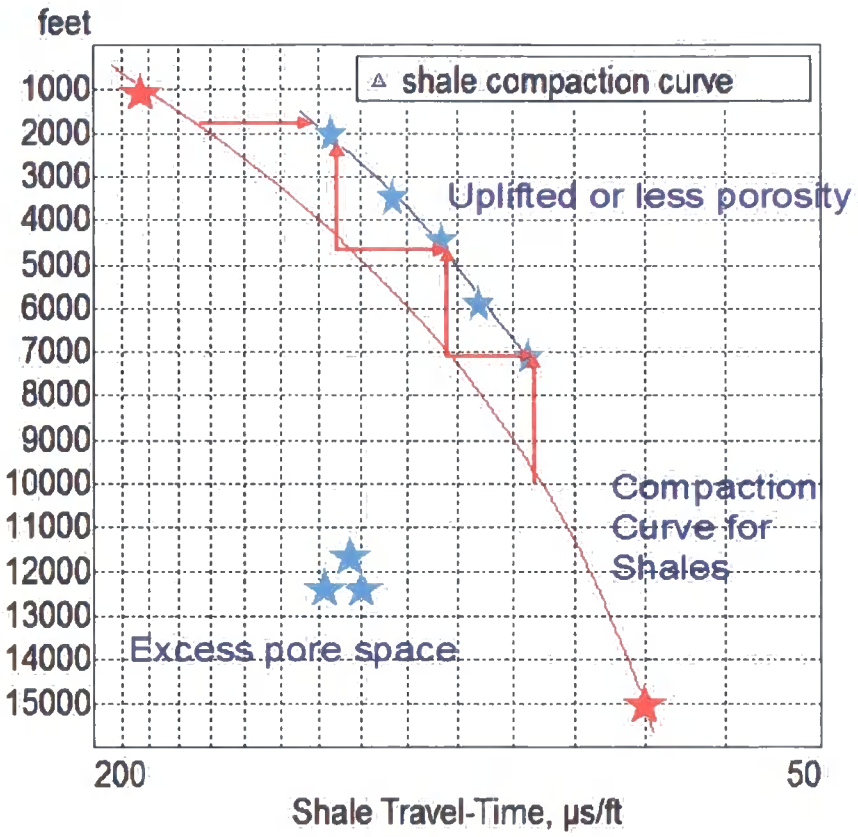

Fig 4.31. Schematic diagram of a shale compaction curve. If shales plot below the normal compaction curve (red curve) they can be interpreted as having a high porosity for their depth, i.e. the shales could be overpressured. If the shales plot above the normal compaction curve, then they have low porosity for their depth. This could mean that there is some secondary porosity loss such as cementation, or they have been at a greater burial depth in the past.

Chapter 3 showed that for the JE Haley 24-1 well, the overpressure in the well is isolated in the Early Permian Wolfcampian Series down to the Mississippian Limestone Formation, whereas the overlying Delaware Group and Bone Spring Formation are normally pressured. This is in agreement with what the shale compaction curve of the JE Haley 24-1 well shows. All the shales below the Bone Spring Formation have high porosity for their depth of burial, and are overpressured. Pore pressure with relevance to wireline logs will be dealt with in more detail in chapter 5. This chapter is more concerned with interpreting the shale compaction profiles of Upper Permian Delaware Group and Bone Spring Formation, in terms of

the Delaware Basin's palaeoburial and uplift history. The questions addressed in this chapter are:

1. Are the shales of the Delaware Basin at maximum burial at present day? If so the shales of the Delaware Group and Upper Bone Spring Formation are significantly more compacted than expected.
2. If the basin has experienced deeper burial in the past, do the compaction curves in the shales of the Delaware Group and Bone Spring Formation represent palaeo normal compaction curves, and does the vertical difference between their present location and the normal compaction curve represents the amount of uplift?

4.2.4.1 Results from shales compaction curve analysis

Utilising the AFTA and vitrinite reflectance (VR) results from the JE Haley 24-1 well, it has been shown that the basin is not at maximum burial at present day, which answers question 1 above. AFTA showed that assuming a palaeogeothermal gradient of 21.8 ^{o}C/km, the JE Haley 24-1 well experienced maximum burial 55 Ma due to an additional 6890 ft (2.1 km) of Mesozoic and Cenozoic sediment. The VR results also suggest that the basin is more thermally mature, and by using a 1D model, 6890 ft of extra burial is enough to explain the high maturity levels.

If shale compaction curves are to be used to quantify uplift, then the assumption that shale compaction is irreversible must be made, i.e. if uplift occurs, then there is negligible elastic rebound or rock dilation (Swarbrick & Osborne 1998). This would mean that at maximum burial the shale would reach a degree of compaction in accordance to its compaction curve. If the shale were then uplifted, its degree of compaction would not change, hence acting as a record of its maximum burial. Numerous experiments have been conducted to analyse mudstone dilation, with Karig and Hou (1992) concluding that compaction is nearly irreversible, however, another study suggests that compaction is reversible (Neuzil & Pollock 1983). One factor which would reduce the amount of dilation is the degree of initial burial and compaction and cementation of the mudstones (Swarbrick & Osborne

1998). The mudstones in the Delaware Basin are heavily compacted with calcite cement being a common feature, suggesting that rebound of the mudstones may not be applicable for this basin.

Based on the results from AFTA and the assumption made above, the present day compaction curve (Fig 4.32 – blue triangles) for the JE Haley 24-1 well was shifted vertically down by 6890 ft (2.1 km) to see if the compaction curve of the Delaware Group represents normal compaction at maximum burial 55 Ma (Fig 4.32 – red circles). The results show that the Delaware Group compaction curve falls very close to the normal compaction curve at that depth, and is just shifted to the right indicating that the shales are still more compact. This deflection could be explained by porosity loss in the Delaware Group through calcite cementation. Thin section analysis of a sand in that Delaware Group indicates that calcite makes up ~20% of the petrology (Fig 4.33), and could explain why the Delaware Group has a lower porosity for its depth. It also needs to be noted that the normal compaction curve used is based on the Lower Bone Spring Formation, and every formation will vary in composition and hence have a differing normal compaction curve. Consequently, it is more than likely that the compaction trend associated with the Delaware Group is representative of maximum burial in the Delaware Basin 55 Ma, where there was an additional 6890 ft of Mesozoic and Cenozoic sediment.

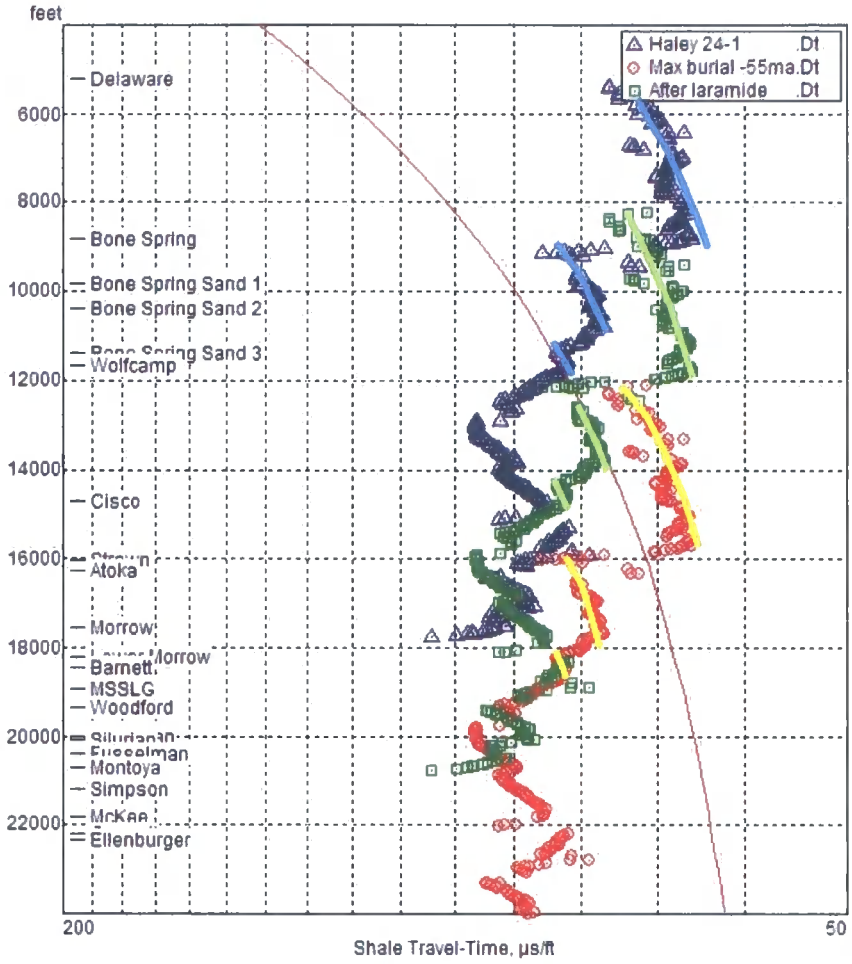

Fig 4.32. Shale sonic data from the JE Haley 24-1 well at present day depth of burial (blue triangles) The data are then dropped vertically down 6890 ft (2.1 km) to represent maximum burial 55 Ma (red circles). The data are then uplifted by 3890 ft to represent the first uplift phase (green squares), when the data for the Upper Bone Spring Formation fall on the normal compaction curve.

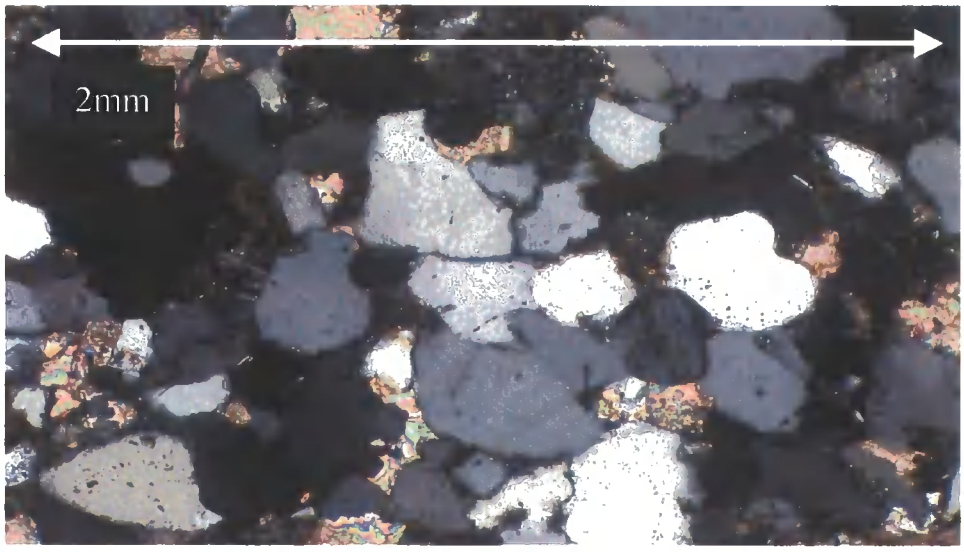

Fig 4.33. Thin section in cross-polarised light of sandstone from the Delaware Mountain Group. The sample contains ~20% of calcite

The compaction trend of the Upper Bone Spring Formation may also represent a palaeo normal compaction curve, and could indicate the period of quiescence after the first uplift phase and then it could give an indication of the amount of uplift the basin experienced in the first cooling episode (55-50 Ma) which could not be uniquely quantified by AFTA but where the range was a minimum amount of 3290 ft (1 km) and a maximum amount of 6890 ft (2.1 km) (refer to sub-section 4.2.1.8 and Fig 4.18). To answer this, the shale compaction curve is then shifted vertically up from its maximum burial position so that the compaction curve of the Upper Bone Spring shales falls on the normal compaction curve (Fig 4.32 – green squares). This represents an uplift of 3890 ft (1185 m), which fits in with scenario three of the possible AFTA burial history scenarios (refer to sub-section 4.2.1.8 and Fig 4.18).

In conclusion, the three shale compaction curves of the Delaware Mountain Group, Upper Bone Spring Formation and Lower Bone Spring Formation could be representative of the time of maximum burial, the period of quiescence after the first uplift event, and present day burial after the second uplift event. Consequently, the difference in depth between the three compaction curves will indicate the amount of uplift that has taken place between each event, and more importantly be able to quantify the amount uplift in the first event, which AFTA could not quantify.

4.2.5 Summary of analysis results

A new burial history scenario is devised for the Delaware Basin

- The sediments in the Delaware Basin have a high thermal maturity for their present depth of burial as shown by AFTA and vitrinite reflectance data.
- Both the AFTA and vitrinite reflectance results from the JE Haley 24-1 well show that in order to achieve the high maturity of the sediments, an additional 6890 ft (2.1 km) of Mesozoic and Cenozoic sediment are needed prior to Cenozoic uplift.
- From the AFTA results the time of maximum burial and the first uplift event was estimated to be around 55 – 50 Ma. AFTA results also uniquely defined a second cooling event 25 – 10 Ma, when there was 3600 ft (1.1 km) of exhumation. It needs to be noted that all AFTA results are dependent on temperature, and for this analysis a palaeogeothermal gradient of 21.8 °C/km was used which is the same as the present day geothermal gradient.
- AFTA is, however, unable to constrain what happened between the two events, which led to three possible scenarios being suggested (refer to section 4.2.1.8 and Fig 4.18).
- Three normal compaction curves can be identified in the shale compaction curve of the JE Haley 24-1 well. These have been interpreted as representing palaeo-normal compaction curves (refer to Fig 4.32).
- The normal compaction curve of the Delaware Group represents normal compaction at the time of maximum burial (55 Ma), and the compaction curve of the Upper Bone Spring Formation represents normal compaction in the period of quiescence after the first uplift event.
- Compaction curves were therefore able to quantify that 3890 ft (1.2 km) of uplift occurred in the first cooling event 55 Ma.
- A new model for the burial and tectonic history of the basin based on results from the JE Haley 24-1 well is therefore suggested (Fig 4.34).
- A new burial history curve is consequently proposed for the Delaware Basin (Fig 4.35). It varies significantly from the burial history curves suggested by Luo et al

(1994) and Barker & Pawlewicz (1987) (refer to Fig 4.1 and Fig 4.4 respectively).

- The timing of each uplift phase corresponds perfectly to two known tectonic events that affected the area at this time:
  - 55-50 Ma – The Laramide Orogeny
  - 25-10 Ma – Basin and Range extension and associated uplift

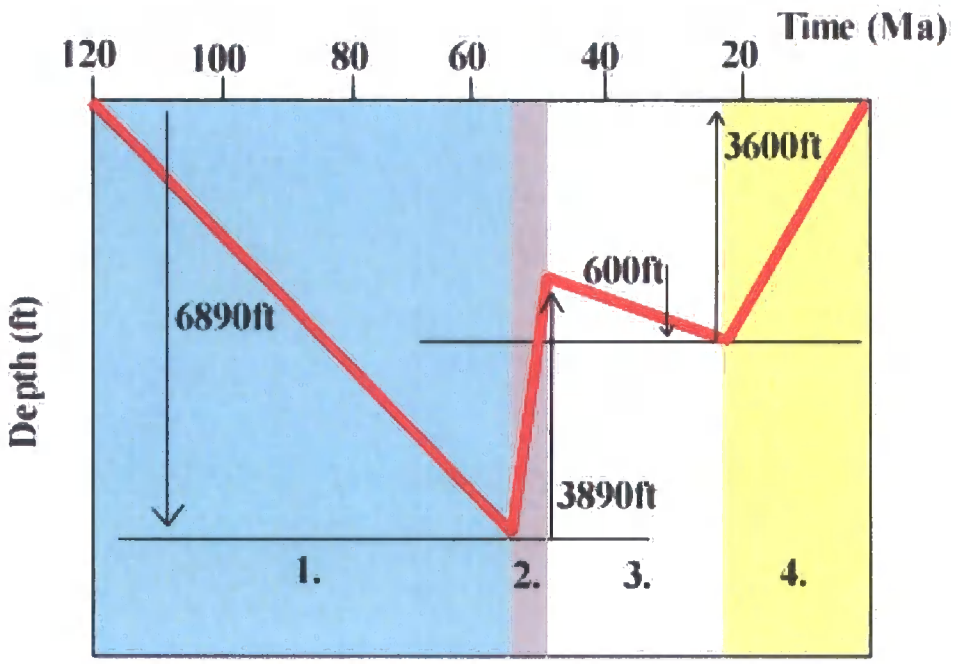

Fig 4.34. A simplified burial history plot for the JE Haley 24-1 well, where two uplift phases and one burial phase have been uniquely defined by AFTA, vitrinite reflectance (VR) and shale compaction data. Episode 1 (blue) represents maximum burial 55 Ma constrained by AFTA and VR data, where an additional 6890ft of sediment is needed to explain the high thermal maturity of sediments recorded in the well. Episode 2 (grey) represents 3890ft of uplift in the 1st cooling event (55-50 Ma) constrained by shale compaction curves. Episodes 3 and 4: AFTA is able to uniquely define the last uplift event (25-10 Ma) and so, 600ft of subsidence and burial is needed during the Oligo-Eocene in order to explain the previous three events.

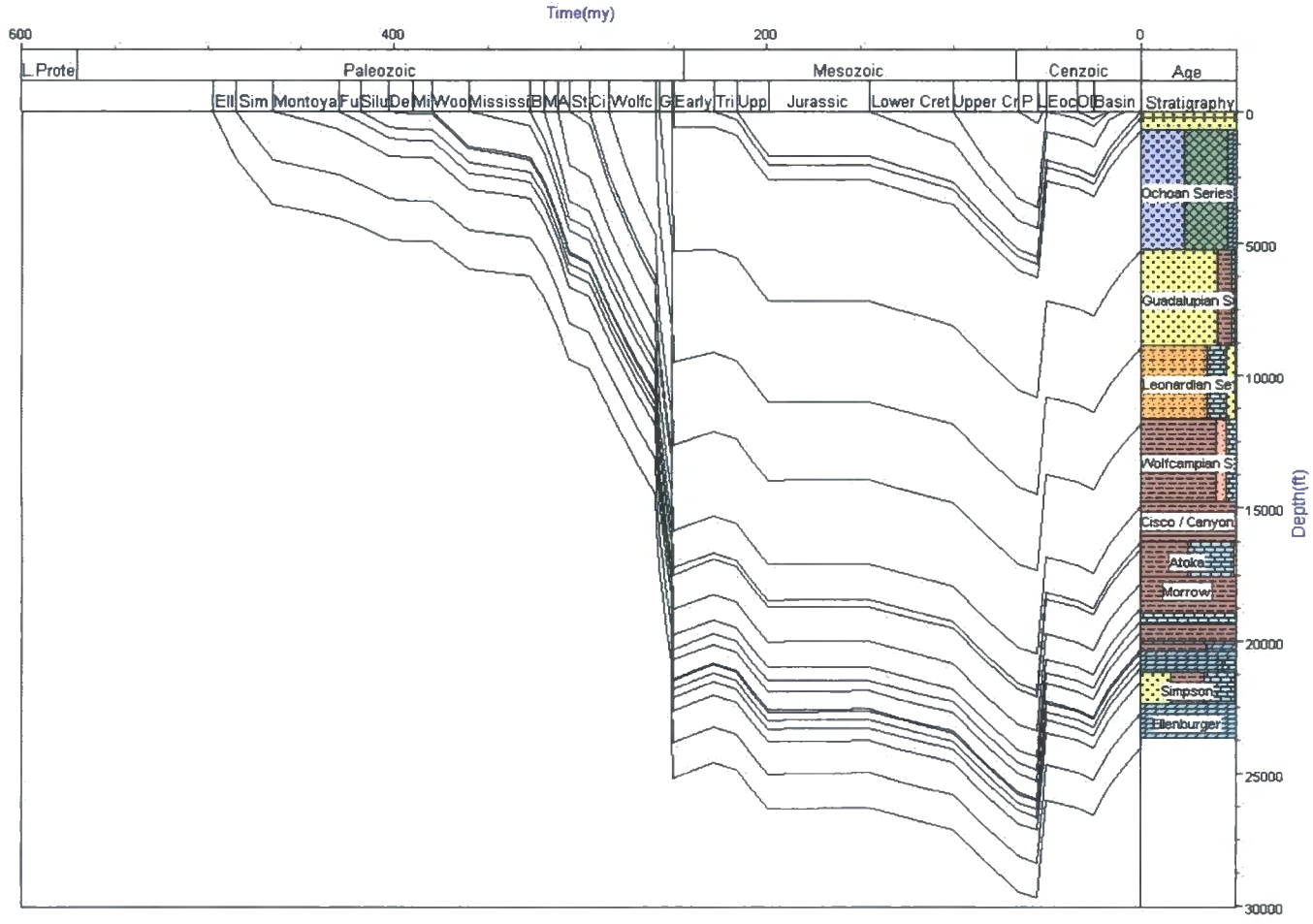

Fig 4.35. A new burial history curve for the JE Haley 24-1 well in the centre of the basin. Maximum burial occurred at the end of the Palaeocene, with two phases of uplift identified in the Cenozoic.

4.3 Discussion: Mesozoic and Cenozoic burial history of the Delaware Basin

From the AFTA, vitrinite reflectance and shale compaction results, a revised burial history has been suggested for the Delaware Basin which is significantly different to previously suggested burial history curves of the basin (Luo et al 1994, and Barker & Pawlewicz 1987). This research suggests that during the Cenozoic and Mesozoic an additional 6890 ft (2.1 km) of sediment was deposited on top of the preserved Triassic, which is seen in the basin today. This contradicts suggestions by numerous authors (Barker & Pawlewicz 1987; Luo et al 1994; Alton-Brown 2004) who proposed Mesozoic deposition of no more than 1640 ft (500m).

This research also shows that during the Cenozoic there were two prominent uplift episodes that affected the basin. The first uplift event (the Laramide orogeny 55-50 Ma) removed 3890 ft (1.2 km) of sediment, then the basin subsided and accumulated another 600 ft (200 m) of sediment, and then the second uplift and cooling phase (the Basin and Range event 25-10 Ma) eroded off a further 3600 ft (1.1 km) of sediment. Again these results do not fit with what previous papers have suggested. Luo et al (1994) suggested there was zero uplift of the basin during the Cenozoic, whereas Barker and Pawlewicz (1987) suggested 3000 ft (900 m), which is less than half the estimate here.

The other area of controversy in the literature concerns which uplift event tilted the basin. Gregory & Chase (1992) and Hill (1996) conjectured that all the tilt and subsequent uplift of the western edge is attributable to the Laramide compression, whereas Horak (1985) and Barker & Pawlewicz (1987) suggested that half of the 7500 ft (2.2 km) of overall flank uplift is due to Laramide compression, and the other half due to Basin and Range. At the other extreme, Elston (1984) and Sahagian (1987) suggested that isostatic uplift associated with the Basin and Range extension could be as much as 6500 ft (2 km).

These three areas of uncertainty are discussed in the following sub-sections.

4.3.1 Determining the palaeogeothermal gradient

This research (sub-section 4.2.5) agrees with Barker & Pawlewicz (1987) and Alton-Brown (2004), who stated that the sediments in the Delaware Basin are too thermally mature for their depth of burial and present geothermal gradient. The results from this research (sub-section 4.2.5) suggest that the high thermal maturity seen in the sediments is a consequence of 6890 ft (2.1 km) of additional burial where the geothermal gradient remained constant through time at 21.8 °C/km. This conflicts with the theories proposed by Barker & Pawlewicz (1987) and Alton-Brown (2004) as to why the sediments have a high thermal maturity. In contrast to the additional burial model as proposed by this research, those authors suggested that a higher palaeo-heat flow is the cause and that a significant amount of extra burial is not needed.

4.3.1.1 Higher heat flow during the Triassic (Alton-Brown 2004)

Alton-Brown (2004) used present day heat flow data and the preserved stratigraphy to model the thermal maturity of the Tubbs well in Winkler County which is located in the centre of the Delaware Basin and is stratigraphically very similar to the JE Haley 24-1 well used in this research. For the 1D model, Alton-Brown (2004) used a present day heat flow of 48 MW/m^2, and that Late Cenozoic tilting of the basin removed 980 ft (300 m) of Late Cretaceous sediment. This initial model significantly underestimates the thermal maturity as measured by vitrinite reflectance (Fig 4.36). Alton-Brown's (2004) models show that if burial and uplift are not modified, then a constant heat flow of 75 MW/m^2 is needed to explain the high thermal maturity; however, this overestimates the modern subsurface temperature. If burial is modified and heat flow remains at 48 MW/m^2, then 9800 ft (3 km) of Late Cretaceous deposition and subsequent erosion is needed (Fig 4.36). Alton-Brown (2004) dismissed the idea of greater burial, and instead suggests that

the palaeo-heat flow varied through time so that the thermal maturity developed under higher heat flow.

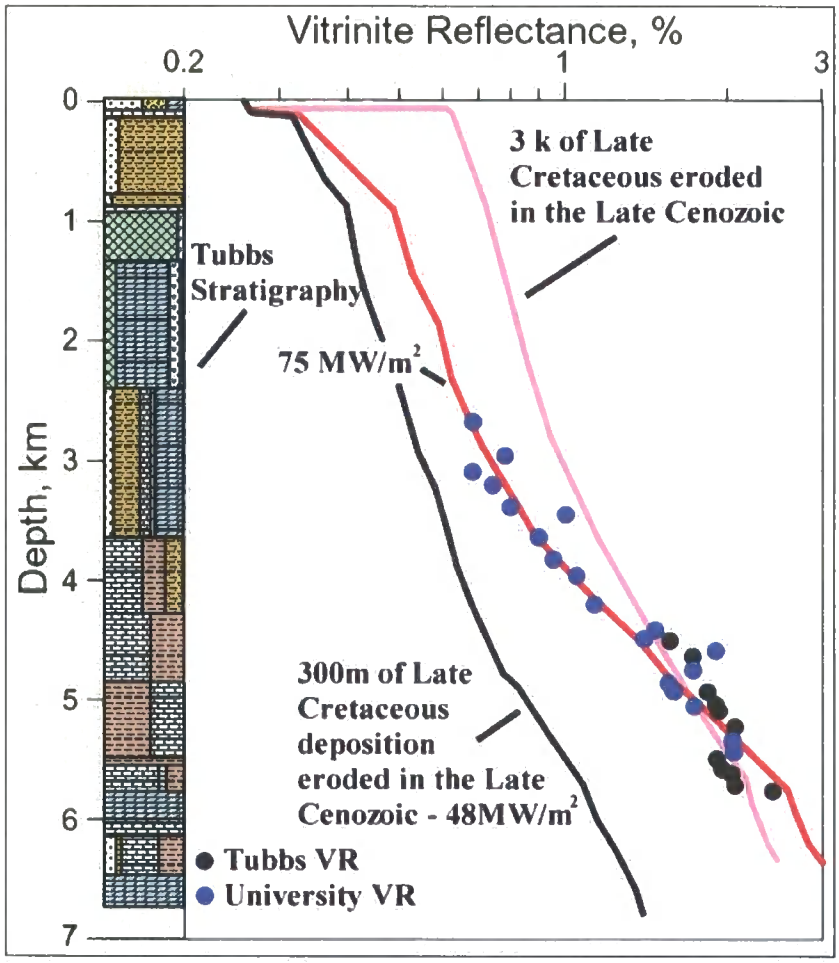

Fig 4.36. Alton-Brown's modelled thermal maturity profiles for the Tubbs well. A present day heat flow of 48 MW/m^2 and 980ft (300m) of Late Cretaceous erosion significantly underestimates the well's thermal maturity. (Taken from Alton-Brown 2004).

Alton-Brown (2004) concluded that the most probable time of heating is a Triassic base-crust tectonic event leading to an Early to Middle Jurassic elevated surface heat flow. The model assumed 980ft (300m) of Late Cretaceous deposition occurred and was eroded during Late Cenozoic basin tilting. Heat flow during the Early to Mid Jurassic reached 85 MW/m^2, which then reduced to the 48 MW/m^2 recorded today in the well. This heat flow model matches the thermal maturity seen in the sediments (Fig 4.37). Alton-Brown (2004) suggested that the Triassic heating

event may have been a consequence either of a short lived period of subduction that would have generated melts that underplated the crust in the Permian Basin area or of southerly absolute plate motion which pushed the southern US over mantle heated by the Early Permian collision.

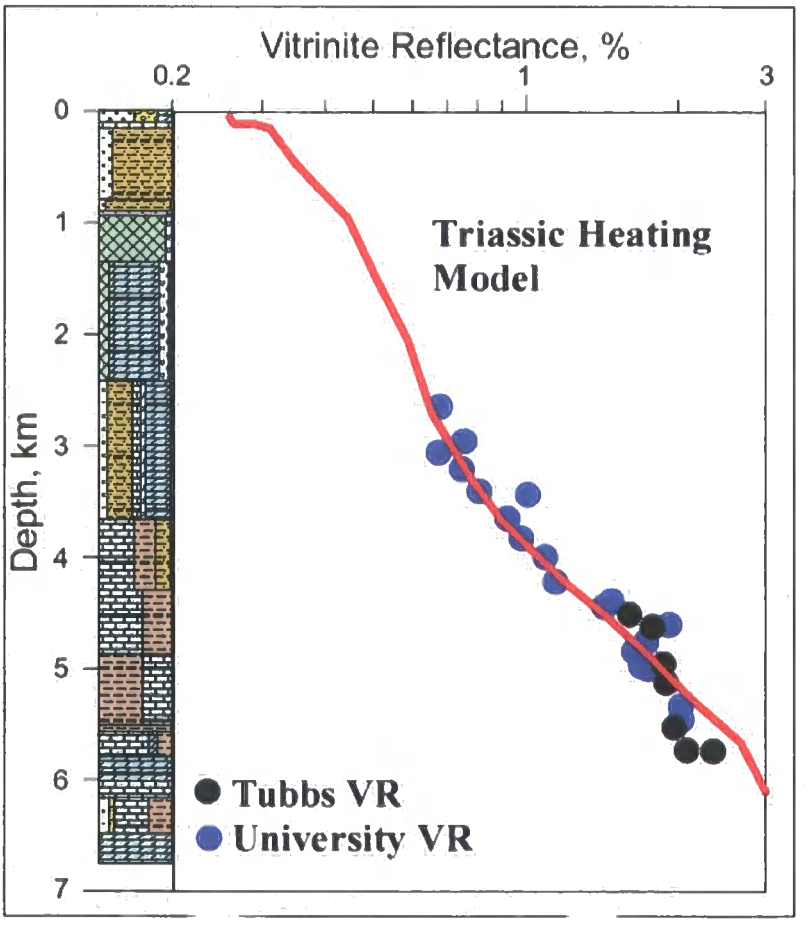

Fig 4.37. Alton Brown's thermal history model for the Tubbs well. The model used a high heat flow of 85 MW/m^2 in the Triassic, which matches the high maturity of the sediments recorded by vitrinite reflectance. Taken from Alton-Brown 2004.

4.3.1.2 Elevated thermal regime during the Tertiary (Barker and Pawlewicz 1987)

Barker and Pawlewicz (1987) also favoured a higher palaeo-heat flow as a mechanism to generate the high thermal maturities seen in the basin and used vitrinite reflectance data as the thermal maturity indicator. Unlike Alton-Brown (2004) who favoured a Triassic heating event, Barker and Pawlewicz (1987) suggested that a higher heat flow existed during the Triassic from the Oligocene through to Late Miocene (33–10 Ma). This was a consequence of a large number of igneous intrusions that were emplaced 33 Ma in the western Delaware Basin and a higher heat flow associated with Basin and Range extension during the Miocene. They suggested that the palaeogeothermal gradient during this time period was up to 50 °C/km.

4.3.1.3 Palaeogeothermal gradient discussion

In contrast to the results published by Barker & Pawlewicz (1987) and Alton-Brown (2004), this research suggests that greater burial did occur in the basin, which would have had the influence of raising the thermal maturity of the sediments. Vitrinite reflectance (VR) was the only method of palaeotemperature estimation used by Barker & Pawlewicz (1987) and Alton-Brown (2004). VR has limitations in that it can only be used to estimate the maximum temperature experienced by the sediments , and that could be a consequence of either greater burial or a higher heat flow. It also cannot put a time frame on the heating episode. Where this research has an advantage over the research undertaken by both Barker and Pawlewicz (1987) and Alton-Brown (2004) is that AFTA was done on samples from the Delaware Basin. AFTA is a definitive research tool for identifying whether sediments are too thermally mature for their present depth of burial, and also for identifying and quantifying phases of uplift and cooling.

The results from the AFTA for this study clearly showed that sediments in the basin are too thermally mature for their present depth of burial. The results also

showed that there were two phases of cooling from maximum palaeotemperatures (55-50 Ma and 25 -10 Ma), indicating that there was greater burial and subsequent uplift of the basin. The amount of burial needed prior to the first uplift event to explain the palaeotemperatures recorded by AFTA, and the amount of uplift experienced in the second event are dependent on the palaeogeothermal gradient. AFTA, however, can put constraints on the maximum palaeotemperatures the sediments may have experienced. With each allowed palaeogeothermal gradient, a differing amount of exhumation was also predicted (Table 4.6).

- Laramide event (55-50 Ma): AFTA allowed a range of palaeogeothermal gradients of 21.5 to 24.5°C/km at 95% confidence limits.
- Basin and Range event (25-10 Ma): AFTA showed that the palaeogeothermal gradient was no more than 22 °C/km at 95% confidence limits.

These results show that even with the highest palaeogeothermal gradient (~25°C/km) allowed, the basin still experienced maximum burial of an additional 4000 ft (1.2 km) of missing sediment prior to the first uplift event (55-50 Ma). This is significantly more than Alton-Brown (2004) used in his 1D modelling, where 980 ft (300 m) of Late Cretaceous deposition and later Cenozoic uplift and erosion was assumed.

The results from the integration of AFTA, vitrinite reflectance and rock eval T-max data, when plotted together (refer to Fig 4.27 & 4.28), show that the palaeotemperature profile was linear and sub-parallel to the present day temperature profile. This indicates that the most likely explanation for the observed heating is deeper burial, and the linear nature of the palaeotemperature profile indicates that a heating pulse is unlikely, which contradicts Alton-Brown's (2004) suggestion.

	Estimates of removed section (metres)	
	Early Cretaceous-Eocene *1 (125 to 50 Ma)	L. Eocene-L. Miocene *1 (40 to 10 Ma)
Maximum Likelihood Estimate	1700	10000
Lower and upper 95% confidence limits	1300 - 2200	1100 - >10000
Fixed paleo-geothermal gradients		
5°C/km	*not allowed*	>10000
10°C/km	*not allowed*	4400-5700
15°C/km	*not allowed*	2250-3150
20°C/km	*not allowed*	1250 -1750
21°C/km	~2200	2100-2700
21.8°C/km	2100 ± 50	1100 ± 150
22°C/km	1950-2050	~1100
25°C/km	~1200	*not allowed*
30°C/km	*not allowed*	*not allowed*
35°C/km	*not allowed*	*not allowed*
40°C/km	*not allowed*	*not allowed*

Table 4.6 Table showing differing exhumation amounts for each episode depending on the palaeogeothermal gradient. This research assumed that the palaeogeothermal gradient remained the same as the present geothermal gradient of 21.8°C/km.

The results also disprove the conjecture of Barker and Pawlewicz (1987) that the palaeogeothermal gradient during the Oligo-Miocene (33-10 Ma) was as high as 50°C/km. According Barker and Pawlewicz (1987), the high palaeogeothermal gradient was a consequence of associated higher heat flow due to igneous intrusions in the western Delaware Basin, and also an associated higher heat flow due to Basin and Range extension. AFTA results from this research show that during the Oligo-Miocene (33-10 Ma) the maximum palaeogeothermal gradient which could have been experienced was only as high as 22 °C/km. Therefore this research suggests that there was no high heat flow associated with the Basin and Range extension, and the igneous intrusions would have had only a localised thermal effect on the stratigraphy

that the intrusion was emplaced into. An example of localised heating due to an igneous intrusion in the western Delaware Basin can be seen in the well Homer Cowden A1, where an igneous sill is emplaced into the Morrow Formation of the Pennsylvanian (Figs 4.38 & 4.39).

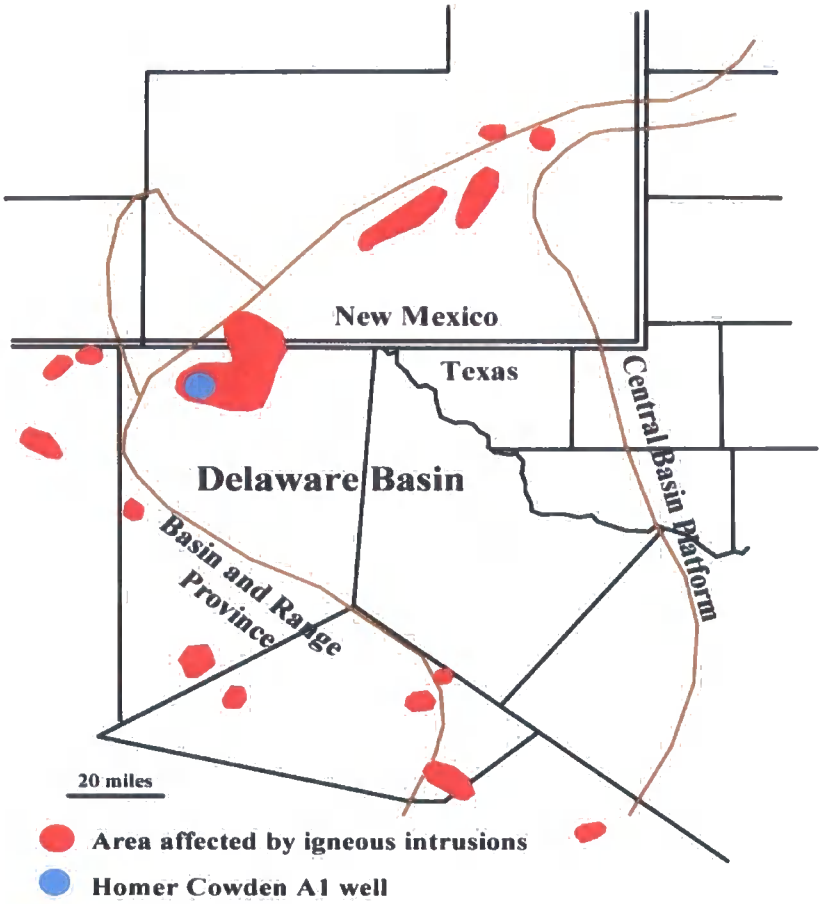

Fig 4.38. Map of the Delaware Basin, highlighting the areas where igneous intrusions have been emplaced, and the location of the Homer Cowden A1 well.

One of Barker and Pawlewicz's (1987) pieces of evidence behind an increased palaeogeothermal gradient due to igneous intrusions in the western basin (Fig 4.38) was that the vitrinite reflectance (VR) in the west of the basin is significantly higher than in the east of the basin, i.e. the sediments appeared more thermally mature in the west (Fig 4.40). The apparent horizontal difference in VR

from east to west is a consequence of the western edge being more uplifted than the centre of the basin. If the VR data are plotted where each sample point reflects the stratigraphic unit it came from (Fig 4.40), then regardless of depth of burial VR results are similar for individual units. The one difference arises with VR results from the Morrow and Woodford formations in the Homer Cowden A1 well, where the samples are more thermally mature than the stratigraphic equivalent in the centre of the basin. This is a consequence of the igneous sill that has been emplaced into the Morrow Formation in the vicinity of the Homer Cowden A1 well (Fig 4.39).

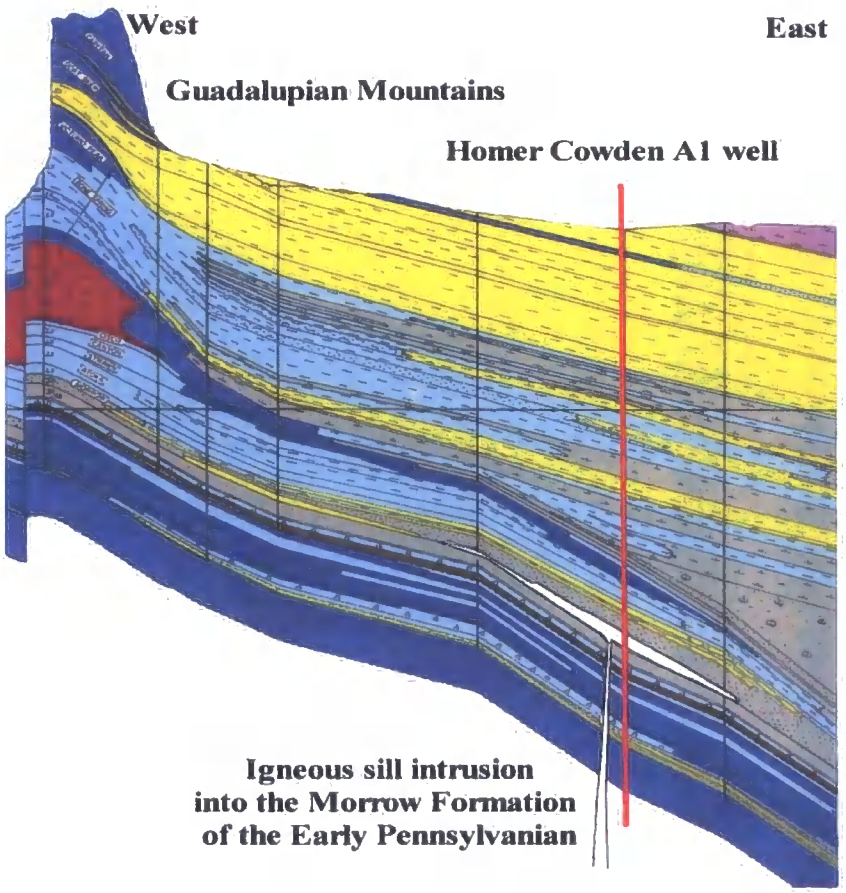

Fig 4.39. Cross-section at the western edge of the basin showing the location of the Homer Cowden A1 well and the sill intrusion into the Morrow Formation of the early Pennsylvanian System (Taken from West Texas Geological Society Publication 94-79).

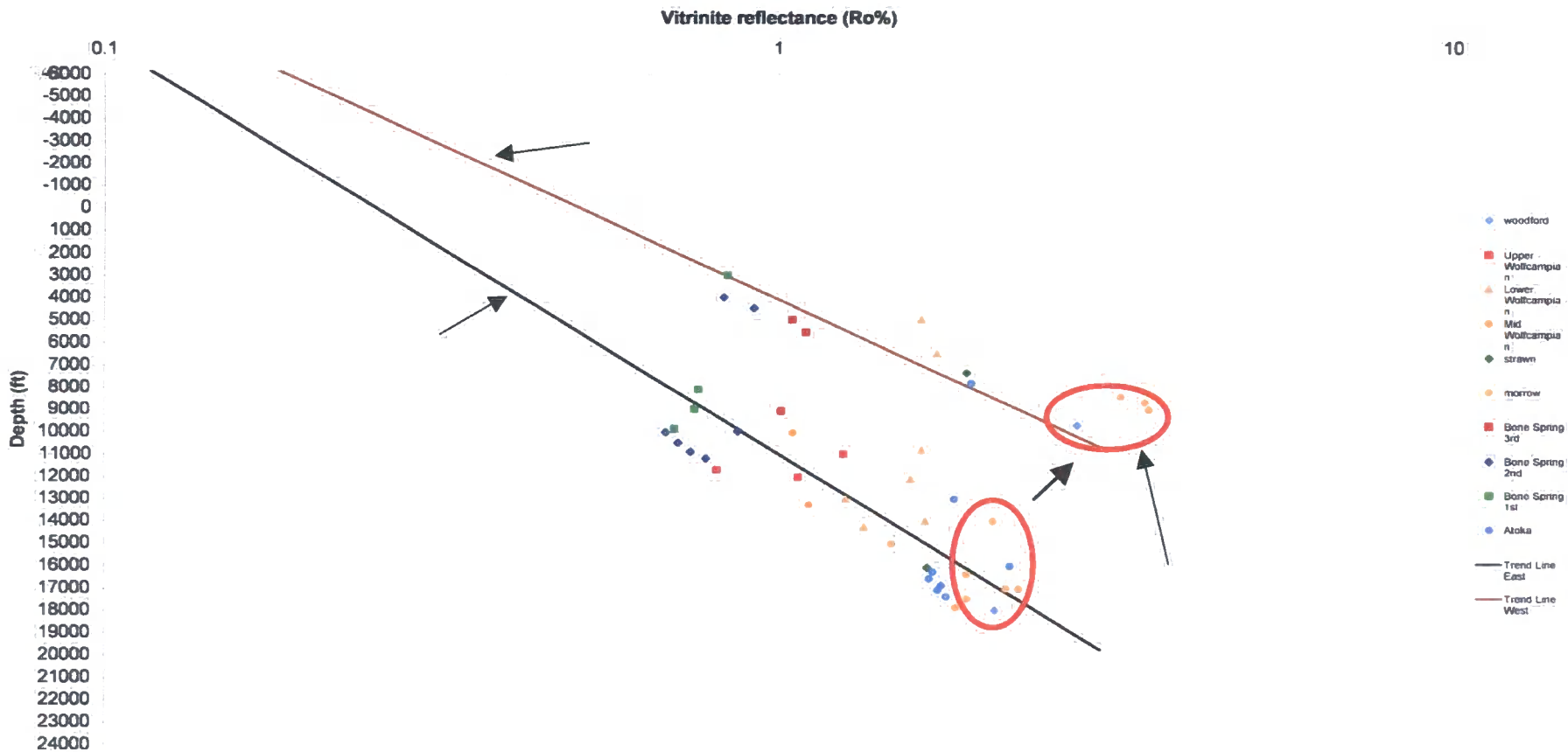

Fig 4.40. Plot of vitrinite reflectance (VR) data against depth for samples taken from the Delaware Basin, where each sample is plotted reflecting its stratigraphic position compared to the well the sample came from (refer to Fig 4.23 & 4.26). Two trends can be seen reflecting samples taken from the western uplifted edge of the basin (trend line west) and samples from the centre of the basin (trend line east). Samples within the same stratigraphic unit from east to west have similar VR readings and differ in depth only. This reflects the tilt of the basin, where units dip to the east. However, Morrow and Woodford samples from the Homer Cowden A1 well are more thermally mature in the west compared to the east as a consequence of the igneous intrusion.

4.3.2 Constraining an accurate burial and tectonic history by qualification of stratigraphy

By using AFTA, vitrinite reflectance data and shale compaction curves, a new burial history curve has been proposed in the results (sub-section 4.2.5 and Fig 4.35). In this sub-section, the stratigraphy is analysed to consider whether the burial and tectonic history that is proposed is actually geologically plausible.

AFTA results showed that the JE Haley 24-1 well experienced maximum burial around 55-50 Ma due to the additional burial by 6890 ft (2.1 km) of sediment above the Triassic unconformity. So what did this 6890 ft consist of? Working from the Triassic through to the end of the Palaeocene, depositional estimates will be made. These estimates are based on identifying the missing sedimentary units and then seeing if these units have been deposited elsewhere in the Delaware Basin, or the neighbouring Midland Basin or even further away in East Texas, and whether they can be correlated back to the Delaware Basin. A summary of Mesozoic and Cenozoic deposition is seen in Table 4.7.

Era	System	Series	Group	Age	Tectonism	Preserved Sediment			
						JE Haley 24-1	Delaware Basin	Permian Basin	Texas
CENOZOIC	TERTIARY	Pliocene			BASIN & RANGE	100ft	500ft	500ft	2000ft in East Texas
		Miocene		5.3 Ma		No deposits	No deposits	No deposits	3000ft in East Texas
		Oligocene		23 Ma		No deposits	No deposits	No deposits	5000ft in East Texas
		Eocene		33.9 Ma	LARAMIDE	No deposits	No deposits	No deposits	8000ft of Eocene sands in East Texas
		Palaeocene		55.8 Ma		No deposits	No deposits	No deposits	~500ft E. Texas
MESOZOIC	CRETACEOUS	Upper Gulfian		65.5 Ma		No deposits	Superficial	Superficial	~2000ft to 3000ft in East Texas
		Lower Comanche	Wash	99.6 Ma		No deposits	~500ft – Pecos – eroded	500ft – Val Verde - eroded	~500ft in East Texas
			Fred*			No deposits	~375ft - Pecos	Undefined from Washita - Val Verde Basin	~500ft in East Texas
			Trinity	145 Ma		No deposits	~375ft - Pecos	~1250ft – Val Verde Basin	~5000ft in East Texas
	JURASSIC			200 Ma		No deposits	No deposits	No deposits	No deposits
	TRIASSIC					~250ft	~500ft - Pecos	~1500ft in Midland Basin	~2000ft in the High Plains

Table 4.7. Table showing amount of preserved Mesozoic and Cenozoic sediment in the JE Haley 24-1 well, Delaware Basin, Permian Basin and Texas. The two cooling episodes are also highlighted.

4.3.2.1 Triassic

Table 4.7 showed that there are only 250 ft (76 m) of preserved Triassic sediment in the JE Haley 24-1 well; however further to the east in the Midland Basin there are up to 1500 ft (500 m) (fig 4.41).

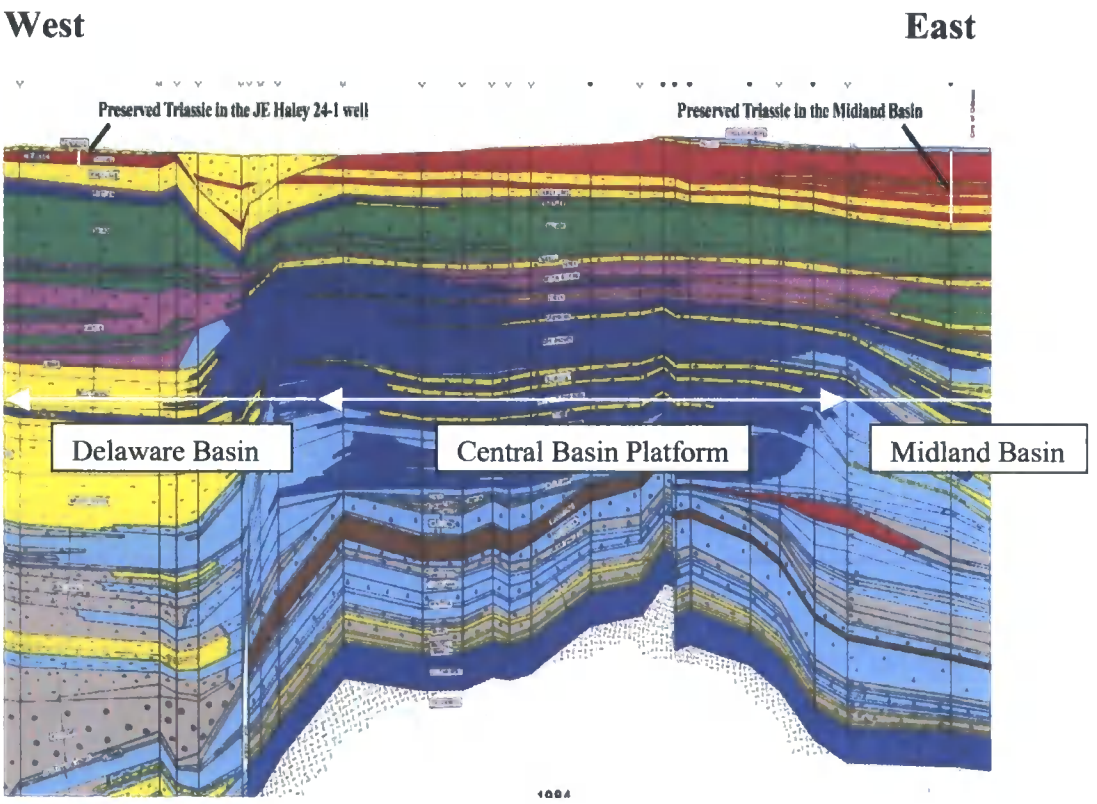

Fig 4.41. Cross-section east to west across the Delaware Basin, the Central Basin Platform and the Midland Basin highlighting the preserved thickness of Triassic sediment. (Taken from the West Texas Geological Society Publication 84-79)

There is also an unconformity on top of the Triassic in the Midland Basin, due to the whole basin being emergent during the Jurassic. Consequently the Triassic may have been thicker, perhaps by 500 ft (150 m) that would coincide with the 2000 ft (600m) of preserved Triassic seen in North Texas.

Assumption: 1750 ft (533 m) of sediment was deposited during the Triassic in the location of the JE Haley 24-1 well.

Missing sediment accounted for: 1750 ft (533 m) of Triassic.

Confidence: Based on preserved Triassic seen in the Midland Basin and in North Texas, and the Basin's proximity to a large sediment source of the Ouachita fold belt (Fig 4.42), 1750 ft of missing Triassic sediment is a likely scenario.

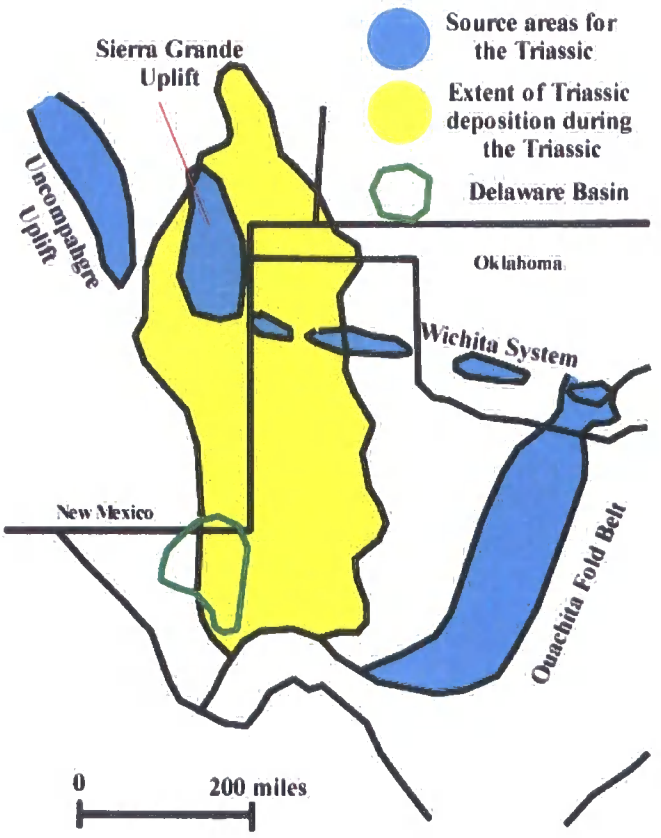

Fig 4.42. Map showing the extent of Triassic deposition during the Triassic, with the major structural features highlighted that could have acted as a source of sedimentation (Adapted from Hill 1996).

4.3.2.2 Jurassic

Hill (1996) and Hills (1984) suggested that West Texas was emergent during the Jurassic, with no Jurassic sediments recorded in the area. An unconformity between the Triassic and Early Cretaceous is evident across West Texas (Hill 1996). Without any further evidence, zero deposition of Jurassic sediment is assumed for this discussion.

4.3.2.3 Lower Cretaceous

In Texas, the Lower Cretaceous consists of the Trinity (oldest), Fredericksburg and Washita (youngest) Groups. Table 4.6 shows that no Lower Cretaceous is preserved in the JE Haley 24-1 well. The Lower Cretaceous is, however, preserved in the southern Delaware Basin in Pecos County, and in the Val Verde Basin with a total of 1250 ft (381 m) preserved. The presence of the Washita Group (although with an eroded surface) in Pecos County indicates that all of the Lower Cretaceous is accounted for in the 1250 ft (381 m).

Assumption: 1250 ft (381m) of sediment was deposited during the Lower Cretaceous in the location of the JE Haley 24-1 well.

Missing sediment accounted for: 3000 ft (914 m) of Lower Cretaceous and Triassic.

Confidence: With the entire Lower Cretaceous preserved in the southern Delaware Basin (+/- 100ft due to an eroded top of the Washita Group), assuming this was extensive, the same thickness can be assumed for the JE Haley 24-1 well.

4.3.2.4 Upper Cretaceous

There is no evidence of any Upper Cretaceous ever being deposited in the Delaware Basin and only a few outcrops are seen larger Permian Basin (Fig 1.1 & Table 4.7). However, the lack of deposits could easily be explained due to uplift and erosion associated with the Laramide Orogeny. Therefore any value given to the

amount of Upper Cretaceous deposition would be a crude estimate. It will be based on the amount of preserved Upper Cretaceous seen in other mid state American basins, and also the remaining amount of sediment needed to total the 6890 ft (2.1 km) required to explain maximum palaeotemperatures. The amount of missing Palaeocene will be estimated first.

4.3.2.5 Palaeocene

There is no Palaeocene recorded in West Texas, and so the estimation of missing Palaeocene sediment from the Delaware Basin is based purely on the 500ft (152m) of Palaeocene deposited in the East Texas basin, which stratigraphically lies on top of the Upper Cretaceous.

Assumption: 500ft of sediment was deposited during the Palaeocene in the location of the JE Haley 24-1 well.

Missing sediment accounted for: 3500ft (1066m) of Triassic, Lower Cretaceous and Palaeocene sediments.

Confidence: The Palaeocene sediment seen in the East Texas basin lies directly on top of Upper Cretaceous and similar deposition could have occurred in the west (Fig 4.43).

4.3.2.6 Upper Cretaceous continued

If maximum burial prior to the Laramide Orogeny 55 Ma was due to an additional 6890 ft (2.1 km) of sediment, and additional Triassic, Lower Cretaceous and Palaeocene may account for 3500 ft (1066 m) of this total, then the Upper Cretaceous would account for the difference, which is 3390 ft (1033 m). Is this large amount of Upper Cretaceous plausible for the Delaware Basin?

In the East Texas Basin (Table 4.7, and Fig 4.43), there are up to 3000 ft (914 m) of Upper Cretaceous sediments in the deepest part of the basin. Deposition of Upper Cretaceous in the Delaware may have been similar to, less than or more than that seen in the East Texas Basin, as it depends on amount of accommodation space

available, but it is plausible that approximately 3000 ft (914 m) of feet of sediment could have been deposited in the Delaware Basin.

Further to the north in Colorado and Wyoming, most of the basins of the Rocky Mountain Region have large accumulations of Upper Cretaceous sediment. The Powder River Basin of Wyoming has up to 5000 ft of preserved Upper Cretaceous sediment (Heasler et al 1994), and there are over 8000 ft plus of preserved Upper Cretaceous sediments further south in the Denver Basin in Northern Colorado (Sutton et al 2004). The Anadarko Basin in Oklahoma, which was dealt with in some detail in chapter 3, has experienced anywhere between 1.5 km (4921 ft) and 3 km (9842 ft) of Cenozoic uplift (Lee and Demming 2002). Carter et al (1998) tried to constrain this value by analysing AFT data, vitrinite reflectance and heat flow data. They inferred that at least 1.5 km (4921 ft) of denudation has occurred since the early to mid Cenozoic with erosion commencing around 50 Ma. They suggested that the missing sediment was of Upper Cretaceous age.

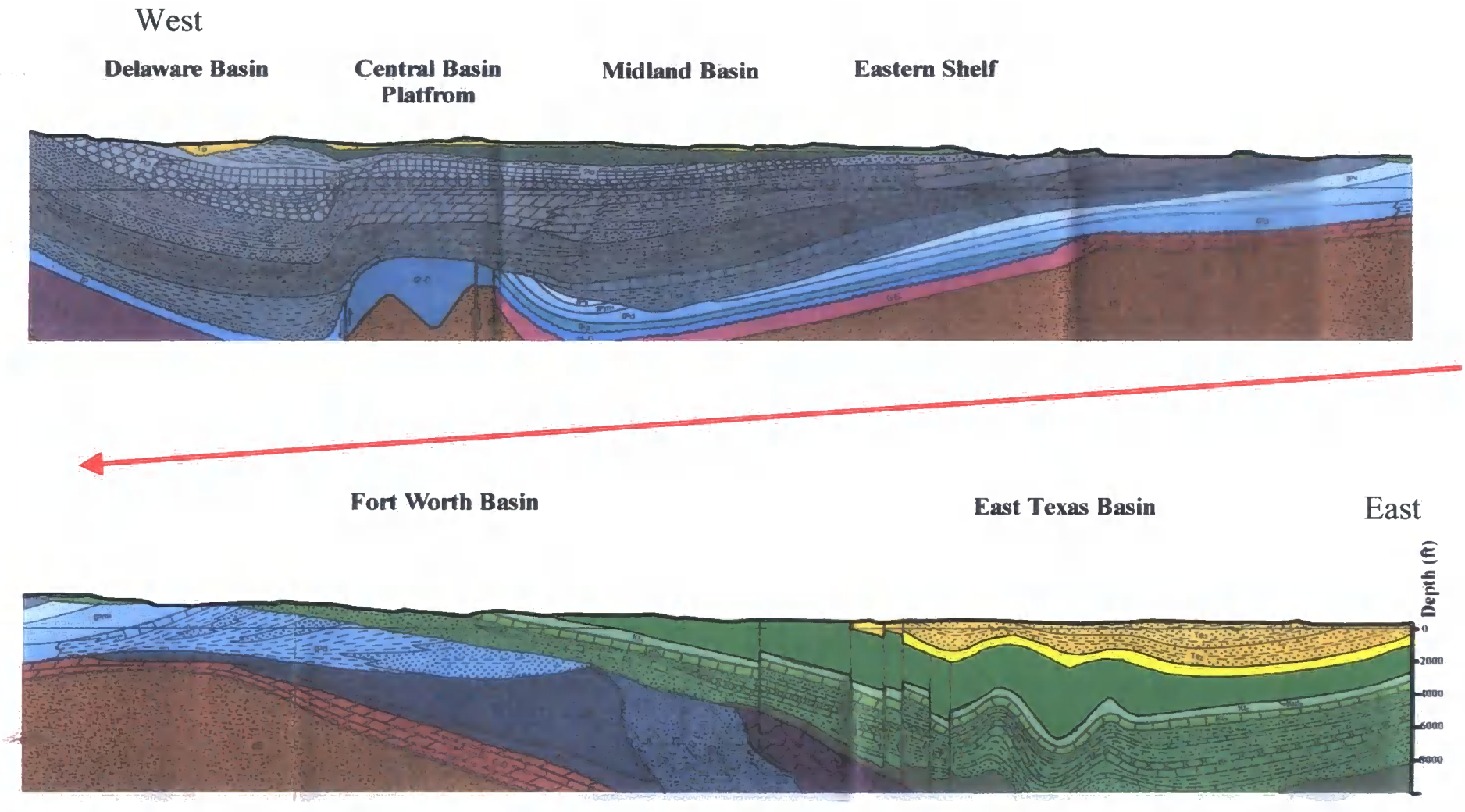

Fig 4.43. X-section across the whole of Texas west to east. In the East Texas Basin, there is preserved Palaeocene (yellow) and Upper Cretaceous (bright green) sediment (Taken from the United States Geological Highway map of Texas).

The depositional environment of the Late Cretaceous was that of a large interior epicontinental seaway (Fig 4.44) which spread across the whole of the mid United States. The sea would have covered the area represented by the Delaware Basin (Fig 4.44), so it is logical to assume that deposition would have occurred in the basin as long as there was sufficient accommodation space. During the Late Cretaceous, the basins of the Rocky Mountain Region to the north of the Delaware Basin were subsiding at a considerable rate due to the emerging Rocky Mountains (Fig 4.45). The Denver Basin, for example, was subsiding by 80 m/My, and assuming that the Late Cretaceous lasted for approximately 30My, then almost 8000 ft (2.4 km) of accommodation space would have been generated. Sloss (1988) did not include West Texas in the Late Cretaceous subsidence rate map (Fig 4.45), possibly because no Upper Cretaceous sediment is preserved and so it was assumed that the area never had any deposition of Upper Cretaceous age sediment and that no subsidence had occurred. However, if West Texas had experienced Late Cretaceous subsidence at a rate of 20-30 m/My, which is similar to the basins on the periphery of the map in the states of Kansas and Nebraska, then up to 3000 ft (900 m) of accommodation space would have been generated.

Assumption: 3390 ft (1033 m) of sediment was deposited during the Late Cretaceous in the location of the JE Haley 24-1 well

Missing sediment accounted for: 6890 ft (2.1 km) of Triassic, Cretaceous and Palaeocene sediments.

Confidence: There is up to 3000 ft (~1 km), of Upper Cretaceous sediment seen in the East Texas Basin, and further to the north in Colorado, large accumulations of 5000 ft plus (1.5 km) are preserved. It is possible that the Late Cretaceous seaway deposited 3390 ft of sediment in the Delaware Basin.

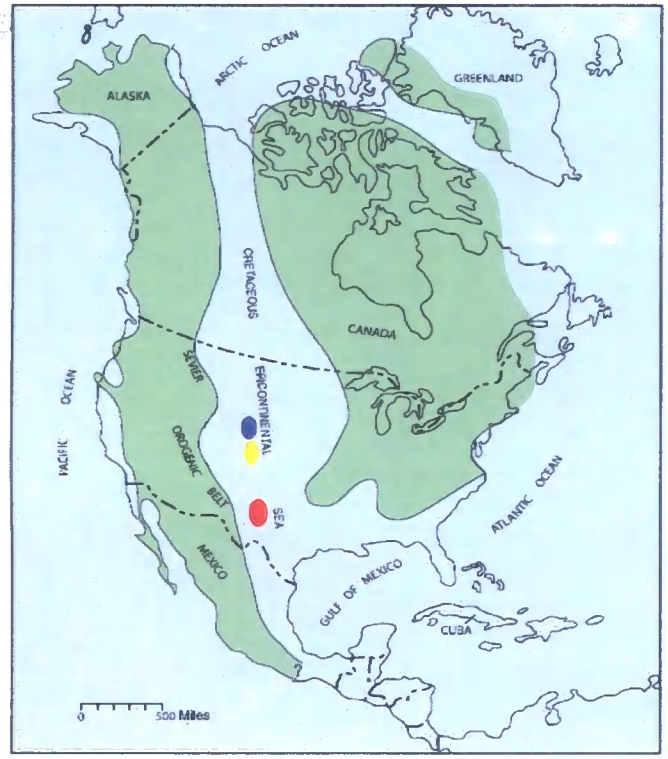

Fig 4.44

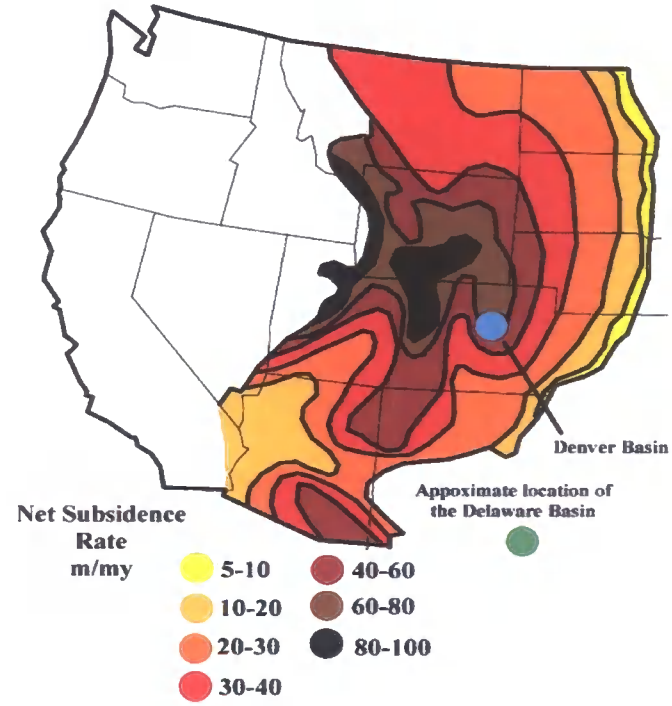

Fig 4.45

Fig 4.44 Map showing the extent of the Late Cretaceous interior seaway. Shown on the map are approximate locations of the Powder River Basin (blue), Denver Basin (yellow) and the Delaware Basin (red).

Fig 4.45. Map showing net subsidence rate of the Late Cretaceous for the foreland basins of the Rocky Mountains. Net subsidence can be interpreted as creation of accommodation space and hence deposition. The Late Cretaceous lasted for ~30My (Adapted from Sloss 1988).

4.3.3 When was the basin tilted?

The last area of discussion focuses on the uncertainty in the literature surrounding the origin of the tilt of the basin. Gregory & Chase (1992) and Hill (1996) concluded that all the tilt and subsequent uplift of the western edge is attributable to the Laramide compression, whereas Horak (1985) and Barker & Pawlewicz (1987) suggested that half of the 7500 ft (2.2 km) of overall flank uplift is due to Laramide compression and half is due to the Basin and Range event.

Shale compaction curves for three wells (Fig 4.45) in the Delaware Basin are used here to distinguish the two uplift events, and to determine which event tilted the basin. In sub-section 4.2.4.1, three distinct normal compaction curves were identified for the JE Haley 24-1 well, where each represented a phase of the well's burial history: present day normal compaction, normal compaction after the Laramide uplift, and normal compaction at maximum burial prior to Laramide uplift. The other wells here for comparison with the JE Haley 24-1 well are the Wigins Orla well in Culberson County on the western edge of the basin and the Weatherby well in Pecos County. The Wigins Orla well is used as a comparison because it is located on the western edge of the basin and this has experienced more uplift (~2300 ft) than the JE Haley 24-1 well due to the tilt of the basin. The Weatherby well in Pecos County is used because stratigraphic units are at the same depths as in the JE Haley 24-1 well, although it is over 100 miles further to the southwest and Lower Cretaceous strata is preserved in the section.

Prior to any uplift event, it is assumed that strata in all wells were at maximum burial (~55 Ma) and all horizons in the basin were horizontal. To simulate maximum burial for the JE Haley 24-1 and Weatherby wells, they are buried by an additional 6890 ft (2.1 km) of sediment. To estimate maximum burial for the Wigins Orla well, the extra uplift due to tilt (~2300 ft) is added to the 6890 ft of missing sediment already calculated. For all wells when the present day compaction curve (blue) is moved down to maximum burial (red curve in Fig's 4.46 & 4.47), the Upper Permian Delaware Group shows evidence for being normally compacted at that depth. Note that the Delaware Group does contain a large proportion of calcite,

making its normal compaction curve shift to the right, which is especially evident in the Weatherby well. If the compaction curve in the Bone Spring for each well is representative of normal compaction after the Laramide orogeny (55-50 Ma), then by shifting the curve vertically so that the Bone Spring compaction curve is in line with the assigned normal compaction curve (green curve in Fig's 4.46 & 4.47), an indication of the amount of Laramide uplift can be estimated.

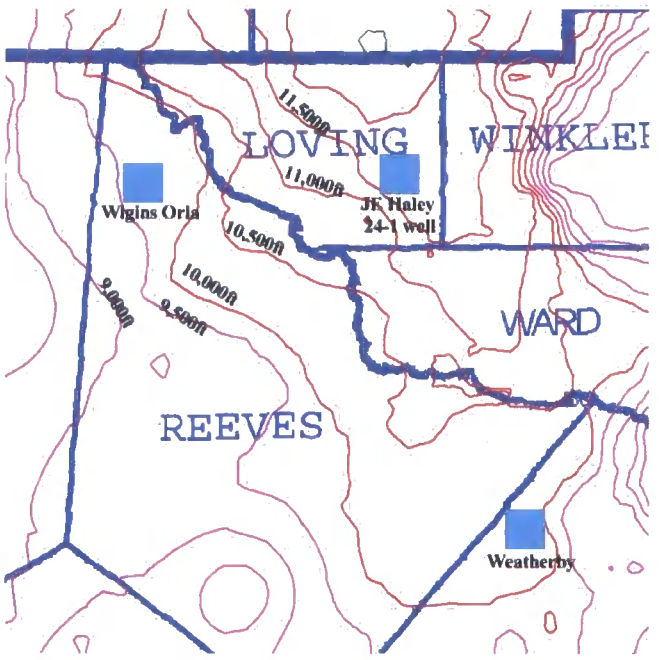

Fig 4.45. Location map showing the wells Wigins Orla, Weatherby and JE Haley 24-1. Depth contours of the top Wolfcampian Series are shown to give an indication of the tilt of the basin to the east, where the top of the Wolfcampian Series for in the Wigins Orla well is 2000 ft (~600 m) higher.

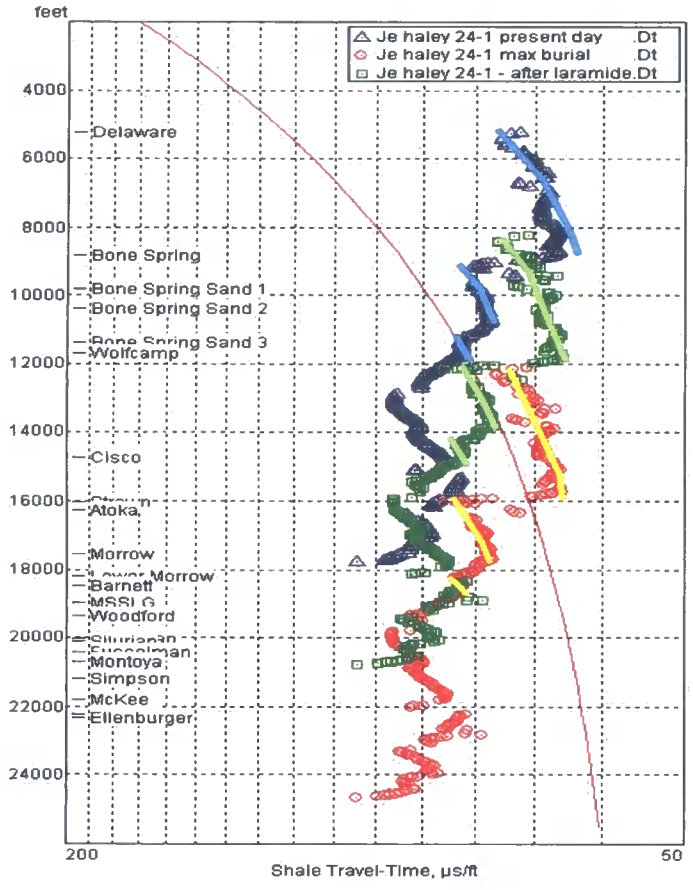

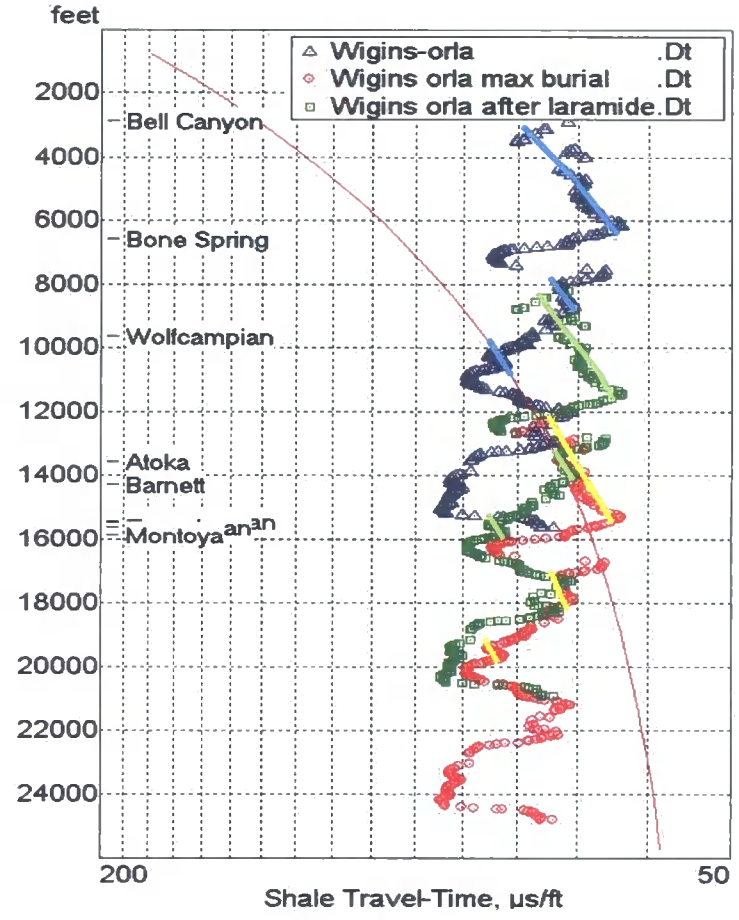

Fig 4.46. Shale compaction curves for the JE Haley 24-1 well and the Wigins Orla well. At present day, three distinct normal compaction curves can be seen for both wells. These correspond to compaction at maximum burial, compaction after Laramide uplift, and compaction at present day.

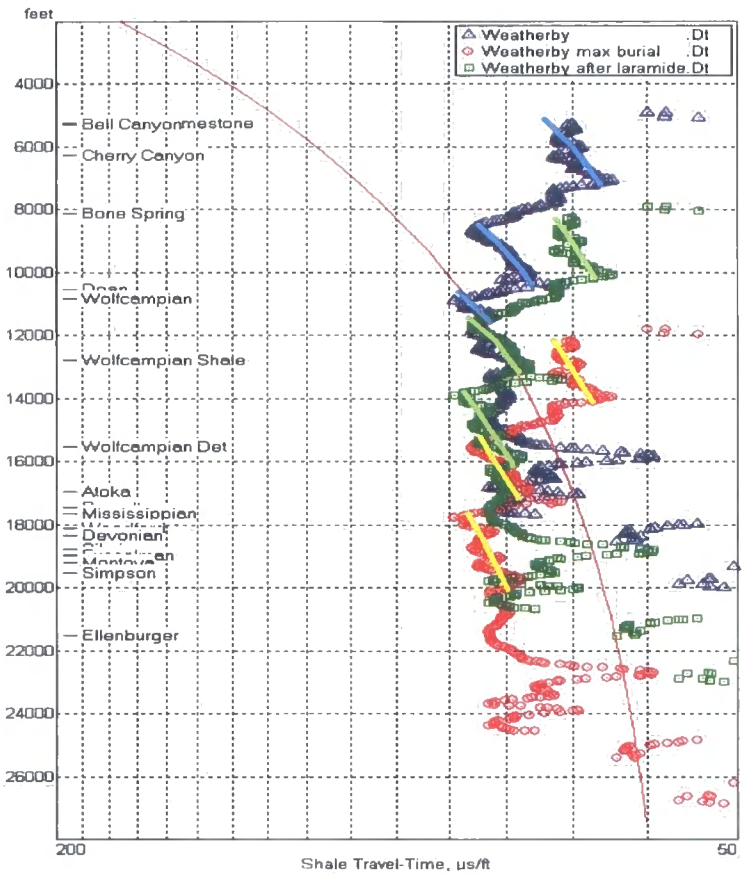

Fig 4.47. Shale compaction curve for the Weatherby well. As with the compaction curves in Fig 4.47, three distinct normal compaction curves can be recognised in the section, which coincide with compaction at maximum burial, then after Laramide uplift, and at present day.

For all three wells, the amount of uplift needed from maximum burial so that the compaction curve in the Bone Spring Formation falls on to the normal shale compaction curve, is identical (3890ft or 2.1km). This suggests that the Laramide uplift (55-50 Ma) event had an equal effect on the whole basin, and did not tilt the basin, which now must be an effect of the later Basin and Range tectonic event (25-10 Ma).

4.4 Conclusions

- Sediments in the Delaware Basin experienced greater temperatures than at present day due to greater burial. There were also two cooling events due to uplift, which coincided with the Laramide Orogeny (55-50 Ma) and the Basin and Range Event (25-10 Ma).
- Assuming a palaeogeothermal gradient of 21.8 °C/km, then maximum burial occurred prior to the Laramide event due to an additional load of 6890ft (2.1km), above the Triassic unconformity, as concluded from AFTA and vitrinite reflectance. The additional load comprised estimated thicknesses of:
    - 1750 ft (500m) of Upper Triassic
    - 1250 ft (400 m) of Lower Cretaceous
    - 3390 ft (1 km) of Upper Cretaceous
    - 500 ft (150 m) of Palaeocene
- The Laramide then uplifted the section by 3890 ft (2.1 km). Shale compaction plots show that the Laramide episode affected the whole basin equally and did not tilt the basin to the east.
- During the Eocene and Oligocene, the basin then subsided by 600 ft (180 m).
- The Basin and Range event (25-10 Ma) as deciphered from AFTA then uplifted the basin by a final 3600 ft (1.1 km).

Chapter 5:

Wireline Data and its Signatures: A Qualitative and a Quantitative Tool for Understanding Sediment Compaction in the Delaware Basin

5.1 Introduction

The Delaware Basin is overpressured (chapter 3), with excess pore pressure of 6000 psi (41 MPa) in some parts of the basin. The overpressure is confined to an isolated section of the basin, with the top of the overpressure in the Early Permian Wolfcampian Formation. The underlying Mississippian and Pennsylvanian Formations also are overpressured. However, the rocks below this interval are normally pressured.

The overpressure is known from direct pressure measurements and from the mud weights used during drilling. All the pore pressures measured in the Delaware Basin were from Drill Stem Tests (DSTs). The DST is a relatively reliable method to determine pore fluid pressures; however, one drawback is that DSTs are only used in porous lithologies, i.e. when a reservoir horizon is encountered while drilling, as the test relies upon fluid flow from the formation into the borehole. It is often assumed that mudrocks in the section have pore pressures, equal or similar, to the reservoir section directly above or below the mudrock interval. In a clastic dominated basin, where mudrock intervals are sparse thin horizons within thick coarse clastic units, measuring the pore pressures exclusively in the coarse clastic horizons would give an accurate reading of the basin's pressure profile. However, the Delaware Basin is between 60 and 70% mudrock dominated, and the isolated overpressured unit is over 7000 ft (2.1 km) thick and 90% mudrock dominated in some parts of the basin. This poses the need for caution when interpreting pore pressure data from DSTs in the basin.

This chapter describes how wireline logs have been used in a quantitative and a qualitative approach to analyse the pore pressures in the mudrocks in the Delaware Basin. The results are compared to the actual pore pressures measured by the DSTs, to check whether wireline logs can be used as a tool for estimating pore pressures. In addition, the mechanism generating the overpressure is investigated using methods suggested by Bowers (2001) and later adapted by Hoesni (2004).

5.1.1 Data

This study has analysed over 600 wells in the Delaware, Midland and Val Verde Basin, of which only 23 wells had digital wireline data available (Fig 5.1). The following wireline logs were analysed for this study:

- Porosity tools
  - Sonic
  - Density
  - Neutron
  - Resistivity
- Gamma ray log
- Caliper log
- Photoelectric factor log

The sonic and gamma ray tools were run in all 23 wells, but the density, resistivity and neutron tools were run in only a few wells. For this reason, the sonic log is the main tool that is used in this study to represent the porosity of the sediments.

The gamma ray log was used to identify shale horizons within the basin, where a gamma ray value of 45 API was used as the cut-off between sand and a mudstone. This value was based on known sandstone horizons within the basin that recorded average gamma ray values of no more than 45 API.

The JE Haley 24-1 well had the most extensive wireline suite, which was in digital and paper format. This well was used as the type well to distinguish the lithologies in the basin, where neutron-density cross-plots and photoelectric factor logs were used to distinguish between non-mudstone lithologies.

All the wireline logs in this chapter are analysed using 'Presgraf', a pore pressure prediction software program developed by Traugott (1999) and licensed to Durham University by BP. The software utilises digital logs that have the .LAS format.

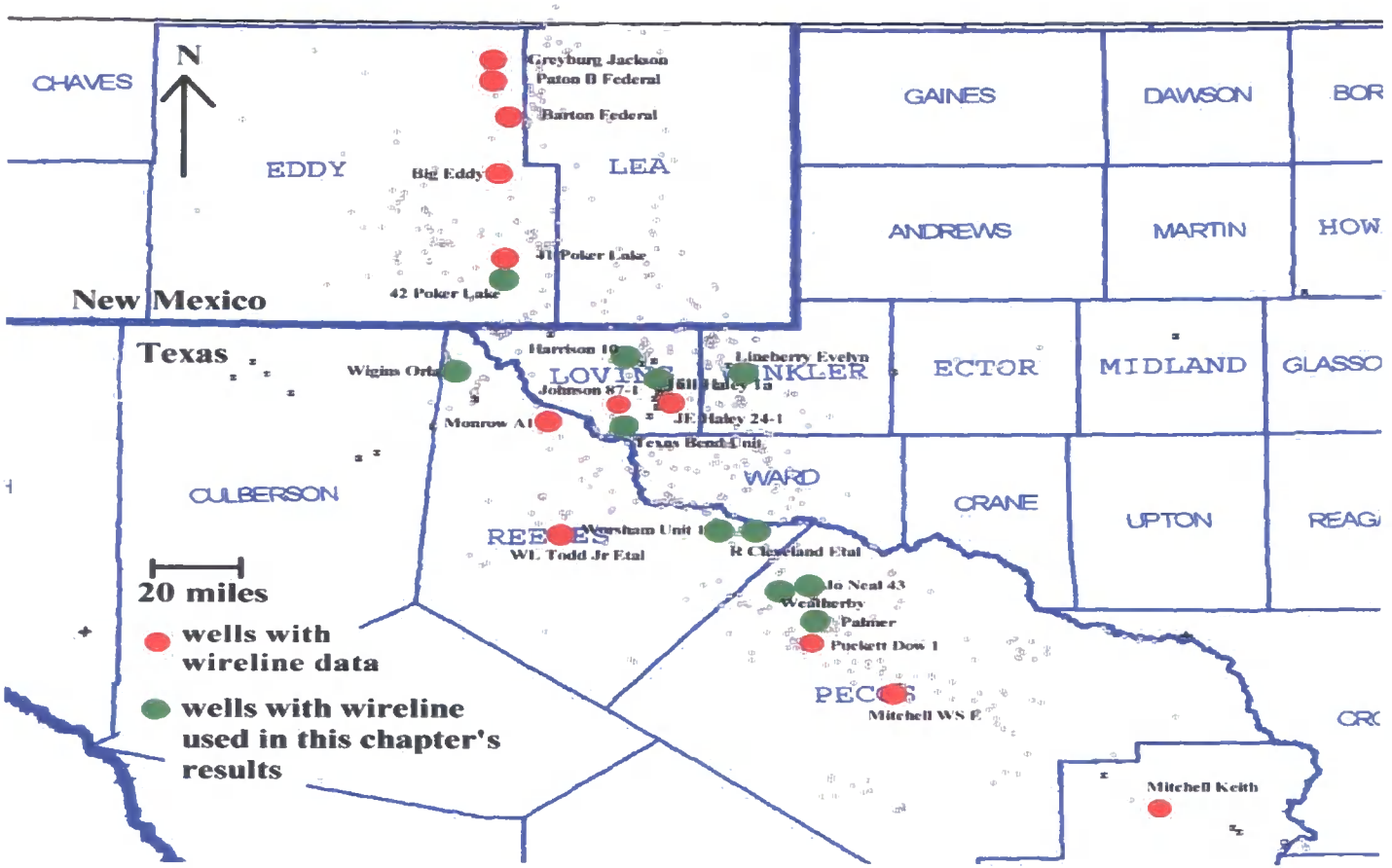

Fig 5.1. Map of West Texas, showing the location of wells with wireline data (red spots) in the Delaware Basin which are to be used in this study.

5.1.1.1 Controls on Data Quality

Borehole Diameter

Before density points can be analysed, it is essential to look at the caliper log. The caliper log shows the diameter of the borehole while drilling, and can be used for two main purposes. The caliper log can be used to see where the casing was set for the well, i.e. the depth at which there is a decrease in the caliper. On a more local scale, the caliper log is used to pick up zones in the well where there are washed out zones or mud cake build up. The density log is strongly influenced by borehole size such that where the borehole is enlarged the density tool records lower than expected values (Fig 5.2).

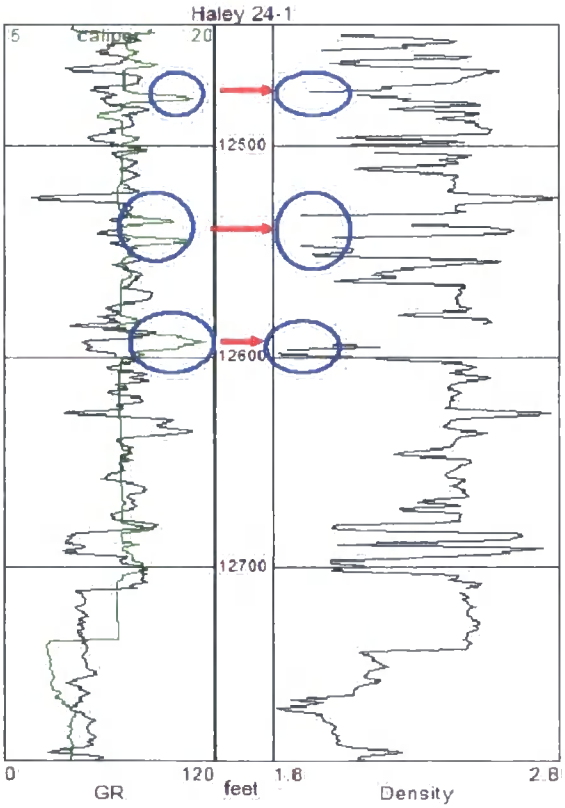

Fig 5.2. A gamma ray and density plot from 12450 ft – 12800 ft from the Hill Halley 24-1 well. From 12450ft – 12730 ft, the casing in the well is 13inches as shown by the caliper log. At the three circled locations, the caliper drastically increases, which coincides with a marked fall in the density. The tools are responding to a cave in the well.

Drilling Fluid

The density tool has a shallow depth of investigation. Most of the density response originates from within 13cm of the tool (Rider 1996). Therefore density is recorded predominantly from the invaded zone. This is an important consideration when the drilling fluid is changed to a higher density drilling mud, such as if barite is added. If this higher density mud infiltrates the invaded zone, then recorded density will be higher (Fig 5.3). The drilling fluid also affects resistivity logs, as an oil-based mud will be highly resistive, while a saltwater-based mud would be highly conductive. Therefore, it is best to analyse a deep resistivity tool, as it measures more closely the true conductivity of the formation water in the uninvaded zone.

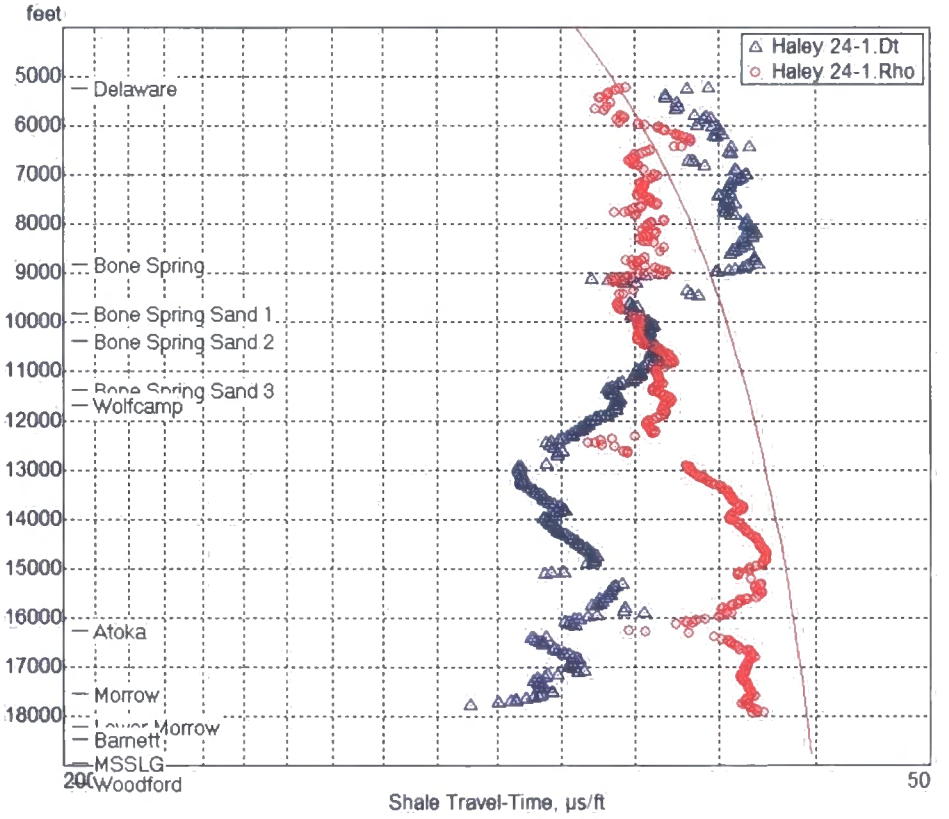

Fig 5.3. Sonic (24-1.Dt) and density (24-1.Rho) plots with depth for the Hill Haley 24-1 well in Loving County. The density values have been converted to travel-time, to enable comparison with the sonic log. While drilling the JE Haley 24-1 well, there was a change from water-based muds to a higher density mud at 12856 ft. At this depth, the density log response increases as a response to the higher density of oil-based drilling mud.

5.2 Pore pressure prediction from wireline logs

Chapter 3 introduced the term effective stress, which is the grain-to-grain contact stress of a rock under burial. Compaction and porosity loss of a compressible sediment is controlled by compressive stresses (vertical and horizontal). Porosity is therefore influenced by the effective stress, where an increase in the effective stress due to overburden decreases the pore space of a sediment as pore fluid is expelled.

If a section experiences overpressure due to disequilibrium compaction (sub-section 3.2.2.2), then the pore pressure is greater than the hydrostatic pressure due to unexpelled water reducing the grain-to-grain contact stress. When no water can escape, the grain-to-grain contact stress remains the same, so the effective stress is constant, and the pore pressure depth profile is parallel to the overburden stress/depth profile (Fig 5.4). This is the principle behind a quantitative approach of pore pressure prediction from wireline logs, where pore pressure in an overpressured section is predicted using the log calculated porosity, and its deviation vertically or horizontally from the normal compaction curve. There are two methods, the Eaton Ratio Method and the Equivalent Depth Method (Fig 5.5).

The Equivalent Depth Method (Hottmann & Johnson 1965) is deterministic and relies on the assumption that shales of equal porosity and similar composition have been subjected to the same maximum vertical effective stress, regardless of their burial depth. This assumption is valid if overpressure was generated by disequilibrium compaction. The Equivalent Depth Method has also been referred to as the vertical method, as in this method; it is assumed that the vertical projection of an overpressured unit to the normal compaction curve corresponds to a line of constant porosity and constant effective stress (Fig 5.5). Therefore the overpressured unit has a porosity equivalent to the unit at the depth directly above on the normal compaction curve. From the acquired equivalent depth porosity, the effective stress can then be worked out using Rubey & Hubbert's equation (1959):

$$\sigma v = 1/\beta \ln(\Phi o/\Phi dT) \quad (5.1)$$

where:

σv = vertical effective stress,

β = empirical constant derived from the compaction trend (compaction coefficient),

Φo = surface porosity, and

ΦdT = sonic derived porosity.

The pore pressure is then worked out using Terzaghi's Law: (5.2)

$$Pf = Sv - \sigma v$$

where:

Pf = pore fluid pressure,

Sv = lithostatic pressure or overburden, and

σv = vertical effective stress.

The Eaton Ratio Method is empirical and uses the ratio of the observed log porosity value and the expected log porosity value for a normally pressured rock to determine pore pressure at the same depth. This method is also known as the horizontal method, as the measured value and the value taken for normally pressured are taken at the same depth (Fig 5.5). This method commonly uses sonic travel time, resistivity or seismic interval velocity data. The equation can be summarised for travel time below. For resistivity or velocity data, substitute (dTn / dT) by (Vn / V) or (Rn / R) respectively.

$$P_p = P_{OB} - (P_{OB} - P_n)(dT_n/dT)^{EE} \quad (5.3)$$

where

P_p = predicted pore pressure gradient,

P_{OB} = overburden gradient,

P_n = normal (hydrostatic) pore pressure gradient,

dT_n = normal sonic travel time,

dT = observed sonic travel time, and

EE = Eaton exponent (sonic =3; resistivity =1.2; velocity =3).

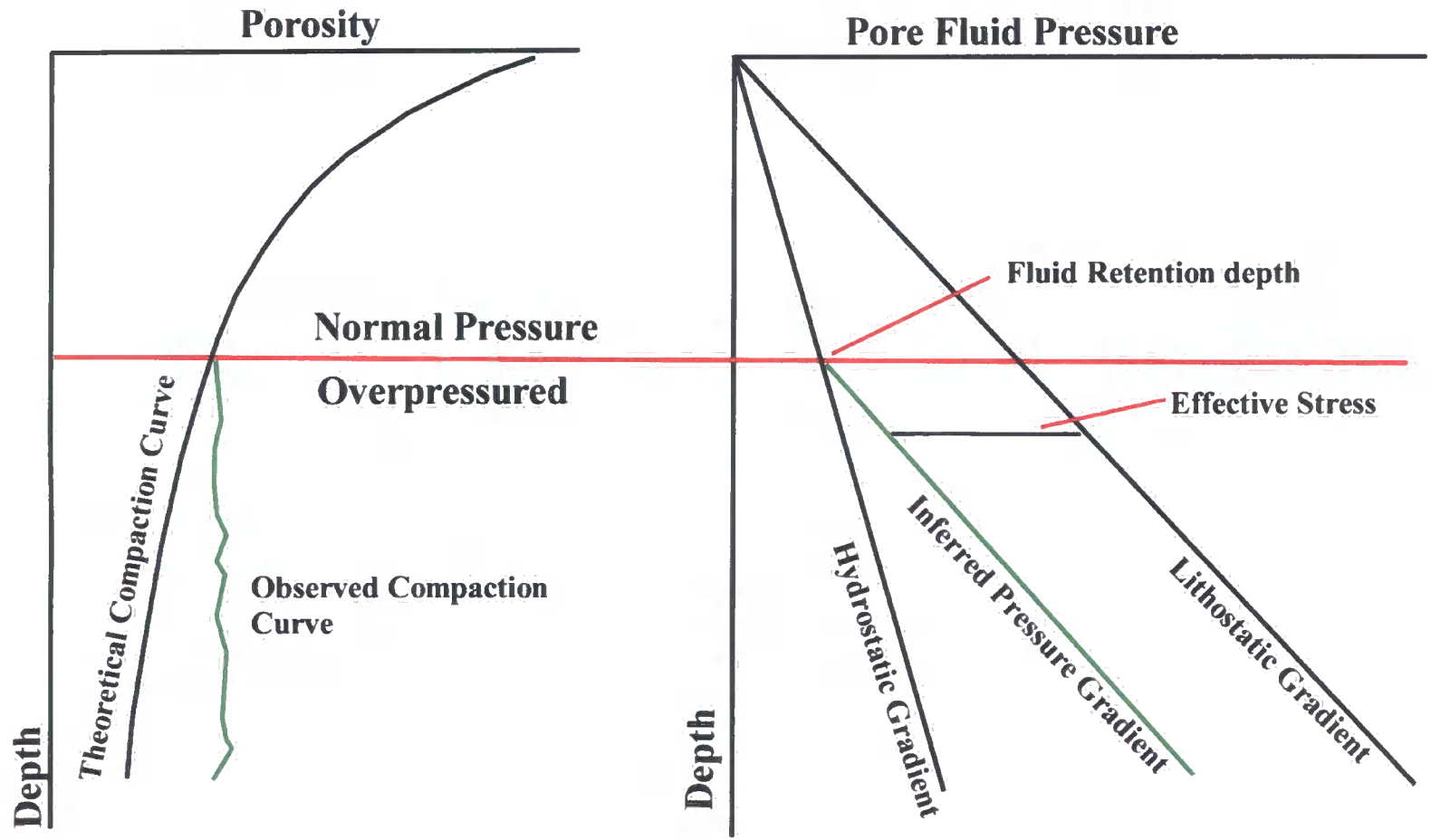

Fig 5.4. Porosity will decrease with depth as a consequence of increasing vertical effective stress and follow a theoretical compaction curve where pore pressure is hydrostatic. Where overpressure is generated through disequilibrium compaction, effective stress remains constant and porosity will remain constant with depth.

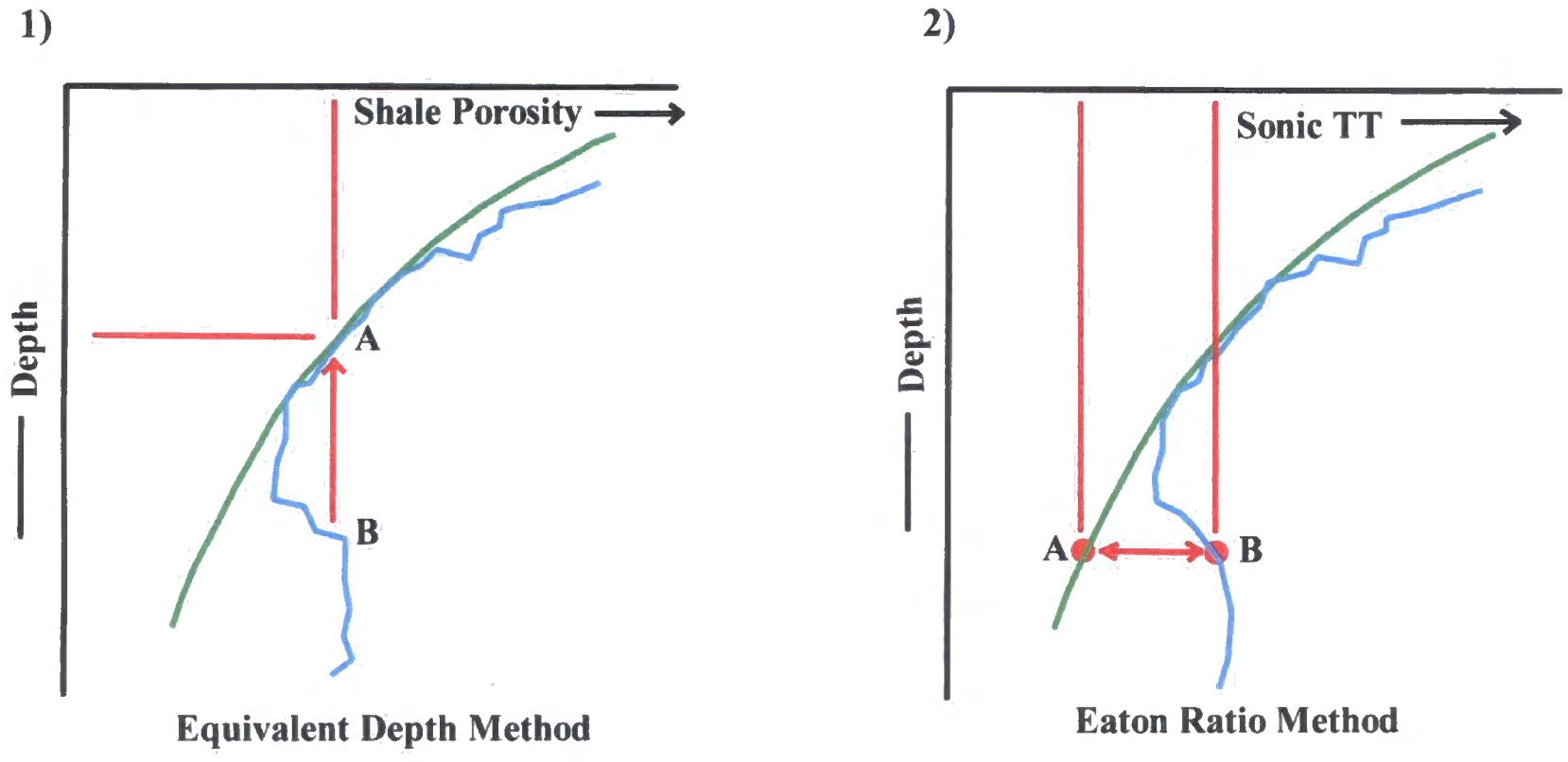

Fig 5.5. Predicting pore pressure from wireline logs: 1) The Equivalent Depth Method, assumes that vertical projection to the normal compaction curve corresponds to a line of constant porosity and constant effective stress. 2) The Eaton Ratio Method assumes that the ratio of the measured log value (B) to the log value on the normal compaction curve (A) is empirically related to the ratio of the vertical effective stress at B and A.

5.2.1 Factors affecting pore pressure prediction

Predicting pore pressure from wireline logs, is highly dependent on the selection of a number of parameters and processing methods. These critical factors are briefly discussed in this sub-chapter making the reader aware of the constraints on using pore pressure prediction methods.

5.2.1.1 Normal compaction

Both the Equivalent Depth Method, and the Eaton Ratio Method are reliant on an accurate normal compaction curve for the shales of the basin if pore pressures are to be determined by these methods. Chapter 4 (sub-section 4.2.4) dealt with shale compaction curves in the Delaware Basin and in the JE Haley 24-1 well, this study has suggested that the Mid Permian shales of the Bone Spring 3rd Sand Formation are normally compacted at present day. Through the use of mercury injection porosimetry analysis on shales of the Bone Spring 3rd Sand Formation, a porosity value of 10% can be assigned to these shales to aid in calibration. A porosity-depth profile can be produced within the software 'presgraf', which is based on Hubbert & Rubey's relationship (Equation 4.3) (Fig 5.6). Due to a lack of data, an initial starting porosity of 60% is assumed for the equation, which is a good default value for the initial porosity of mudstones if the true value is unknown. Within presgraf, the compaction coefficient is a variable between 4000 – 7000. A value of 5200 was used to create the compaction curve (Heppard, P., *pers comm.*).

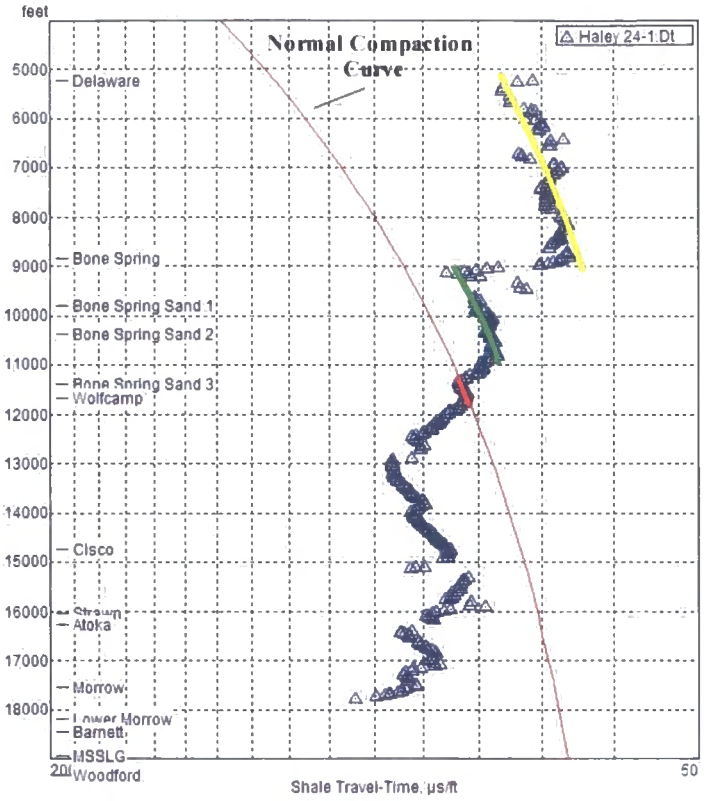

Fig 5.6. Shale compaction curve for the JE Haley 24-1 well. 'The Presgraf' assigned normal compaction curve (based on Hubbert and Rubey's (1959) compaction relationship), is indicating that the shales of the Bone Spring 3rd Sand Unit are normally compacted at present day.

Assigning normal compaction curves to mudstones within Palaeozoic basins can create a degree of uncertainty regards accuracy.

5.2.1.1.1 Uplift

In chapter 4 it was concluded that the Delaware Basin underwent significant uplift and erosion during the Cenozoic. Following uplift, the sediments may no longer be at their maximum effective stress, and for this reason it has been suggested that porosity depth curves should not be made in uplifted areas due to the inaccuracies involved (Giles et al 1998). Uplift in the Delaware Basin has had an influence on the shale compaction curves (Fig 5.6), because the Delaware Group and the Upper Bone Spring Formations display porosity values less than expected for the present day depth of burial.

This study, however, suggests that the pore pressure system in the Delaware Basin is dynamic rather static, and at present day certain mudstone beds (Bone Spring 3rd Sand in the JE Haley 24-1 well) have dewatered and equilibrated back to hydrostatic pressure and normal compaction. It is these horizons that the normal compaction curves are based upon for the pore pressure prediction methods.

5.2.1.1.2 Heterogeneity of sediments

Another consideration is that for the pore pressure prediction methods, a single normal compaction curve is assumed for the whole mudstone sequence, which is making the assumption that the mudstone sequence is homogenous. In reality, the porosity-depth curve for one mudstone sequence of Devonian age is likely to be very different to the porosity-depth curve of mudstones from the Late Permian. This is highlighted by the large variation of published porosity depth curves (Chilingarian 1974) (refer to Fig 4.30). Dzevanshir et al (1986) suggested lithology, mineralogy, sorting, and amount and nature of the cement will have an impact on the trend of the curve. Yang & Aplin (2004) suggested that the clay fraction of the mudstone is the dominant control on the compaction profile.

This study suggested in chapter 4 (sub-section 4.2.4.1 and Figs 4.33 & 4.34) that the mudstones of the Delaware Group in the JE Haley 24-1 well (Fig 5.6) appear to have low porosity for their present depth of burial as a consequence of both Cenozoic uplift and calcite cement that makes up 20% of the matrix.

For the mudstones below the normally compacted Bone Spring 3rd Sand Formation of the JE Haley 24-1 well in the Delaware Basin, the recorded porosity from the sonic log is a response to the overpressure in the basin, which masks any normal compaction curves. Therefore the assumption that the overlying normally compacted sediments have the same porosity depth relationship as the overpressured mudstones has been applied for this study. It is applied reluctantly as this is unlikely to be the case, however, without the relevant data, it is the simplest assumption to make.

5.2.1.2 Non-mechanical compaction

The Equivalent Depth Method, and the Eaton Ratio Method only work if the mudstone is normally compacted or undercompacted for its depth of burial. In cases where porosity has been destroyed by chemical processes following normal compaction, or effective stress has been reduced by fluid expansion mechanisms, then pore pressure prediction methods will not provide reliable estimates of the pore pressure, but will underestimate it. By using velocity-density cross-plots, the distinction between mechanical compaction related porosity and effective stress reduction through unloading can be made (Bowers 2001), and will be discussed in sub-section 5.3.

5.2.1.3 Other parameters

Other factors are also likely to influence pore pressure prediction methods, but detailed evaluation of their control on the Delaware Basin was beyond the scope of this study.

Goulty (2004) suggested that using porosity-vertical effective stress relationships in a compressional basin may result in the underestimation of pore pressure.

According Giles (1998), high temperature may also have an effect on the wireline properties, but the effect of high temperature is greater in young basins where the sediments have immature mineralogies. Hoesni (2004) found that a high geothermal gradient had an effect on the porosity of sandstones in the Malay Basin Indonesia. However, the effect on mudstones in the basin was not investigated.

5.2.2 Results of pore pressure prediction

The Equivalent Depth Method, and the Eaton Ratio Method were applied to eleven wells in the Delaware Basin, providing a comprehensive spread across the basin (Fig 5.1):

- Eddy County: 42 Poker Lake well
- Loving County: Hill Haley 1a; Harrison 10; and the Texas Bend well
- Winkler County: Lineberry Evelyn well
- Reeves County: Worsham Unit 1; R Cleveland etal 2; and the Wigins Orla well
- Pecos County: Weatherby; Jo Neal 43; and the Palmer well

The wells were chosen where a normal compaction curve could be assigned to each well.

The sonic log was used for analysis, as it was the one porosity wireline tool that was used in all the wells. The sonic log is also accurately responsive towards zones of overpressure in the basin. The density log was run in the Hill Haley 1a well; however, as already illustrated, the density log is sensitive to drilling fluid (Fig 5.3), and so was not analysed in this study.

All result plots have the same key, where pore pressure estimation from the Equivalent Depth Method is a straw-coloured curve (.D43), and from the Eaton Ratio Method, a blue curve (D.46). The pore pressure data points were obtained from DSTs from the well being analysed, or from other wells located within close proximity to that well. The name of the well and the formation where the pressure data were obtained is listed in the key.

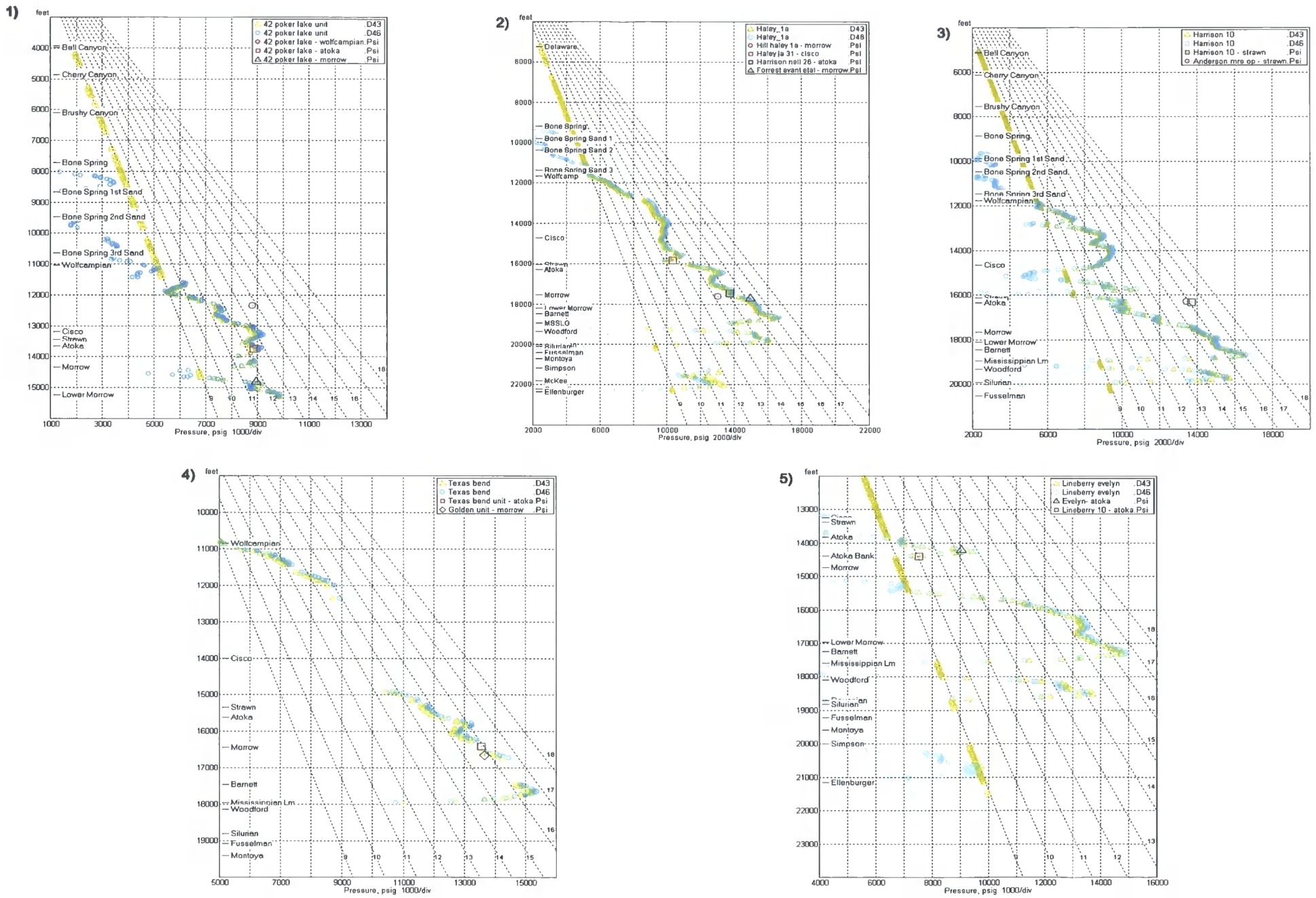

Fig 5.7. Pore pressure prediction plots using the Equivalent Depth Method (D. 43 - straw coloured curve) and the Eaton Ratio Method (D.46 – blue curve) on sonic log curves of wells in the Delaware Basin: **1)** 42 Poker Lake well; **2)** Hill Haley 1a well; **3)** Harrison 10 well; **4)** Texas Bend well; **5)** Lineberry Evelyn well.

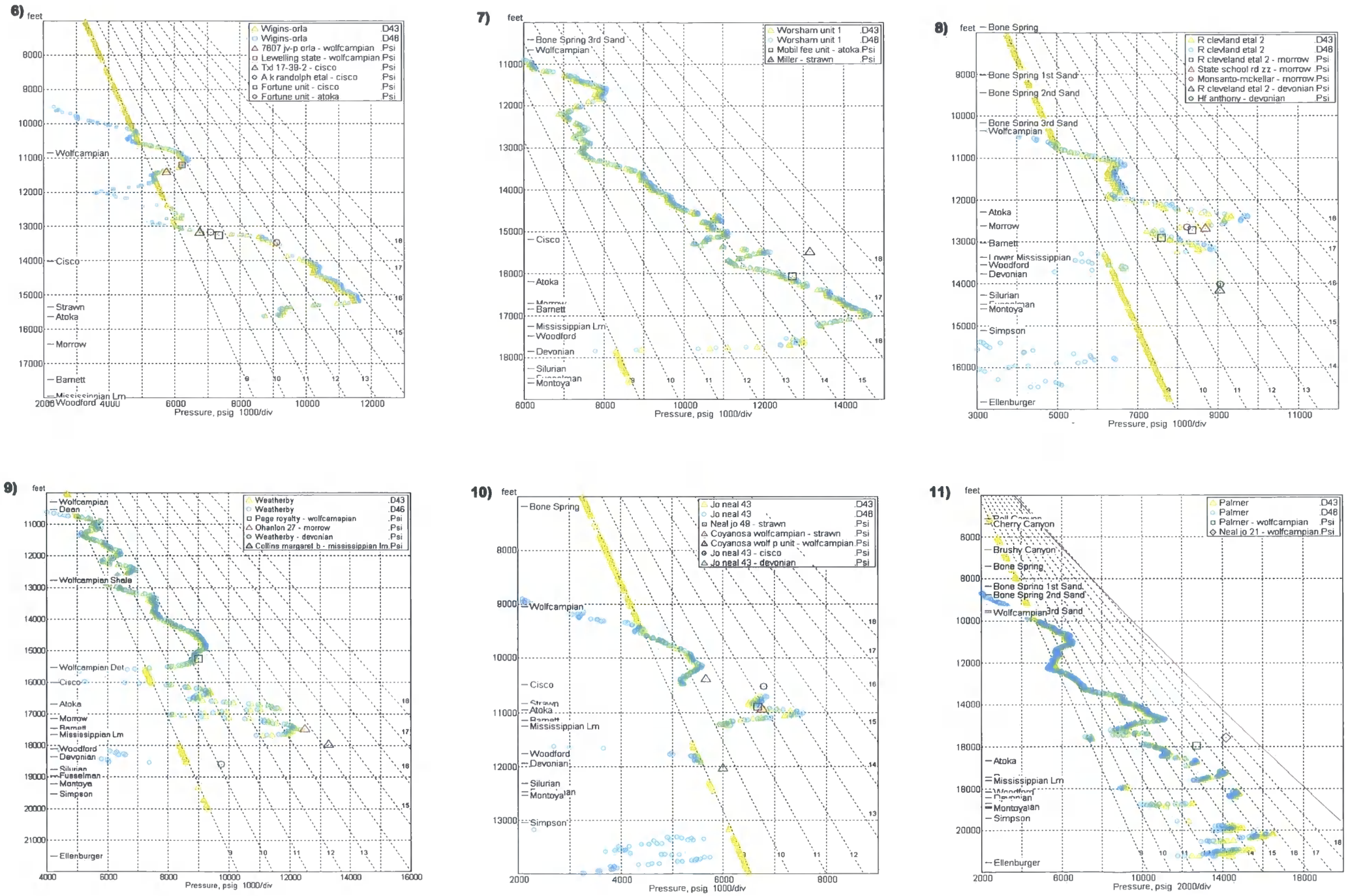

Fig 5.8. Pore pressure prediction plots using the Equivalent Depth Method (D. 43 - straw coloured curve) and the Eaton Ratio Method (D.46 – blue curve) on sonic log curves of wells in the Delaware Basin: **6)** Wigins Orla well; **7)** Worsham Unit 1 well; **8)** R Cleveland etal 2 well; **9)** Weatherby well; **10)** Jo Neal 43 well; **11)** Palmer well.

The results from the pore pressure prediction are summarised below in table 5.1.

Formation	Location	Pressure predicted = **Mechanical compaction**	Pressure underpredicted = **Unloading**
Early Permian:			
Wolfcampian Series	Eddy County		√
	Winkler County		√
	Reeves County	√ √	
	Pecos County	√	√ √ √
Pennsylvanian System:			
Cisco Formation	Loving County	√ √	
	Reeves County	√ √ √	
	Pecos County		√
Strawn Formation	Loving County		√ √
	Reeves County		√
	Pecos County	√ √	
Atoka Formation	Eddy County	√	
	Winkler County	√ √	
	Loving County	√ √ √ √	
	Reeves County	√ √	
Morrow Formation	Eddy County	√	
	Loving County	√ √ √	
	Reeves County	√ √ √	
	Pecos County	√	
Mississippian	Pecos County		√
Devonian	Reeves County		√ √
	Pecos County		√ √

Table 5.1. A summary of the results from the pore pressure prediction analysis. The number of ticks equals the number of true formation pore pressure readings taken from DST readings from wells

The results (Figs 5.7 & 5.8, and Table 5.1) from the pore pressure prediction analysis using the Equivalent Depth Method (EDM) and the Eaton Ratio Method on sonic logs thought the Delaware Basin, first of all show that the EDM and the Eaton method provide very similar pore pressure predictions to each other. The one difference is for sediments that are overcompacted for their present depth of burial, for example the mudstones of the Upper Bone Spring Formation (refer to Fig 5.6). In this case, the Eaton method predicts that the pore pressures are below hydrostatic, i.e. they are underpressured, whereas the EDM predicts that the pore pressures are hydrostatic (Fig 5.7 No. 2). It is known that, in the Delaware basin, the mudstones of the Upper Bone Spring Formation are actually hydrostatically pressured at present day (Webster. R.W., *pers comm*).

Mechanical Compaction

The results also show that both methods accurately predict the pore pressure in a number of wells. The Atoka and Morrow Formations of the Pennsylvanian System, for example, have 19 true formation pressure readings taken from DSTs in a number of wells, and each value is accurately predicted from the two methods. This suggests that these two formations are undercompacted as a response to loading, i.e. disequilibrium compaction.

Other formations pressures (in the Wolfcampian, Cisco and Strawn Formations) are also accurately predicted by the methods, suggesting that overpressure in these wells is a consequence of disequilibrium compaction, where mechanical compaction has been halted.

Evidence for unloading

There are also some results where both methods underpredict pore pressures. This is seen particularly in the Devonian, Mississippian Limestone and the Strawn Formation. Some pore pressures of the Wolfcampian are also underpredicted in some areas of the basin (Eddy, Winkler and Pecos County). As mentioned in sub-section 5.2.1.2, the EDM and Eaton method only accurately predict pore pressures, if the mudstone is normally compacted or undercompacted for its depth of burial. In cases where porosity has been destroyed by chemical processes following normal

compaction, or effective stress has been reduced by fluid expansion mechanisms, then pore pressure prediction methods will not provide a reliable estimation of the pore pressure, and will underestimate the pore pressure.

These results subsequently may be showing evidence of unloading mechanisms occurring in the basin. Velocity / density cross-plots will provide further evidence as to the existence of unloading processes and will be dealt with in the next sub-section.

5.3. Mechanism for overpressure generation

Discrepancies between the predicted pore pressures using the EDM and Eaton method and the measured formation pressures have been used as an indication of additional pressuring mechanisms other than disequilibrium compaction (Hart et al 1995; Mudford 1988). Bowers (2001) and Bowers & Katsube (2002) suggested a method involving velocity-density cross-plots to differentiate between overpressure generated by disequilibrium compaction and unloading processes.

5.3.1 Methodology behind velocity / density cross-plots

The sonic, resistivity, neutron and density logs are used to give an indication of a formation's porosity. However, in some basins throughout the world, the sonic and resistivity log give a response to zones of overpressure, whereas the density and neutron logs do not (Hermanrud et al 1998; Bowers 2002). Hermanrud et al (1998) investigated the sensitivity of sonic, resistivity, neutron and density logs to overpressure in the Haltenbanken area of offshore Norway. The same unit of shale was tracked over 28 wells, where its pore pressure ranged from normal to relatively highly overpressured (>3000psi or 20 MPa). They noticed no significant change in the density or neutron log response between the normal and overpressured zones, whereas the resistivity and the sonic logs showed a marked decrease when entering

the overpressured zone (Fig 5.9). Because the shales were from similar depths and exhibited little lateral variation, Hermanrud et al (1998) ruled out diagenesis as a possible cause.

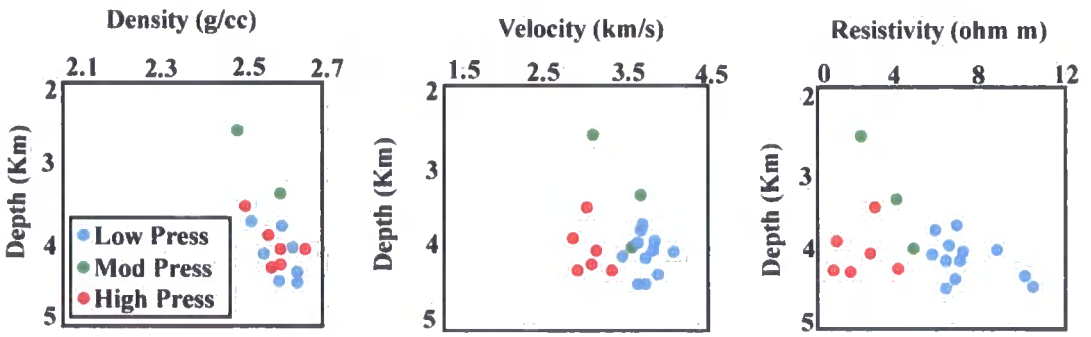

Fig. 5.9. Sonic, density and resistivity data from the Not formation in Haltenbanken, offshore Norway (Hermanrud et al 1998). The velocity and resistivity data are showing responses to high overpressure, whereas density data increases with depth regardless of pore pressure change.

It has been proposed by Katsube et al (1992) that rock pore structures are a combination of relatively large high aspect ratio storage pores, which are linked together by a network of smaller, lower aspect ratio connecting pores. The contribution of storage and connecting pores to the bulk properties of the rock are weighted equally, in the density and neutron log responses. The sonic and resistivity logs, however, are sensitive to the transport properties of a rock, and in relation to the storage and connecting pores, the effect of the connecting pores is more dominant.

Bowers and Katsube (2002) proposed that the difference between the transport properties (sonic and resistivity) and the bulk properties (density and neutron) of the rock to overpressure can be explained by this storage pore/connecting pore model.

Where overpressure is generated by disequilibrium compaction, the effect is the slowing down or halting of the compaction process, it cannot cause effective stress reduction. The slowing down of compaction will have the same effect on the

connecting pores as well as the storage pores, therefore the bulk and transport properties will respond equally. Hence the density log will have the same trend as the sonic or resistivity log.

Bowers and Katsube (2002) found out that connecting pores are mechanically flexible and are capable of elastic rebound, whereas any volume reduction in storage pores tends to be permanent. Therefore where effective stress is reduced by the overpressure generation mechanism of fluid volume increase, the connecting pores widen due to their flexibility, but the storage pores remain unchanged. The transport properties (sonic and resistivity) of the rock thus respond to the widening of the connecting pores, whereas the bulk properties (density and neutron) remain unchanged. The mismatch between sonic and density recorded in the mudstones of the Haltenbanken area of offshore Norway (Hermanrud et al 1998) (Fig 5.9) was attributed to fluid expansion mechanisms.

Fig 5.10 can be used to interpret velocity / density cross-plots, where four mechanisms can be identified from the trends. If the sediment is normally compacted or overpressured as a consequence of disequilibrium compaction, then the trend of the data will follow the published trend lines (Bowers 2001). Lithology changes are characterised by a shift to the left (sandy) and right (clay rich) relative to the trend lines. Unloading can be recognised by a near vertical trend in the data, where velocity decreases and density remains constant (Bowers 2001). Where chemical compaction or clay diagenesis has occurred, then trend shows increasing density with almost constant velocity (Hoesni 2004). A hybrid trend of moderately decreasing velocity with increasing density has been recognised by Lahann (2002), and is suggested by Hoesni (2004) to be a consequence of combination of chemical compaction and unloading effects.

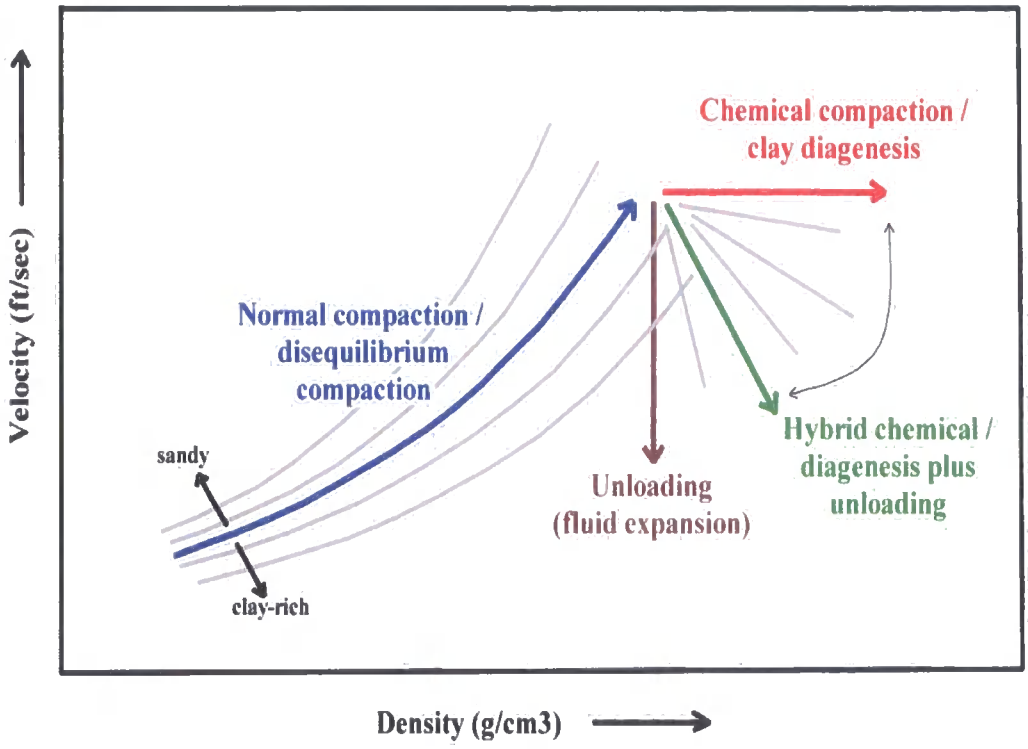

Fig 5.10. Summary of velocity / density trends for different processes (Taken from Hoesni 2004).

5.3.2. Results of velocity / density cross-plots for the Delaware Basin

Velocity / density cross-plots were constructed for three wells (Hill Haley 1a; Worsham Unit 1; Harrison 10 well) in the Delaware Basin, and interpreted based on the work by Bowers and Katsube (2002) and Hoesni (2004). Only three wells were analysed due to the lack of density logs for wells in this study. These three wells were earlier analysed by pore pressure estimation methods (sub-section 5.2.2), where the true pore pressures in the Hill Haley 1a well were accurately predicted in the Morrow Formation of the Pennsylvanian System, suggesting overpressure was generated as a consequence of disequilibrium compaction. In the Worsham Unit 1 well and the Harrison 10 well, the pore pressures were underpredicted in the Strawn

Formation of the Pennsylvanian System, suggesting unloading mechanisms may be the cause.

The pore pressures of the Devonian and the Mississippian Limestone Formations were also underpredicted in some wells; however, in no wells were both the density and the sonic log run through these two formations, meaning that velocity / density cross-plots could not be constructed to aid in the understanding of why he pore pressures were underpredicted.

Hill Haley 1a well

Velocity / density cross-plots were run through the Atoka, Morrow, and Barnett Formation of the Hill Haley 1a well. Earlier pore pressure prediction methods accurately predicted the pore pressure of the Morrow Formation.

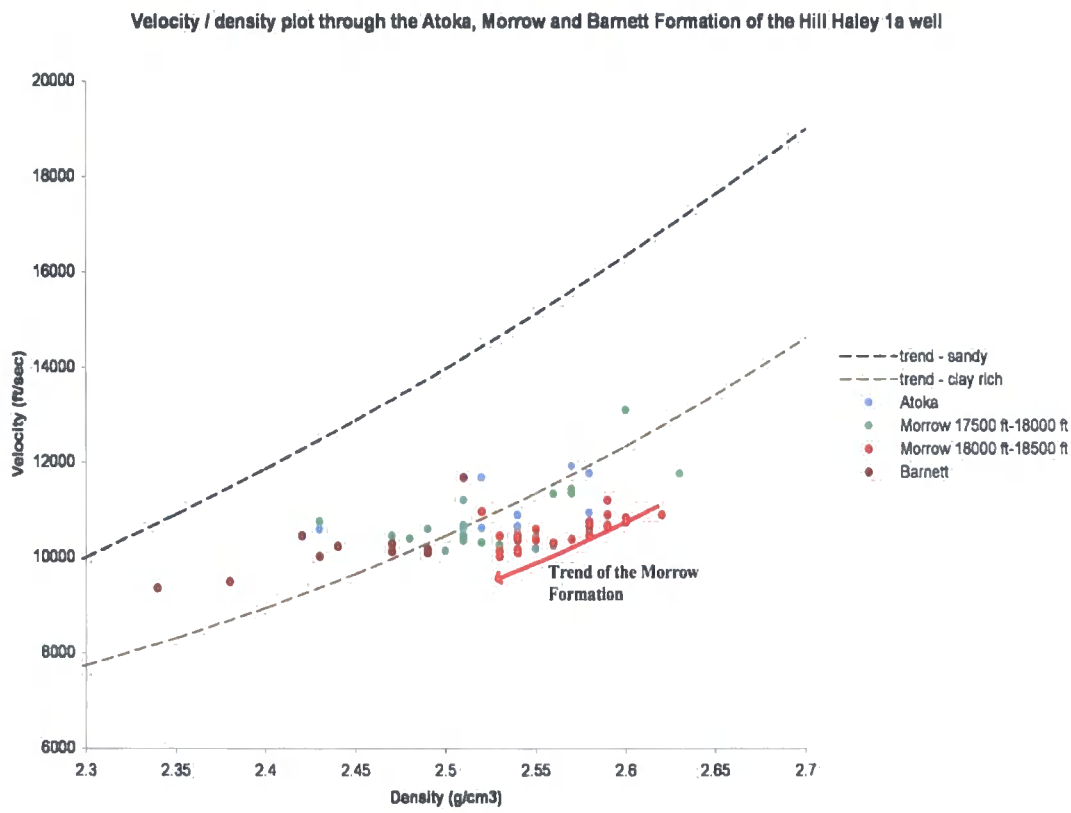

Fig 5.11. Velocity / density cross-plot for the Hill Haley 1a well.

The results for the Hill Haley 1a well show that although the plot of the Morrow Formation is quite sporadic, the general trend suggests a compaction trend as a result of overburden. The Morrow Formation is overpressured in this section and so the results suggest disequilibrium compaction as the mechanism behind overpressure. The overlying and underlying Atoka and Barnett Formations respectively also display compaction as a result of mechanical processes. These results are in agreement to the pore pressure prediction results of the Morrow Formation in the Hill Haley 1a well (Fig 5.7 No. 2), where the methods were accurately predicting the overpressure in the Morrow Formation, indicating that the overpressure was a consequence of disequilibrium compaction.

Harrison 10 well

Velocity / density cross-plots were created for the Cisco Formation and Strawn Formation of the Harrison 10 well. Earlier pore pressure predicting methods were underpredicting the overpressure in this zone.

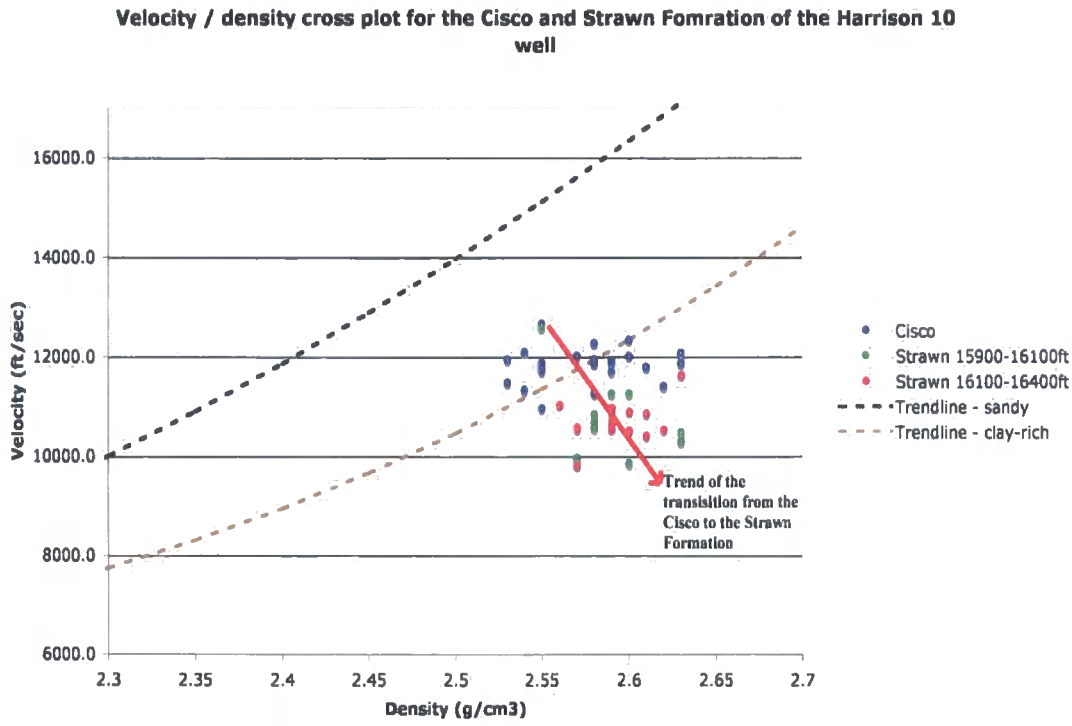

Fig 5.12. Velocity / density cross-plot for the Harrison 10 well.

The results for the Harrison 10 well show a trend suggesting a hybrid combination of unloading and chemical compaction in the transition between the Cisco Formation and the Strawn Formation. This is in agreement with the pore pressure prediction result for the Harrison 10 well (Fig 5.7 No. 3), where the methods were underpredicting the overpressure in the Strawn Formation, which could suggest that the pore pressure was a consequence of unloading. In conclusion based on both these sets of results, the Strawn Formation in the Harrison 10 well is indicating evidence of unloading.

Worsham Unit 1 well

Velocity / density cross-plots were created for the Strawn Formation of the Worsham Unit 1 well. Earlier pore pressure predicting methods were underpredicting the overpressure in this zone.

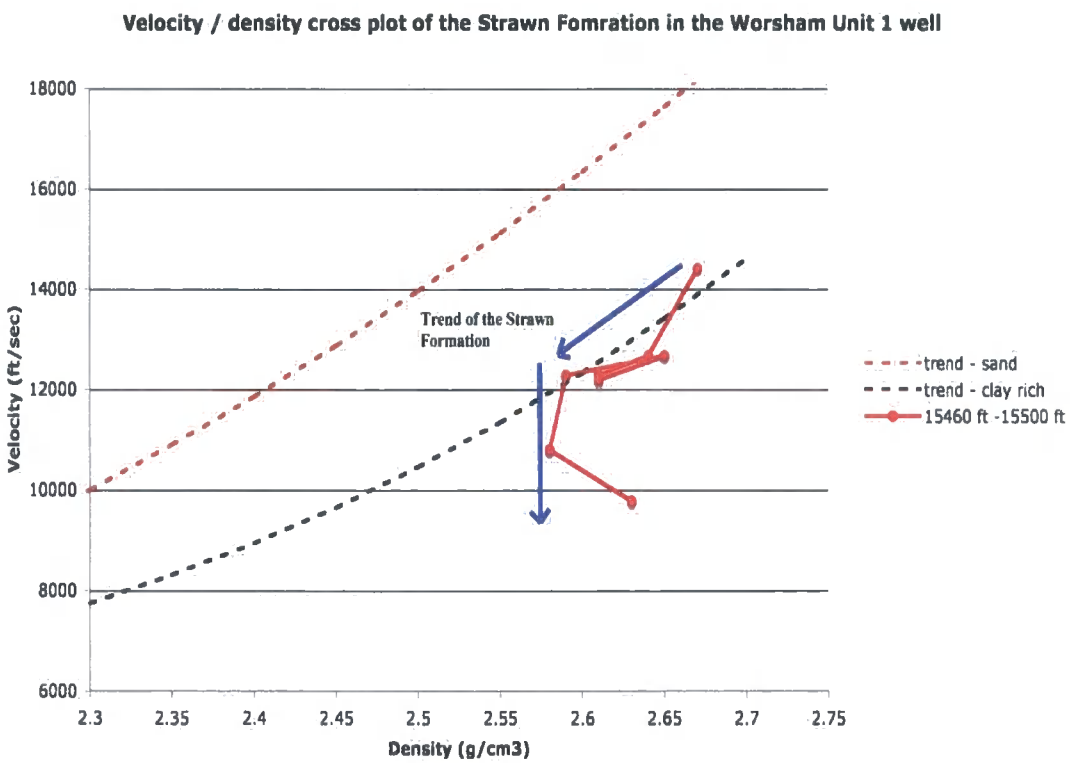

Fig 5.13. Velocity / density cross-plot for the Worsham Unit 1 well.

The results from the Worsham Unit 1 well, show evidence of unloading in the Strawn Formation. This unloading pattern is on a small scale (~ 50 ft or 15m), but the depth corresponds exactly to the overpressure reading that was being underpredicted by the Equivalent Depth Mehtod and the Eaton Ratio Method (Fig 5.8 No.7), and to a peak of high porosity as represented by the sonic compaction curve (Fig 5.14).

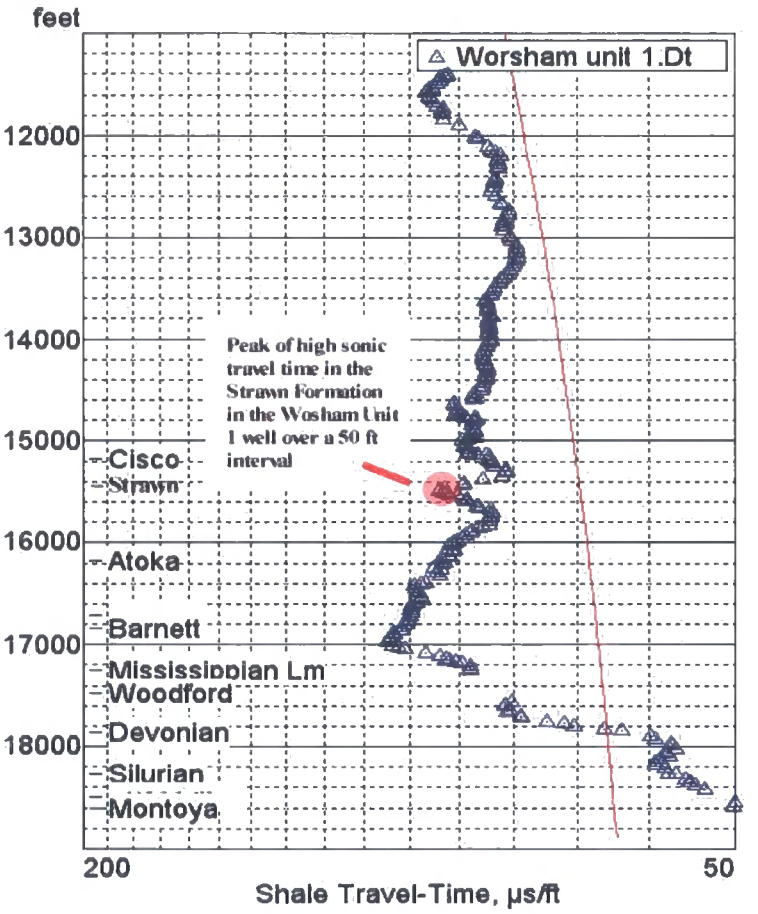

Fig 5.14. Shale compaction curve of the Worsham Unit 1 well using sonic travel time data from the well. A peak of high travel time (i.e. porosity) is seen around 15500 ft, which corresponds to a high overpressure reading (Fig 5.8 No. 7). This zone is also showing evidence of unloading (Fig 5.13).

This study suggests that this horizon may be a reservoir horizon where unloading processes are occurring such as gas generation through oil to gas cracking, gas expansion on uplift or lateral transfer.

5.4 Discussion: Application of sonic logs in pore pressure analysis

Sonic logs are recognised as a useful tool for the analysis of pore pressure in a basin. Previous work has used sonic logs to predict pore pressure (Harrold et al 1999; Ruth & Hillis 2000; Hoesni 2004), or has used velocity data from sonic logs in combination with density data to analyse the mechanism of pore pressure generation (Hermanrud et al 1998; Bowers & Katsube 2002; Hoesni 2004), or has used the sonic response to recognise the onset of overpressure in a well (Carlin & Dainelli 1998; Heppard et al 1998; Hoesni 2004). With the exception of Ruth and Hillis (2000), whose work was conducted in the Permian Cooper Basin of South Australia, the use of sonic logs to understand pore pressure is predominantly undertaken in 'young' Tertiary basins, where the sedimentary fill is homogeneous, and overpressure has been generated through disequilibrium compaction. However, the results of this study have shown that the sonic log can be a useful pore pressure analysis tool in Palaeozoic heterogeneous aged shales of the Delaware Basin. This is dependent on an accurate assignment of a present day normal compaction curve that is complicated by the complex burial and tectonic history of the basin; the shales are not currently at their maximum effective stress.

5.4.1 Evidence for pore pressure dewatering

The results from this chapter have shown that sonic logs respond accurately to pore pressure change where overpressure was generated by disequilibrium compaction and compaction is controlled by vertical stress. Then interpretation of the shale compaction trend based on sonic logs can give an indication of the present day overpressure pattern (Fig 5.15). In chapter 4 it has already been suggested that the present day shale compaction curve shows evidence for palaeo-normal compaction curves within the Delaware Group and the Upper Bone Spring Formation. These trends are overcompaction trends at their present day depths of burial and represent phases in the basin's burial history when these units were normally compacted. The

Delaware Group was normally compacted 55 Ma when the basin was at maximum burial, and the palaeo-normal compaction curve of the Upper Bone Spring Formation represents a period of quiescence after the Laramide uplift (55-50 Ma) (Fig 5.15). These palaeo-normal compaction curves suggest that since maximum burial the basin has been attempting to reach pressure equilibrium, with certain horizons being able to dewater at different stages of the basin's history, hence showing that the pressure system in the basin is dynamic compared to static. Interpretation of the overpressured section from the compaction curve suggests that dewatering is still occurring at the present day (Fig 5.15).

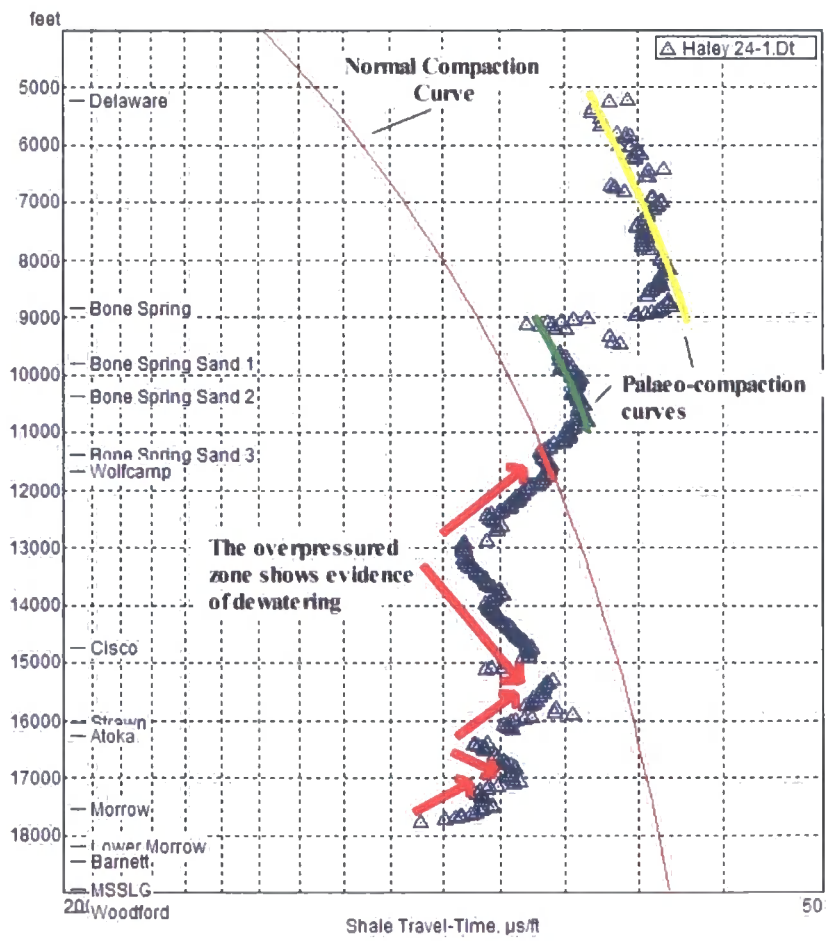

Fig 5.15. Interpretation of the shale compaction curve for the JE Haley 24-1 well.

Further analysis of the dewatering pattern shows that the high peaks of sonic velocity correspond to carbonate horizons in the basin (Fig 5.16). These carbonate beds have low sonic travel time readings of around 50 µs/ft which equates to a porosity of about 2-3 %, indicating that they may be tight horizons, which are controlling the dewatering of the overpressured zone.

Further analysis of the dewatering pattern and the influence of the limestone horizons on the pore pressure history is dealt with further in the later discussion (chapter 7).

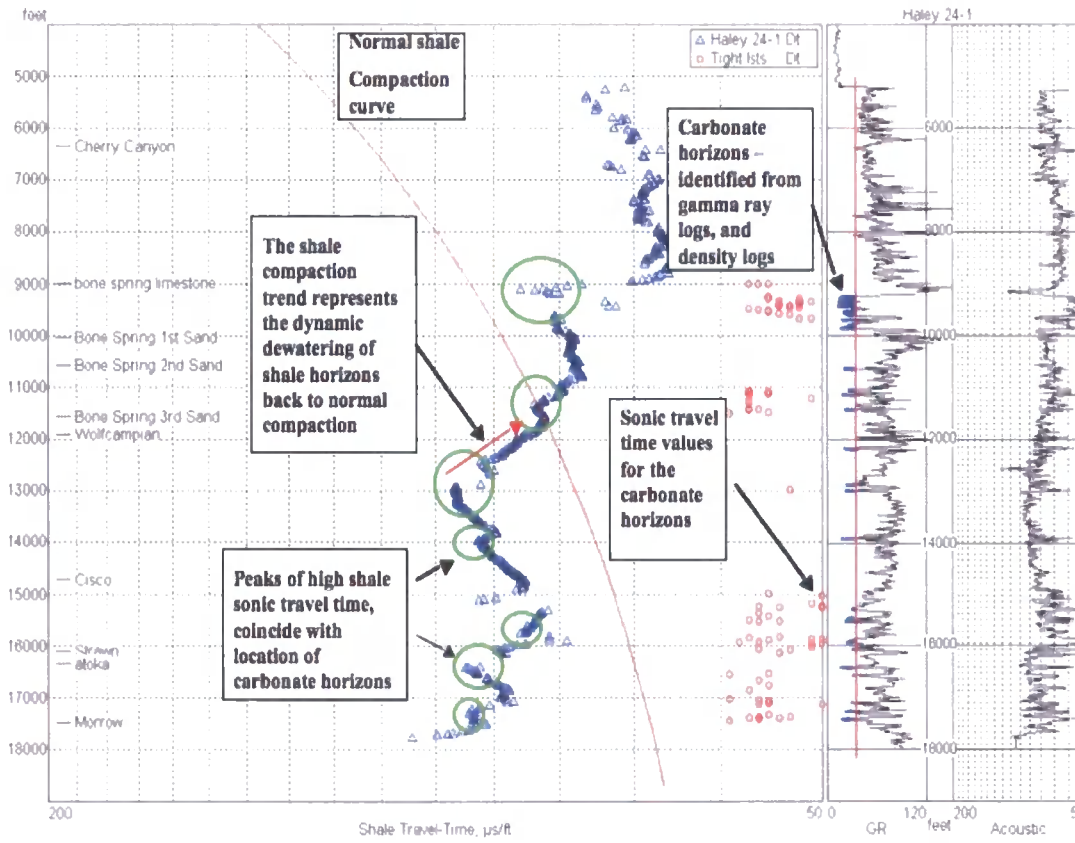

Fig 5.16. Correlation of the shale compaction curve to the gamma ray log. The peaks of high sonic velocity correspond to limestone horizons in the basin, suggesting that these horizons may be controlling the dewatering of the basin.

5.5 Conclusions

5.5.1 Pore pressure prediction

In this chapter, 11 wells were analysed using the sonic travel time to predict overpressure using the Equivalent Depth Method and the Eaton Ratio Method. The results showed a very accurate fit with the true formation pressures (Figs 5.7 & 5.8), which indicates that the formation pressures recorded in the wells are a consequence of disequilibrium compaction. The methods, however, underpredicted the pore pressure for certain horizons:

- In the Devonian Formation, all pore pressure was underpredicted in the chosen wells.
- Mississippian Limestone Formation was underpredicted in one well.
- The Lower Wolfcampian Series was underpredicted in three wells.
- Within the Pennsylvanian System
    - The Strawn Formation was underpredicted in two wells.
    - The Cisco Formation was underpredicted in one well.

The Equivalent Depth Method and the Eaton Ratio Method only accurately predict pore pressure if the shale is normally compacted or undercompacted due to disequilibrium compaction for its depth of burial. Where porosity has been destroyed by chemical processes following normal compaction, or where pore pressure has increased as a result of fluid expansion, then these methods will not provide a reliable estimation of pore pressure, but will underestimate the pore pressure. The results suggest that unloading mechanisms may be a secondary feature in certain horizons in some wells, and is more likely to be a localised effect in the reservoir.

5.5.2 Mechanism of generation using velocity / density cross-plots

Velocity / density cross-plots were also created for the Hill Haley 1a well, Worsham Unit 1 well, and the Harrison 10 well, where the results back up the previous pore pressure prediction results.

- **Hill Haley 1a well**. The pore pressure prediction method accurately predicted the pore pressure of the Morrow Formation in the well. Using velocity-density cross-plots, the results confirm that the Morrow Formation is undercompacted for its depth of burial.
- **Harrison 10 well**. The pore pressure prediction method underpredicted the pore pressure of the Strawn formation. Velocity / density cross-plots, suggest that in the well the Strawn Formation is not simply mechanically compacted but has experienced unloading and chemical diagenesis.
- **Worsham Unit 1**. The pore pressure prediction method underpredicted the Strawn Formation. The velocity / density cross-plots of the Strawn Formation shows that over a small horizon (50ft) unloading processes are occurring, which could be indicative of gas generation via source rock maturation, oil to gas cracking in a reservoir, lateral transfer of high pressures from deeper units, or gas expansion due to uplift.

5.5.3 Dynamic or static pressure system

Interpretation of the shale compaction curve from the sonic log indicates that pore pressure dewatering is occurring in the overpressured section of the basin at present day. This shows that the pore pressure in the basins is in a dynamic state, where the overpressured units are attempting to return to pressure equilibrium. The zones of highest preserved porosity in the overpressured zone correspond to limestone horizons in the basin suggesting that they may be controlling the dewatering.

Chapter 6:
Basin Modelling of the Delaware Basin

6.1 Introduction

Basin analysis is the study of the interactions between sediment deposition and compaction, thermal changes, fluid flow, tectonic forces, sea level variations, hydrocarbon production and accumulation in evolving sedimentary basins (Lerche 1993). Basin modelling is a numerical tool that integrates the above interactions within a basin and displays the results of the basin analysis in a one, two, or three-dimensional (1D, 2D, 3D) perspective through time. Basin modelling is predominantly used in industry for the modelling of burial history, thermal regimes, pore pressure prediction, source rock maturation, hydrocarbon generation, expulsion, secondary migration and entrapment (Dore 1993). Also, because the search for new hydrocarbon reserves within the worlds basins is becoming ever more challenging, basin modelling is being used increasingly as a predictive tool by the oil and gas industry, to reduce risk in prospect evaluation (Duppenbecker and Iliffe 1998).

For the simulation of these processes in any basin, a number of parameters need to be specified for input to the program, in order to define the:

- Burial History
    - The present day geometry of the basin.
    - Lithology for each stratigraphic horizon.
    - Porosity and permeability relationships for each lithology.
    - Known hiatuses and fault evolution.
- Thermal history
    - Present and palaeo surface temperature.
    - Present and palaeo heat flow.
    - Crust and lithosphere properties.
- Hydrocarbon generation and expulsion.
    - Known source rock horizons.
    - Geochemistry of the source rock.

This chapter will look at several of the key parameters involved in basin modelling software, particularly the parameters needed to reflect present conditions in the Delaware Basin.

It is important to note that, as a consequence of the numerous parameters needed in basin modelling and the sensitivity of the parameters to minor change, the end results can vary significantly depending on the values used. Therefore unless a precise value is known for each parameter for a particular basin, modelling cannot provide a unique answer to a geological system. It can only provide a better understanding through insight into how the basin and its individual components evolved through time, and contribute to answering the geological questions.

This is the premise behind the use of basin modelling in this study. It will not be used to generate a definitive answer of what generated overpressure or how it is maintained. However, the basin modelling is used as a tool to test the results and the theories presented up till now from the previous chapters. The model will illustrate if the results suggested so far are geologically plausible.

6.1.1 Aims of basin modelling

The purpose of this chapter is to address the following two main questions with the aid of basin modelling.

1. How did overpressure generate in the Delaware Basin?
2. How is the overpressure maintained in the Delaware Basin

6.2 Data input and methodology for 1D and 2D basin modelling

1D modelling

A 1D model uses data from a single well in a basin, and therefore looks at the interaction between sediment deposition, compaction, thermal changes, and pore pressure etc. within the constraints of a vertical or sub-vertical well. 1D modelling is often referred to as maturity modelling (Waples 1998), and the commercial 1D modelling software 'Genesis' developed by the company Zetaware was used for this study. The 1D model of the Delaware Basin created for this study is based on the JE Haley 24-1 well in Loving County. Lithological and chronological information needed to create the 1D model was taken from work already done on the basin (Barker & Pawlewicz 1987; Hills 1994; Luo et al 1994; Hill 1996; Dutton 2005). An example of the 1D model output and the lithologies used to create it is shown below (Fig 6.1).

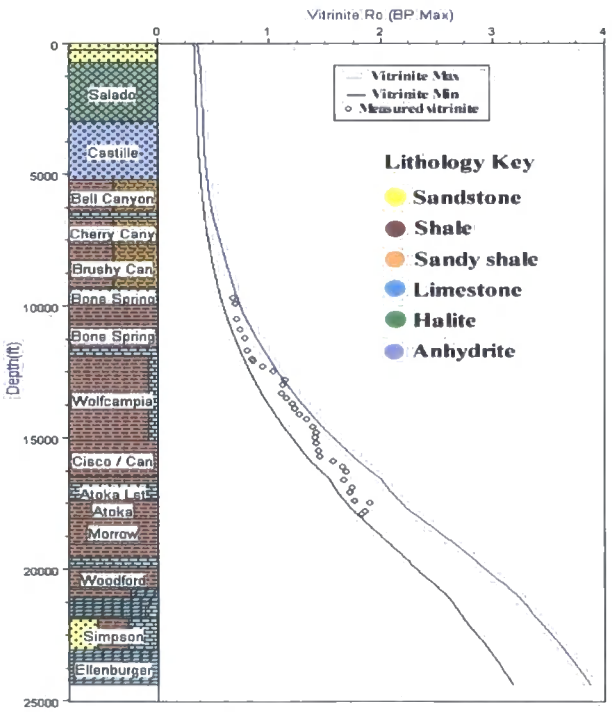

Fig 6.1. Example of a 1D model using the JE Haley 24-1 well. In this example, the recorded vitrinite data is plotted against expected vitrinite results. Using the heat flow history concluded in chapter 4, true vitrinite reflectance data match the predicted values, indicating the thermal history scenario is correct (sub-section6.2.3.1).

2D modelling

2D modelling has the advantage over 1D modelling that the basin can be viewed in a vertical cross-section perspective, which means that lateral fluid flow can be modelled. This advantage over 1D modelling means that pore pressure can be accurately modelled. The software Temis 2D version 4.0 was used for this study. Temis 2D is a finite volume commercial software package that enables the user to simulate basin subsidence, thermal history and hydrocarbon generation and migration as in a sedimentary basin. The details of the algorithms and the modelled processes are given in Ungerer et al (1990).

The present day geometry of the Delaware Basin which used to create the 2D model, was based on a USGS cross-section of the basin from east to west, which encompasses the Central Basin Platform and the neighbouring Midland Basin further to the east. The 2D model creates individual cells within the cross section, and each cell can be assigned its own lithological parameters (Fig 6.2), making the 2D model as realistic as possible.

The Temis 2D licence for Durham University is limited in that it can only model two pore fluid phases, water and hydrocarbons. This means that oil and gas cannot be modelled as two different fluids. This two-phase modelling is more than adequate for the purposes of 2D modelling in this study.

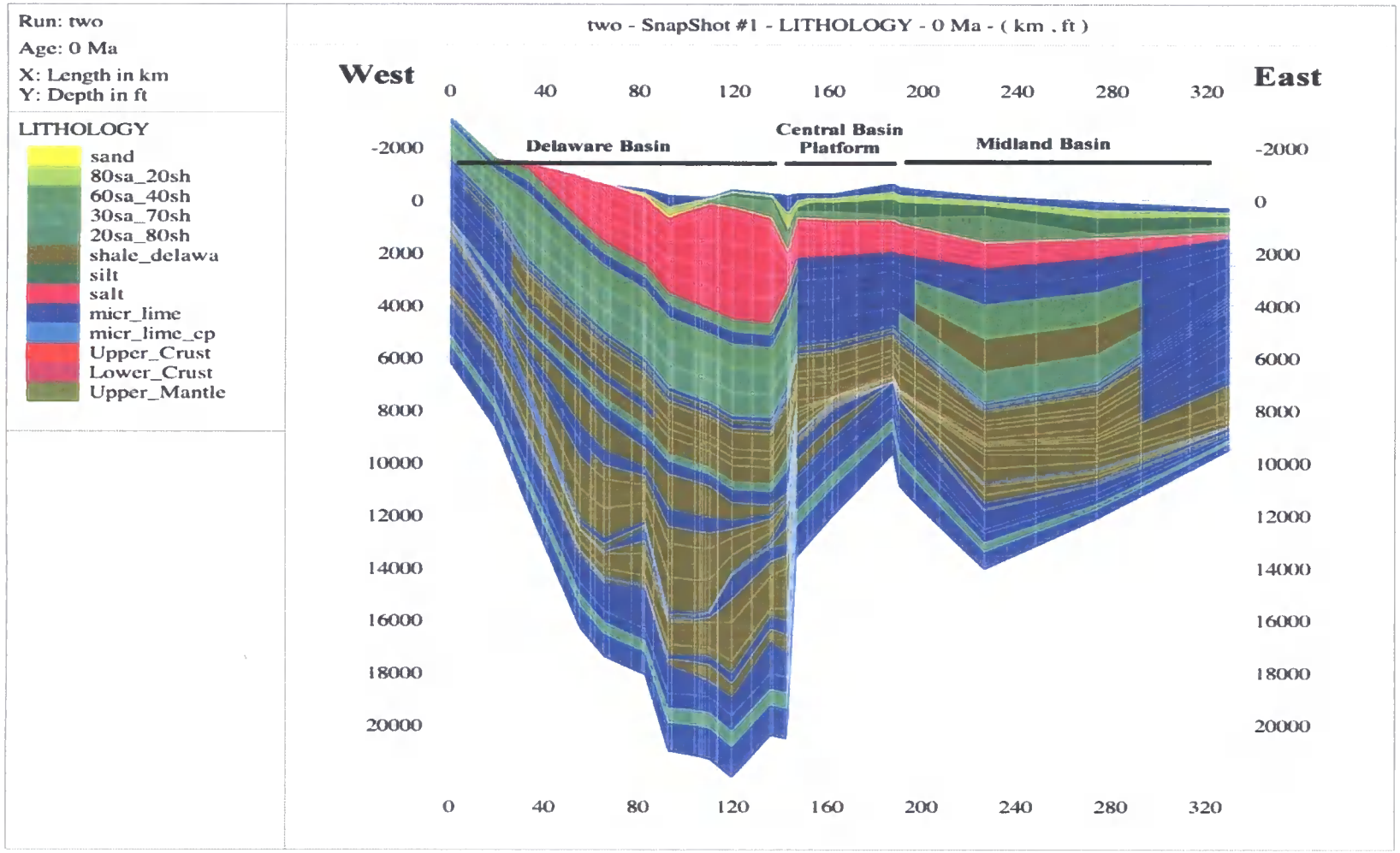

Fig 6.2. Cross section of the basin as represented in a 2D model using the software 'Temis 2D'.

6.2.1 Basin subsidence and compaction

Both the 1D and 2D modelling software use a "backstripping" method in the computation of subsidence and compaction. The present day geometry is backstripped, whereby the sedimentary layers are removed one by one, bringing the sediments back to the basin's surface where they were originally deposited. This geometrical restoration defines the sedimentary and stratigraphic evolution of the basin based on the initial input parameters the user defines. To decompact layers and hence define the initial thickness, a porosity-depth or effective stress-depth relationship for each lithology is needed as an input parameter. Porosity-depth or effective stress-depth relationships are essential to basin modelling, as they are used to calculate as well as the subsidence history, properties such as heat capacity, thermal conductivity and permeability (Giles et al 1998). The more accurate the porosity-depth relationships are, the more accurate the results from the basin model will be.

This study has used shale compaction curves and mercury porosimetry analysis to create a porosity-depth curve to be assigned for the shales of the Delaware Basin, based on the Hubbert and Rubey relationship (1959) (chapter 4.2.4). This curve has been used for both the 1D and 2D models used in this study. For all other lithologies, default porosity-depth relationships from the modelling software are used, due to the lack of available data needed to construct them.

It is important to note that the Delaware Basin has been uplifted in the past; this means that all sediments in the basin have experienced higher values of effective stress than at present. This makes estimating porosity-depth relationships for any sediment very difficult, and it is advisable to avoid uplifted sediments when trying to recreate porosity-depth curves (Giles et al 1998).

6.2.2 Fluid flow

Fluid flow in a basin is effectively controlled by the permeability of the sediments, as permeability is the parameter defining the ease with which fluid flows through a porous medium. Darcy's Law defines the flow rate as:

$$Q = k(P1-P2)A / \mu L \quad (6.1)$$

where:

Q = flow rate,

k = permeability,

P1-P2 = pressure drop,

A = cross-sectional area,

μ = viscosity, and

L = Length.

In a basin model, permeability is usually expressed as a simple function of the porosity, and is estimated using a power function of the type:

$$k = k_0 (e/e_0)^c \quad (6.2)$$

where:

k_0 is the reference permeability,

e_0 is the reference void ratio of the sediment,

e is the current void ratio: $e = \phi /(1-\phi)$, and

c is a coefficient which is influenced by sediment lithology.

This is the method by which permeability is calculated in the 'Genesis' 1D-modelling program. A default value of the coefficient (c) is generally used for all mudstones, and the value of 3.5 is used as default for mudstones in the Genesis model.

Several permeability models have been developed which are based on the Hagen-Poiseuille equation, which describes Newtonian flow in a straight tube of circular cross-section. The Kozeny-Carman relationship is one of these theoretical approaches to model permeability, and is the method used in Temis 2D modelling.

The Kozeny-Carmen relationship relates permeability to specific surface area and porosity. For permeable sediments (ϕ >10%), the equation is:

$$k = 0.2\phi^3 / (S_o^2 (1-\phi)) \quad (6.3)$$

where:
k = permeability (m^2),
S_o = specific surface area (m^2/m^3), and
ϕ = porosity.

For sediments of a low permeability (ϕ < 10%), the Kozeny-Carman relationship has been modified:

$$K = 20\phi^5 / (S_o^2 (1-\phi)) \quad (6.4)$$

The equations above show how a basin model computes the permeability evolution of a lithological package through geological time. However, the output modelled permeability is entirely dependant on the inputs. To aid in the calibration, present day permeability measurements were taken from seven mudstone samples through the basin using a mercury injection procedure. This was undertaken at Newcastle University, with the following vertical permeabilities being recorded:

- Bell Canyon Formation: 3.33 E^{-21} m^2
- Cherry Canyon Formation: 3.1 E^{-21} m^2
- Brushy Canyon Formation: 1.84 E^{-21} m^2
- Bone Spring Formation: 6.12 E^{-21} m^2
- Wolfcampian Series: 2.83 E^{-21} m^2
- Pennsylvanian System: 2.61 E^{-21} m^2
- Mississippian System: 3.02 E^{-21} m^2

6.2.3 Thermal history

Heat flow in a sedimentary basin is derived from two sources. Radiogenic heat from the lithosphere is generated by the radioactive decay of isotopes of uranium, thorium and potassium. For Palaeozoic crust, the radiogenic heat flow is around 28.8 mW/m^2 (Rudnick 1995) which is the value used in both 1D and 2D models. Heat flow from the mantle is the other main source of heat for a sedimentary basin. The inputs into a basin model include the thickness of the crust and its thinning history and the thickness of the mantle lid. For the modelling of the Delaware Basin, the crust thickness was set at 32 km for the duration of the foreland basin's history. The thickness of the mantle lid was set at 98km.

The transfer of heat in a sedimentary basin is achieved by thermal conduction through rocks and convection through fluids (Allen & Allen 1990). In both the 1D and the 2D models, only conduction is used to transmit heat. A 1D model cannot directly handle convection, because convective movement is not one-dimensional (Waples 1998). With the 2D Temis model, convection was not possible, because it was not an option in the thermal history setup that was used in the model.

6.2.3.1 Heat flow history

This study has defined a new burial and tectonic history for the Delaware Basin (Chapter 4). It was based on thermochronology results from apatite fission track analysis (AFTA), vitrinite reflectance (VR) and shale compaction curves. Based on the results, the following burial history scenario was suggested (Fig 6.3):

- Assuming a present and a palaeogeothermal gradient of 21.8° C/km (constant heat flow of 47 mW/m^2 during the Mesozoic and Cenozoic).
- The surface temperature has been constant at 20 °C through time.
- Maximum burial occurred in the basin 55 Ma. To explain the high thermal maturity of the sediments, an additional 6890 ft of Mesozoic and

Cenozoic sediment is needed on top of preserved Triassic at maximum burial.

- The first uplift event (Laramide) occurred at 55-50 Ma, when 3890ft of sediment was eroded.
- The basin then subsided and 600 ft of Cenozoic Oligo-Eocene sediment was deposited.
- A second uplift event occurred 25-10 Ma (Basin and Range) resulting in 3600 ft of uplift and erosion.

The thermal history scenario can be constrained by modelling the present-day vitrinite reflectance data. If this thermal history scenario is correct, then the model will accurately predict the true present-day values (Fig 6.1).

For both the 1D and 2D models, heat flow was computed as a transient heat flow model compared to a steady state model. Transient heat flow takes into account the thermal blanketing effect of rapid burial, as well as the cooling of sediments resulted from the dumping of colder sediment on top.

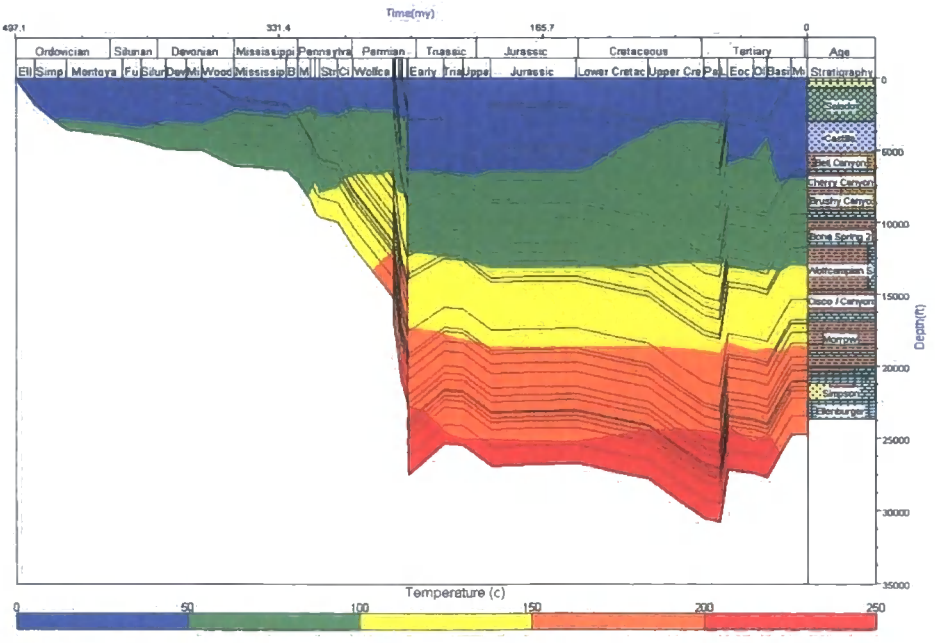

Fig 6.3. Burial history plot showing the temperature profile for the Delaware Basin based on results from chapter 4. The basal heat flow was modelled as constant at 47 mW/m^2.

6.2.4 Hydrocarbon generation and expulsion

Hydrocarbon generation was modelled using the 'Genesis' 1D program. Within the Delaware Basin, there are six known source rocks (Hill 1996; Dutton et al 2005):

- Bone Spring 1st Sand Formation of the Lower Permian
- Bone Spring 2nd Sand Formation of the Lower Permian
- Wolfcampian Series of the Lower Permian
- Barnett Formation of the Upper Mississippian
- Woodford Formation of the Devonian
- Simpson group of the Mid Ordovician.

To determine what kerogen type source rocks have, samples from each source rock need to be analysed, to determine the hydrogen index (HI) and the oxygen index (OI), and then these results plotted against each other (Fig 6.4). Each kerogen type has a distinctive initial HI, and with maturation during burial the kerogen will move down the indicated pathway toward the origin of the axes (black arrow). From this, the present-day level of maturation can be determined and hence the kerogen type can be identified (Cornford 2001).

Samples from the source rocks of the Delaware Basin were analysed for HI and OI (Fig 6.5). The results show that the Wolfcampian and the Barnett are Type III source rocks. The other source rocks are harder to interpret as they are highly mature, and plot right on the axes of almost zero OI. Samples from the Simpson source rock have high levels of HI, and this suggests that they originated from a type I or a type II source rock. For the purpose of modelling they will be classed as type II. The source rocks of both the Bone Spring Formations were also classed as type II / type III oil/gas prone. The Woodford source rock has been classed as a type III gas prone source rock (Webster. R., *pers comm.*). The following initial HI's were therefore assigned to the source rocks:

- Bone Spring Formations – HI = 350 mg/g/TOC
- Wolfcampian – HI = 200 mg/g/TOC
- Barnett – HI = 200 mg/g/TOC

- Woodford – HI = 200 mg/g/TOC
- Simpson – HI = 450 mg/g/TOC.

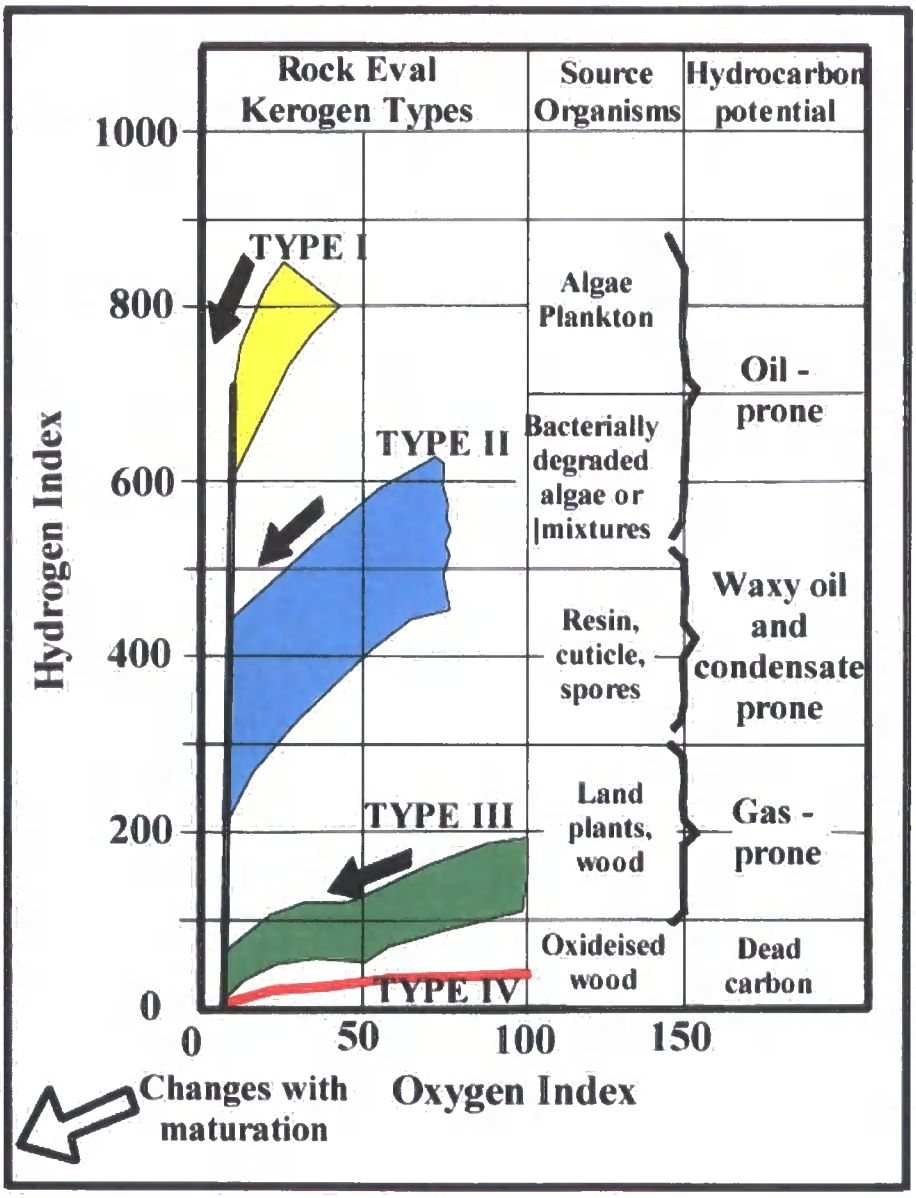

Fig 6.4. Kerogen type and maturity can be determined from a plot of hydrogen index against oxygen index. As the kerogens mature, they move down the predicted pathway towards the axes. Taken from Cornford 2001.

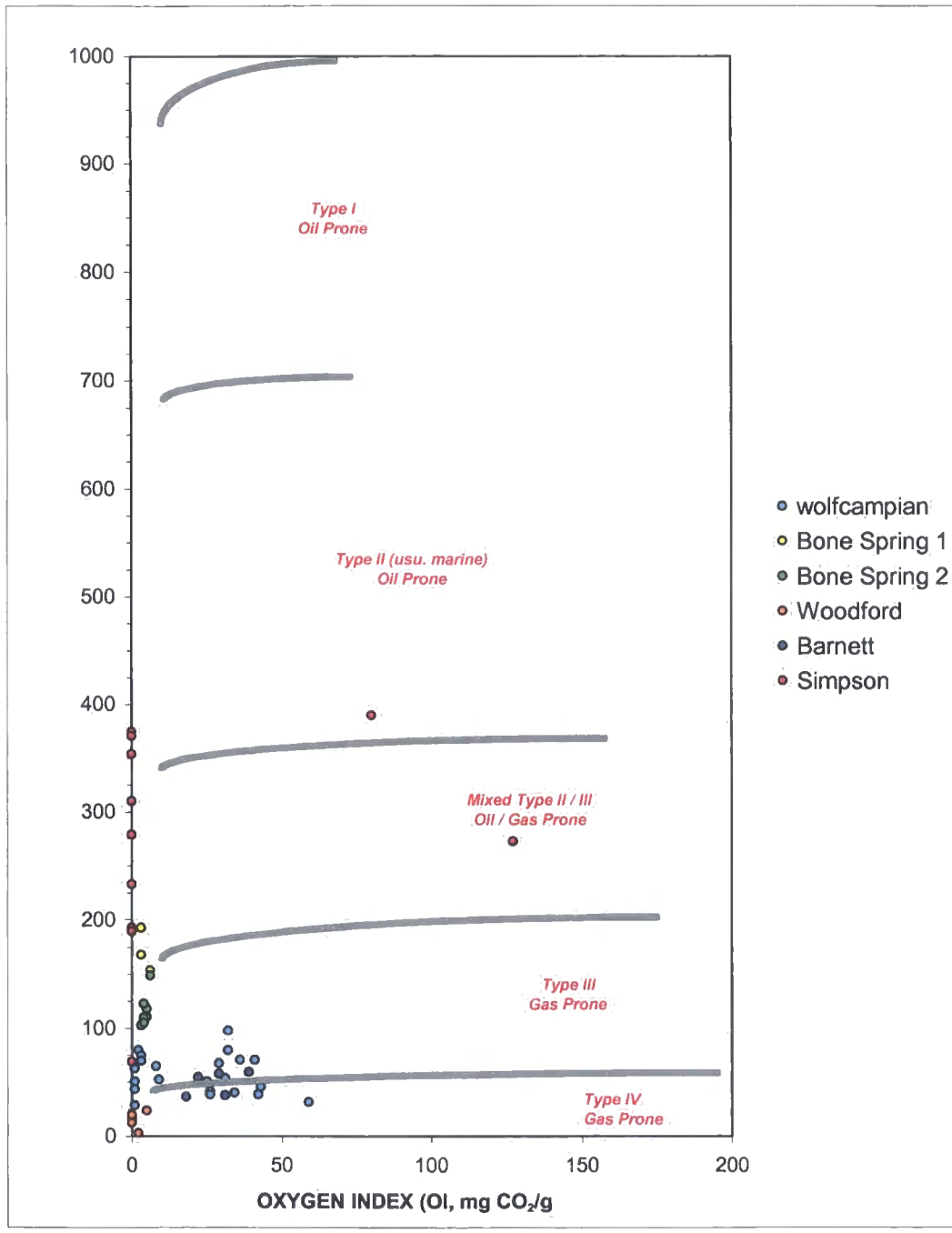

Fig 6.5. Plot of hydrogen index (HI) against oxygen index (OI) for the source rocks of the Delaware Basin. Apart from the Wolfcampian and the Barnett source rocks, the other source rocks are highly mature (OI close to zero), which makes identifying their kerogen type harder.

The final input parameters needed for the modelling of hydrocarbon generation is the initial total organic carbon (TOC) value of the source rocks. The present day TOC (% wt) values for the sources rocks are:

- Bone Spring 1st Sand, TOC = 2.40
- Bone Spring 2nd Sand, TOC = 1.87
- Wolfcampian, TOC = 1.24
- Barnett, TOC = 4.23
- Woodford, TOC = 3.92
- Simpson, TOC = 0.11

During thermal maturation, the source rock's TOC will decrease with time, and so the measured present day TOC of the source rock will be less than its initial TOC when it was buried. To work out the initial TOC levels of the source rocks from the Delaware Basin, 1D modelling was used to model the decrease in the TOC for each source rock (Fig 6.6). An initial TOC was first estimated for a particular source rock, and then modelled to see if it decreased sufficiently to match the final measured TOC. If it did not match, then the initial TOC was corrected accordingly.

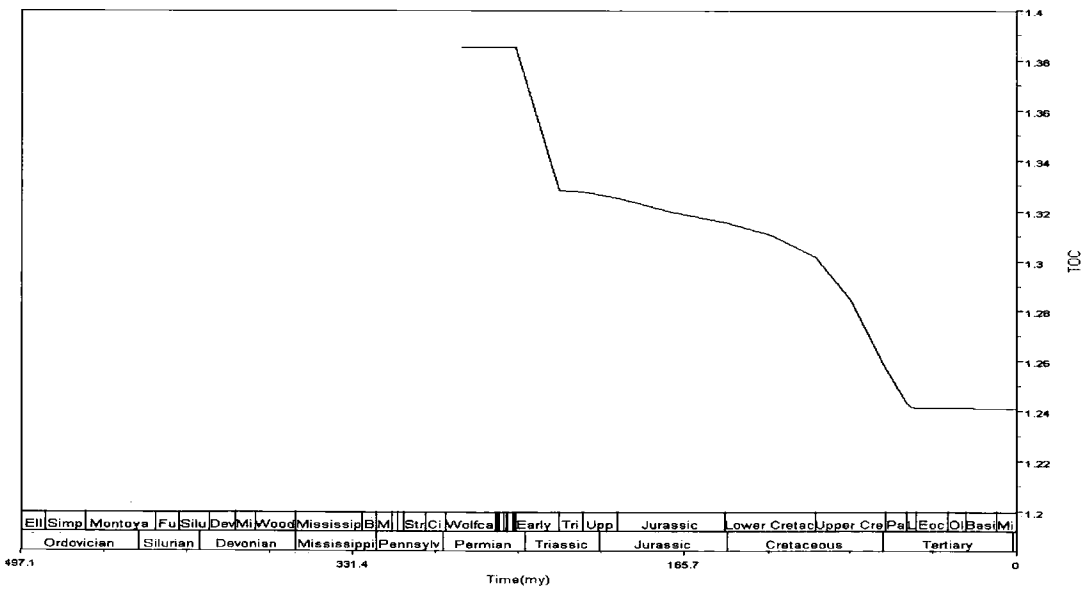

Fig 6.6. A 1D model plot of the decrease in the TOC content of the Wolfcampian source rock through time. The measured present day TOC is 1.24, and the model shows that an initial TOC content of 1.385 is needed to explain the present day value.

The 1D modelling of TOC decrease was applied on all source rocks. The following initial TOC values were used as input parameters for both the 1D and 2D models:

Source rock	Initial TOC values
Bone Spring 1st Sand	2.62 %wt
Bone Spring 2nd Sand	2.25% wt
Wolfcampian	1.385 %wt
Barnett	4.9 %wt
Woodford	4.5 %wt
Simpson	0.5 %wt

6.2.5 Sensitivity of basin modelling input parameters: Constraints on accurate pore pressure prediction.

One of the controlling factors of overpressure generation and retention is the permeability of the sediments. The ability of a sedimentary unit to dewater during and after burial is a function of its permeability, and this will determine whether or not overpressure can develop through disequilibrium compaction and be retained through geological time.

Since permeability is a function of the porosity, the assigned porosity-depth or effective stress-porosity curve for the mudrock affects its permeability and the amount of overpressure it may retain. Tests show that with a grater decrease in porosity with compaction, the amount of overpressure retained in the rock column could triple (Schneider et al 1993) (Fig 6.7). It is therefore important to ensure that the porosity-depth or porosity-effective stress curve is as accurate as possible.

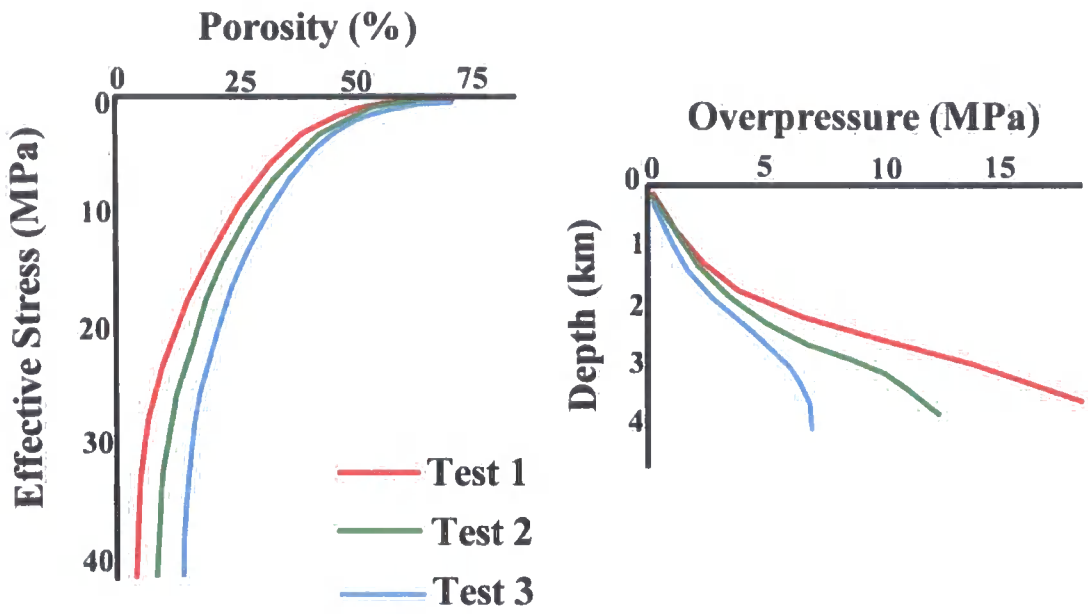

Fig 6.7. Example of the influence of porosity-effective stress relationship on overpressure generation. Tests were carried out on a single lithofacies and a constant sedimentation rate. The greater decrease of porosity with compaction causes a greater decrease of permeability using the Kozeny-Carman formula (Equation 6.2) (Taken from Schneider et 1993).

Another area that will cause uncertainty within a basin model is the great lithological heterogeneity of mudstones (Aplin et al 1995). This will have an effect on all models where permeability is estimated.

As mentioned previously, the coefficient used in equation 6.2, is normally a default value. However due to the great heterogeneity of mudstones, this value is likely to vary greatly as its influenced primarily by the grain size of the sediment, which can be described by the sediment's clay fraction (wt % particles smaller than 2μm diameter) (Aplin et al 1995; Yang & Aplin, 1998). A study by Tokunga et al (1998) used 2D modelling to model the effect that changing the coefficient c had on a number of parameters in the basin. The model used values of c ranging from 0 to 9, where increasing the value increases the rate at which permeability decreases with porosity loss (depth). The study showed that with a higher value of c (higher clay content in the mudstones), overpressure was more developed in the section, as the

mudstones had a lower permeability, and less pore fluid was expelled, and so the compaction of the sediments was retarded (Fig 6.8).

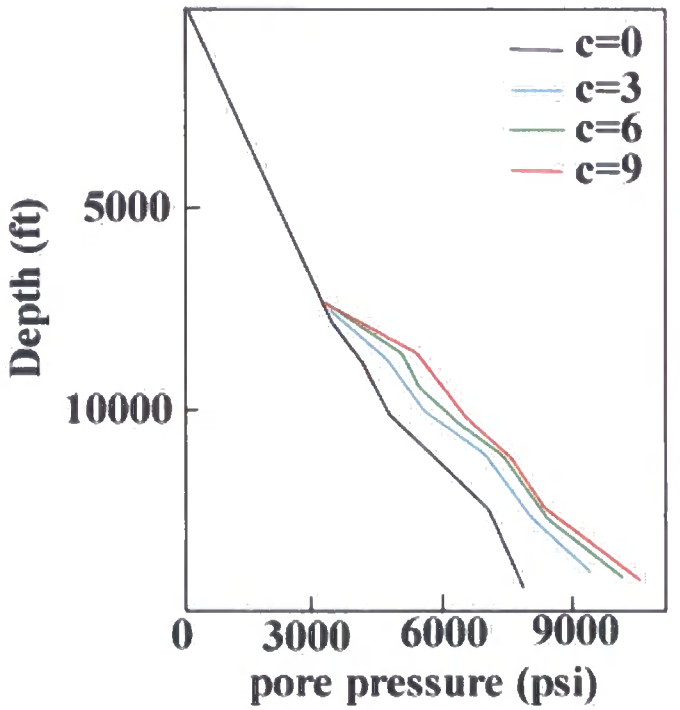

Fig 6.8. Pore pressure versus depth plot for different values of the compaction coefficient c. is altered with every model. For c =0 the section is close to hydrostatic, and with an increase in c the amount of overpressure also increases as the sediments become less permeable. Taken from Tokunga et al (1998).

Another consequence of the large heterogeneity of mudstones is that there is a large variation in published porosity-permeability curves. Published permeability data (Neuzil 1994) suggest that mudstone permeability can vary by three orders of magnitude at a given porosity (Fig 6.9). This variation is due to the lithological variability of mudstones, in particular the grain size. This places huge restrictions on the modelling of fluid flow and pressure in basins (Yang et al 2002), where most models assume that a single porosity-permeability function is sufficient for the whole mudstone sequence. In reality, mudstones may differ lithologically over a small depth interval.

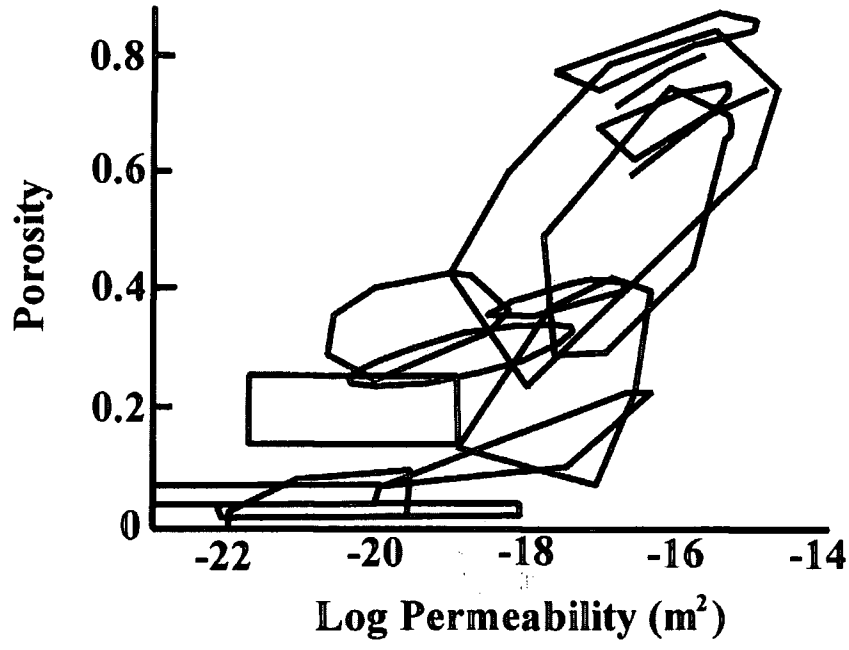

Fig 6.9. Published permeability data for mudstones. There is a large variability of mudstone pemeabilities, where at a single porosity, permeability varies over three orders of magnitude. Taken from Neuzil (1994).

One method of estimating the clay fraction content of mudstones is by using computer programs that analyse wireline data. One such program 'shale quant' was developed by Newcastle University (Aplin & Yang). Unfortunately this study did not have access to 'shale quant', and so the clay fraction of the mudstones in the Delaware Basin is unknown. Therefore accurate porosity-permeability relationships cannot be assigned to the modelling for this study.

6.3 Results of 1D and 2D modelling

As stated earlier in sub-section 6.1, this study has used basin modelling as a tool to test the results and the theories presented up till now from the previous chapters, regarding overpressure generation and its retention in the Delaware Basin.

6.3.1 Mechanism behind overpressure generation in the basin

Chapter 3 (sub-section 3.3) showed that up to 8500 psi of overpressure exists in the Delaware Basin. Chapter 5 (sub-section 5.5) concluded through the use of wireline analysis that the overpressure was predominantly generated through disequilibrium compaction, however, in certain horizons such as the Pennsylvanian aged Strawn Formation there is evidence to suggest that the overpressure may have been enhanced through unloading mechanisms. Basin modelling has been used to test these conclusions.

6.3.1.1 Overpressure generation through disequilibrium compaction.

Disequilibrium compaction occurs when there is rapid deposition of sediment, and the underlying sediments cannot dewater quickly enough. Compaction is halted, causing the pressure of the pore fluids to rise above the hydrostatic generating overpressure. It is commonly associated with mudstones where a low permeability aids in the inability of the sediment to dewater. During the Permian in the Delaware Basin, up to 19000 ft (5.8 km) of uncompacted sediment was deposited in 35 million years (285-250 Ma) (Fig 6.10). This rapid deposition of sediment has the potential to generate overpressure via disequilibrium compaction in the basin.

A 2D section was created in 'Temis 2D' which ran east-west across the Delaware Basin, Central Basin Platform and the Midland Basin, and was used to

model burial through time and the generation of overpressure by disequilibrium compaction.

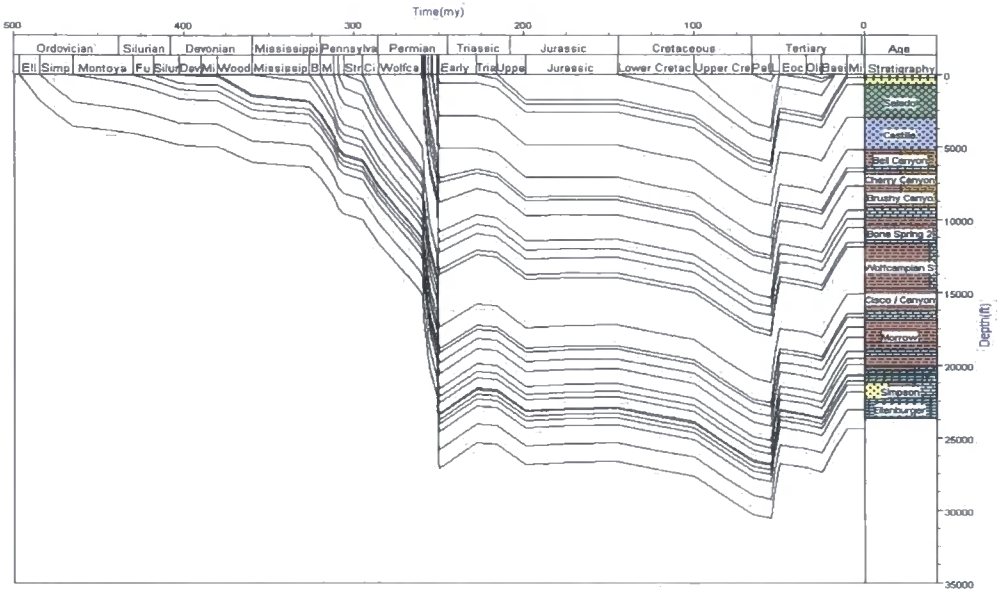

Fig 6.10 Burial history curve of the Delaware Basin using 1D modelling based on well information from the JE Haley 24-1 well in the centre of the Delaware Basin. Rapid deposition occurred between 285-250 Ma, when 15000 ft of Late Permian sediment was deposited.

The results are shown as cross-sections at particular times, with different colours representing the levels of excess pore pressure on the plots. Alongside the cross-section are plots of excess pore pressure with depth for a well in the centre of the basin at that particular period of time. Cross-sections for the following times are:

- 270 Ma – Top Wolfcampian Series of the Early Permian (fig 6.11)
- 251 Ma – Top Delaware Mountain Group of the Late Permian (fig 6.12)
- 250.6Ma – Top Ochoan Series of the Late Permian (fig 6.13)

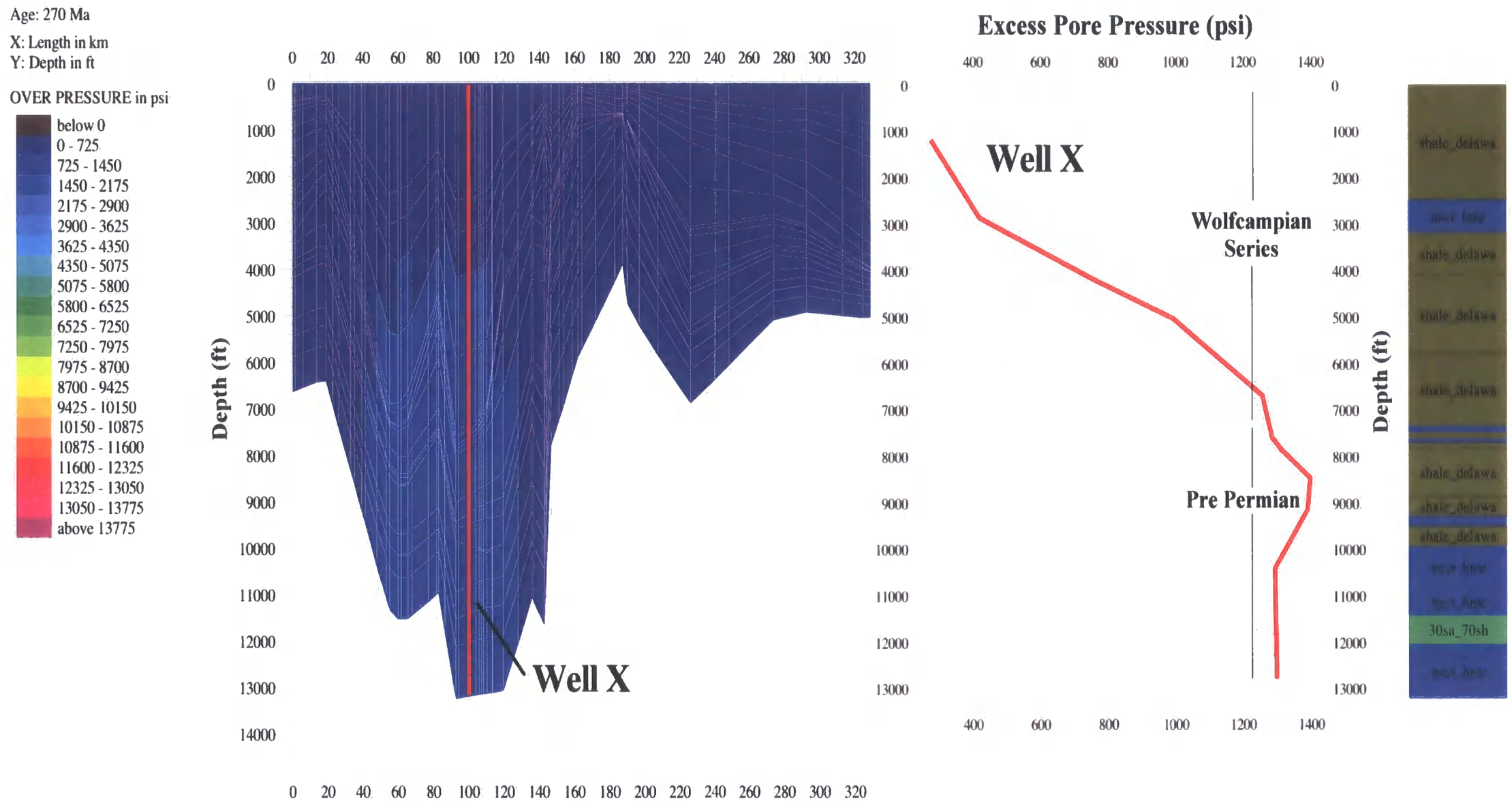

Fig 6.11. A 2D modelling plot showing the distribution and scale of overpressure in the Delaware Basin at top Wolfcampian Series 270Ma. Overpressure is starting to build up in the basin due to the deposition of 7500 ft (2.3km) of dominantly mudrocks of the Early Permian Wolfcampian Series.

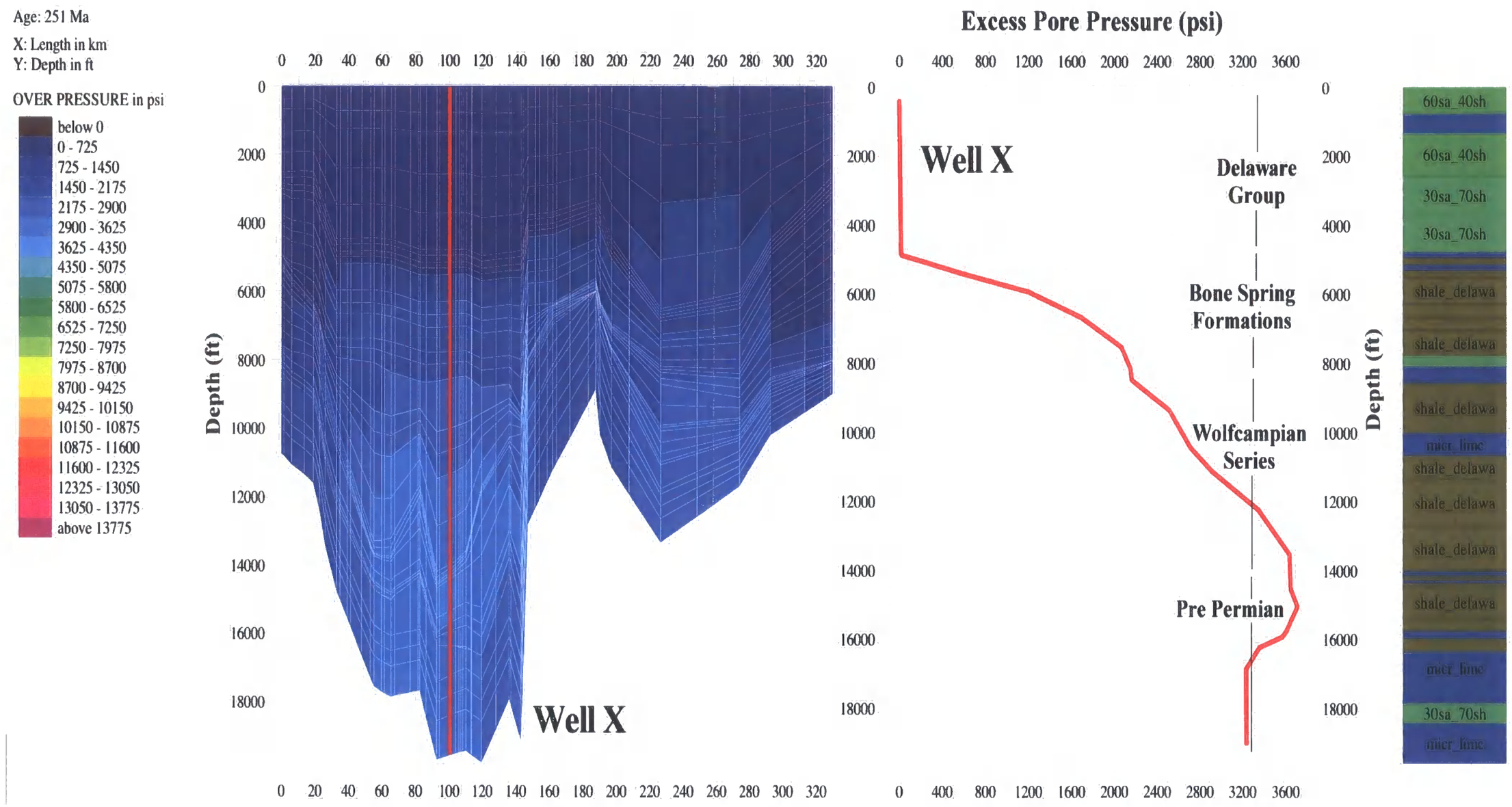

Fig 6.12. A 2D modelling plot showing the distribution and scale of overpressure in the Delaware Basin at top Delaware Mountain Group 251 Ma. The continued rapid deposition of the Delaware Mountain Group and the Bone Spring Formations resulted in the continued rise of overpressure in the basin.

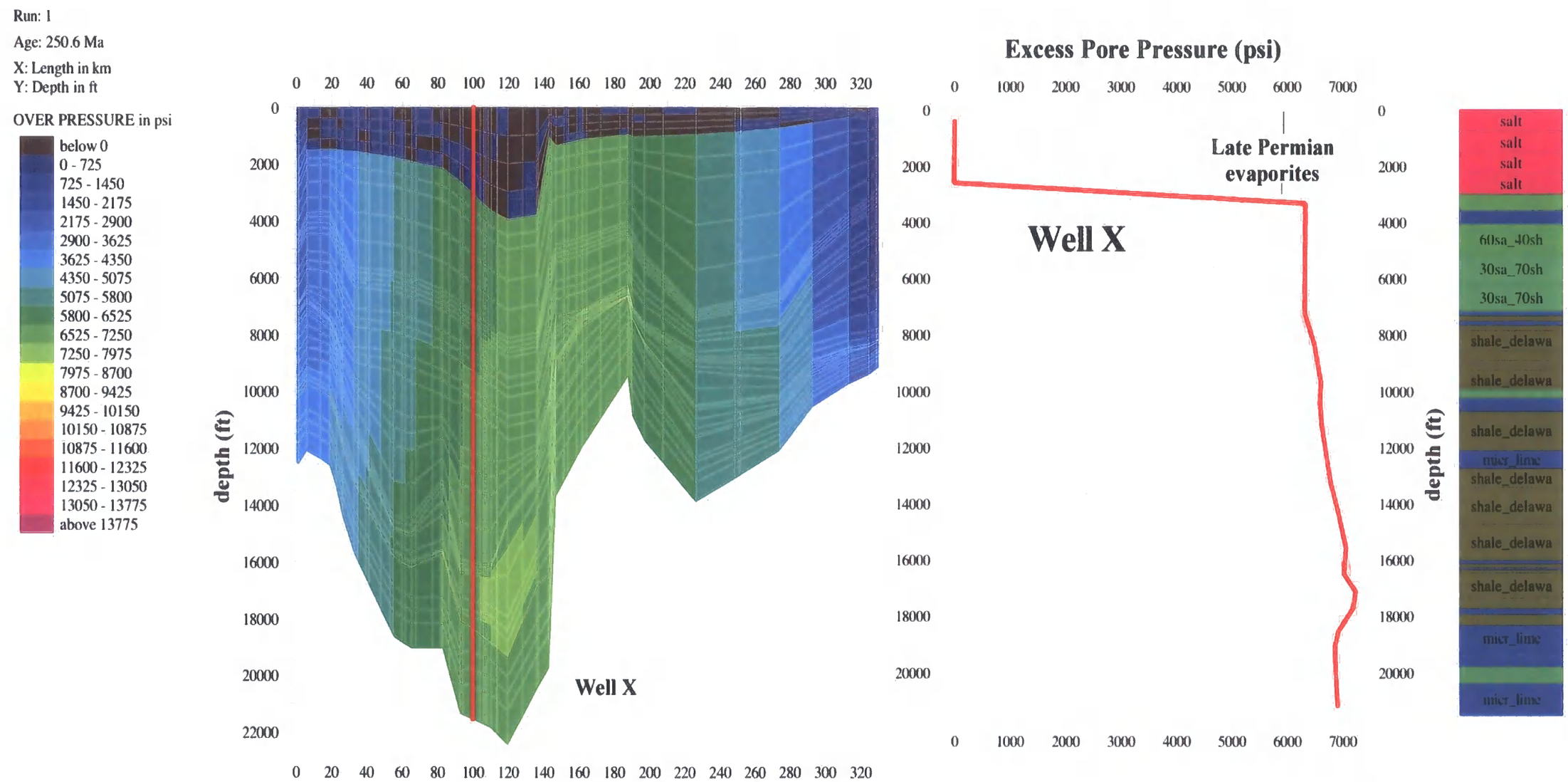

Fig 6.13. . A 2D modelling plot showing the distribution and scale of overpressure in the Delaware Basin at Top Ochoan Series 250.6 Ma. The overpressure in the basin ramps up due to the deposition of up to 4000 ft (1.2 km) of Late Permian evaporites across the whole basin.

Summary of results from the 2D pore pressure generation modelling

The results from the basin modelling (Figs 6.11 – 6.13) show that overpressure was generated through disequilibrium compaction in the Delaware Basin. During the Permian, rapid deposition of sediment caused the underlying shales of the Pennsylvanian and Mississippian System to become overpressured through their inability to dewater quick enough at a rate to allow pressure equilibrium.

The deposition of 7500ft (2.3km) of the mudrock dominated Early Permian Wolfcampian Series 270 Ma (Fig 6.11), generated up to 1400 psi of overpressure in the underlying section. Permeability measurements on the Wolfcampian mudstones (sub-section 6.2.2) showed a measured vertical permeability of $2.83E^{-21}$ m^2 (10^{-6} mD). This low permeability would halt the effective dewatering of the underlying sediments. This low permeability sequence of overlying mudrocks coupled with a further 8500 ft (2590 m) of Mid to Late Permian deposition enabled the overpressure to rise to 3600 psi in the underlying sediments (Fig 6.12).

The overpressure in the basin suddenly ramped up to 7000 psi with the deposition of the Late Permian of the Ochoan Series from 251 Ma to 250.6 Ma (Fig 6.13). During this time, up to 4000 ft (1.2 km) of evaporites were deposited across the whole basin. This rate agrees well with other studies of evaporite deposition. For example, in the Mediterranean, up to 1 km of evaporites were deposited within 400 kyr during the Messinian (Martin & Braga 1994). The evaporites in the Delaware Basin acted as an impermeable top seal and inhibited the escape of pore fluids from the basin. The result of this perfect top seal was that the whole of the basin became excessively pressured at the end of the Permian.

It needs to be noted that in order to make the 2D basin model realistic, the salt was not modelled as a continuous impermeable unit from east to west. Therefore at each edge of the model, the evaporites were modelled as a mix of 50% anhydrite and 50% mudstone. This allowed some bleed off of fluid pressures after its deposition. It is geologically likely that on the edges of the salt, some dissolution may have occurred, or the salt may not have covered the entire basin after deposition, and so by adding the pathways, it makes the model more realistic.

6.3.1.2 Overpressure generation through non-stress related mechanisms

In Chapter 5, it was concluded that in certain horizons such as the Pennsylvanian aged Strawn Formation there is evidence to suggest that overpressure may have been enhanced through alternative mechanisms other than disequilibrium compaction. These mechanisms have been explained in Chapter 3 (sub-section 3.2.5.1). Within the time frame and analytical capabilities of this research, the main non-stress related mechanisms were analysed via modelling to substantiate the conclusions made in chapter 5.

1D and 2D basin modelling has been used to look at the petroleum system of the Delaware Basin. In particular gas generation from the source rock and in-situ oil to gas cracking have been analysed, as these two processes have the potential to be main mechanisms that could generate overpressure within a sedimentary basin (Swarbrick & Osborne 1998; Swarbrick et al 2002).

Within a tilted horizon, the lateral transfer of deep basinal high overpressures up dip to a shallower depth will also inflate overpressures in a basin (sub-section 3.2.5.1.2). Modelling of this mechanism is beyond the capabilities of the basin modelling software package used for this study. However, a 3D surface visualisation software package (Oilfield Data Manager) has been used to model the basin and highlight areas where lateral transfer may be occurring.

Other non-stress related mechanisms such as gas expansion on uplift, and mineral transformation could not be modelled due to the limitations of the software available and time constraints of the research. The likelihood of these mechanisms contributing to the overpressure system in the Delaware Basin will be looked at in more detail in the later discussions (chapter 7.2.3).

Gas generation from source rocks

Based on 1D modelling of vitrinite reflectance data from the source rocks, all six source rocks in the Delaware Basin have reached a high enough thermal maturity to produce hydrocarbons (Fig 6.14). Only the source rocks below and including the

Lower Wolfcampian have entered the gas window. These results from the 1D vitrinite modelling are confirmed by an oil and gas exploration company, which is currently exploring in the basin (Webster, R.W., *pers comm.*).

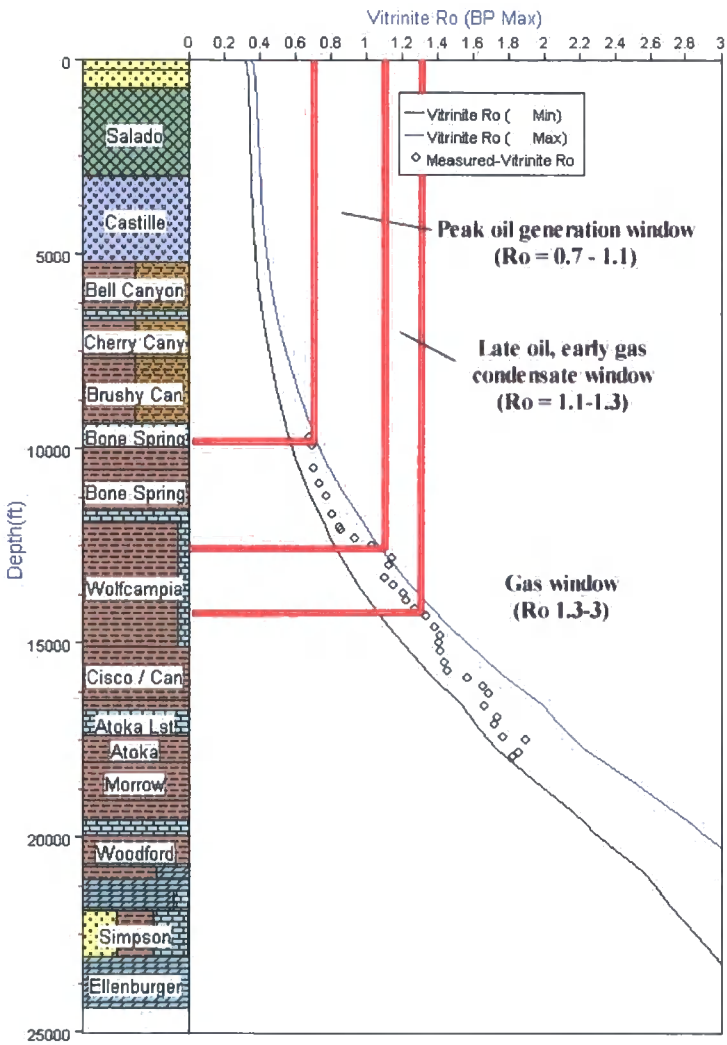

Fig 6.14. A 1D modelling plot of vitrinite data from the JE Haley 24-1 well. The results show that the source rocks of the Bone Spring Formation and Upper Wolfcampian are currently in the oil window while the Lower Wolfcampian and the Barnett, Woodford and Simpson source rocks are in the gas window.

The following four plots (Figs 6.15 – 6.18) show 1D modelling results where the rate of gas generation was modelled against time and burial history for the Lower Wolfcampian, Barnett, Woodford and Simpson source rocks.

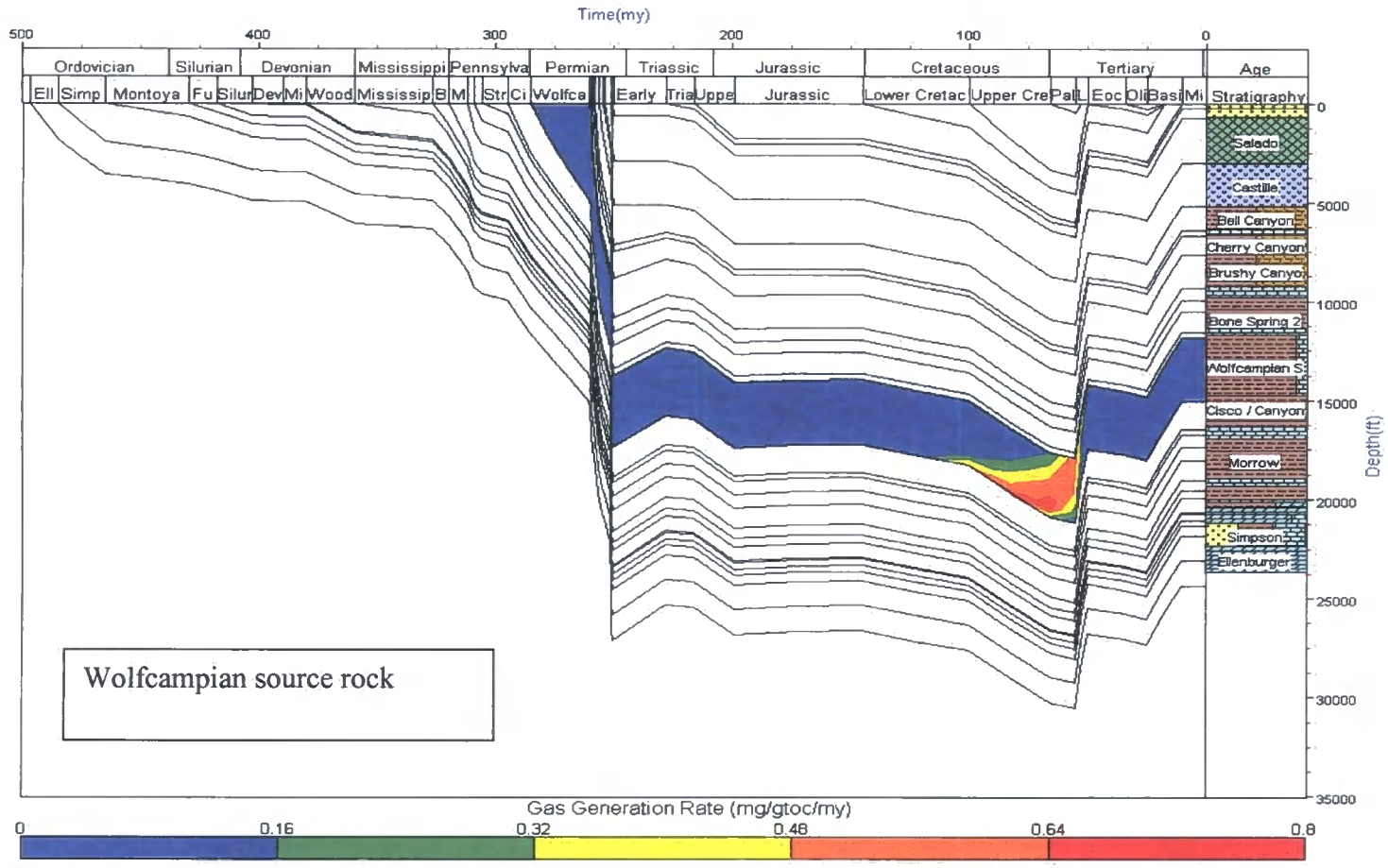

Fig 6.15. A 1D modelling plot of the gas generation rate of the Wolfcampian source rock. Maximum generation of gas in the source rock occurs at 70 Ma within the Lower Wolfcampian.

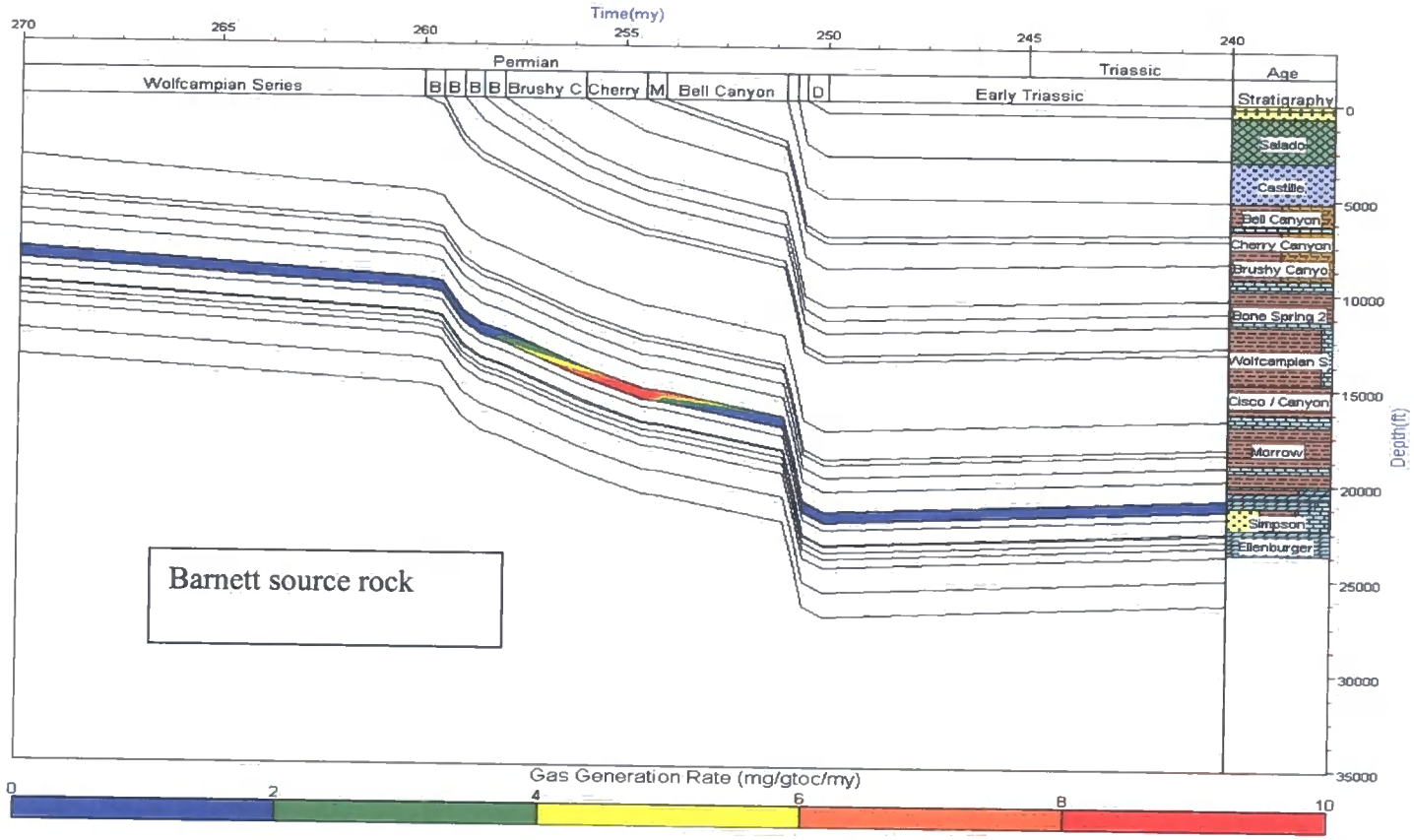

Fig 6.16. A 1D modelling plot of the gas generation rate of the Mississippian System Barnett source rock. Gas generation occurs during the rapid burial of the overlying Mid-Upper Permian 250-260 Ma.

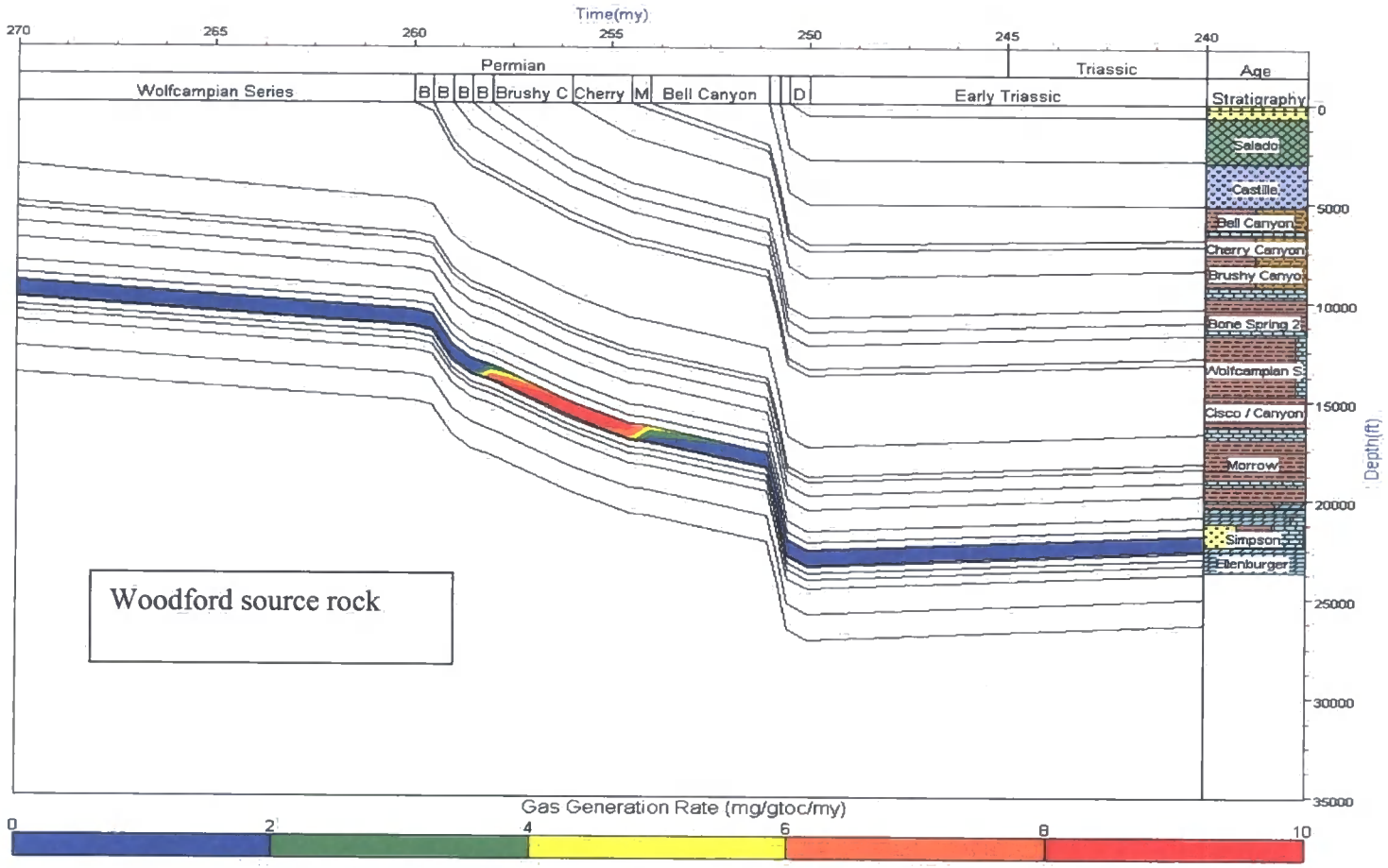

Fig 6.17. A 1D modelling plot of the gas generation rate of the Devonian Woodford Formation. The generation of gas occurs during the rapid burial of the overlying Mid-Upper Permian (250-260 Ma).

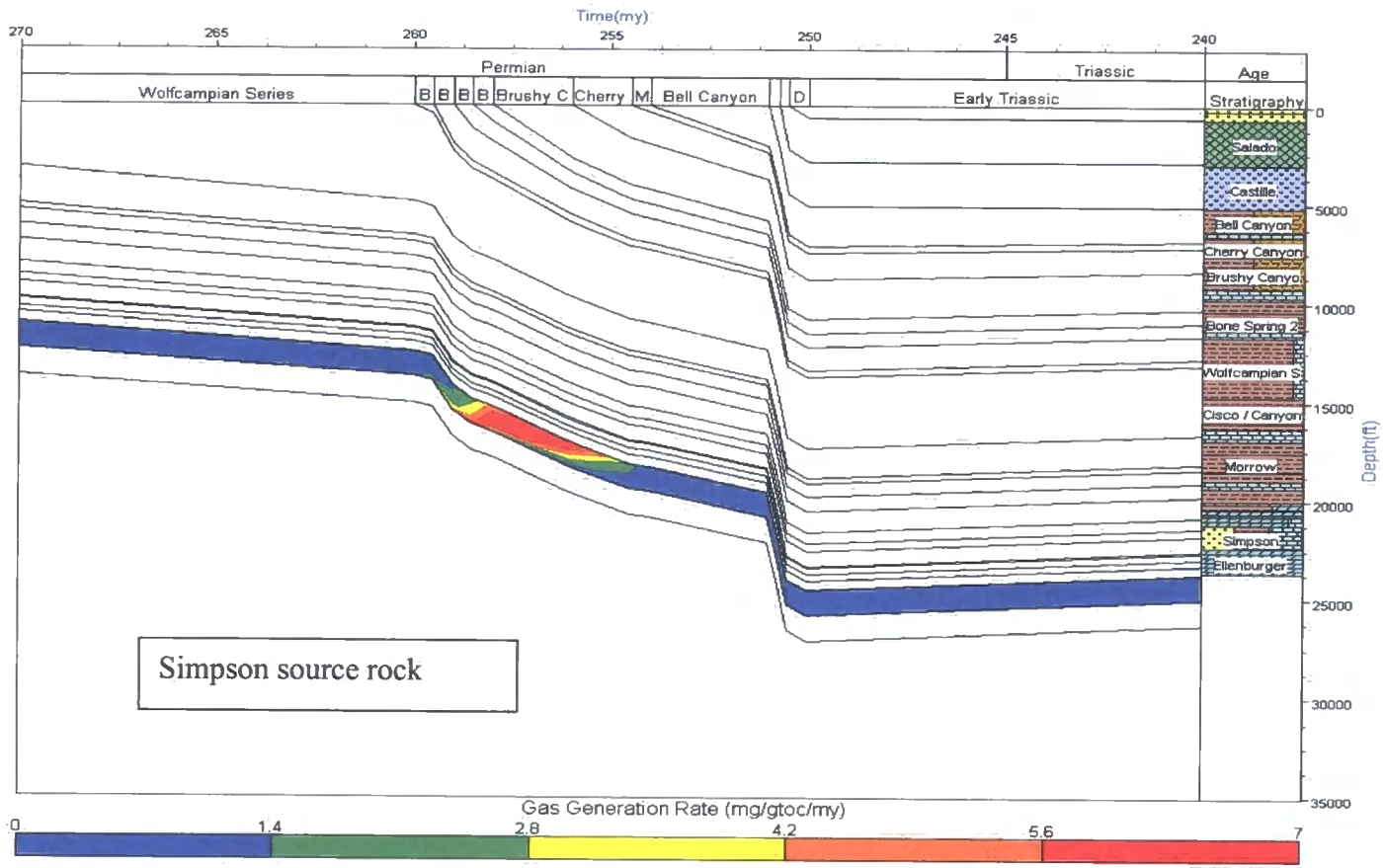

Fig 6.18. A 1D modelling plot of the gas generation rate in the Ordovician Simpson source rock. Gas generation occurs during the rapid burial of the overlying Mid-Upper Permian sequence (250-260 Ma)

The results from the 1D source rock modelling show that the basin has undergone two main phases of gas generation. The Wolfcampian source rocks started to generate gas prior to maximum burial around 70 Ma, whereas the underlying source rocks, the Barnett, Woodford and Simpson, all generated gas during rapid basin subsidence during the Permian.

2D modelling of the source rocks was also undertaken to complement the 1D results. The 2D model is able to show the total amount of generated hydrocarbons (Fig 6.19) from the source rocks. The results show that the Bone Spring, Woodford and the Barnett source rocks produced most hydrocarbons, where the Bone Spring total would have been 100% oil as the source rock has not entered the gas window. The Wolfcampian and the Simpson source rocks produced less hydrocarbons, due to their low initial TOC values. The 2D modelling also showed that total generation of the hydrocarbons in all source rocks had ceased prior to maximum burial at 55 Ma.

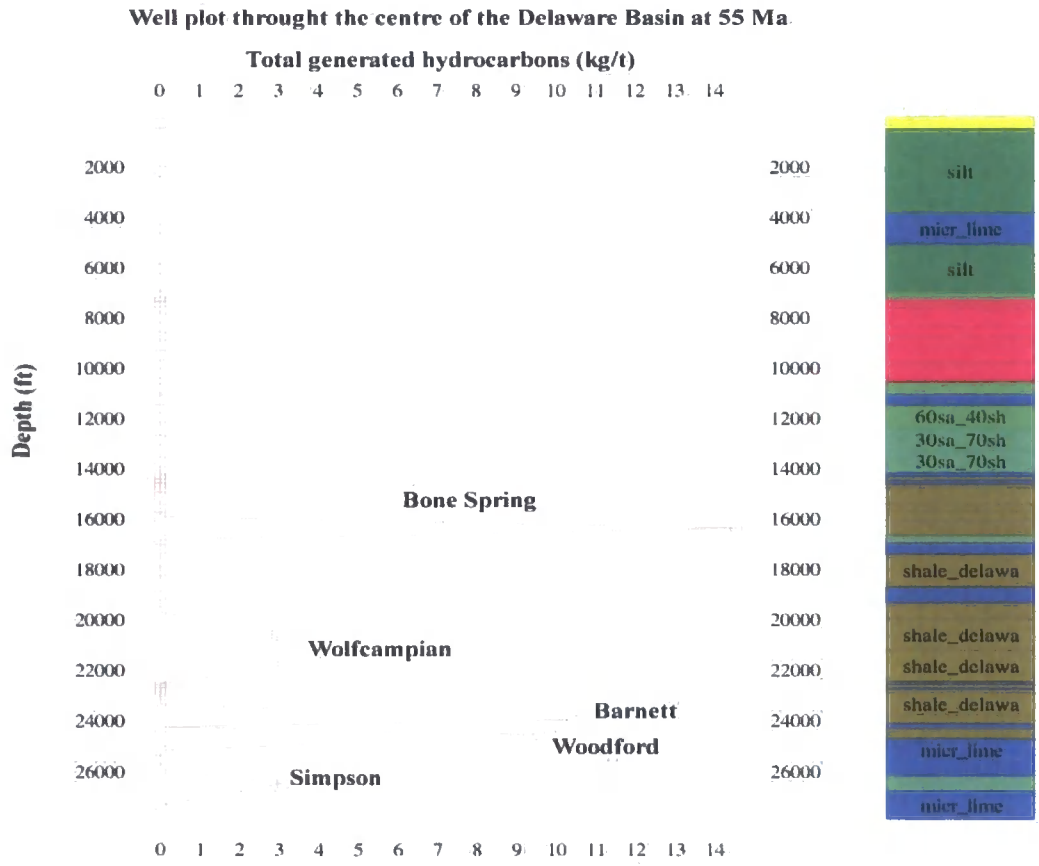

6.19. A plot from 2D modelling showing total generated hydrocarbons from the source rocks 55 Ma. No more generation occurred after this time.

Potential for oil to gas cracking in the reservoir

Modelling has also been used to look at the potential for oil to gas cracking in-situ in the reservoir, where a large volume increase can occur and hence generate overpressure (Swarbrick et al 2002).

The licence of 'Temis 2D' that Durham university has been granted is only a two-phase model, where only water and hydrocarbons can be generated. Therefore modelling oil cracking into gas in not plausible for this study. However what can be modelled is the timing and degree of saturation of hydrocarbons in the surrounding reservoirs, and the modelling of formation temperatures. Oil to gas cracking initiates at temperatures between 120-140 °C and complete cracking to gas is achieved at temperatures in excess of 180 °C (Mackenzie & Quigley 1988). 1D modelling is used to show the temperature history of the basin (Fig 6.20).

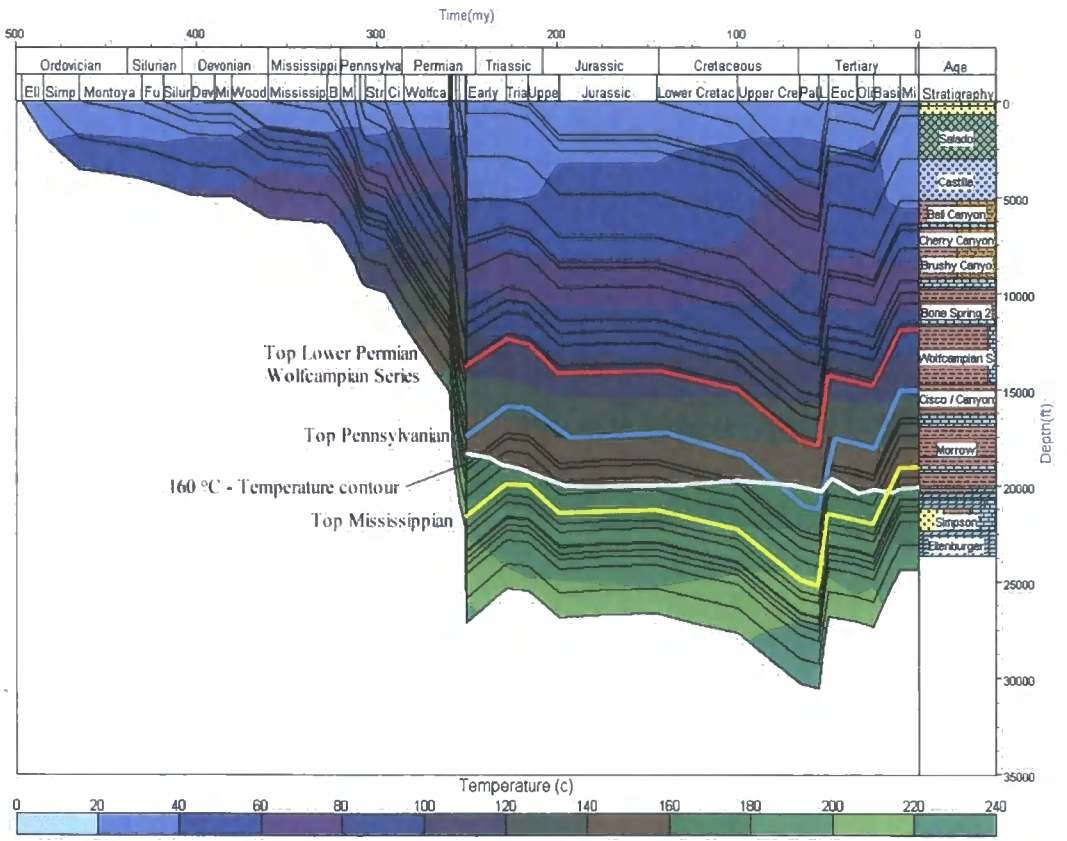

Fig 6.20. A 1D temperature history plot of the Delaware Basin showing the top Wolfcampian Series, Top Pennsylvanian and Top Mississippian along with the 160 °C contour.

As shown in Fig 6.20, the Lower Wolfcampian Series would have reached 160 °C as a consequence of the extra burial during the Mesozoic and the Cenozoic (175-160 Ma). The saturation of hydrocarbons within the Wolfcampian at this time reached 4% according to 2D modelling (Fig 6.21). The upper formations of the Pennsylvanian System would also have reached the required cracking temperature from 100 Ma as the Upper Cretaceous started to be deposited. This extra deposition meant all units below the Mississippian System achieved temperatures of 180 °C and greater (Fig 6.20), creating prime conditions for any oil to gas cracking in the reservoirs, with maximum hydrocarbon saturation within the units below the Wolfcampian occurring around 200 Ma (Fig 6.22).

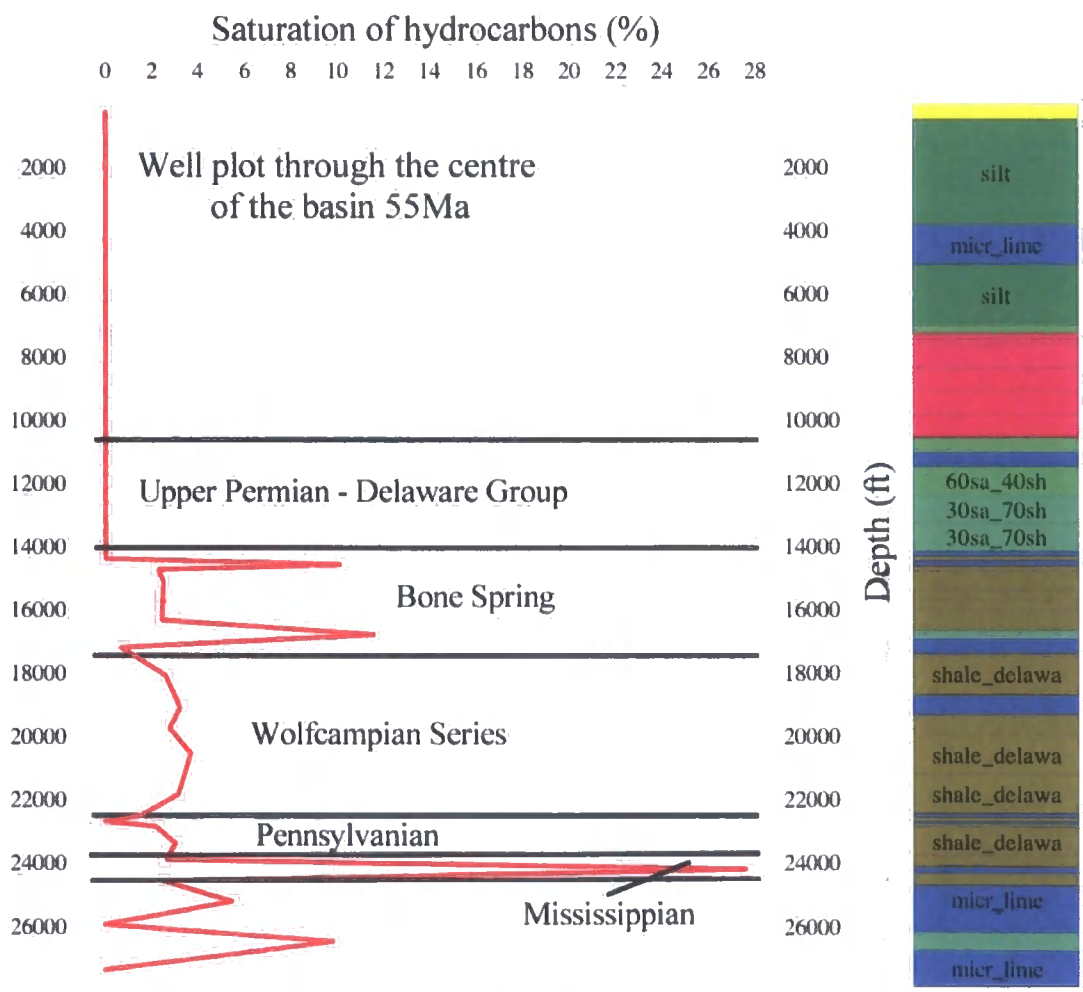

Fig 6.21. A well plot through the centre of the Delaware Basin showing degree hydrocarbon saturation in the section, using 2D modelling.

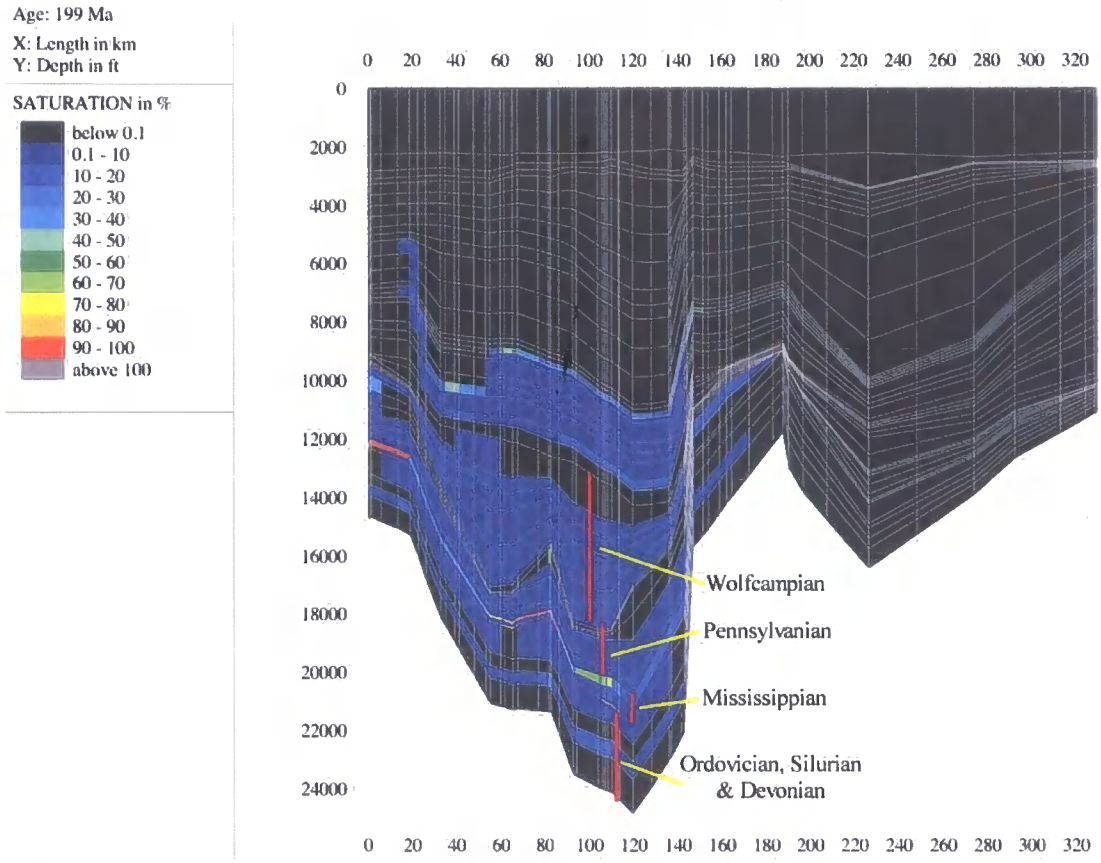

Fig 6.22. A 2D model plot of the basin at 199 Ma showing saturation of hydrocarbons. Complete saturation in the units below the Wolfcampian was achieved at this time. Units below the Top Mississippian are already at temperatures above 180 °C, and the Pennsylvanian units reached this temperature 100 Ma.

Lateral Transfer of overpressure

The basin modelling software packages used for this study, cannot model overpressure enhancement at structural crests by the lateral transfer of fluids from deep. However 3D surface visualisation models can be used to see if the mechanism is viable.

The Jo Neal 43 well is located in Pecos County in the deep section of the basin. Pore pressure prediction methods were used on the sonic log from the well (sub-chapter 5.2.2). The results showed that the methods were under predicting pore pressures for the Pennsylvanian aged Cisco Formation. This well is located at the apex of domal anticline (Fig 6.23), which formed during the Ouachita orogeny (sub-

section 2.2.2.1). The top of the Cisco Formation in this well sits at 10400 ft (3169 m). This compares to the Palmer well downdip of the structure to the south (Fig 6.23), where the Cisco Formation is at 16000 ft (4876 m). If a pressure gradient of 0.45 psi/ft is used, then the pressure differential between these two wells for the Cisco Formation could be up to 3000 psi. This would significantly enhance the overpressure in the Jo Neal 43 well.

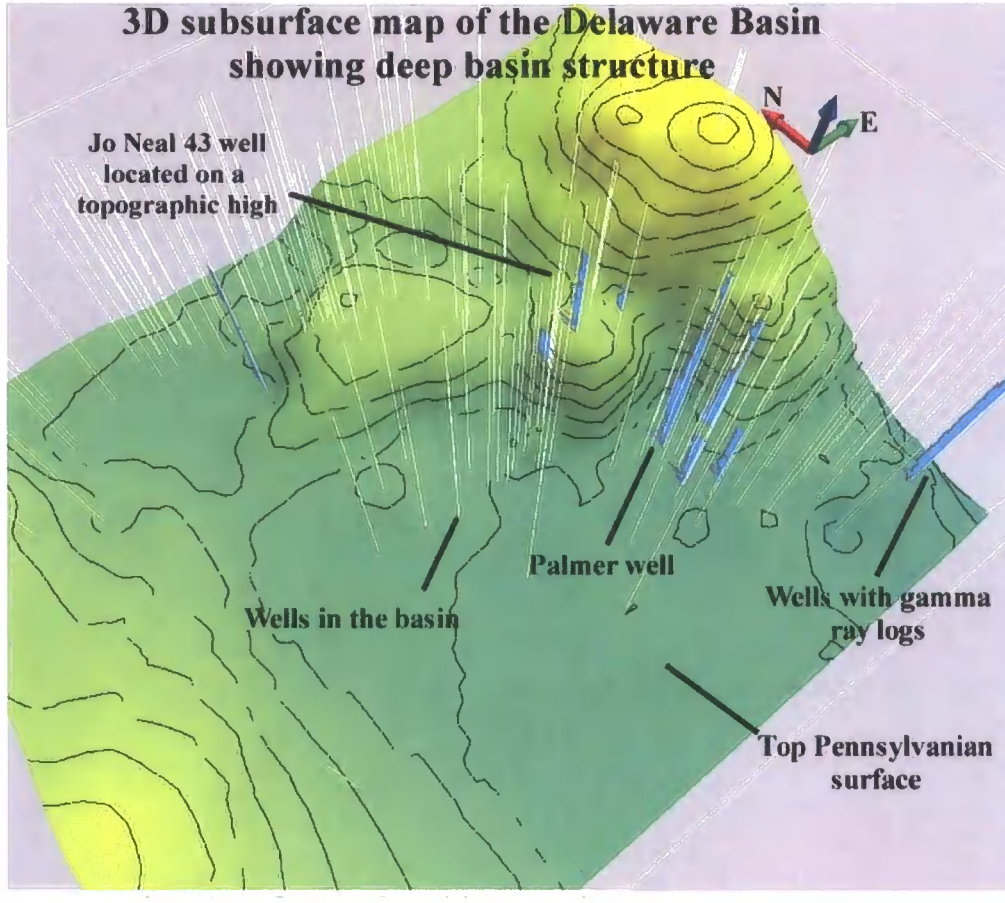

Fig 6.23. A 3D subsurface map showing the top of the Pennsylvanian in Pecos County, which is situated in the centre of the Delaware Basin. The Jo Neal 43 well shows evidence of inflationary overpressures and with the well located on a structural crest, the lateral transfer of fluids from deep may be an explanation for the overpressures recorded.

The Cisco Formation is also a sandstone horizon (Fig 6.24 and Webster, R.W., *pers comm.*). This is necessary if any lateral transfer of deep overpressure is to occur, as the unit needs to be permeable.

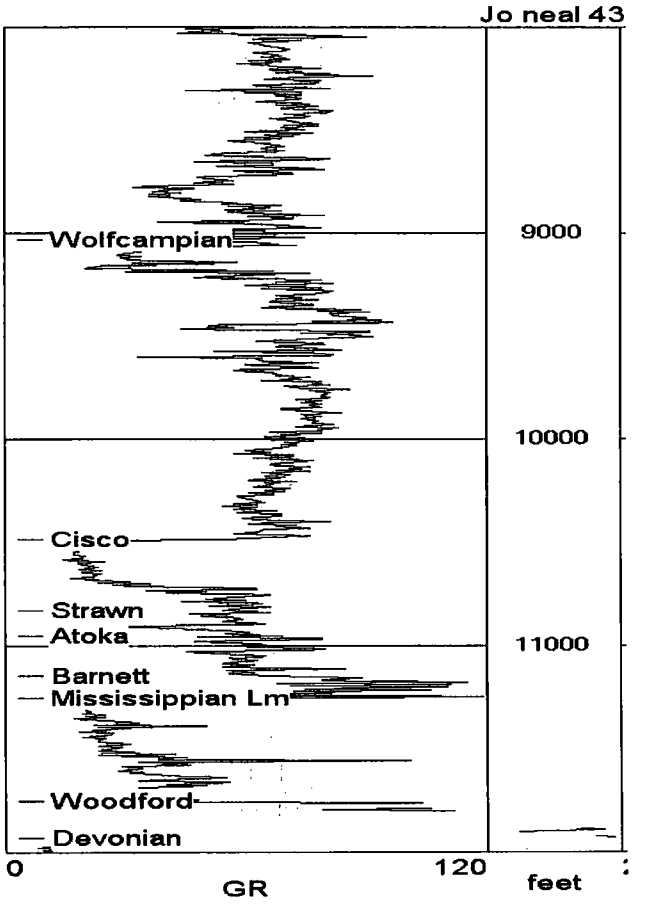

Fig 6.24. A gamma ray log for the Jo Neal 43 well. The Cisco Formation has a low gamma ray reading indicating that it has a low mudstone content and may be a sand. This is confirmed by an oil and gas exploration company, which is currently exploring in the basin.

Summary of non-stress related overpressure generation modelling.

The results from the modelling of source rock generation, oil to gas cracking and lateral transfer is summarised below.

Source rock generation.

- Vitrinite reflectance data and 1D modelling of the source rocks show that both source rocks of the Bone Spring Formation are only oil producing,

whereas the source rocks of the Wolfcampian Formation (in particular the Lower Wolfcampian), Barnett Formation, Woodford Formation and the Simpson Group, have all entered the gas window.

- Gas generation in the Wolfcampian source rock occurred around 70 Ma, which is 200 Myr after its deposition. This research has shown that the Delaware Basin experienced greater burial than previously thought, with a further 6890 ft (2.1 km) being deposited prior to maximum burial (55 Ma). This extra burial during the Mesozoic and Cenozoic is the reason why the Wolfcampian source rock reached a high enough thermal maturity for gas production.
- Gas generation in the Barnett, Woodford and Simpson source rocks occurred due to the rapid input of Mid-Late Permian sediment (250 – 260 Ma).
- 2D basin modelling results show that all the source rocks reached maximum generation prior to maximum burial 55 Ma.
- The best producing source rocks in the basin are the Bone Spring, Barnett and Woodford.

Potential for oil to gas cracking

- 1D and 2D modelling has shown that all units from the Lower Wolfcampian downwards reached the required temperatures needed for oil to gas cracking to occur in reservoirs.
- The Lower Wolfcampian Series reached the required temperatures for cracking around 75 Ma, and by maximum burial 55 Ma the section was saturated with hydrocarbons.
- Units below the Top Pennsylvanian were fully saturated by 199 Ma, with the Pennsylvanian units reaching required cracking temperatures at 100 Ma.
- Units below the Top Mississippian have been in the required temperature zone since the end of the Permian (250 Ma).

Lateral Transfer

- The Ouachita orogeny during the Pennsylvanian created domal anticlinal structures, giving tilted reservoir horizons such as the Cisco Formation.

Implications for overpressure development

- The modelling has shown that gas generation did occur in the source rocks below and including the Wolfcampian Series. It also showed that for the same section, the conditions needed for potential oil to gas cracking in reservoirs was in place. Therefore a volume change associated with either of these two processes may have added to the overpressure already generated by disequilibrium compaction.
- More significantly however, the Upper Wolfcampian Series never reached the required temperatures for oil to gas cracking despite being saturated with hydrocarbons. Therefore the overpressure seen in this section at present day would only have been generated primarily through disequilibrium compaction according to the modelling, ad the amount of gas generation from the source rock was minor.
- Any high overpressure in the deep basin created during the rapid burial of the Permian section could have been transferred up-dip through lateral transfer in a permeable aquifer, so that any overpressure on the crest may have been enhanced. For example the Jo Neal 43 well in Pecos County.
- Note, that high overpressures recorded in the crest of a reservoir could be also due to oil to gas cracking, or hydrocarbon buoyancy.

Note, these results are all theoretical, as the modelling software could not compute overpressure generation through non-stress related mechanisms. However the modelling does show that conditions in the basin were viable for the above mechanisms to occur.

6.3.2 Modelling the retention of overpressure in the basin

The modelling results in sub-section 6.3.1 showed that overpressure could be generated in the Delaware Basin by disequilibrium compaction and theoretically by non-stress related mechanisms, by the following timeline:

- 260 – 250 Ma: Gas generation in the Barnett, Woodford and Devonian source rocks.
- ~ 250 Ma: Disequilibrium compaction
- ~ 250 Ma: Lateral transfer of fluids to structural crests.
- ~ 100 Ma: Reservoirs below Top Pennsylvanian reached conditions for oil to gas cracking.
- ~ 70 Ma: Gas generation in the Wolfcampian source rock.
- ~ 55 Ma: Reservoirs in the Lower Wolfcampian reached conditions suitable for oil to gas cracking.

Basin modelling has therefore been used to see how overpressures could be retained in the basin until present day. Due to the limitations of the basin modelling software, the following results are only based on where overpressures have been generated by disequilibrium compaction.

6.3.2.1 Late Permian evaporites

The deposition of the Late Permian impermeable evaporites is a perfect scenario as to how disequilibrium compaction generated overpressures may have been retained in the basin. The following basin modelling results were run where the evaporites were modelled as a laterally continuous layer across the whole basin (Figs 6.25 – 6.27).

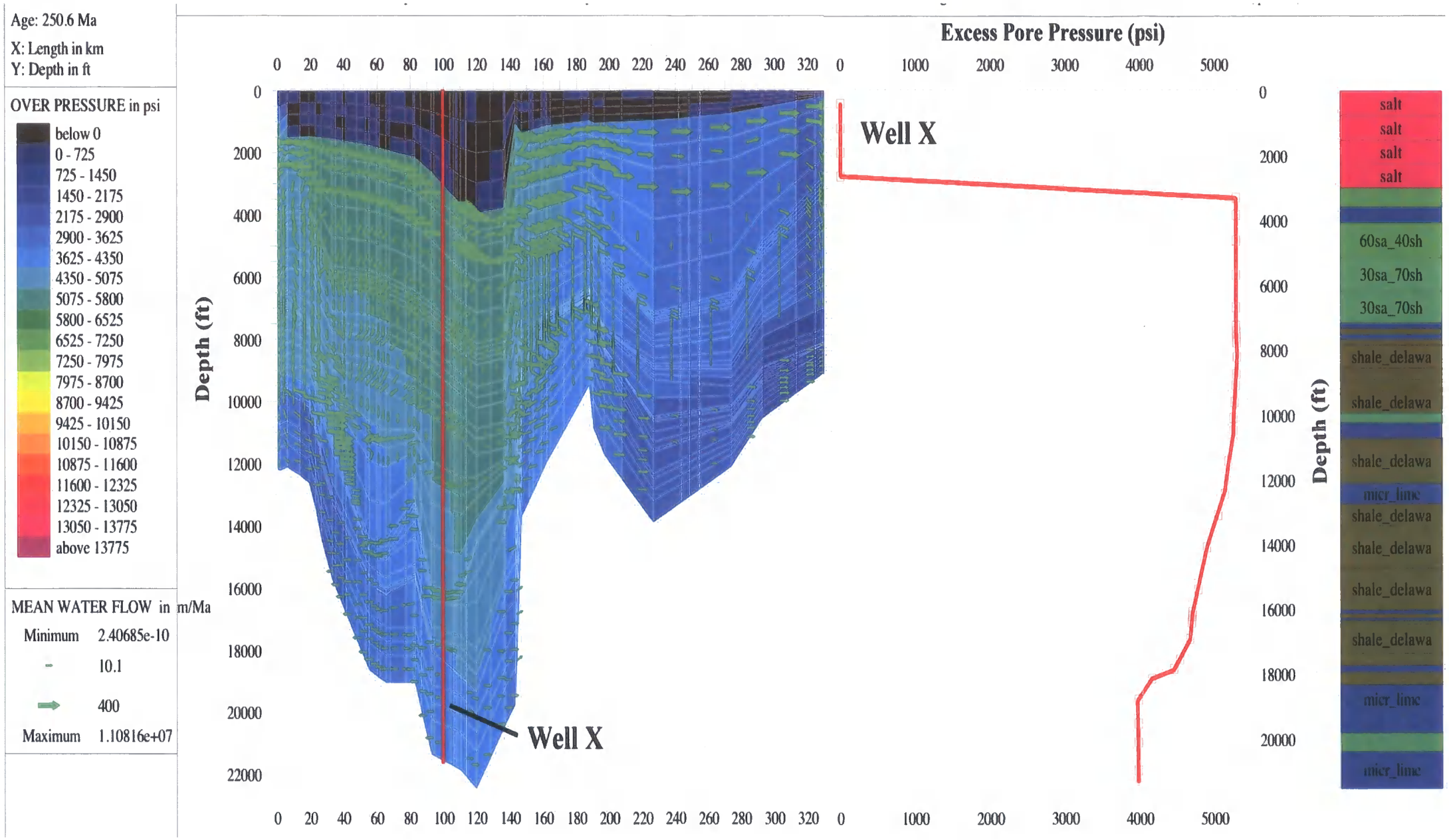

Fig 6.25. A 2D modelling plot showing the distribution and scale of overpressure in the Delaware Basin at top Ochoan Series 50.6 Ma, where the Late Permian evaporites are modelled as a laterally continuous impermeable seal. During the Ochoan, up to 4000ft worth of halite and gypsum was deposited on top of the basin. The plots show that this effectively sealed the whole basin, enabling excess pore pressure to reach in excess of 5000psi.

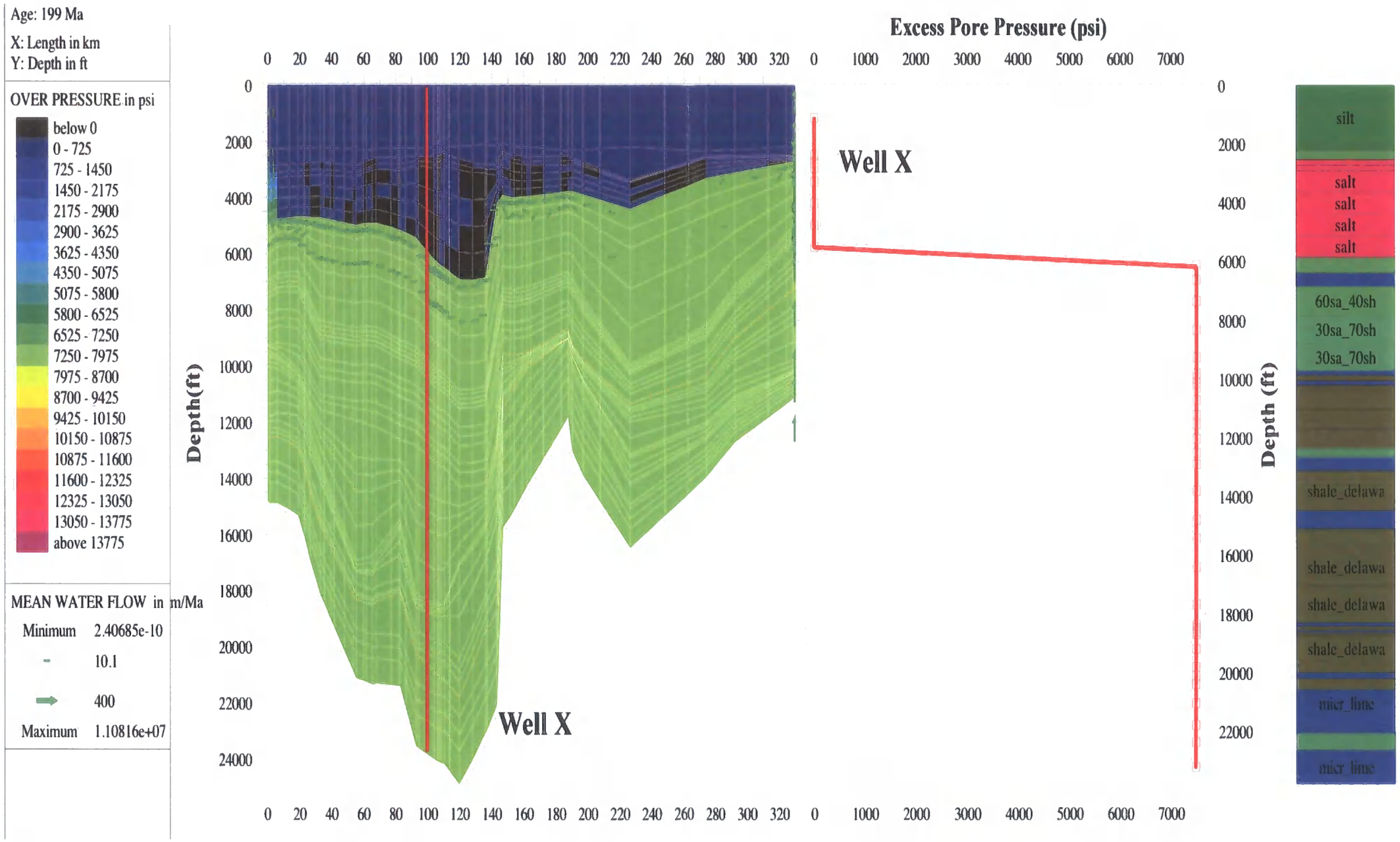

Fig 6.26. A 2D modelling plot showing the distribution and scale of overpressure in the Delaware Basin at top Triassic 199 Ma, where the Late Permian evaporites are modelled as a laterally continuous impermeable seal. Deposition of the Triassic and with the salt acting as a continuous lateral top seal, the pore pressure was able to build up to in excess of 7000psi.

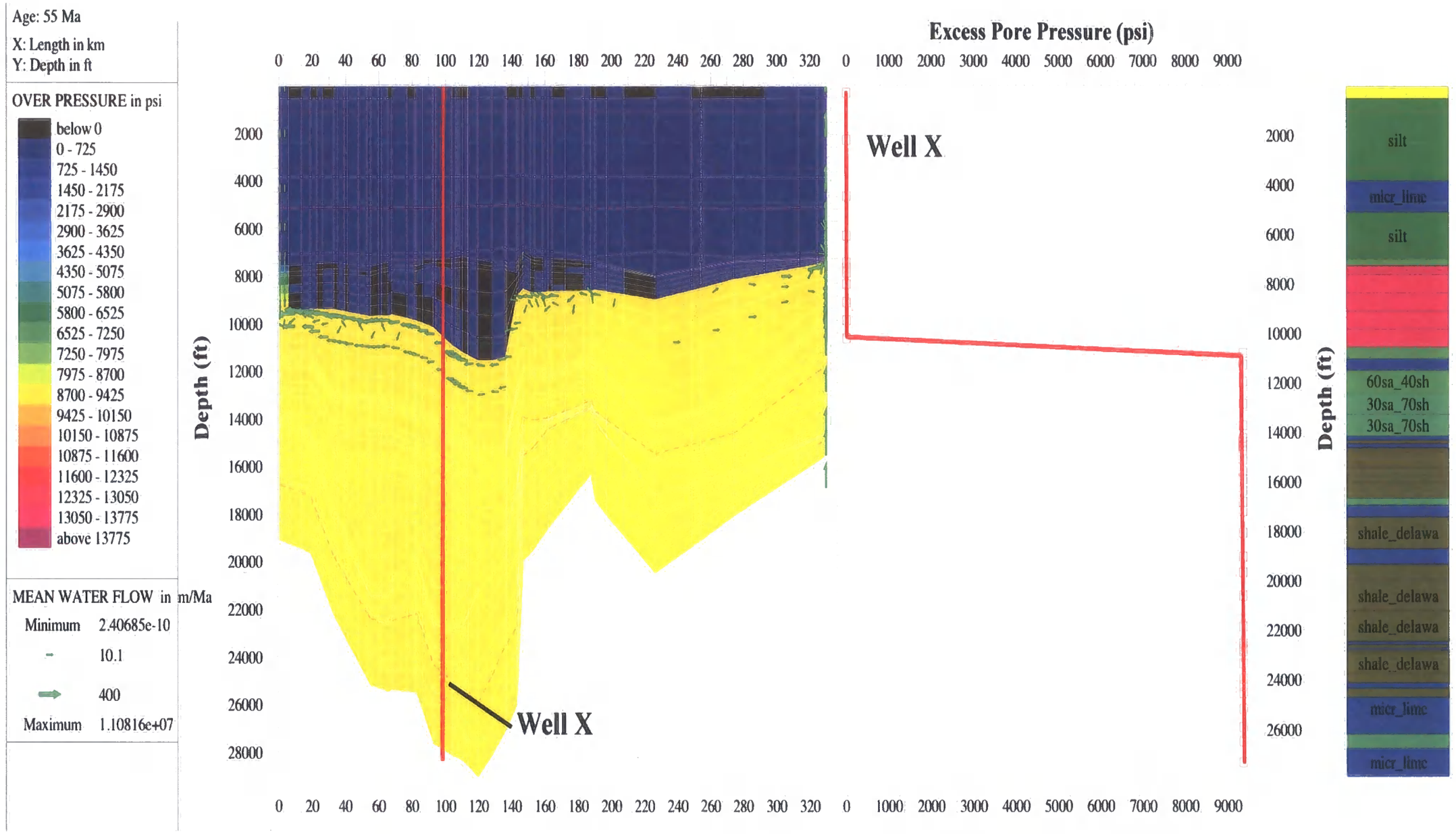

Fig 6.27. A 2D modelling plot showing the distribution and scale of overpressure in the Delaware Basin at maximum burial 55 Ma, where the Late Permian evaporites are modelled as a laterally continuous impermeable seal. Excess pore pressure has reached a maximum of around 9000psi in the whole basin, where every unit below the salt is excessively pressured.

Summary of the modelling results

The modelling results show that if the salt is modelled as a laterally continuous perfect top seal, then the overpressure reaches up to 9000 psi, by maximum burial 55 Ma (Fig 6.27).

However, if the salt was acting as a perfect top seal, it then contradicts the conclusions made in chapter 4 (sub-section 4.2.4.1). Based on shale compaction curves it is suggested that the Upper Permian Delaware Mountain Group was normally pressured at maximum burial, indicating that the basin could dewater. In a geological sense it is unlikely that the salt was a complete barrier to fluid flow, as there may have been some salt dissolution, fracturing, or simply the salt may not have been laterally extensive across the whole basin hence allowing fluids to bleed off.

6.3.2.2 Late Permian evaporites modelled as being permeable on the edges of the basin

It was mentioned in sub-section 6.3.1.1, that to allow the model to be geologically realistic for overpressure modelling, the evaporites were modelled as a mix of 50% anhydrite and 50% mudstone on the flanks of the basin (Fig 6.13). This would allow for some dewatering of fluid pressures to occur in the basin over geological time till present day. The following 2D sections (Figs 6.28 – 6.31) show the results of this modelling from 199 Ma through to present day and follow on from Fig 6.13, which models the basin at 250.6 Ma.

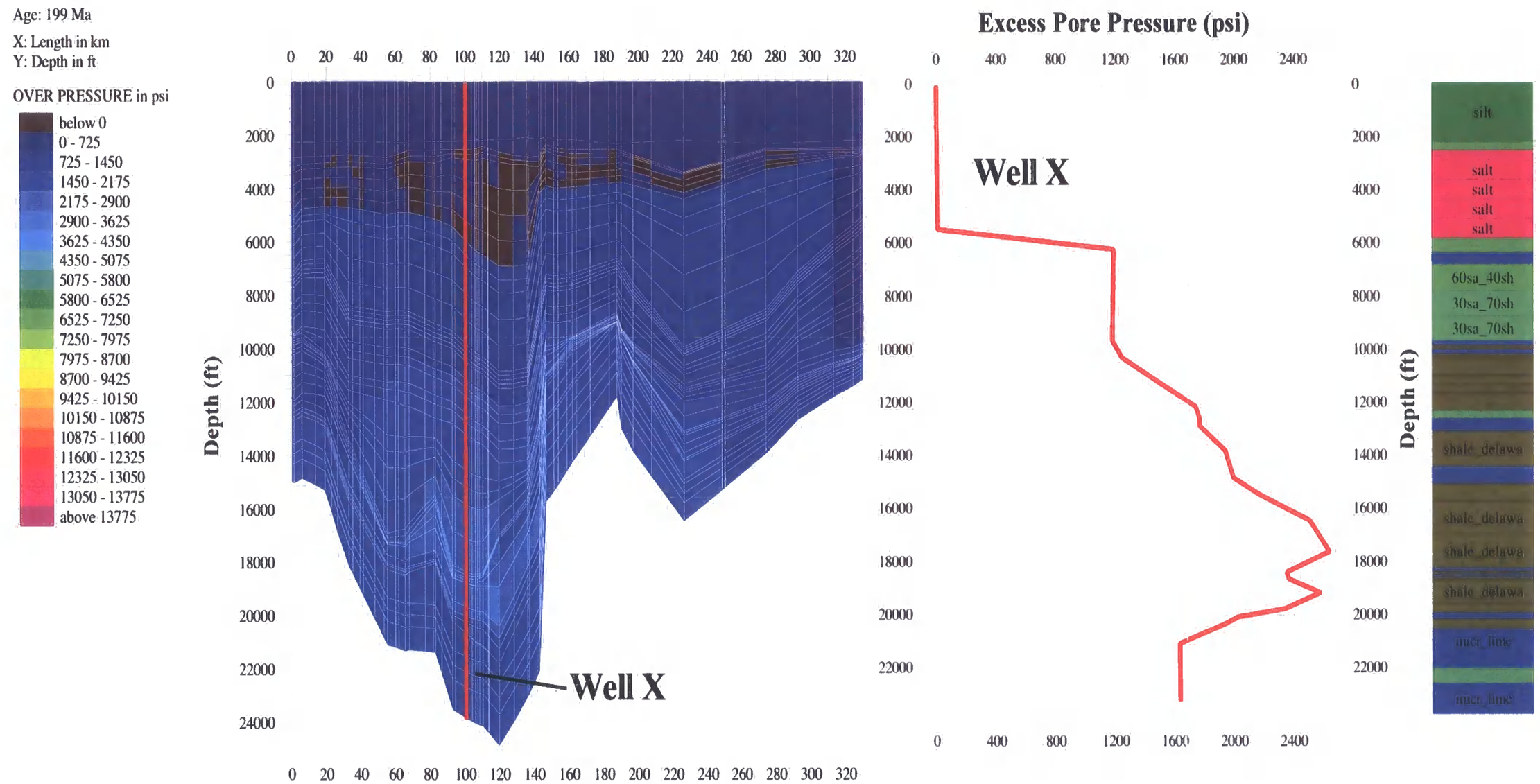

Fig 6.28. A 2D modelling plot showing the distribution and scale of overpressure in the Delaware Basin at top Triassic 199 Ma, where the Late Permian evaporites are modelled to allow some dewatering to occur on the flanks of the basin. Little deposition has occurred in the basin since the Late Permian. This has allowed the basin the dewater, and equilibrate, reducing the degree of overpressure in the basin.

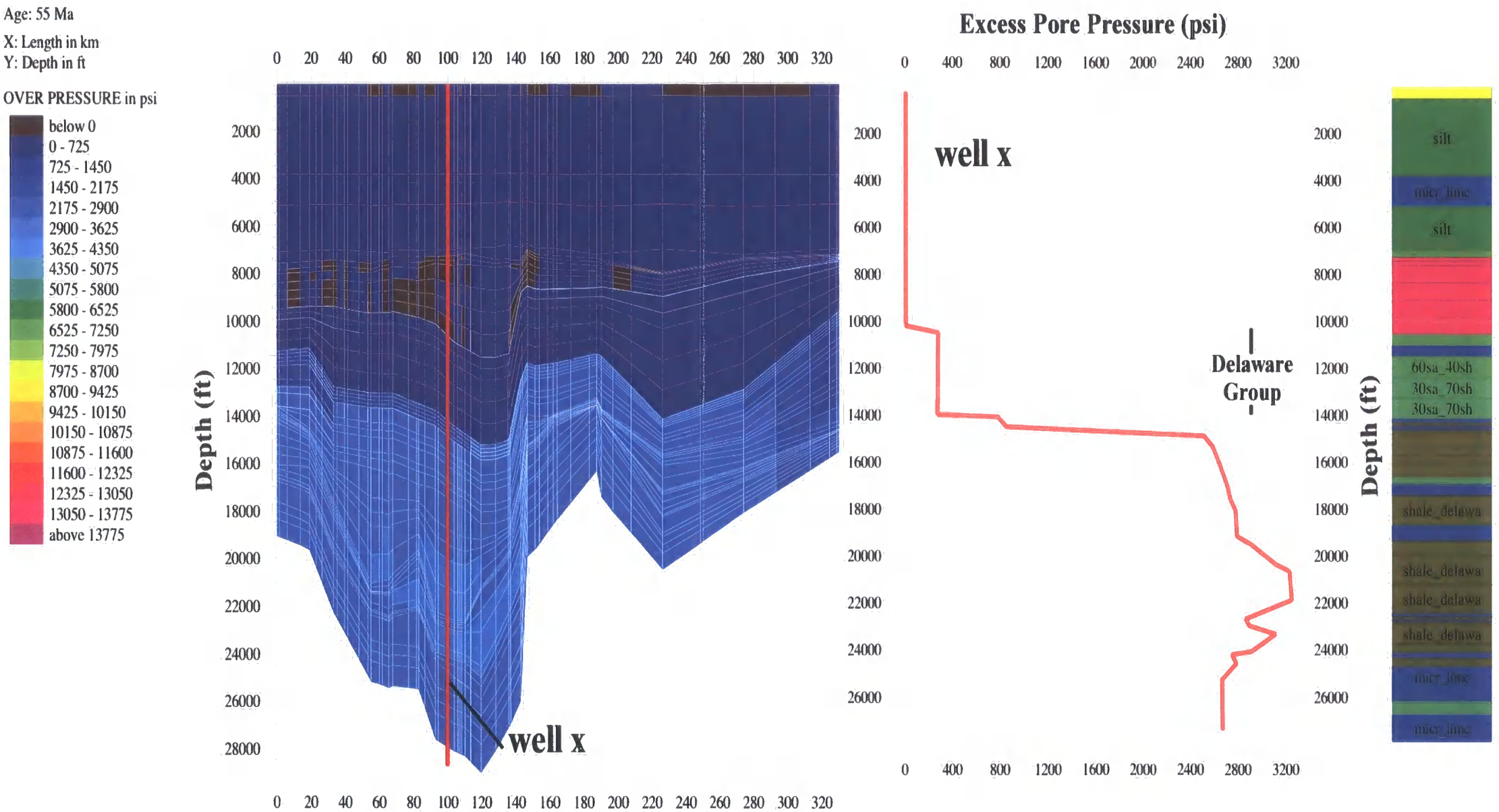

Fig 6.29. A 2D modelling plot showing the distribution and scale of overpressure in the Delaware Basin at maximum burial 55 Ma, where the Late Permian evaporites are modelled to allow some dewatering to occur on the flanks of the basin. The deposition of around 5000 ft of Cretaceous and Palaeocene sediments meant that overpressures increased in the basin.

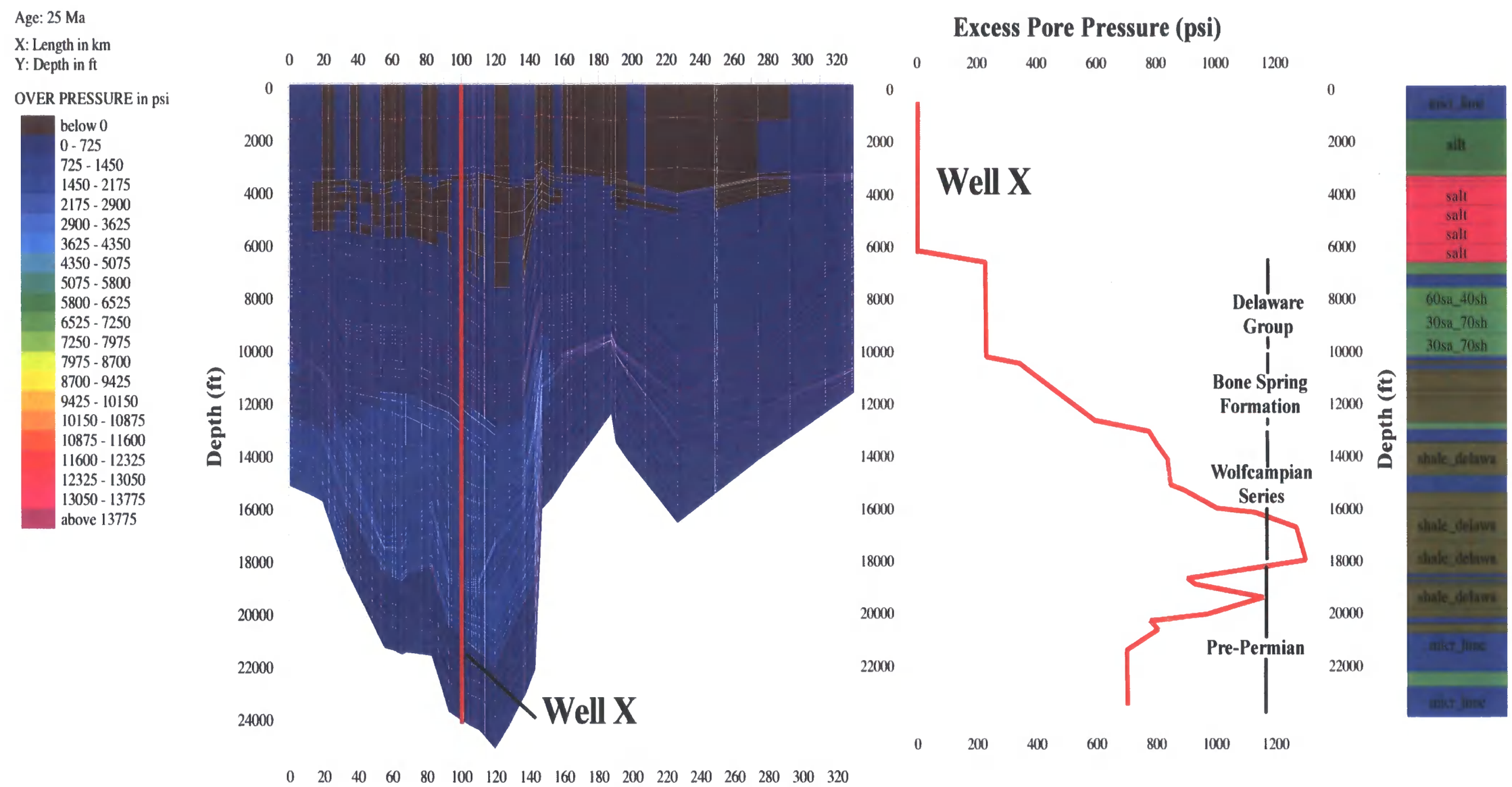

Fig 6.30. A 2D modelling plot showing the distribution and scale of overpressure in the Delaware Basin at 25 Ma, prior to the second uplift event. The Late Permian evaporites are modelled to allow some dewatering to occur on the flanks of the basin.

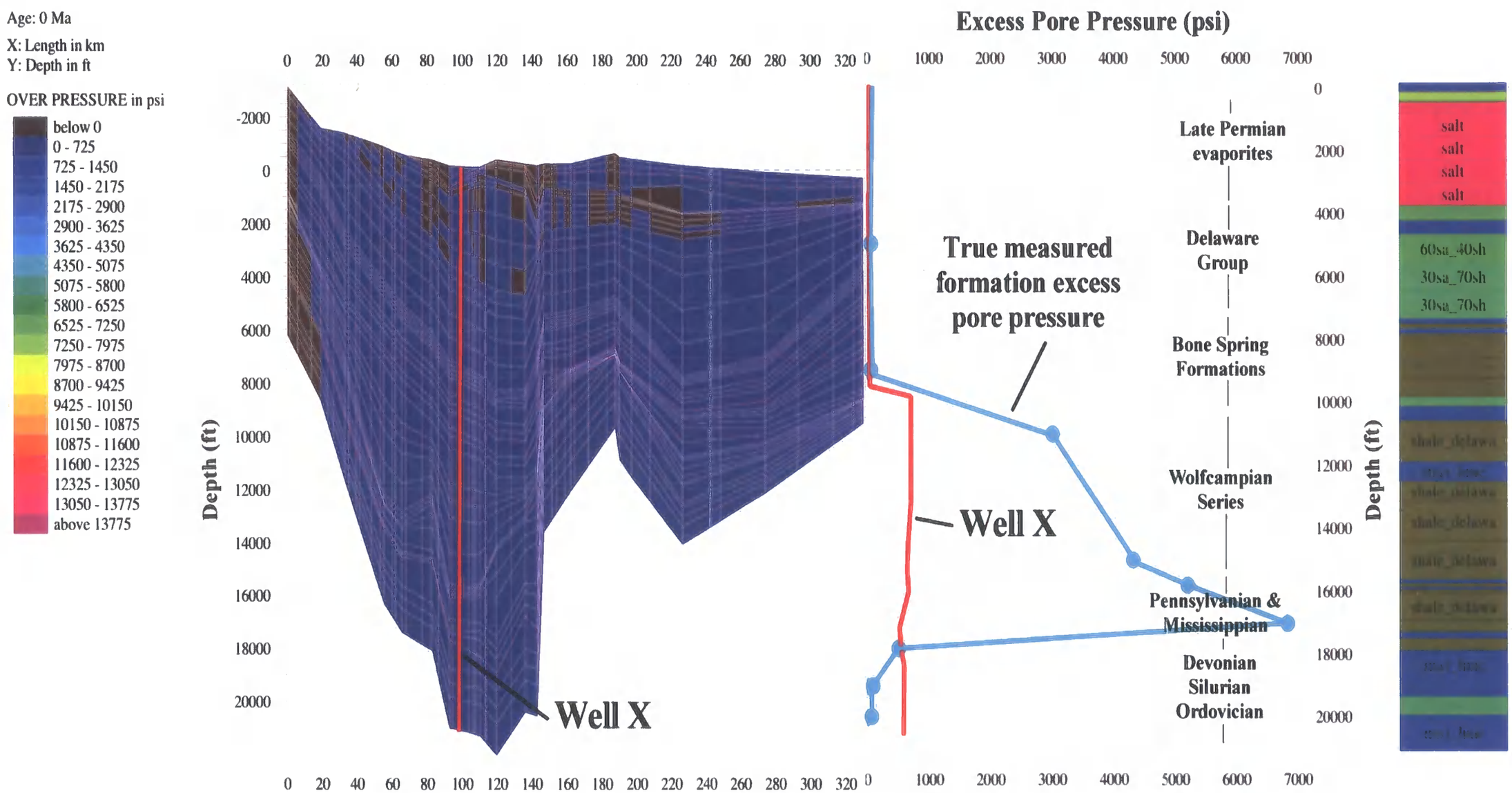

Fig 6.31. A 2D modelling plot showing the distribution and scale of overpressure in the Delaware Basin at present day, where the Late Permian evaporites are modelled to allow some dewatering to occur on the flanks of the basin. The model shows the basin to be not highly overpressured at present day.

Summary of the modelling results

When the model is run where the evaporites are modelled as a mix of anhydrite and mudstone on the edges of the basin (Figs 6.28 – 6.31), the pressure history of the basin is dramatically different then when the evaporites are modelled as a perfect top seal (Fig 6.25 – 6.27). By allowing some dewatering to occur on the flanks of the basin, the overpressure is not contained in the basin to as large a degree. For example at 55 Ma, there was 9400 psi of overpressure in the entire basin when the evaporites were modelled as a perfect top seal (Fig 6.27). This compares to Figure 6.29 where overpressures in the Wolfcampian Series only reach up to 3200 psi, if dewatering can occur on the flanks of the basin.

By making the Late Permian evaporites more permeable on the edges of the basin, this modelling has achieved the following results:

- Despite allowing overpressures to dissipate, the basin is still overpressured at the end of the Triassic 199 Ma, with overpressures up to 2400 psi being modelled in the Wolfcampian Series (Fig 6.28). The overpressure is being maintained by the low permeability (10^{-6} mD) mudstones of the Bone Spring Formation and Wolfcampian Series. The evaporites will still also be a very effective regional seal, as it is only on the flanks of the basin where they have been modelled to be more permeable.
- The deposition of almost 7000 ft (2.1 km) of Cretaceous and Palaeocene sediment had the effect of ramping up the pressures in the section underlying the Delaware Mountain Group (Fig 6.29).
- However, the more sand rich Delaware Mountain Group is able to dewater and become close to being hydrostatically pressured at maximum burial 55 Ma. This agrees with the results made in chapter 4 (sub-section 4.2.4.1), where based on shale compaction curves it was concluded that the Delaware Mountain Group was normally pressured at maximum burial. The modelling does show that the Delaware Mountain Group is still slightly overpressured at 55 Ma (300 psi of overpressure) and not hydrostatic (Fig 6.29). However, this could just be a limitation of 2D modelling where dewatering can only occur in a 2D perspective. A 3D model would have more drainage paths and may allow complete dewatering to occur.

- Chapter 4 showed that the basin underwent two phases of uplift in the Cenozoic. Uplift has the impact of decreasing the pore pressure in sediments. This happens due to the slight porosity increase through the rebound of the sediments on uplift, and the shrinkage of pore fluids due to a temperature decrease. This pressure decrease coupled with continued dewatering explains the decrease in overpressure at 25 Ma compared to 55 Ma (Figs 6.29 & 6.30), and why the basin is close to hydrostatic at present day (Fig 6.31).
- The model is inaccurately representing the pressure history at present day. The model is showing overpressures no more than 600 psi in the whole basin. Whereas measured pressures through DSTs indicate overpressures up to 7000 psi in the Pennsylvanian and Mississippian System for example (Fig 6.31). This shows that if the evaporites are not the pressure seal, then overpressures cannot be retained in the basin till present day, and another method of pressure retention is therefore needed.

6.3.2.3 Tight laterally extensive carbonates

Chapter 5 (sub-section 5.4.1) through the use of wireline analysis concluded that lateral tight carbonates horizons are controlling the dynamic dewatering of the overpressured zone in the basin (Fig 5.16). The model used in sub-section 6.3.2.2 was adapted by making the limestone horizons that corresponded with the peaks of high mudstone sonic travel time (Fig 5.16), tighter with regards their permeability. The limestones that were altered were the:

- Top Bone Spring Formation.
- Base of the Bone Spring Formation.
- Mid Wolfcampian Series.
- Top Pennsylvanian System.
- The Mississippian Limestone Formation

The tight limestones can be identified in the stratigraphic column by a light blue colour coding.

The present day vertical permeability of these limestones was modelled in the order of 10^{-8} mD, which is tighter than the mudstones in the basin by two orders of magnitude. The modelling results are shown in figures 6.32 – 6.36, as cross-sections for the following times:

- 250.6 Ma – Top Ochoan evaporites (Fig 6.32).
- 199 Ma – Top Triassic (Fig 6.33).
- 55 Ma – Maximum burial (Fig 6.34).
- 25 Ma – Prior to Basin and Range associated uplift (Fig 6.35).
- 0 Ma – Present day (Fig 6.36).

In the model, the tight carbonates were only modelled for the Delaware Basin and not the neighbouring Midland Basin. This was so that the Midland Basin could become normally pressured, as no overpressure is recorded in the basin at present day.

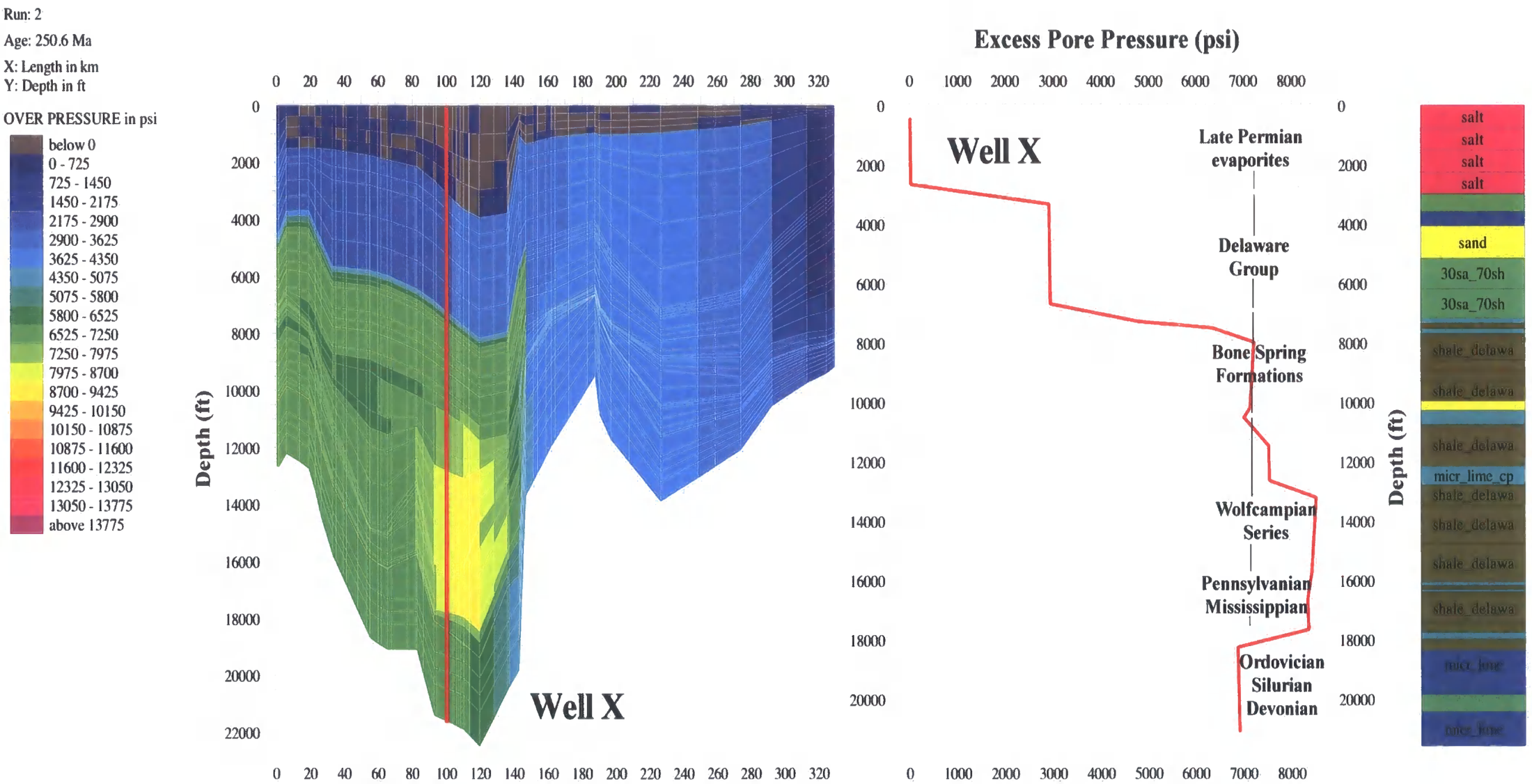

Fig 6.32. A 2D modelling plot showing the distribution and scale of overpressure in the Delaware Basin at top Ochoan Series 250.6 Ma. The Late Permian Ochoan Series evaporites are modelled to allow some dewatering to occur on the flanks of the basin and tight low permeability limestones are modelled in the stratigraphy.

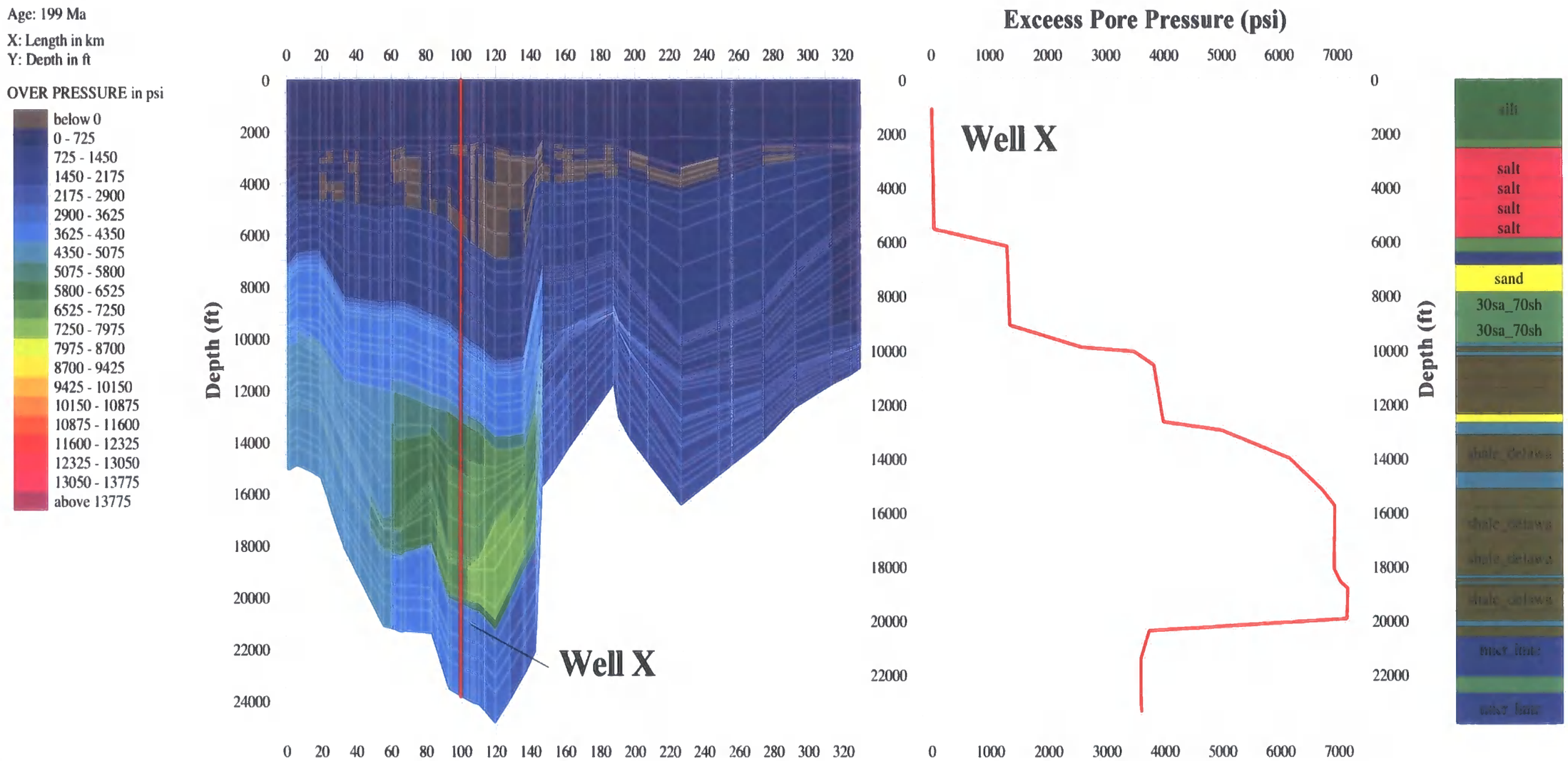

Fig 6.33. A 2D modelling plot showing the distribution and scale of overpressure in the Delaware Basin at top Triassic 199 Ma. The Late Permian Ochoan Series evaporites are modelled to allow some dewatering to occur on the flanks of the basin and tight low permeability limestones are modelled in the stratigraphy laterally across the Delaware Basin.

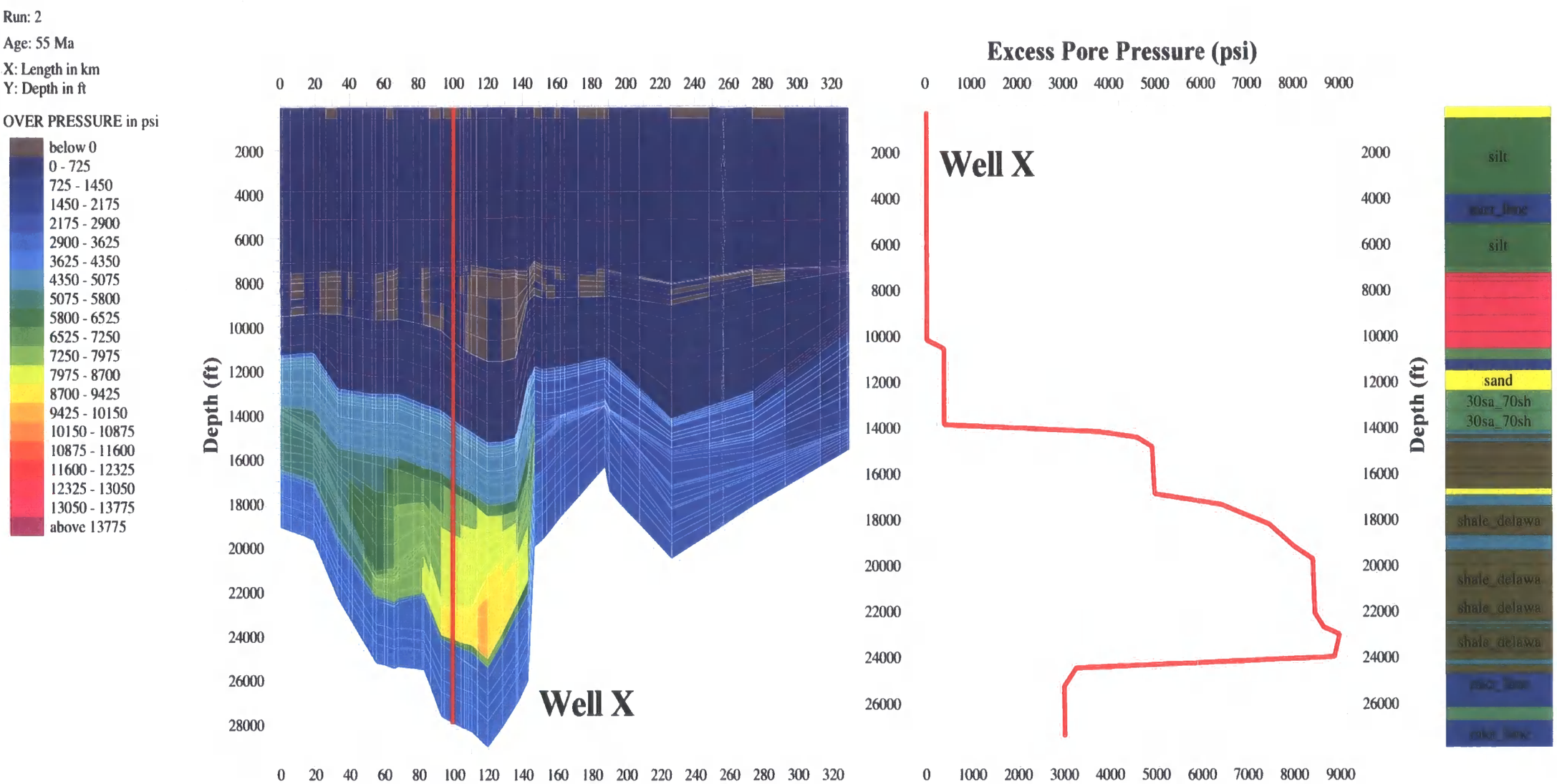

Fig 6.34. A 2D modelling plot showing the distribution and scale of overpressure in the Delaware Basin at maximum burial 55 Ma. The Late Permian Ochoan Series evaporites are modelled to allow some dewatering to occur on the flanks of the basin and tight low permeability limestones are modelled in the stratigraphy laterally across the Delaware Basin.

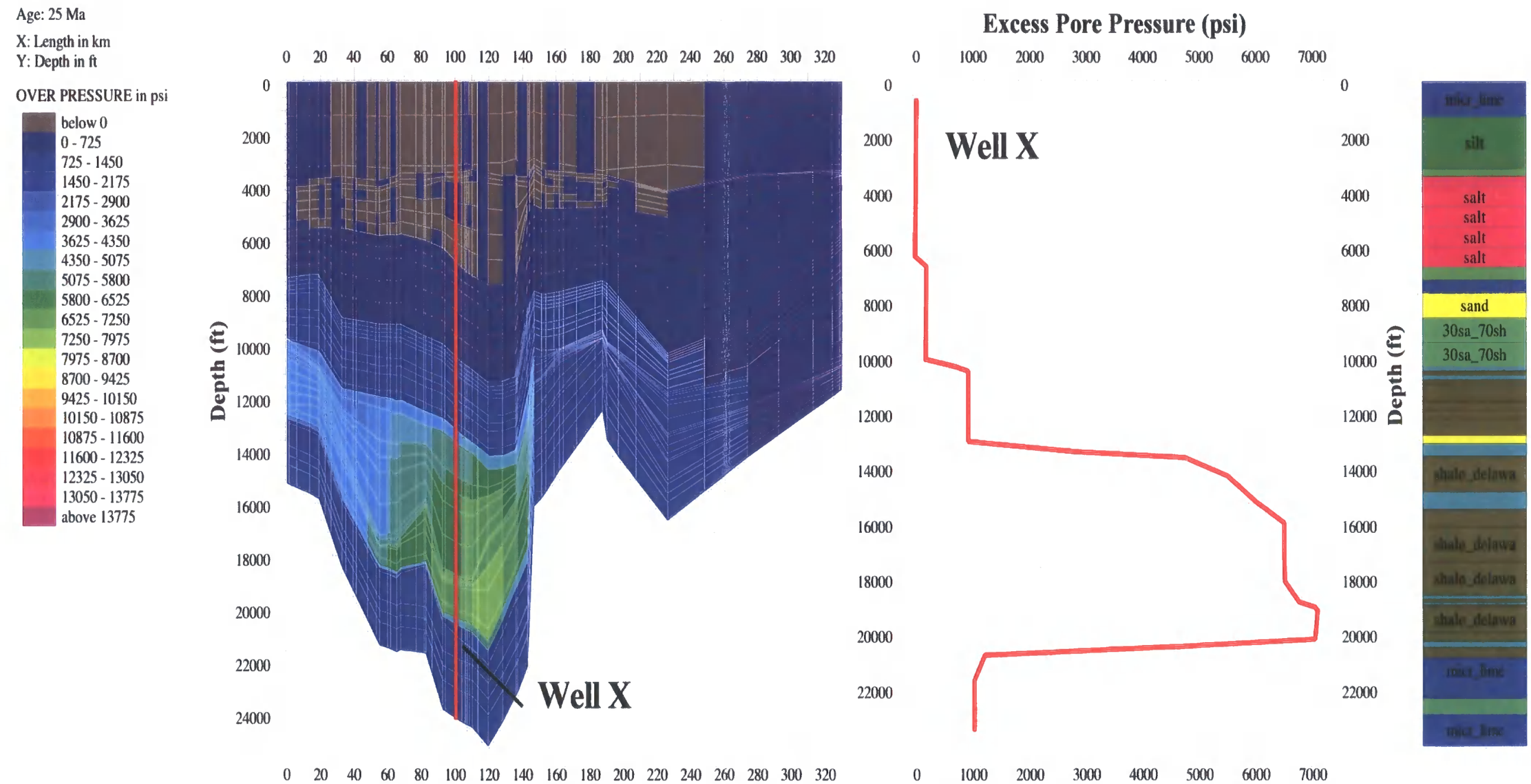

Fig 6.35. A 2D modelling plot showing the distribution and scale of overpressure in the Delaware Basin prior to the Basin and Range associated uplift event 25 Ma. The Late Permian Ochoan Series evaporites are modelled to allow some dewatering to occur on the flanks of the basin and tight low permeability limestones are modelled in the stratigraphy laterally across the Delaware Basin.

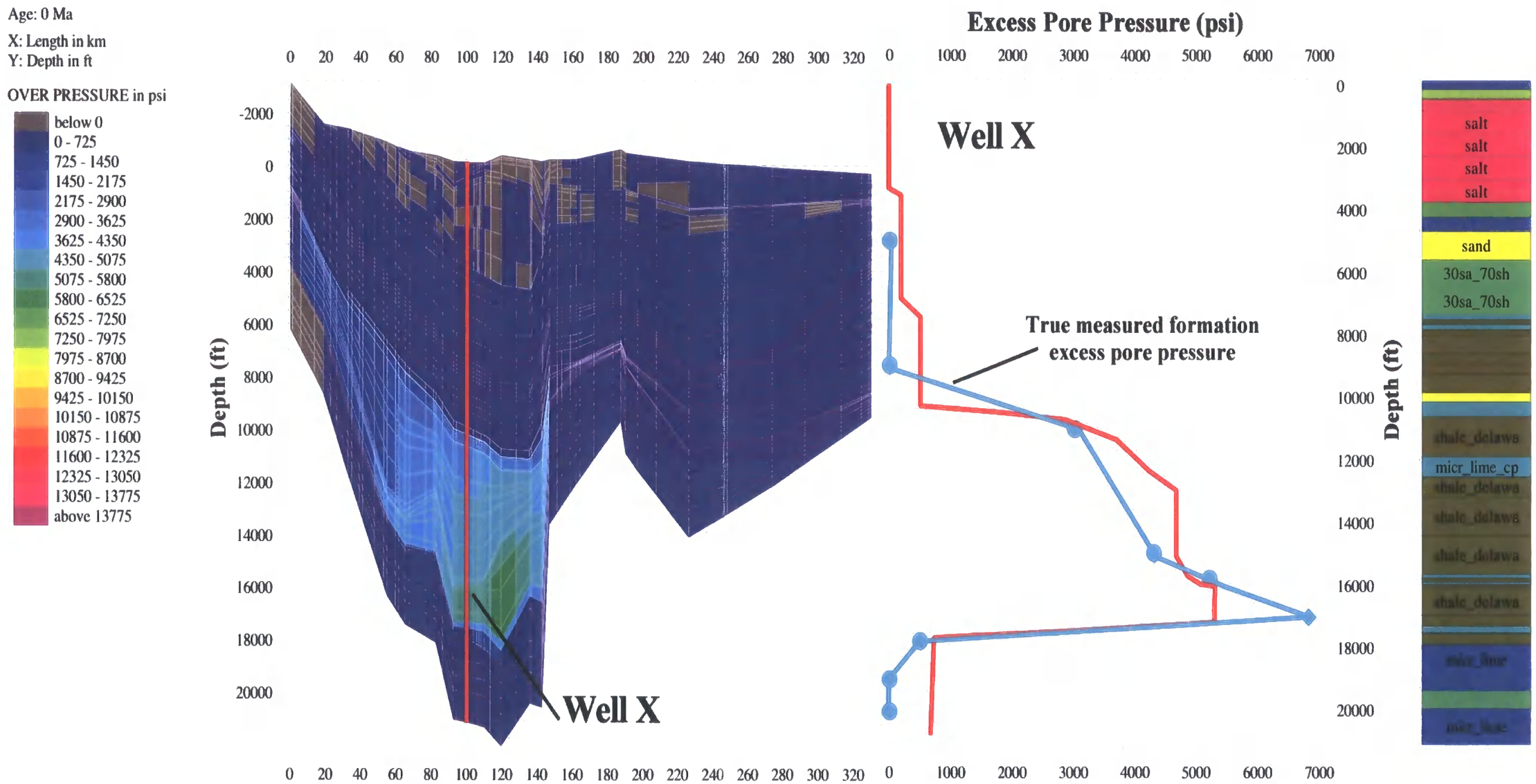

Fig 6.36. A 2D modelling plot showing the distribution and scale of overpressure in the Delaware Basin at present day. The Late Permian Ochoan Series evaporites are modelled to allow some dewatering to occur on the flanks of the basin and tight low permeability limestones are modelled in the stratigraphy laterally across the Delaware Basin.

Summary of the modelling results

The latest modelling results show that if certain limestones horizons in the basin are modelled as being tighter (lower vertical permeability), then significantly more overpressure is retained in the basin through geological time.

At maximum burial 55 Ma (Fig 6.34), between 7000 and 9000 psi of overpressure is being modelled in the Wolfcampian Series and in the Pennsylvanian and Mississippian System. This compares to the on average 3000 psi of overpressure seen when tight limestones were not added to the model (Fig 6.29). No tight limestones were added within or above the Delaware Mountain Group, meaning that this section was able to dewater and return close to hydrostatic pressure by maximum burial.

Prior to the Basin and Range uplift event (25 – 10 Ma), the model (Fig 6.35) is still showing high overpressures (6000 – 7000 psi) in the Wolfcampian Series, the Pennsylvanian System and in the Mississippian System. The pressures have decreased by around 2000 psi since 55 Ma and this is likely to be a consequence of the Laramide uplift event (55 – 50 Ma), where uplift will reduce pore pressure through elastic rebound and shrinkage of pore fluids. Overpressure has also decreased in the Permian Bone Spring Formation and the underlying Ordovician, Silurian and Devonian. Where pressures are modelled at around 1000 psi above hydrostatic.

At present day (Fig 6.36), the model is showing almost hydrostatic pressures in the Delaware Mountain Group, Bone Spring Formation, Ordovician, Silurian and the Devonian. With the uplift and tilt of the basin, dewatering can occur a lot quicker. This is due to erosion of the salt, and potential conduit horizons such as the sand rich Delaware Mountain Group now having connectivity to the surface. The presence of the tight carbonates, has enabled an overpressure cell to remain in the centre of the basin, in the Wolfcampian Series, Pennsylvanian System and the Mississippian System. The results are actually very similar to the true pressures recorded in the basin via DSTs at present day.

It needs to be noted that the modelled pressures may well be on the high side because it was run as a 2D model. In a 3D model, there would be more drainage

pathways, allowing more effective dewatering of certain horizons. For example, at maximum burial 55 Ma (Fig 6.34), the Delaware Mountain Group still has around 300 psi of overpressure. In a 3D model, it may be fully hydrostatic. The same principle could be applied to the Bone Spring Formation at 25 Ma (Fig 6.35). This is unfortunately one of the uncertainties associated with a simple 2D model.

6.4 Discussion: A sensitivity analysis

As mentioned at the start of this chapter, all modelling results are dependant on the initial input parameters. This discussions section aims to look at the porosity-depth function of mudstones and its impact on modelling results.

6.4.1 Impact of different shale compaction curves on pore pressure modelling

Figure 6.8 in sub-section 6.2.5 showed the effect that a change in the porosity-depth curve for a mudstone would have on the retention of overpressure in a basin, since permeability is a function of the porosity. In this sub-section three different shale compaction curves are used in 1D modelling of the Delaware Basin to view the effect it has on the pore pressure retention in the basin.

As seen from published shale compaction curves (Fig 4.29 sub-section 4.2.4), there is a large degree of variation at any depth. For example, at 10000 ft (3 km) there may be up to a 15% difference in the porosity value between curves. For this 1D model experiment, the three compaction curves differ by as much as 4% in porosity at a depth of 12000 ft (3.6 km) (Fig 6.37). The initial starting porosity is 60% for each curve.

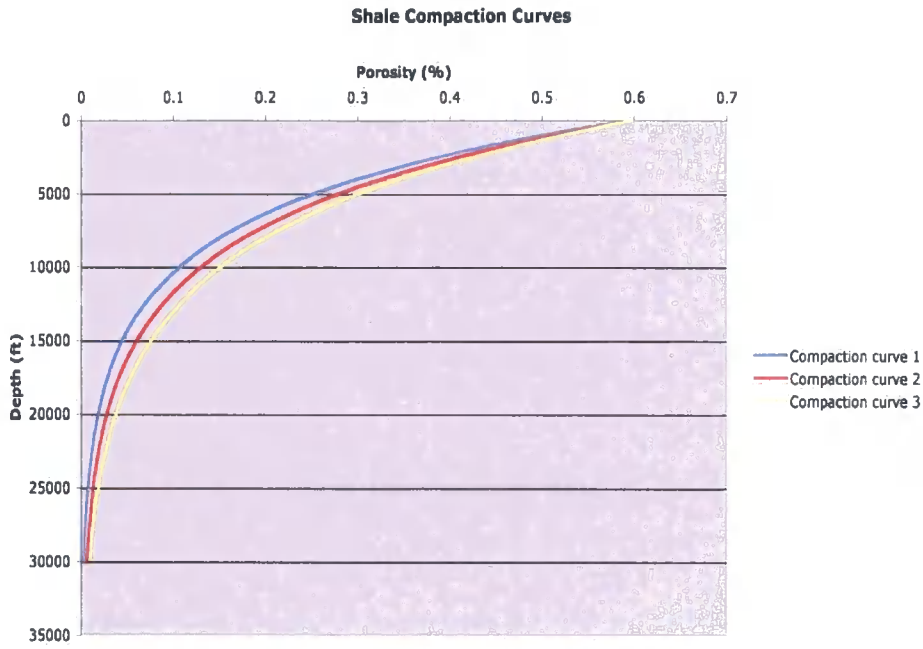

Fig 6.37. A 1D model showing three different shale compaction curves. Each curve has an initial starting porosity of 60%. At 12000 ft they vary in porosity from 8% - 12%. Compaction curve 2 is the compaction curve used previously for this study.

Results of 1D modelling

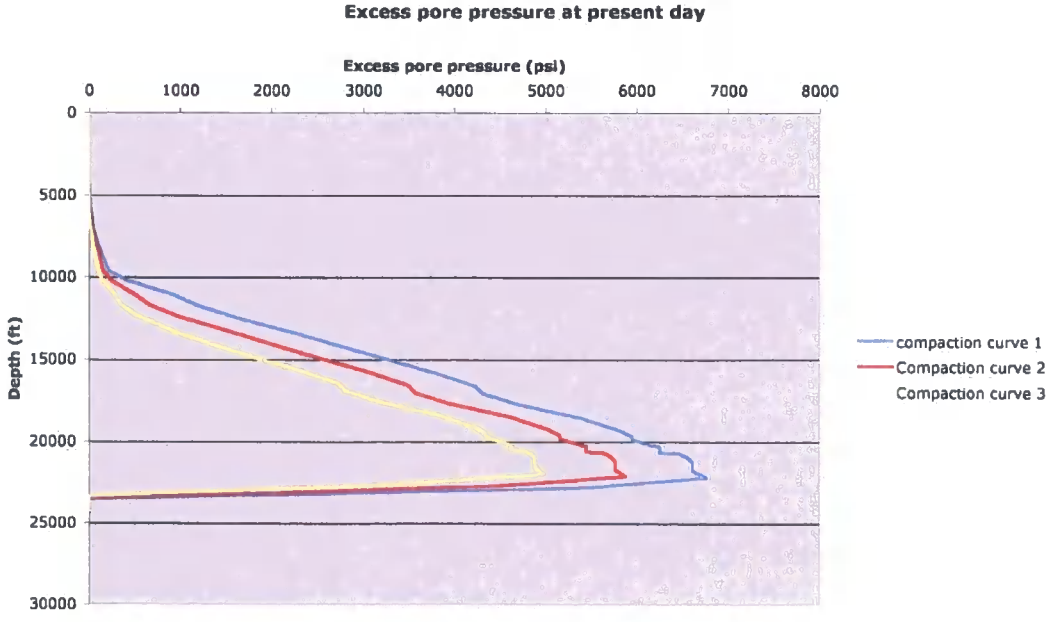

Fig 6.38 1D modelling results showing amount of excess pore pressure in the well at present day for the three different shale compaction curves.

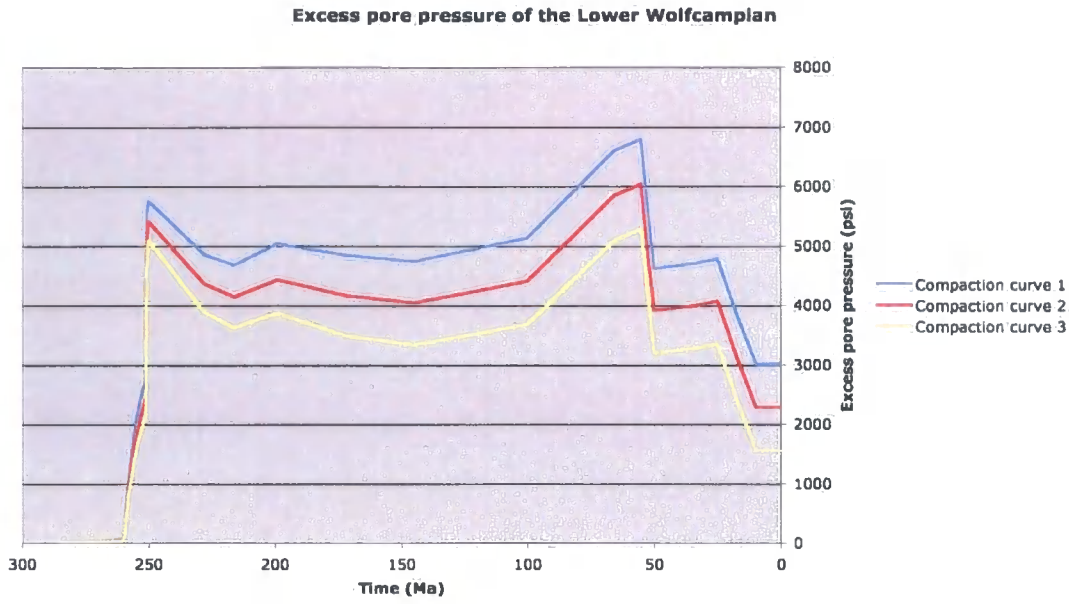

Fig 6.39 1D modelling results showing degree of excess pore pressure in the Lower Wolfcampian Unit through time for the three different shale compaction curves.

The results from the 1D modelling show that with only a 4% change in the porosity at 12000 ft (3.6 km), the effect on the excess pore pressure history of the Delaware Basin is quite significant. Excess pore pressures at present day could be about 2000 psi (13.7 MPa) greater if compaction curve 3 was used instead of curve 1 (Fig 6.38). Fig 6.39 shows the difference in excess pore pressure in the Lower Wolfcampian Unit when different shale compaction curves are used. Prior to uplift at 55 Ma, the difference is 1500 psi (10.3 MPa). These results are in agreement with the conclusions drawn by Schneider et al (1993) (Fig 6.8).

6.5 Conclusions of basin modelling

The following conclusions can be drawn from the basin modelling of the Delaware Basin.

Mechanism of overpressure generation in the Delaware Basin

Disequilibrium compaction

- Overpressure in the Delaware Basin can be generated through disequilibrium compaction (Fig 6.13, sub-section 6.3.1.1). The rapid burial of 20000 ft (6 km) of the mudrock dominated Permian sequence, coupled with a low permeability (10^{-6} mD) enables overpressure to build up to 7000 psi.

Non-stress related mechanism

A limitation of the modelling software used, is that overpressure generation through non-stress related mechanisms cannot be modelled. However, implications can be made based on modelling results.

- The Barnett, Woodford, and Simpson source rocks all generated gas during the rapid burial of the Permian sediments (Fig 6.16 – 6.18). It is possible that overpressure may have developed in these units as a result of the gas generation.
- The Wolfcampian source rock produced gas by 70 Ma, however, not many hydrocarbons were produced due to a low initial TOC content. It therefore unlikely that any overpressure was generated by gas production in this formation.
- All units below the Pennsylvanian System had the required conditions to allow oil to gas cracking to occur if a reservoir was oil-filled, so additional overpressure generation via this mechanism is plausible.
- Overpressures within a permeable unit may have been enhanced at structural crests by lateral transfer (Fig 6.23).

From the modelling results it is concluded that the primary mechanism for overpressure generation within the Delaware Basin would have been disequilibrium compaction. However, it is geologically possible that overpressure was enhanced on a localised scale in certain horizons through non-stress related mechanisms. For example the Pennsylvanian age Cisco Series is a reservoir in the basin and as shown from the modelling, the conditions are favourable for oil to gas cracking or lateral transfer to occur.

The modelling has also shown that regardless of the generating mechanism, all overpressure would have been generated prior to maximum burial 55 Ma (sub-section 6.3.2).

Overpressure retention in the basin

- The Late Permian evaporites would have been a perfect top seal if laterally continuous across the whole basin, and acted as an impermeable barrier to flow (Fig 6.27, sub-section 6.3.2.1).
- Taking into account results from chapter 4 (sub-section 4.2.4.1), where it was suggested that the Delaware Mountain Group was hydrostatically pressured at maximum burial, the model was adapted to allow limited flow on the flanks of the basin. The results showed that in this scenario the basin would not retain any significant overpressure through time, and the model therefore underestimates the overpressures at present day (Fig 6.31).
- If certain limestones horizons are modelled as "tight" (10^{-8} mD) in the basin, then this will compartmentalise the basin and overpressures are maintained through to present day. In this scenario the model accurately predicts overpressures similar to those recorded in the basin (Fig 6.36).

Sensitivity analysis

- The parameters used in basin modelling have a large impact on the pore pressure distribution predicted in the basin. For example, different shale compaction curves result in different values of permeability, and affect the ability of a mudrock to retain overpressure.

Chapter 7:

Synthesis and Discussions:

The Generation and Maintenance of Overpressure in the Delaware Basin

7.1 Introduction to the discussions

This research project set out to answer the following questions about the Palaeozoic successions in the Delaware Basin:

1. How was overpressure generated in the basin?
2. How is excess pore fluid pressure maintained in the basin?

By integrating the results presented here with findings in previous publications, this discussions chapter aims to answer the above questions and aid in the further understanding of overpressure in other old Palaeozoic basins.

This research includes the first use of apatite fission track analysis (AFTA) to investigate the burial history of the Delaware Basin. Synthesis of the AFTA results, well logs and basin modelling has provided a much better understanding of the pore pressure history in the basin.

This chapter will briefly discuss the main mechanisms and maintenance of overpressure in basins using the Delaware Basin as an example. However, the emphasis will be on how overpressure in maintained in 'old' sediments and its applications.

The results of this study will be highly relevant and applicable for further research and exploration in many other basins with excess pore pressures but especially where the excess pore pressure is found in 'old' basins of Palaeozoic age, e.g. the Val Verde Basin in West Texas and the Anadarko Basin in Oklahoma.

7.2 Mechanisms of overpressure generation

7.2.1 An overview

The mechanisms by which overpressure can be generated were described in chapter 3 (sub-section 3.2.5.1) as either stress related or non-stress related (unloading mechanisms). Stress related mechanisms include disequilibrium compaction and

tectonic compression. Unloading mechanisms generate overpressure by reducing the effective stress, by such methods as aquathermal expansion, smectite dehydration, smectite to illite transformation, lateral transfer and hydrocarbon generation (Osborne & Swarbrick 1997). Swarbrick et al (2002) have analysed the magnitude of overpressure generated as a consequence of the above mechanisms, and shown that the two main mechanisms which have the potential to produce a large amount of overpressure are disequilibrium compaction and gas generation, either through source rock generation or oil to gas cracking in the reservoir (Table 7.1).

Overpressure is more commonly associated with young rapidly subsiding basins with a high sedimentation rate, such as the Tertiary deltas in the Gulf of Mexico or off the west coast of Africa where overpressure has developed through disequilibrium compaction. In these basins, the maintenance of overpressure in the system is controlled by the low permeability of the mudrocks (around 10^{-3} mD), which enabled overpressure to develop in the first place as a consequence of disequilibrium compaction.

Where overpressure is found in Palaeozoic Basins, the excess pore pressure may have been generated during the Palaeozoic or Mesozoic as a consequence of disequilibrium compaction. Mudrock permeabilities of 10^{-3} mD would enable any excess pore pressure to be dissipated within tens to hundreds of millions of years. A very low shale permeability (10^{-9} mD) is therefore needed to maintain the overpressure over this length of time (Lee & Demming 2002). The lowest permeabilities ever measured in sedimentary rocks are in the range of $10^{-7} - 10^{-8}$ mD (nanoDarcy to picoDarcy) (Lee & Demming 2002). It is for this reason that overpressure in old Palaeozoic basins has often been attributed to later fluid expansion mechanisms such as gas generation, where any overpressure generated has only been maintained for a shorter time.

This study, however, suggests that disequilibrium compaction was the main mechanism for overpressure generation in the Delaware Basin as a consequence of the rapid burial of Permian sediment. Fluid expansion mechanisms may have enhanced the overpressure and would be on a localised scale, such as on a structural crest or within a reservoir (Table 7.1)

Author	Study area	Age	Methods of analysis	Mechanism of overpressure generation	Maintenance of overpressure
This study	Delaware Basin, West Texas, US	Palaeozoic	- Pressure data from DSTs. - Burial history analysis - AFTA, VR & shale compaction curves - 1D & 2D basin modelling	- Disequilibrium compaction - Unloading as a secondary mechanism	Numerous pressure seals within the basin
Luo et al (1994)	Delaware Basin, West Texas, US	Palaeozoic	- Pressure data from DSTs - Burial history analysis	- Disequilibrium compaction - Hydrocarbon generation - Clay dehydration - Aquathermal expansion	Two pressure seals within the basin
Lee & Williams (2000) & Hansom & Lee (2005)	Delaware Basin, West Texas, US	Palaeozoic	2D Basin Modelling	- Disequilibrium compaction - Hydrocarbon generation	One pressure seal within the basin
Lee & Demming (2000)	Anadarko Basin, Oklahoma, US	Palaeozoic	- Pressure data from DSTs - Mathematical modelling	Gas generation	Gas capillary sealing
Hoesni (2004)	Malay Basin, Malaysia	Tertiary	- Basin modelling - Velocity / density cross plots - Pore pressure prediction form wireline logs	- Disequilibrium compaction - Chemical compaction	N/A
Wilson et al 91998)	Piceance Basin, Colorado, US	Palaeozoic	- Well data - Basin Modelling	Gas generation	Pressure seals

Author	Study area	Age	Methods of analysis	Mechanism of overpressure generation	Maintenance of overpressure
Spencer (1987)	Williston Basin, Rocky Mountains, US	Palaeozoic	Core and well log	Hydrocarbon generation	N/A
Luo et al (2003)	Yinggehai Basin, South China Sea	Cenozoic	Modelling	Disequilibrium compaction	Pressure seal
Swarbrick et al (2000)	Judy Field, Central North Sea	Cenozoic	Modelling	Disequilibrium compaction	Overlying Cretaceous chalk seal.
Hunt & Cathles (1998)	Gulf Coast, Louisiana	Tertiary	- pressure data from DST's - Core data	Gas generation	Pressure seals
Mello & Karner (1996)	Gulf of Mexico	Tertiary	Modelling	Disequilibrium compaction	N/A
Williamson (1995)	Sable Basin, offshore Nova Scotia	Mesozoic	Modelling	- Disequilibrium compaction - Gas generation	N/A

Table 7.1. Examples of overpressured basins from around the world, showing the mechanism of overpressure generation and how it is maintained.

7.2.2 Disequilibrium compaction

The results from this research demonstrate that disequilibrium compaction was the main generating mechanism for overpressure in the basin. This conclusion contradicts the findings by Luo et al (1994), Lee & Williams (2000) and Hansom & Lee (2005) (Table 7.1), who considered hydrocarbon generation to have been of equal or greater importance than disequilibrium compaction to explain the generation of overpressure in the Delaware Basin.

Chapter 4 illustrated that the burial and tectonic history of the Delaware Basin has been misinterpreted in the past by numerous authors (Barker & Pawlewicz 1987; Luo et al 1994; Hill 1996; Lee & Williams 2000; Alton-Brown 2004; Hanson & Lee 2005), who assumed simplistic burial history scenarios based on the preserved stratigraphy in the basin at present day.

Luo et al (1994) suggested that no extra Mesozoic sediment was deposited on top of the preserved Triassic in the basin, and therefore subsequently there was no uplift of the basin during the Cenozoic (Fig 7.1). This study has shown through the analysis of apatite fission tracks, vitrinite reflectance plots and shale compaction curves (chapter 4) that the basin had a significantly more complex Mesozoic and Cenozoic burial and tectonic history than was previously known (Fig 7.2). Prior to maximum burial (55 Ma), the basin experienced 6890 ft (2.1km) of extra burial on top of the preserved Triassic. During the Cenozoic this Mesozoic deposition was removed by two uplift events, the Laramide event (55-50 Ma) and the Basin and Range event (25-10 Ma).

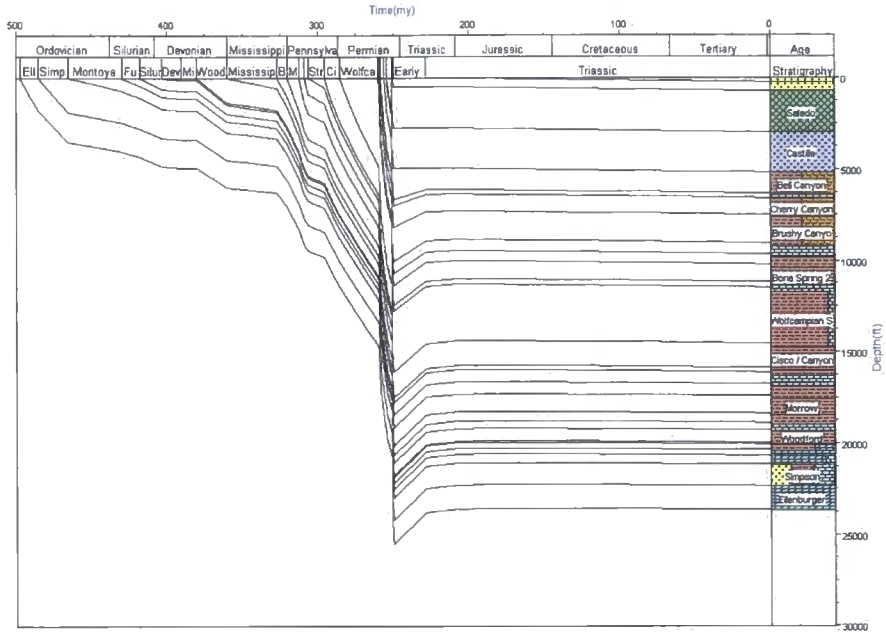

Fig 7.1. Burial history used by Luo et al (1994) for their analysis of the pore pressure history of the Delaware Basin.

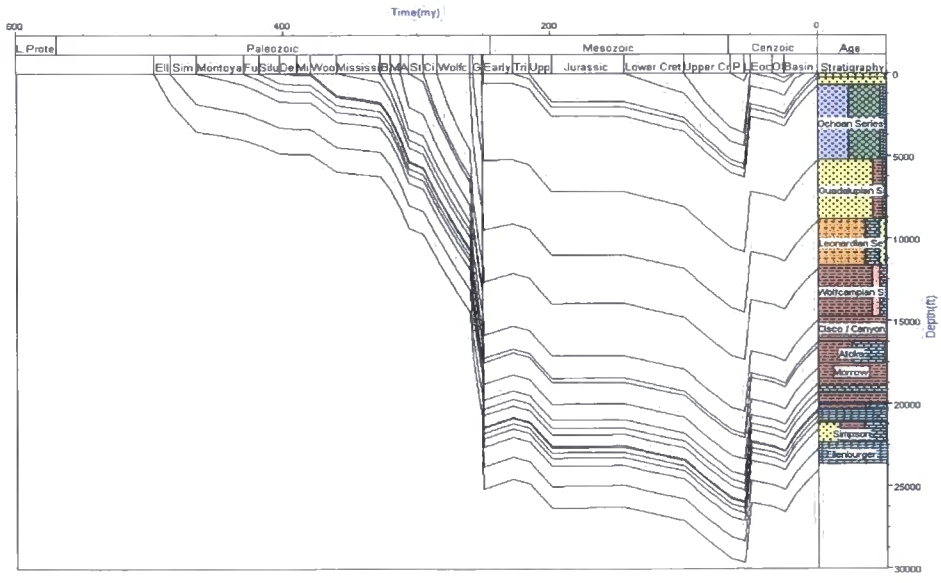

Fig 7.2. A revised burial history curve for the Delaware Basin based on results from this research (refer to chapter 4).

Luo et al (1994) argued against disequilibrium compaction as a dominant mechanism for overpressure generation in the basin due to the inability of this mechanism to generate similar overpressures to those recorded in the basin at present

day (up to 8500 psi). Luo et al (1994) based the relationship between sedimentation and pore pressure generation on the sedimentation rate of the overpressured units, stating that due to the low sedimentation rate of the Pennsylvanian System, disequilibrium compaction would not have generated overpressure in these units. Disequilibrium compaction can easily be generated in mudstones that have been deposited slowly provided they subsequently experience rapid burial by overlying units. This is seen in the Delaware Basin, where the mudrocks of the Pennsylvanian section were overlain by 20000 ft (6 km) of Permian section that was deposited in 35 My. The results through the use of basin modelling in chapter 6 (Fig 6.13, sub-section 6.3.1.1) have shown that overpressures can reach up to 7000 psi in the basin by the end of the Permian through disequilibrium compaction alone. This study has also shown that due to the extra 6890 ft of deposition during the Cretaceous and Palaeocene (Fig 7.2), overpressures will increase by a further 2000 psi in the centre of the basin (Fig 6.34 & 6.35). These results demonstrate that in the Delaware Basin disequilibrium compaction alone can generate a large magnitude of overpressure.

The research conducted by Lee and Williams (2000) and Hansom and Lee (2005) used 2D basin modelling to study the pore pressure history of the basin. In both studies a burial history scenario (Fig 7.1) similar to Luo et al (1994) was used in the modelling. The thickness and lateral variability of the stratigraphy used in the models was based upon present day stratigraphic fills and architecture. However, the Permian stratigraphy has varied greatly in thickness and lateral extent through time as a consequence of the additional Mesozoic deposition and subsequent Cenozoic erosion as suggested in this study. Correctly modelling the lateral extent of the Late Permian evaporites and the tectonic history of the basin through time, has an important influence on the pore pressure history of the basin. In the models, Lee and Williams (2000) and Hansom and Lee (2005) modelled the Late Permian evaporites as not being laterally extensive across the whole basin through time (Fig 7.3).

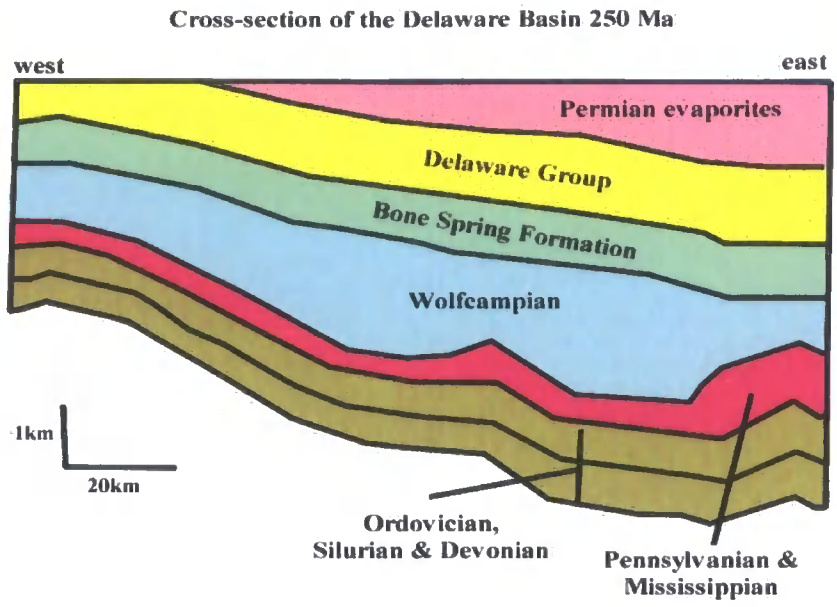

Fig 7.3. Cross section used by Lee and Williams (2000) and Hansom and Lee (2005) for the basis of their modelling. Their model has assumed present day stratigraphic thicknesses and lateral extent in the geological past (Taken from Lee & Williams 2000).

Lee & Williams (2000) and Hansom & Lee (2005) acknowledged that pore pressure as a consequence of disequilibrium compaction could build up to 5000 psi (34.4 MPa) above hydrostatic as an outcome of the rapid burial of the Permian section. However, they concluded that despite this generation of overpressure, it cannot be retained in the basin due to the lack of a suitable pressure seal. The dissipation of excess pore pressures would have begun at the end of the Permian (250 Ma). An alternative mechanism for overpressure generation was therefore needed to explain the present day magnitude of overpressure in the basin.

In contrast, this study has shown that even if there were no pressure seals and the evaporites were modelled to allow fluid flow on the edges of the basin, then there is still some overpressure in the basin at the end of the Triassic (199 Ma) (Fig 6.28, sub-section 6.3.2.2). This overpressure is then increased further by the deposition of Cretaceous and Palaeocene sediments, so that by the time of maximum burial (55 Ma) overpressures are being modelled at up to 3200 psi (Fig 6.29). It is likely that this overpressure is retained in the basin at 55 Ma as a consequence of low permeability (10^{-6} mD) mudstones in the section, as well as the Late Permian

evaporites. Despite the evaporites being modelled to allow flow on the edges of the basin, it is still laterally extensive and would be a very effective seal across the rest of the basin helping to maintain the overpressure. However, this research does show through modelling that the overpressure is not maintained from 55 Ma through to present day if pressure seals are not present (Fig 6.31). Uplift of the basin during the Laramide Orogeny (55 – 50 Ma) reduced the overpressure by 2000 psi (Fig 6.29 – 6.30) through elastic rebound of the pore space and through shrinkage of the pore fluids with cooling. The later Basin and Range uplift event (25 – 10 Ma) tilted the basin and speeded up the dewatering process by eroding off the evaporites on the western edge and allowing connectivity of permeable conduit zones to the surface. This study therefore agrees with Lee & Williams (2000) and Hansom & Lee (2005), where the need for pressure seals in the basin is essential if disequilibrium compaction generated overpressure is to be maintained till present day. The discussion regarding the presence of pressure seals in the Delaware Basin will be looked at later in sub-section 7.3.

This study has shown that a full burial history obtained using AFTA, vitrinite reflectance and shale compaction curves, is required before the pore pressure history can be appreciated. In addition it is important to appreciate the petrophysical nature of the sediments and their lateral extent.

In Cenozoic basins undergoing active (rapid) sedimentation (e.g. Gulf Coast, Table 7.1), overpressuring can be readily attributed to the high deposition rates of coarse clastics overlying low permeability mudstones (10^{-3} – 10^{-6} mD). The Delaware Basin is very different from such a setting, and exhibits the need for an in-depth study of 'old' (Palaeozoic) basins. The approach used in this study has enabled a better understanding of complex compartmentalised basins, where disequilibrium compaction is the predominant mechanism for overpressure generation.

7.2.3 Non-stress related mechanisms (unloading)

This study has used pore pressure prediction methods (chapter 5.2), which depend on the sediment being mechanically compacted. If the pore pressure prediction methods underestimate the true formation pressures, it suggests that unloading mechanisms contributed to the overpressure. The Devonian Formation shows evidence in four wells that its pore pressure may be the consequence of unloading processes. Other formations to show evidence of unloading in some wells are the Strawn and Cisco formations of the Pennsylvanian System and the Lower Wolfcampian Formation. Velocity / density cross-plots were created for the Strawn Formation in two wells (Figs 5.12 & 5.13, sub-section 5.3.2) and the results showed that unloading mechanisms had taken place.

This discussions sub-section will integrate results presented in this study with findings in previous publications, to suggest viable mechanisms to explain the unloading recorded in some horizons.

Hydrocarbon generation

Hydrocarbon generation has been suggested as one of the main methods for generating overpressure in the Delaware Basin (Luo et al 1994; Lee & Williams 2000; Hansom & Lee 2005). Hansom and Lee (2005) conclude by saying that oil and gas generation can cause excess pore pressure up to 40% and 110%, respectively, of that generated by compaction only. This study does not rule out hydrocarbon generation as a potential mechanism, as numerous authors have shown that there is potential for an increase in pore pressure via this method (Meissner 1978; Ungerer 1983). Recent studies (Swarbrick & Osborne 1998; Swarbrick et al 2002) have shown that it is only gas generation from the source rock or in-situ oil to gas cracking within a reservoir can generate large magnitudes of overpressure.

Basin modelling (sub-section 6.3.1.2) of the Mississippian Barnett, Devonian Woodford and Ordovician Simpson source rocks demonstrates that gas was generated as a consequence of the burial of the Permian section (255 Ma), which is in agreement to what has been previously published in the literature (Barker &

Pawlewicz 1987; Luo et al 1994; Hill 1996; Lee & Williams 2000; Hansom & Lee 2005). None of these source rocks, however, show any evidence of being overpressured at present day. This lack of overpressure in the deep section is most likely to do with effective dewatering of the sediments after the Basin and Range event (25-10 Ma), so the deep section may have been overpressured in the past.

The only source rock that is overpressured is the Early Permian Wolfcampian Series, which reached the gas window 70 Ma (refer to Fig 6.15). Basin modelling showed that, due to an initial low TOC value (1.24%) for the Wolfcampian source rock, the amount of hydrocarbons generated is low in comparison to the other basinal source rocks. For example, the Kimmeridge Clay source rock of the Central Graben in the North Sea averages a TOC of 6%. All these factors lead this study to suggest that hydrocarbon generation within the Wolfcampian source rock would not have generated the magnitude of overpressure that is seen in this formation. Luo et al (1994) recognised that the Wolfcampian is not a gas producing source rock, but stated that oil generation from the Wolfcampian would have generated overpressure. Again this seems unlikely following the work by Swarbrick et al (2002), who state that oil generation is unlikely to generate large volumes of overpressure.

Swarbrick et al (2002) suggested that a more likely overpressure generating mechanism is oil to gas cracking in the reservoir, where in a tightly sealed reservoir, the potential exists for a significant volume expansion. Basin modelling from this study (Fig 6.20, sub-section 6.3.1.2) has shown that units below and including the Lower Wolfcampian Series would have reached the required conditions for oil to crack to gas in the reservoir by the time of maximum burial (55 Ma). For oil to gas cracking to be a viable mechanism in some reservoirs, the oil needs to be trapped within a reservoir. In the Delaware Basin there are numerous Palaeozoic structural highs that could be suitable traps for hydrocarbons. For example, the Jo Neal 43 well is located in Pecos County in the deep section of the basin. Pore pressure prediction methods were used on the sonic log from the well (sub-chapter 5.2.2). The results showed that the methods were underpredicting pore pressures for the Wolfcampian Series, the Pennsylvanian Cisco Formation, and the Devonian Formation. The well is located at the apex of a structural high, where oil could be trapped (refer to Fig 6.23 sub-section 6.3.1.2) and the conditions in these reservoirs permit oil to gas cracking

to take place. Known deep basin reservoir plays exist in the Wolfcampian Series, Pennsylvanian System, Devonian Formation, Ordovician and Silurian (Dutton et al 2005). In conclusion, overpressure generation as a consequence of oil to gas cracking may be occurring in the deep basin but on localised scale within some tightly sealed compartmentalised horizons.

Lateral Transfer

The lateral transfer of fluids from deep overpressured parts of the basin along laterally extensive inclined aquifers will enhance overpressure on the structural high (Yardley & Swarbrick 2000). Pressure differences up to 3000 psi have been recorded in the South Caspian Sea, believed to be a consequence of lateral transfer (Swarbrick 2003). Chapter 6 (sub-section 6.3.1.2) demonstrated that Palaeozoic structures in the Delaware Basin have produced tilted reservoirs, where lateral transfer may be occurring, for example, the Jo Neal 43 well in Pecos County (Fig 6.23). If this mechanism did occur in the Delaware Baisn, then it would be only to enhance the overpressure that had already generated in the basin.

Gas expansion with uplift

The expansion of a gas with uplift has the potential to create high overpressures if it is in a well sealed system (Osborne & Swarbrick 1997). However, there has been very little quantification of this mechanism in the literature and so its potential to be a mechanism of overpressure generation in the Delaware Basin is entirely hypothetical. What is known through the results of this study is that the Delaware Basin has experienced significant uplift during the Cenozoic (chapter 4). All source rocks below and including the Lower Wolfcampian reached the gas window prior to uplift 55 Ma. Also the mudstones in the basin are very tight (10^{-6} mD) and with the inclusion of tight limestones, there is the potential to create a well sealed system. More research is therefore needed on the role and importance that this mechanism may have on the pressure system in the basin, but it has the potential to have a significant impact.

Smectite to Illite transformation

Luo et al (1994) attributed smectite to illite transformation as one of the mechanisms behind overpressure generation in the Delaware Basin. However, the only evidence Luo et al (1994) used to base this conclusion on, is that the overpressured zone in the basin corresponds to the temperature range that is favourable for smectite to illite transformation (70-150 °C). In a discussion and reply to Luo et al (1994), Swarbrick (1995) stated that the contribution to overpressure by smectite to illite transformation in the Delaware Basin cannot be evaluated based on the data given by Luo et al (1994). This study has not produced any further evidence other than agreeing with Luo et al (1994) regarding the temperature profile of the basin (Fig 6.20, sub-section 6.3.1.2). Also Swarbrick et al (2002) suggested that any overpressure generated by this mechanism would most likely be insignificant and so is not considered to be a major contributor to overpressure in this study. Therefore further specific research on the mudstones in the basin needs to be carried out gain a better understanding of this mechanism and its applicability to the Delaware Basin.

Hydrocarbon buoyancy

For this to be a viable mechanism of overpressure generation, then a large hydrocarbon column height is needed (Swarbrick & Osborne 1998). This study had limited pressure data that was taken from the same formation. Often only one DST measurement was taken. Therefore analysing the pressure gradients and hence identifying a hydrocarbon column within the basin was not possible. Also this mechanism is restricted to structural and stratigraphic traps and cannot cause regional overpressure (Swarbrick & Osborne 1998). For these reasons, this mechanism has not been analysed further. However, it would be advisable to know the hydrocarbon column height of a play if it is about to be drilled, as pressures could be enhanced by up to 1000 psi if a 1km dry gas column was present (Swarbrick et al 2002).

7.3 Maintenance of overpressure in the Delaware Basin

Chapter 5 (Fig 5.16, sub-section 5.4.1) showed that shale compaction trends in sonic logs indicate that dewatering of mudstones in the basin continues at present day. If the basin is currently dewatering, then the pressure system in the basin is in a dynamic compared to static state, in agreement with the definition of overpressure by Swarbrick (2003):

"Overpressure results from the inability of pore fluids to escape at a rate which allows equilibration with a column of static water connected to the surface."

The evidence of dewatering at present day suggests the overpressure has been maintained in the geological past.

The very existence of overpressure in young basins that are rapidly subsiding, such as the Tertiary deltas of the Mississippi, Nile and Mahakam, can be easily explained through disequilibrium compaction related to the high sedimentation rates and the predominance of low permeability lithologies. These geological settings maintain overpressure through continuous burial without the need of a seal. However, what is not well understood is how overpressure can exist in older basins that have not undergone active sedimentation in tens to hundreds of millions of years.

Basin modelling results (Fig 6.13, sub-section 6.3.1.1) showed that the whole basin became overpressured as a consequence of the rapid burial of the Permian section (270 Ma – 250.6 Ma). However, results from chapter 4 (Fig 4.32, sub-section 4.2.4.1) showed that the Late Permian Delaware Mountain Group was normally pressured by the time of maximum burial 55 Ma. This shows that the pressure system in the basin has always been in a dynamic state attempting to reach pressure equilibrium and the Late Permian evaporites must have allowed some fluid flow to occur out of the basin if geological units are returning to hydrostatic pressures. Modelling results then showed that if the basin carried on in a dynamic state, little overpressure would remain in the basin at present day with the model underpredicting the magnitude of true recorded overpressures by up to 6000 psi (Fig

6.31, sub-section 6.3.2.2). Modelling does show that low permeability mudstones (10^{-6} mD) and the Late Permian evaporites (modelled to allow flow on the edges) can maintain overpressures in the basin since generation (~270 Ma) through to 25 Ma (Figs 6.28 – 6.31). However, the modelled magnitude is less than the true recorded values of overpressure in the basin and another method of maintaining the overpressure is therefore needed.

Either gas capillary seals (Boult et al 1997; Lee & Demming 2002; Cranganu & Villa 2006), or pressure seals (Bradley & Powley 1994; Luo et al 1994; Al-Shaieb et al 1994; Lee & Williams 2000; Lee & Demming 2002) are able to maintain overpressure for long periods of geological time (Table 7.1), and their applicability to the Delaware Basin is discussed in sub-sections 7.3.1 and 7.3.2.

7.3.1 Gas capillary seals

A gas capillary seal is a seal that restricts the flow of hydrocarbons, and is formed when the capillary pressure across the pore throats (a function of the surface tension between the wetting fluid and the migrating hydrocarbon) is greater than or equal to the buoyancy pressure of the hydrocarbons. Gas capillary sealing has been proposed as the mechanism for maintaining overpressure in the Andarko Basin, Oklahoma (Cranganu 2004; Lee & Demming 2002), the Laramide basins of Wyoming (Surdam et al 1997), and the Ermonanga Basin, Australia (Boult & Theologou 1997). It is common to find gas systems associated with geopressure systems that are both over and underpressured (Hunt 1990, and Law 2002).

The association between gas and anomalous pressures suggests a relationship between gas and reduced permeability. This, however, cannot explain all situations and although the Delaware Basin has deep centred gas (R. Webster pers. comm.), no evidence has been found from wireline logs to link the compartmentalised overpressured section with gas horizons. In this study, the lack of density and neutron logs run in the same wells has hindered the identification of strata that are saturated with gas.

One suggested example of a location in the basin where gas capillary sealing may be occurring, but cannot be proved, is in the JO Neal 43 well in Pecos County (Fig 6.23). This well is located at the apex of an anticlinal trap, where hydrocarbons could be saturated in suitable reservoirs. Pore pressure prediction methods using sonic log were underpredicting overpressures in the Wolfcampian, Cisco and Devonian formations, suggesting unloading mechanisms such as oil to gas cracking may have an influence. Therefore without suitable proof to identify the presence of gas in the trap and its stratigraphic relationship to the overpressured units, gas capillary sealing can only be hypothesized in the basin.

7.3.2 Pressure seals

A pressure seal is a seal that restricts the flow of both hydrocarbons and brine. It is formed where the pore throats become effectively closed, and the permeability approaches zero (Bradley and Powley 1994). Generally, a pressure seal can be any lithological unit that prevents fluid movement over substantial intervals of geological time (Hunt 1990). The existence of pressure seals is widely accepted as a mechanism for the maintenance of overpressure in basins (Bahr et al 1994; Luo et al 1994; Drzewiecki et al 1994; Surdam et al 1994; Wilson et al 1998; Lee & Williams 2000; Luo et al 2003).

The results from chapter 5 showed that calcite-rich horizons within the basin coincided with the peaks of high shale travel time (Fig 5.16). This is evidence to suggest that lithological horizons may act as pressure seals in the basin and control the dewatering of the basin. This is in agreement with Luo et al (1994), who concluded that pressure seals do exist in the Delaware Basin and that calcite cementation is a likely cause of the seal. Other authors (Hunt 1990; Drzewiecki et al 1994) also concluded that calcite cementation is a controlling factor on the sealing capacity in other basins (e.g. Michigan Basin). Within the overpressured section of the Delaware Basin, there are potentially five pressure seals (Fig 5.16) that may be creating compartmentalisation within the basin and controlling the maintenance of the overpressure (Fig 7.4)

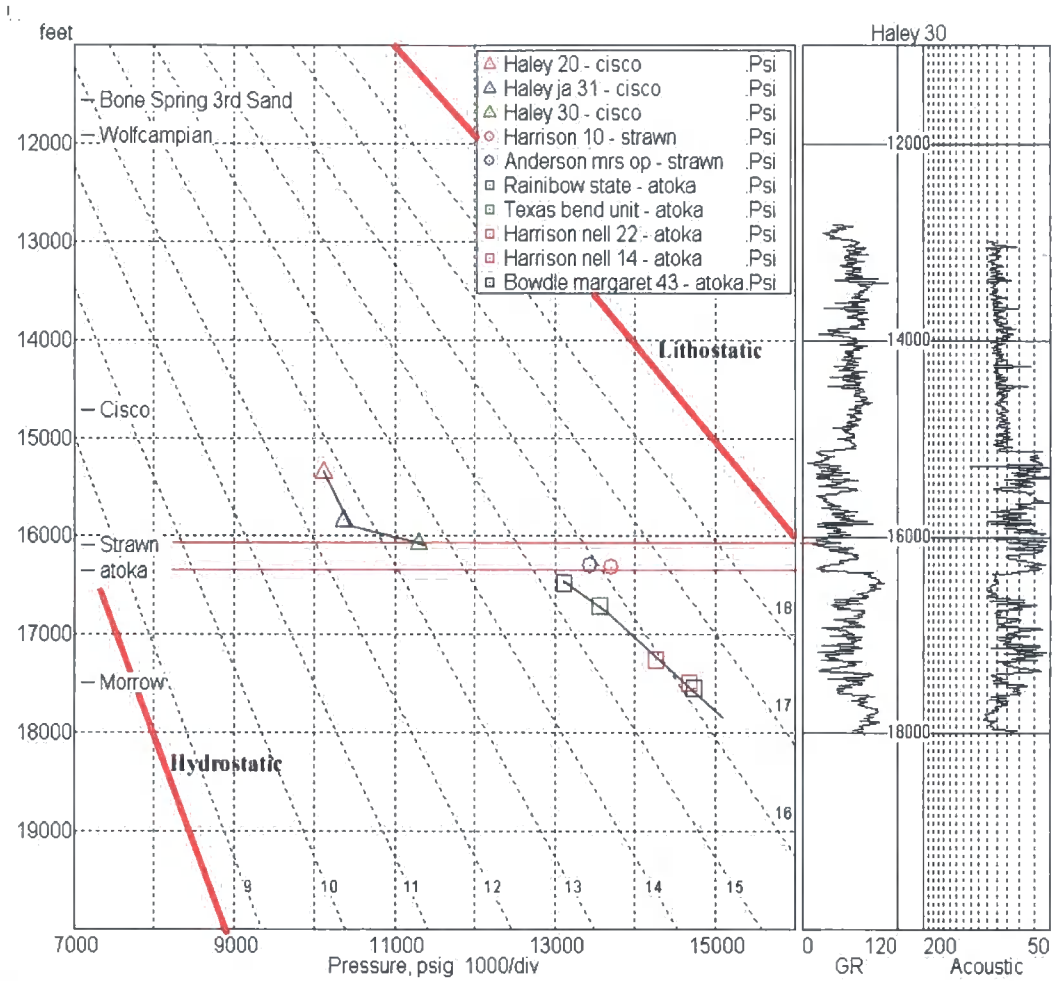

Fig 7.4. Example of two pressure seals in the Delaware Basin. Carbonate beds are located at the bottom of the Cisco Formation and at the top of the Atoka Formation, influencing the overpressure in each section.

Lee and Williams (2000) stated that pressure seals in the Delaware Basin would require a nanoDarcy scale of permeability in order to retain the overpressure. Using this suggested permeability, basin modelling was used to model the effect of pressure seals in the Delaware Basin with respect to the overpressure maintenance in the basin (Figs 6.32 – 6.36, sub-section 6.3.2.3).

The results from the pressure seal modelling show that if tight lithologies acting as pressure seals are present in the basin, then significantly more overpressure can be maintained in the basin at present day. Also the modelled present day overpressure pattern is very similar to that of present day (Fig 6.36). The model is also showing the Delaware Mountain Group to be almost hydrostatically pressured at maximum burial (55 Ma) as well as the Bone Spring formations at 25 Ma, agreeing with conclusions made in chapter 4 that these horizons would be normally compacted at 55 Ma and 25 Ma respectively. Although the model is predicting slight overpressures in these horizons, it needs to be remembered that a 2D model has limitations. A basin is 3D in nature and fluid flow can occur along three dimensions. Therefore, the model may be overpredicting the overpressure, as there may be more drainage pathways allowing more effective dewatering of certain horizons.

7.4. Discussion: A summary

This chapter has integrated the results of this research with other ideas and conclusions from published work, and shown the complexities involved in analysing the pore pressure histories of 'old' Palaeozoic basins such as the Delaware Basin. It has been shown that a complete understanding of the burial and tectonic history of a Palaeozoic basin is essential prior to modelling the pressure history. An important aspect of overpressure that has been highlighted is its maintenance through time, because overpressure has been maintained in the Delaware Basin for over 270 Myr.

Chapter 8:

Conclusions

The Delaware Basin is the largest sub-division of the Permian Basin lying to the east of the Basin and Range uplift. The basin extends eastward across parts of western Texas and southeastern New Mexico. The basin is perhaps most famous geologically for the Capitan Reef of Upper Permian age, but economically has long been explored for hydrocarbons and its stratigraphy and tectonic history are now reasonably well constrained. Although old and now tectonically quiescent, the Delaware Basin is extensively overpressured. The origin of the overpressure and its maintenance has been unconvincingly explained with limited data sets in previous publications (e.g. Luo et al 1994; Lee & Williams 2000; and Hanson & Lee 2005).

Overpressure is commonplace worldwide in young, actively subsiding basins undergoing rapid compaction (e.g. the Gulf Coast basin of the United States). H However, it is less common and has rarely been documented in detail from mature Palaeozoic basins, such as the Delaware Basin, where there has been insignificant sedimentation for the last 250 Myr. The preservation of overpressure to the present day in the Delaware Basin has long required an explanation. This study has incorporated large data sets from several hundred wells (666) with some outcrop field data and used analytical techniques such as, apatite fission track analysis, vitrinite reflectance, shale compaction curves, wireline logs, well pressure testing and basin modelling to provide a better understanding of (i) the generation of overpressure in the Delaware basin; (ii) the maintenance and distribution of overpressure in the Delaware basin; and (iii) how techniques can be effectively applied to constrain overpressure distribution in basins to aid in hydrocarbon exploration and recovery.

The key conclusions are provided below.

8.1 Key Findings

8.1.1 Origins of overpressure

- The presence of overpressure in the basin is explained by disequilibrium compaction as the main process.
  - Basin modelling conclusively showed that rapid deposition of the Permian section inhibited the underlying sediments from dewatering at a rate that would enable pressure equilibrium to occur in the basin.
  - Pore pressure prediction methods (equivalent depth method and the Eaton ratio method) using sonic logs accurately predicted the measured formation pressures in the overpressured section of the basin, indicating that the sediments are undercompacted.
  - A velocity / density cross-plot was made for the overpressured Pennsylvanian Morrow Formation of the Hill Haley 1a well in the centre of the basin. The results agreed with the pore pressure prediction methods, suggesting that the section is overpressured due to disequilibrium compaction.

- Unloading mechanisms may have contributed to overpressure to a lesser extent, on a localised scale within certain formations in the basin.
  - Analysis of the overpressured Pennsylvanian Strawn Formation in two wells, using velocity / density cross-plots, indicates that unloading mechanisms are affecting the sediments.
  - Based on pore pressure prediction methods only, other formations that may have experienced unloading effects include the Wolfcampian Series (Early Permian), Pennsylvanian Cisco Formation, Mississippian Limestone Formation and the Devonian Formation (Early Devonian).
  - Basin modelling showed that the Wolfcampian source rock had entered the gas window prior to maximum burial 55 Ma. The amount

of gas generated from this source rock would have been small, however, due to a low initial TOC. It is therefore unlikely that any significant overpressure would have been generated through gas generation in the Wolfcampian Series.

- Basin modelling shows that for reservoirs below and including the Lower Wolfcampian, if a suitable trap is present, then the units will be saturated with hydrocarbons and by maximum burial (55 Ma) the temperature conditions would be suitable for oil to gas cracking. Known reservoir plays in the basin include the Devonian Formation and the whole of the Pennsylvanian System. Overpressure generation through oil to gas cracking in the Devonian Formation or in the Pennsylvanian System is therefore a likely scenario, however, it is still theoretical as there is no conclusive evidence.
- Lateral transfer may enhance overpressures at structural crests in Palaeozoic reservoirs within the basin. For example the Jo Neal 43 well in Pecos County may be experiencing enhanced overpressure within the Pennsylvanian Cisco Formation due to lateral transfer.
- Other unloading mechanisms may have influence on the overpressure system in the basin, such gas expansion with uplift or hydrocarbon buoyancy. However, this study does not have enough conclusive evidence to categorically state whether these mechanisms may have an influence in the Delaware Basin, but this study cannot rule them out.

8.1.2 Maintenance of overpressure

- Basin modelling showed that overpressure in the basin is controlled by a number of pressure seals.
  - Overpressure generated in the basin primarily due to disequilibrium compaction due to the burial of the Permian section. The Late Permian evaporites coupled with low permeability mudstones within

the basin, hindered the initial dewatering of the sediments and overpressure developed within the whole basin (250.6 Ma).

- Laterally extensive tight carbonates (< 2% porosity and nanoDarcy scale permeability) within the basin acted as pressure seals, and compartmentalised the basin. They maintained the overpressure in the Lower Permian Wolfcampian Series, Pennsylvanian System and the Devonian Formation. All other units above and below, have not been effectively sealed, and pore pressures have returned to hydrostatic by present day.

8.1.3 Techniques

- An important conclusion to draw from the results is that overpressure in the Delaware Basin is a dynamic rather than a static system. The shale compaction curves based on the sonic logs show evidence of palaeo and present day dewatering patterns in low permeability mudstones.
- This study suggests that sonic logs are a very useful tool for representing the porosity of the mudstones, and for determining the basin's present day pore pressure.

8.2 Summary comments

All the conclusions that have been stated in this chapter are dependent on an accurate burial history. This is the first study on the Delaware Basin that has used apatite fission track analysis alongside vitrinite reflectance and shale compaction curves to assess the basin's burial history.

The burial history that has been deduced is significantly different to the previously published scenarios, where there was no significant deposition on top of the preserved Triassic in the basin, and the well published Cenozoic tectonic events

were never quantified on the effect they had on the basin. This research has found that maximum burial occurred in the basin 55 Ma as a result of a further 6890 ft of Mesozoic and Cenozoic deposition on top of the preserved Triassic. The Cenozoic was a period of tectonic activity in the basin, with two uplift and erosion events affecting the basin. The Laramide event (55-50 Ma) uplifted the entire basin and eroded off 3890 ft of Palaeocene and Upper Cretaceous sediments. The basin then subsided and a further 600 ft of Oligo-Miocene sediment was deposited. The last phase in the basin's tectonic history was the Basin and Range event (25-10 Ma), when the basin underwent further uplift and erosion tilting the basin to the east.

The improved understanding of the burial history of the Delaware Basin will provide a better insight into other Palaeozoic basins in the United States and elsewhere. Numerous Palaeozoic Basins within the US have tight reservoir horizons in the centre of the basin, which are prospective for gas but are also significantly overpressured (Law 2002). Understanding the burial, tectonic, pore pressure and petroleum system history of these Palaeozoic basins, will aid in the future exploration of basin centred gas systems hosted in them.

8.3 Further Work

- This study has suggested that the whole basin became overpressured due to the deposition of Permian section, but certain horizons were able to dewater through time. This hypothesis can be verified by doing fluid inclusion analysis on samples from the present-day hydrostatically pressured units. Fluid inclusion analysis can provide palaeo-pressure estimates, allowing the user to know if a sample was ever overpressured. This study did initially set out to undertake fluid inclusion analysis. However, for fluid inclusion analysis to be successful, a sandstone sample is required because the fluid inclusions are found in quartz overgrowths. The fluid within the inclusion also needs to be of a hydrocarbon nature. The samples provided for this study did not include any fluid inclusions that matched the required criteria and so

this analysis could not be undertaken. If good samples can be found, then fluid inclusion analysis is highly recommended tool for understanding a basin's pore pressure history.

- A lot of the research carried out on this study was dependent on an accurate understanding of the porosity-depth relationships for the mudstones in the basin. One controlling factor of a mudstone porosity is the clay content of the sample. For any future work, the analysis of the clay fraction of the mudstones would be recommended.
- 3D analysis of a basin through basin modelling, or lithological correlation is necessary to gain a complete understanding of the basin in terms of fluid flow, lateral extent of horizons, etc.
- The Delaware Basin is part of the larger Permian Basin. The Midland Basin to the east, and the Val Verde Basin to the south have a similar burial and tectonic history to the Delaware Basin. These two basins however, do not have any overpressure preserved in their section (R.Webster *pers comm).* This study had no data available for the two basins and so an accurate correlation to the Delaware could not be made. It is therefore advisable that a complete basinal study is conducted for the two basins, if the pore pressure history of the Delaware Basin is to be understood further.

References

AL-SHAIB, Z., PUCKETTE, J.O., ABDALLA, A.A., & ELY. P.B., 1994. Megacompartment complex in the Anadarko Basin: A completely sealed overpressure phennomeneon. *In:* ORTOLEVA, P.J. (ed.). *Basin Compartments and Seals.* The American Association of Petroleum Geologists Memoir. **61.** 55-69.

AL-SHAIB, Z., PUCKETTE, J.O., ABDALLA, A.A., & ELY, P.B., 1994. Three levels of compartmentalisation within the overpressured interval. *In:* ORTOLEVA, P.J., (ed.). *Basin Compartments and Seals.* The American Association of Petroleum Geologists Memoir. **61.** 69-85.

ALLEN, P.A., & ALLEN, J.R. 1990. *Basin Analysis.* Blackwell Science. pp.440.

ALLEN, P.A., & ALLEN, J.R. 1990. *Basin Analysis Second Edition.* Blackwell Science.pp. 549.

ALTON-BROWN, A., 2004. Estimating paleo heat flow in cratonic and foreland basins. A proposed methodology with application to the Delaware Basin, West Texas and New Mexico. Poster. *Personal communication.*

APLIN, A.C., 2000. Confocal microscopy of fluid inclusions reveals fluid pressure histories of sediments and an unexpected origin of gas condensate. *Geology.* **28 (11).** 1047-1050.

APLIN, A.C., YANG, Y., & HANSON, S., 1995. Assessment of β, the compression Coefficient of mudstones, and its relationship to detailed lithology. *Marine and Petroleum Geology.* **12.** 955-963.

APLIN, A.C., LARTER, S.R., BIGGE, M.A., MACLEOD, G., SWARBRICK, R.E., & GRUNBERGER, D., 2000. Confocal microscopy of fluid inclusions reveals fluid-pressure histories of sediments and an unexpected origin of gas condensate. *Geology.* **28.** 1047-1050.

ARMAGNAC, C., et al. 1989. Estimating the thickness of sediment removed at an unconformity using vitrinite reflectance data. . *In:* NAESER, N.D., & MCCULLOH, T., (eds.). *Thermal history of sedimentary basins – methods and case histories.* Springer-Verlag. New York. 217-239.

ARMSTRONG, P.A., 2005. Thermochronometers in sedimentary basins. *Reviews in Mineralogy and Geochemistry.* **58.** 499-525.

ATHY, L.F., 1930. Density, porosity and compaction of sedimentary rocks. *The American Association of Petroleum Geologists Bulletin.* **14.** 1-24.

BACHU., H.U., MICHAEL, K., & BUSCHKUEHLE, B.E., 2002. The relation between stratigraphic elements, pressure regime, and hydrocarbons in the Alberta deep basin (with emphasis on select Mesozoic units): Discussion. *The American Association of Petroleum Geologists Bulletin.* **86 (3).** 525-528.

BAHR, J.M., MOLINE, G.R., & NADON, G.C., 2004. Anomalous pressures in the deep Michigan Basin. *In:* ORTOLEVA, P.J., (ed.). *Basin Compartments and Seals.* The American Association of Petroleum Geologists Memoir. **61.** 153-167.

BARKER, C., 1990. Calculated volume and pressure changes during the thermal cracking of oil to gas in reservoirs. *The American Association of Petroleum Geologists Bulletin.* **74(8).** 1254-1261.

BARKER, C.E., & PAWLEWICZ, M.J., 1987. The effects of igneous intrusions and higher heat flow on the thermal maturity of Leonardian and younger rocks, Western Delaware Basin, Texas. *In:* CROMWELL, D.W., & MAZZULLO, L., (eds) *The Leonardian facies in W. Texas and S.E. New Mexico.* Society of Economic Palaeontology and Mineralogy. 69-84.

BEHNKEN, F.H., 1975. Leonardian and Guadalupian (Permian) conodont Biostratigraphyy in western and southwestern United States. *Journal of Palaeontology.* **49.** 284-315.

BISTER, B.S., STEPHENS, W.C., & NORMAN, G.A., 2002. Structure, stratigraphy, and Hydrocarbon system of a Pennsylvanian pull apart basin in north-central Texas. *The American Association of Petroleum Geologists Bulletin.* **86 (1).** 1-20.

BLOCH, S., LANDER, R.H., & BONNELL, L., 2002. Anomalously high porosity and permeability in deeply buried sandstone reservoirs: origin and predictability. *The American Association of Petroleum Geologists Bulletin.* **86 (2).** 301-328.

BOLAS, H.M.N., HERMANRUD, C. & TEIGE, G.M.G., 2004. Origin of overpressure in shales: Constraints from basin modelling. *The American Association of Petroleum Geologists Bulletin.* **88.** 193-211.

BORGE, H., 2002. Modelling generation and dissipation of overpressure in sedimentary basins: an example from the Halton Terrace, offshore Norway. *Marine and Petroleum Geology.* **19.** 377-388.

BOULT, P.J., THEOLOGOU, P.N., & FODEN, J., 1997. Capillary seals within the Eromanga Basin, Australia: Implications for exploration and production. *In:* SURDAM, R.C., (ed.). *Seals Traps and the Petroleum System.* The American Association of Petroleum Geologists Memoir. **67.** 143-167.

BOWERS, G.L., 2001. Determining an appropriate pore pressure estimation strategy. *Offshore Technology Conference.* Houston. Texas. OTC 13042.

BOWERS, G.L., & KATSUBE, T.J., 2002. The role of shale pore structure on the sensitivity of wireline logs to overpressure. *In:* HUFFMAN, A.R., & BOWERS, G.L., (eds.). *Pressure regimes in sedimentary basins and their prediction.* The American Association of Petroleum Geologists Memoir **76.**

BRADLEY, J.S., & POWLEY, D.E., 1994. Pressure compartments in sedimentary basins: A review. *In:* ORTOLEVA, P.J., (ed.). *Basin Compartments and Seals.* The American Association of Petroleum Geologists Memoir. **61.** 3-26.

BRAUN, J., VAN DER BEEK, P., & BATT, G., 2006. *Quantitative Thermochronology* Cambridge University Press. pp. 257.

BRAY, R.J., GREEN, P.F., & DUDDY, I.R., 1992. Thermal history reconstruction using Apatite fission track analysis and vitrinite reflectance; a case study from the UK East Midlands and southern North Sea. *In:* HARDMAN, R.F.P., (ed.). *Exploration Britain; geological insights for the next decade.* Geological Society Special Publications. **67.** 2-25.

BREDEHOEFT, J.D., HANSHAW, B.B., 1968. On the maintenance of anomalous fluids; 1, Thick sedimentary sequences. *Geological Society of American Bulletin.* **79 (9).** 1097-1106.

BREDEHOEFT, J.D., DJEVANSHIR, R.S., & BELITZ, K.R., 1988. Lateral fluid flow in a compacting sand shale sequence: South Caspian Basin: *The American Association of Petroleum Geologists Bulletin.* **72.** 416-424.

BROWN, R.W., SUMMERFIELD, M.A., & GLEADOW, A.J.W., 1994. Apatite fission track analysis; its potential for the estimation of denudation rates and implications for models of long-term landscape development. *In:* KIKBY, M.J., (ed.) *Process models and theoretical geomorphology.* John Wiley and sons. 25-53.

BRUCE, C.H., 1984. Smectite dehydration – its relation to structural development and hydrocarbon accumulation in Northern Gulf of Mexico Basin. *The American Association of Petroleum Geologists Bulletin.* **68.** 673-683.

BURRUS, J., KUHFUSS, B., DOLIGEZ, B., & UNGERER, P., 1991. Are numerical models useful in reconstructing the migration of hydrocarbons? A discussion based on Northern Viking Graben. *In:* ENGLAND, W.A., & FLEET, A.J., (eds.). *Petroleum Migration.* The Geological Society of London, Special Publication **59.** 89-211.

BURRUS, J., et al 1993. Source rock permeability and petroleum expulsion efficiency: Modelling examples from the Mahkam delta, the Williston Basin and the Paris Basin: *In:* PARKER, J.R., (ed.). *Petroleum geology of northwest Europe: Proceedings of the 4th Conference.* The Geological Society, London. 1317 – 1332.

BURRUS, J., SCHNEIDER, F., & WOLF, S., 1994. Modelling overpressures in sedimentary basins: consequences for permeability and rheology of shales, and petroleum expulsion efficiency. *The American Association of Petroleum Geologists International Conference.* Kuala Lumpur. August 21-24. 1994. (abstract).

BUSBY, C.J., & INGERSOLL, R.V., 1995. *Tectonics of Sedimentary Basins.* Blackwell Science. pp. 579.

CARLIN, S., & DAINELLI, J., 1998. Pressure regimes and pressure systems in the Adriatic foredeep (Italy). *In:* LAW, B.E., ULMISHEK, G.F., & SLAVIN, V.I., (eds.). *Abnormal pressures in hydrocarbon environments.* The American Association of Petroleum Geologists Memoir. **70.** 145-160.

CARLSON, W.D., 1990. Mechanism and kinetics of apatite fission track annealing. *American Mineralogist.* **75.** 1120-1139.

CARTER, L.S., et al. 1998. Heat flow and thermal history of the Anadarko Basin Oklahoma. *The American Association of Petroleum Geologists Bulletin.* **82 (2).** 291-316.

CHILINGARIAN, G.V., & RIEKE, H.H., 1974. Compaction of argillaceous sediments. *Developments in Sedimentology.* **16.** 424.

CONANT, L.C., & SWANSON, V.E., 1961. Chattanooga shale and related rocks of Central Tennessee and nearby areas. *US Geological Survey Professional Paper.* **357.** p57.

CORNFORD, C., 2001. The use of organic geochemistry in hydrocarbon acreage Evaluation. IGI ltd. Organic Geochemistry course. Royal Holloway University.

CORRIGAN, J., 1992. Annealing models under the microscope. *On Track.* **2.** 9-11.

CRANGANU, C., 2004. Capillary sealing in the Anadarko Basin, Oklahoma. *Northeast Geology and Environmental Sciences.* **26. 1-2.** 35-42.

CROMWELL, D.W., 1984. The Upper Delaware Mountain Group, Permian (Guadalupian), southeast New Mexico and West Teaxas. *In:* MAZZULLO, S.J., (ed.). *The geological evolution of the Permian Basin.* Permian Basin Section symposium. Midland, Texas. 32-34.

CROWLEY, K.D., CAMERON, M., & SCHAEFER, R.L., 1991. Experimental studies of annealing of etched fission tracks in apatite. *Geochimica et Cosmochimica Acta.* **55.** 1449-1465.

DALZIEL, I., 2002. http://www.ig.utexas.edu/research/projects/plates/

DAVIES, T.B., 2004. Subsurface pressure profiles in gas-saturated basins. *In:* MASTERS, J.A., (ed.). *Elmworth – case study of a deep basin gas field.* American Association of Petroleum Geologists Memoir. **38.** 189-203.

DICKINSON, G., 1953. Geological aspects of abnormal reservoir pressures in Gulf Coast Louisiana. *The American Association of Petroleum Geologists Bulletin.* **37.** 410-432.

DICKNINSON, W.R., 1981. Plate tectonic evolution of the southern Cordillera. *In:* DICKINSON, W.R., & PAYNE, W.D., (eds.). *Relations of tectonics to ore Deposits in southern Cordillera.* Arizona Geological Society Digest. **14.** 113-135.

DONELICK, R.A., O'SULLIVAN, P.B., & KETCHMAN, R.A., 2005. Apatite fission track analysis. *Reviews in Mineralogy and Geochemistry.* **58.** 49-94.

DORE, A.G., 1993. *Basin Modelling: Advances and Applications.* Elsevier. Amsterdam.

DOROBEK, S.L., 1995. Synorogenic carbonate platforms and reefs in foreland basins: Controls on stratigraphic evolution and platform / reef morphology. *In:* DOROBEK, S.L., & ROSS. G.M., (eds.). *Stratigraphic Evolution of Foreland Basins.* Society for Sedimentary Geology. Special Publication. **52.**

DOWNEY, M.W., 1984. Evaluating seals for hydrocarbon accumulations. *The American Association of Petroleum Geologists Bulletin.* **68 (11).** 1752-1763.

DREZEWIECKI, P.A., et al. 1994. Diagenesis, diagenetic banding, and porosity evolution of the Middle Ordovician St. Peter sandstone and Glenwood Formation in the Michigan Basin. *In:* ORTOLEVA, P.J., (ed.). *Basin Compartments and Seals.* The American Association of Petroleum Geologists Memoir. **61.** 153-167.

DUDDY, I.R., et al. 1988. Thermal annealing of fission tracks in apatite 3. Variable temperature behaviour. *Chem. Geology (Isot. Geosci. Sect.)* **73.** 25-38.

DUDDY, I.R., 2006. Delaware Basin AFTA final report and appendix.

DUPPENBECKER, S. J., & ILIFFE, J. E., 1988. *Basin Modelling: Practice and Progress.* Geological Society of London, Special Publications. **141.**

DUTTON, S.P., FLANDERS, W.A., & BARTON, M.D., 2003. Reservoir characterisation of a Permian deep-water sandstone, East Ford field, Delaware Basin, Texas. *The American Association of Petroleum Geologists Bulletin.* **87.** 609-627.

DUTTON, S.P., KIM, E.M., BROADHEAD, R.F., RAATZ, W.D., BRETON, C.L., RUPPEL, S.C., & KEARNS, C., 2005. Play analysis and leading-edge oil reservoir development methods in the Permian Basin: Increased recovery through advanced technologies. *The American Association of Petroleum Geologists Bulletin.* **89.** 553-576.

DZEVANSHIR, R.D., BURYAKOVSKIY, L.A., & CHILINGARIAN, G.V., 1986. Simple quantitative evaluation of porosity of argillaceous sediments at various depths of burial. *Sedimentary Geology.* **43 (3-4).** 169-175.

ELSTON, W.E., 1984. Subduction of young oceanic lithosphere and extensional orogeny in southwestern North America during mid Tertiary time. *Tectonics.* **3(2).** 229-250.

FEINSTEIN, S., KHON, B.P., & EYAL, M., 1989. Significance of combined vitrinite reflectance and fission track studies in evaluating thermal history of sedimentary basins. . *In:* NAESER, N.D., & MCCULLOH, T., (eds.). *Thermal history of sedimentary basins – methods and case histories.* Springer-Verlag. New York. 197-217.

FISHER, A.T., & ZWART, G., 1996. Relation between permeability and effective stress along a plate boundary fault, Barbados accretionary complex. *Geology.* **24.** 307-310.

FLAWN, P.T., 1956. *Basement rocks of Texas and southeast New Mexico: Austin.* Bureau of Economic Geology, University of Texas, Publication number 5605. pp. 261.

FLEISCHER, R.L., PRICE, P.B., & WALKER, R.M., 1975. *Nuclear tracks in solids.* University of California Press.

FOWLER, C.M.R., 1990. *The Solid Earth.* Cambridge University Press. pp.472.

FRENZEL, H.N., HUGH, N., BLOOMER, R.R., & CLINE, R.B., 1988. The Permian Basin region. *In:* SLOSS, L.L., (ed.). *Sedimentary Cover – North American Craton; U.S.* Geological Society of America, The Geology of North America, v. D-2.

FRIEDMAN, G.M., JACKSON, D.R., & WORDON, C.O., 1986. Reservoir rock of the Northwest Shelf and the Delaware Basin of southeastern New Mexico. *In:* PYRON, A.J., PETERSON, J.W., & KING, R.T., (eds.). *Reservoir rock of the Northwest Shelf and the Delaware Basin southeastern New Mexico.* American Association of Petroleum Geologists, southwest section, Rudisoo. pp 142.

GALLAGHER, K., HARMAN, R., BROWN, R., RAZA, A., & BIZZI, L., 1998. Accelerated dunudation and tectonic/geomorphic reactivation of the cratons of northeastern Brazil during the Late Cretaceous. *Journal of Geophysical Research.* **103.** 105.

GALLEY, J.E., 1958. Oil and geology in the Permian Basin of Texas and New Mexico *In:* WEEKS, L.G., (ed.). *Habitat of oil.* American Association of Petroleum Geologists Special Publication. 395-446.

GIES, R.M., 1984. Case history for a major Alberta deep basin gas trap – the Cadomin Formation. *In:* MASTERS, J.A., (ed.). *Elmworth – case study of a deep basin gas field.* American Association of Petroleum Geologists Memoir. **38.** 115-140.

GILES, M.R., INDRELID, S .L., & JAMES, D. D., 1998. Compaction – the great unknown in basin modellinig. *IN:* DUPPENBECKER, S. J., & ILIFFE, J. E., (eds). *Basin Modelling: Practice and Progress.* Geological Society of London, Special Publications. **141.** 15-43

GLEADOW, A.J.W. et al. 1986. Confined fission track lengths in apatite – a diagnostic tool for thermal history analysis. *Contr. Min. Petr.* **94.** 405-415.

GLUYAS, J., & SWARBRICK, R. 2004. *Petroleum Geoscience.* Blackwell Science. pp 359.

GOULTY, N.R., 1998. Relationships between porosity and effective stress in shales. *First Break.* **16.** 413-419.

GOULTY, N.R., 2004. Mechanical compaction behaviour of natural clays and implication for pore pressure estimation. *Petroleum Geoscience.* **10.** 73-79.

GREEN, P.F., 1988. The relationship between track shortening and fission track age reduction in apatite: Combined influences of inherent instability, annealing anisotropy, length bias and system calibration. *Earth Planetary and Scientific Letters.* **89.** 335-352.

GREEN, P.F., DUDDY, I.R., GLEADOW, A.J.W., TINGATE, P.R., & LASLETT, G.M., 1986. Thermal annealing of fission tracks in apatite 1. A qualitative description. *Chem. Geology (Isot. Geosci. Sect.)* **59.** 237-253.

GREEN, P.F., et al. 1989. Apatite Fission Track Analysis as a palaeotemperatures indicator for hydrocarbon exploration. *In:* NAESER, N.D., & MCCULLOH, T., (eds.). *Thermal history of sedimentary basins – methods and case histories.* Springer-Verlag. New York. 181-195.

GREEN, P.F., 1993. Mechansims and kinetics of apatite fission track annealing: Discussion. *American Mineralogist.* **78.** 441-445.

GREGORY, K.M., & CHASE, C.G., 1992. Tectonic significance of palaeobotanically estimated climate and altitude of the Late Eocene erosion surface, Colorado. *Geology.* **20.** 581-585.

HAGEN, E.S., 1989. Thermal evolution of Laramide-style basins: Constraints from the northern Bighorn Basin. *In:* NAESER, N.D., & MCCULLOH, T., (eds.). *Thermal history of sedimentary basins – methods and case histories.* Springer-Verlag. New York. 277-297.

HALL, P.L., 1993. Mechanisms of overpressuring – an overview. *In:* MANNING, D.A.C., HALL, P.L., & HUGHES, C.R., (eds.). *Geochemistry of clay-pore Fluid interactions.* Chapman and Hall. London. 265-315.

HANSOM, J., & LEE, M-K., 2005. Effects of hydrocarbon generation, basal heat flow and sediment compaction on overpressure development: a numerical study. *Petroleum Geoscience.* **11.** 353-360.

HARRIS, P.M., & GROVER, G.A., 1989. *Subsurface and outcrop examination of the Capitan shelf margin, northern Delaware Basin.* SEPM Core Workshop No. 13 pp 481.

HARROLD, T.W.D., SWARBRICK, R.E., & GOULTY, N.R., 1999. Pore pressure estimation from mudrock porosities in Tertiary Basins, Southeast Asia. *The American Association of Pertroleum Geologists Bulletin.* **83 (7).** 1057-1067.

HART, B.S., FLEMMINGS, P.B., & DESHPANDE, A., 1995. Porosity and pressure: Role of compaction disequilibrium compaction in the development of geopressures in a Gulf Coast Pleistocene Basin. *Geology.* **23.** 45-48.

HAYES, P.T., 1964. *Geology of the Guadalupe Mountains, New Mexico.* US Geological Survey, Professional Paper 446. pp 69.

HEASLER, H.P., SURDAM, R.C., & GEORGE, J.H., 1994. Pressure compartments in the Powder River Basin, Wyoming Montana, as determined from drill stem test data. *In:* ORTOLEVEA, P.J., (ed.). *Basin Compartments and seals.* The American Association of Petroleum Geologists Memoir. **61.** 235-263.

HENNING, A., YASSIR, N., ADDIS, T., WARRINGTON, A., & KRAVIS, S., 1998. Pore pressure estimation in an active thrust region and its impact on exploration and drilling. *American Association of Drilling Engineers Industry Forum on Pressure Regimes in Sedimentary Basins and their Prediction.*

HENRY, C.D., & MCDOWELL, F.W., 1986. Geochronology of magnetism in the Tertiary volcanic field, Trans-Pecos Texas. *In:* PRICE, J.G., et al (eds.). *Igneous geology of Trans-Pecos Texas.* Bureau of Economic Geology, University of Austin Texas. Report 96. pp 48.

HEPPARD, P.D., CANDER, H.S., & EGGERTSON, E.B., 1998. Abnormal pressure and the occurrence of hydrocarbons in offshore eastern Trinidad West Indies. *In:* LAW, B.E., ULMISHEK, G.F., & SLAVIN, V.I., (eds.). *Abnormal pressures In hydrocarbon environments.* The American Association of Petroleum Geologists Memoir. **70.** 65-85.

HERMANRUD, C., 1993. Basin modelling techniques – an overview. *In:* DORE, A.G., (ed.). *Basin Modelling: Advances and Application.* Elsevier. Amsterdam. p 1-34.

HERMANRUD, C.L., WENSAAS, L., TEIGE, G.M.G., BOLAS, H.M.N., HANSEN. S., & VIK, E., 1998. Shale porosities from well logs on Haltenbanken (offshore Mid-Norway) show no influence of overpressuring. *In:* LAW, B.E., ULMISHEK, G.F., & SLAVIN, V.I., (eds.). *Abnormal pressures in hydrocarbon environments.* The American Association of Petroleum Geologists Memoir. **70.** 65-85.

HILL, C.A., 1996. *Geology of the Delaware Basin, Guadalupe, Apache, and Glass Mountains New Mexico and West Texas.* Permian Basin section-SEPM Publication No. 96-39. pp 480.

HILLS, J.M., 1963. Late Palaeozoic tectonics and mountain ranges, western Texas to southern Colorado. *The American Association of Petroleum Geologists Bulletin.* **47.** 1709-1725.

HILLS, J.M., 1984. Sedimentation, tectonism, and hydrocarbon generation in Delaware Basin, West Texas and southeastern New Mexico. *The American Association of Petroleum Geologists Bulletin.* **68 (3).** 250-267.

HILLS, J.M., 1985. Structural evolution of the Permian Basin of West Texas and New Mexico. *In:* DICKERSON, P.W., & MEUHLBERGER, W.R., (eds.). *Structure and tectonics of Trans-Pecos Texas.* West Texas Geological Society, Guidebook Publication. **85-81**. 89-99.

HOESNI, M.J., 2004. *Origins of overpressure in the Malay Basin and its influence on petroleum systems.* PhD Thesis University of Durham.

HOLBROOK, P., 2002. The primary controls over sediment compaction. *In:* HUFFMAN, A.R., & BOWERS, G.L., (eds.). *Pressure regimes in sedimentary basins and their prediction.* The American Association of Petroleum Geologists Memoir **76.**

HORAK, R.L., 1985. Trans-Pecos tectonism and its effect on the Permian Basin. *In* DICKINSON, P.W. & MUEHLBERGER, W.R. (eds.). *Structure and tectonics of the Trans-Pecos, Texas.* West Texas Geological Society Guidebook Publication **85-81.**

HOTTMANN, C.E., & JOHNSON, R.K., 1965. Estimation of formation pressures from log derived shale properties. *Gulf Coast Association of Geological Societies.* **15.** 178-186.

HUBBERT, M.K., & RUBEY, W.W., 1959. Mechanics of fluid filled porous solids and its application to overthrust faulting. Role of fluid pressures in mechanics of overthrust faulting. *GSA Bulletin.* **70.** 115-205.

HUNT, D.W., FITCHEN, W.M., & KOSA, E., 2002. Syndepositional deformation of the Permian Capitan reef carbonate platform, Guadalupe Mountains, New Mexico, USA. *Sedimentary Geology.* **154.** 89-126.

HUNT, J.M., 1990. Generation and migration of petroleum from abnormally pressured fluid compartments. *The American Association of Petroleum Geologists Bulletin.* **74(1).** 1-12.

HUNT, J.M., WHELAN, J.K., EGLINTON, L.B., & CATHLES III, L.M., 1988. Relation of shale porosities, gas generation, and compaction to deep overpressures in the U.S. Gulf Coast. *In:* LAW, B.E., ULMISHEK, G.F., & SLAVIN, V.I., (eds). *Abnormal pressures in hydrocarbon environments.* The American Association of Petroleum Geologists Memoir. **70.** 87-104.

HUNT, J.M., WHELAN, J.K., EGLINTON, L.B., & CATHLES, L.M., 1994. Gas generation – a major cause of deep Gulf Coast overpressure. *Oil and Gas Journal.* **92.** 59-63.

HUTCHINGS, W.D., 2001. Sequenece stratigraphy of the Permian Delaware Mountain Group, basin floor setting, Delaware Basin, West Texas and southeastern New Mexico: Application of stacking pattern analysis. *The American Association of Petroleum Geologists.* Annual Meeting. Denver. Colorado. June 3rd-6th.

INGERSOLL, R.V., 1988. Tectonics of sedimentary basins. *Geological Society of America Bulletin.* **100.** 1704-1719.

JAPSEN, P., 1998. Regional velocity depth anomalies, North Sea chalk: A record of overpressure and Neogene uplift and erosion. *American Association of Petroleum Geologists Bulletin* **82.** 2031-2074.

JIAO, Z.S., & SURDAM, R.C., 1997. Characteristics of anomalously pressured Cretaceous shales in the Laramide Basins of Wyoming. *In:* SURDAM, R.C., (ed.). *Seals Traps and the Petroleum System.* The American Association of Petroleum Geologists Memoir. **67.** 243-253.

JORDON, T.E., 1981. Thrust loads and foreland basin evolution, Cretaceous, West United States. *The American Association of Petroleum Geologists Bulletin.* **65(12).** 2506-2520.

KARIG, D.E., & HOU, G., 1992. High-stress consolidation experiments and their geologic implications. *Journal of Geophysical Research.* **97.** 289-300.

KATAHARA, K.W., & CORRIGAN, J.D., 2002. Effect of gas on poroelastic response to burial or erosion. *In:* HUFFMAN, A.R., & BOWERS, G.L., (eds.). *Pressure regimes in sedimentary basins and their prediction.* The American Association of Petroleum Geologists Memoir **76.** 73-79.

KATSUBE, T.J., WILLIAMSON, M., & BEST, M.E., 1992. Shale pore structure evolution and its effect on permeability. *The Log Analyst.* **33 (2).** 174.

KEARY, P., & VINE, FJ., 1992. *Global Tectonics.* Blackwell Science. pp. 296.

KOHN, B.P., et al. 2005. Visualizing thermotectonic and denudation histories using apatite fission track thermochronology. *Reviews in Mineralogy and Geochemistry.* **58.** 527-565.

KYLE, J.R., 1990. Geological history and mineral resources development of the northern Trans-Pecos region, Texas and New Mexico. *In:* KYLE, J.R., (ed.). *Industrial mineral resources of the Delaware Basin, Texas and New Mexico. Guidebook.* **8.** 84-96.

LAHANN. R., 2002. Impact of smectite diagnesis on compaction modelling and compaction equilibrium. *In:* HUFFMAN. A.R., & BOWERS. G.L., (eds.). *Pressure regimes in sedimentary basins and their prediction.* The American Association of Petroleum Geologists Memoir **76.** 61-73.

LAW, B.E., 2002. Basin centered gas systems. *The American Association of Petroleum Geologists Bulletin.* **86 (11).** 1891-1919.

LAW, B.E., & DICKINSON, W.W., 1985. Conceptual model for origin of abnormally pressured gas accumulations in low-permeability reservoirs. *The American Association of Petroleum Geologists Bulletin.* **69 (8).** 1295-1304.

LEE, M-K., & WILLIAMS, D.D., 2000. Paleohydrology of the Delaware Basin, Western Texas: Overpressure development, hydrocarbon migration and ore genesis. *The American Association of Petroleum Geologists Bulletin.* **84(7).** 961-974.

LEE, Y., & DEMING, D., 2002. Overpressures in the Anadarko Basin , southwestern Oklahoma: static or dynamic. *The American Association of Petroleum Geologists Bulletin.* **86 (1).** 145-160.

LERCHE, I., 1993. Theoretical aspects of problems in basin modelling. *In:* DORE, A.G.,(ed.). *Basin Modelling: Advances and Applications.* Elsevier. Amsterdam. p 35-66.

LORENZ, J.C., STERLING, J.L., SCHECTER, D.S., WHIGHAM, C.L., & JENSEN, J.L., 2002. Natural fractures in the Spraberry formation, Midland Basin, Texas: The effects of mechanical stratigraphyon fracture variabilityand reservoir behaviour. *The American Association of Petroleum Geologists Bulletin.* **86 (3).** 505-523.

LUO, M., BAKER, M.R., & LEMONE, D.V., 1994. Distribution and generation of the overpressure system, eastern Delaware Basin, western Texas and southern New Mexico. *The American Association of Pertroleum Geologists Bulletin.* **78 (9).** 1386-1405.

LUO, X., BRIGAUD, F., & VASSEUR, G., 1993. Compaction coefficients of argillaceous sediments: their implications, significance and determination. *In:* DORE, A.G., (ed.). *Basin Modelling: Advances and Applications.* Elsevier. Amsterdam. p. 321-332.

LUO, X., DONG, W., YANG, J., & YANG, W., 2003. Overpressuring mechanisms in the Yinggehai Basin, South China Sea. *The American Association of Petroleum Geologists Bulletin.* **87.** 629-645.

MACKENZIE, A.S., & QUIGLEY, T.M., 1988. Principles of geochemical propect appraisal. *The American Association of Petroleum Geologists Bulletin.* **72.** 399-415.

MARTINSEN, R.S., 1994. Summary of published literature on anomalous pressures. Implications for the study of pressure compartments. *In:* ORTOLEVA, P.J., (ed.). *Basin Compartments and Seals.* The American Association of Petroleum Geologists Memoir **61.**

MAZZULLO, S.J., 1986. Mississippi valley-type sulfides in Lower Permian dolomites, Delaware Basin, Texas; implications for basin evolution. *American Association of Petroleum Geologists Bulletin.* **70.** 943-952.

MEISSNER, F.F., 1978. Petroleum Geology of the Bakken Formation Williston Basin, North Dakota and Montana. *In: 24th annual conference, Williston Basin, Symposium: Montana.* Geological Society. 207-227.

MELLO, U.T., & KARNER, G.D., 1996. Development of sediment overpressure and its effect on thermal maturation: Application to the Gulf of Mexico Basin. *The American Association of Petroleum Geologists Bulletin.* **80.** 1367-1396.

MONTGOMERY, S.L., 1997. Permian Bone Spring formation: Sandstone play in the Delaware Basin, part I– slope. *American Association of Petroleum Geologists Bulletin.* **81(8).** 1239-1258.

MONTGOMERY, S.L., 1997. Permian Bone Spring formation: Sandstone play in the Delaware Basin, part II – basin. *American Association of Petroleum Geologists Bulletin.* **81(9).** 1423-1434.

MUDFORD, B.S., 1988. Modelling the occurance of overpressure on the Scotian Shelf, Offshore Eastern Canada. *Journal of Geophysical Researh.* **93.** 7845-7855.

MCCULLOH, T.H., & NAESER, N.D., 1989. Thermal history of sedimentary basins: Introduction and overview. *In:* NAESER, N.D., & MCCULLOH, T., (eds.). *Thermal history of sedimentary basins – methods and case histories.* Springer Verlag. New York. 181-195.

NAESER, N.D., 1993. Apatite fission track analysis in sedimentary basins – a critical appraisal. *In:* DORE, A.G., (ed.). *Basin Modelling: Advances and Applications.* Elsevier. Amsterdam. p. 147-160.

NAESER, N.D., NAESER, C.W., & MCCULLOH, T.H., 1989. The application of fission track dating to the depositional and thermal history of rocks in sedimentary basins. *In:* NAESER, N.D., & MCCULLOH, T., (eds.). *Thermal history of sedimentary basins – methods and case histories.* Springer-Verlag. NewYork. 157-181.

NEUZIL, C.E., 1994. How permeable are clays and shales? *Water Resources Research.* **30.** 145-150.

NEUZIL, C.E., & POLLOCK, D.W., 1983. Erosional unloading and fluid pressures in hydraulically tight rocks. *Journal of Geology.* **91.** 179-193.

OKUI, A., & WAPLES, D.W, 1993. Relative permeabilities and hydrocarbon expulsion from source rocks. *In:* DORE, A.G., (ed.). *Basin Modelling: Advances and Applications.* Elsevier. Amsterdam. p. 293-302.

ORTOLEVA, P.J., 1994. Basin compartmentalisation: Definitions and Mechanisms. *In:* ORTOLEVA, P.J., (ed.). *Basin Compartments and Seals.* The American Association of Petroleum Geologists Memoir. **61.** 39-53.

OSBORNE, M.J., & SWARBRICK, R.E., 1997. Mechanisms for generating overpressure in sedimentary basins: a reevaluation. *The American Association of Petroleum Geologists.* **81 (6).** 1023-1042.

OSBORNE, M.J., & SWARBRICK, R.E., 1999. Diagensis in North Sea HPHT clastic reservoirs – consequences for porosity and overpressure prediction. *Marine and Petroleum Geology.* **16.** 337-353.

PAWLEWICZ, M.W., BARKER, C.E., & MCDONALD, S., 2005. Vitrinite reflectance data for the Permian Basin, West Texas and southeast New Mexico. USGS Open File Report. **2005-1171.**

PRICE, J.G., & HENRY, C.D., 1984. Stress orientations during Oligocene volcanism in Trans-Pecos Texas: Timing the transition from Laramide compression to Basin and Range tension. *Geology.* **12.** 238-241.

REVIL, A., CATHLESS, L.M.III., SHOSA, J.D., PEZARD, P.A., & DE LAROUZIERE, F.D., 1998. Capillary sealing in sedimentary basins; a clear field example. *Geophysical Research letters.* **25 (3).** 389-392.

RICHEY, S.F., WELLS, J.G., & STEPHENS, K.T., 1985. *Geohydrology of the Delaware Basin and vicinity, Texas and New Mexico.* US Geological Survey, Water Resources Report. **84-4077.** pp 99.

RIDER, M., 1996. *The Geological Interpretation of Well Logs.* Whittles Publishing. pp. 279.

RUDNICK, R.L., & FOUNTAIN, D.M., 1995. Nature and composition of the continental crust: a lower crustal perspective. *Review of Geophysics.* **33.** 267-309.

RUTH, P.V., & HILLIS, R., 2000. Estimating pore pressure in the Cooper Basin South Australia: sonic log method in an uplifted basin. *Exploration Geophysics* **31.** 441-447.

SAHAGIAN, D., 1987. Epeirogeny, and eustatic sea level changes as inferred from Cretaceous shoreline deposits – application to the central and western United States. *Journal of Geophysical Research.* **92.** 4895-4904.

SARG, J.F., 1991. Tectonics, eustasy and sequence stratigraphy – the Pennsylvanian-Wolfcampian of the Permian Baisn. *The Geological Society of America. Rocky Mountain section-south Central section, Albuquerque. New Mexico.* **23 (4).** p90.

SCHNEIDER, F., BURRUS, J., & WOLF, S., 1993. Modelling overpressures by effective stress / porosity relationships in low permeability rocks: empirical artifice or physical reality? *In:* DORE, A.G., 1993. Basin Modelling: Advances and Applications. Elsevier. Amsterdam. p. 333-342.

SCHNEIDER, R.V., & HINOJOSA, J.H., 1991. Tectonic history of southwestern New Mexico and southeastern Arizona – a thermal perspective. *The Geological Society of America. Rocky Mountain section-south Central section, Albuquerque. New Mexico.* **23 (4).** p90.

SCHOLLE, P.A., ULMER, D.S., & MELIM, L.A., 1992. Late stage calcites in the Permian Capitan Formation and its equilalents, Delaware Basin margin, west Texas and New Mexico: evidence for replacement of precursor evaporates. *Sedimentology.* **39.** 207-234.

SHUMAKER, R.C., 1992. Paleozoic structure of the Central Basin Uplift and adjacent Delaware Basin, West Texas. *The American Association of Petroleum Geologists Bulletin.* **76 (11).** 1804-1834.

SLAVIN, V.I., & SMIRNOVA, E.M., 1998. Abnormally high formation pressure; orgin, prediction, hydrocarbon field development and ecological problems. *In:* LAW, B.E., ULMISHEK, G.F., & SLAVIN, V.I., (eds). *Abnormal pressures in hydrocarbon environments.* The American Association of Petroleum Geologists Memoir. **70.** 104-114.

SLOSS, L.L., 1988. Tectonic evolution of the craton in Phanerozoic time. *In:* SLOSS, L.L., (ed). *Sedimentary Cover – North American Craton; U.S.* Geological Society of America, The Geology of North America, v. D-2.

SPEED, R.C., & SLEEP, N.H., 1982. Antler orogeny and foreland basin: A model. *Geological Society of America Bulletin.* **93.** 815-828.

SPENCER, C.W., 1987. Hydrocarbon generation as a mechanism for overpressuring in Rocky Mountain region. *The American Association of Petroleum Geologists Bulletin.* **71 (4).** 368-388.

SURDAM, R.C., JIAO, Z.S., & MARTINSEN, R.S., 1994. The regional pressure regime in Cretaceous sandstones and shales in the Powder River Basin. *In:* ORTOLEVEA, P.J., (ed.). *Basin Compartments and seals.* The American Association of Petroleum Geologists Memoir. **61.** 213-235.

SURDAM, R.C., JIAO, Z.S., & HEASLER, H.P., 1997. Anomalously pressured gas compartments in Cretaceous rocks of the Laramide Basins of Wyoming. A new class of hydrocarbon accumulation. *In:* SURDAM, R.C., (ed.). *Seals Traps and the Petroleum System.* The American Association of Petroleum Geologists Memoir. **67.** 199-222.

SYLVESTER, A.G., 1988. Strike-slip faults. *Geological Society of America Bulletin.* **100.** 1666-1703.

SWARBRICK, R.E., 1995. Distribution and generation of the overpressure system, Eastern Delaware Basin, Western Texas and Southern New Mexico: Discussion. *The American Association of Petroleum Geologists Bulletin.* **79 (12).** 1817-1821.

SWARBRICK, R. E., 2003. Pressures and Overpressures in the Subsurface. Geopressure Technology Course 25th – 27th March 2003.

SWARBRICK, R.E., & OSBORNE, M.J., 1996. The nature and diversity of pressure transition zone. *Petroleum Geoscience.* **2.** 111-116.

SWARBRICK, R.E., & OSBORNE, M.J., 1998. Mechanisms that generate abnormal pressures: an overview. *In:* LAW, B.E., ULMISHEK, G.F., & SLAVIN, V.I., (eds). *Abnormal pressures in hydrocarbon environments.* The American Association of Petroleum Geologists Memoir. **70.**

SWARBRICK, R.E., OSBORNE, M.J., GRUNBERGER, D., YARDLEY, G.S., MACLEOD, G., APLIN, A.C., LARTER, S.R., & AULD, H.A., 2000. Integrated study of the Judy Field (Block 30/7a) – an overpressured North Sea oil/gas field. *Marine and Petroleum Geology* **17.** 993-1010.

SWARBRICK, R.E., OSBORNE, M.J., & YARDLEY, G.S., 2002. Comparison of overpressure magnitude resulting from the main generating mechanisms. *In:* HUFFMAN, A.R., & BOWERS, G.L., (eds.). *Pressure regimes in sedimentary basins and their prediction.* The American Association of Petroleum Geologists Memoir **76.**

TOKUNAGA, T., HOSOYA, S., TOSAKA, H., & KOJIMA, K., 1998. An estimation of the intrinsic permeability of argillaceous rocks and the effects on long term fluid migration. *In:* DUPPENBECKER, S.J., & ILIFFE, J.E., (eds.). *Basin Modelling: Practice and Progress.* Geological Society. Special Publication. **141.** 83-95.

TREVENA, A. S., & CLARK, R. A., 1986. Diagenesis of sandstone reservoirs in the Pattani Basin, Gulf of Thailand. *The American Association of Petroleum Geologists Bulletin.* **70.** 299-308.

UNGERER, P., 1993. Modelling of petroleum generation and expulsion. *In:* DORE, A.G., (ed.). *Basin Modelling: Advances and Apllications.* Elsevier. Amsterdam. p. 219-232.

UNGERER, P., BURRUS, J., DOLIGEZ, B., CHENET, P.Y., & BESSIS, 1990. Basin evaluation by integrated two-dimensional modelling of heat transfer, fluid flow, hydrocarbon generation, and migration. *The American Association of Petroleum Geologists Bulletin.* **74.** 309-335.

WAGNER, M., ALTHERR, R., & VAN DEN HAUTE, P., 1992. Apatite-fission track analysis of Kenyan basement rocks; constraints on the thermotectonic evolution of the Kenya Dome; a reconnaissance study. *Tectonophysics.* **204 (1-2).** 93-110.

WANG, H.F., CROWLEY, K.D., & NADON, J.C. 1994. Thermal history of the Michigan Basin from apatite fission track analysis and vitrinite reflectance. *In:* ORTOLEVEA, P.J., (ed.). *Basin Compartments and seals.* The American Association of Petroleum Geologists Memoir. **61.** 167-179.

WAPLES, D.W., 1998. Basin Modelling: How well have we done? *In:* DUPPENBECKER, S.J., & ILIFFE, J.E., (eds.). *Basin Modelling: Practice and Progress.* Geological Society. Special Publication. **141.** 1-15.

WAPPLES, D.W., & KAMATA, H., 1993. Modelling porosity reduction as a series of chemical and physical processes. *In:* DORE, A.G., (ed.). *Basin Modelling Advances and Applications.* Elsevier. Amsterdam. p. 303-320.

WEEDMAN, S.D., BRANTLEY, S.L., & ALBRECHT, W., 1992. Secondary compaction after secondary porosity: Can it form a pressure seal? *Geology.* **20.** 303-306.

West Texas Geological Society Publication 84-79. 1984. Cross section through the Permian Basin of West Texas.

WIGGINS, W.D., HARRIS, P.M., & BURRUSS, R.C., 1993. Geochemistry of post-uplift calcite in the Permian Basin of Texas and New Mexico. *Geological Society of America Bulletin.* **105.** 779-790.

WILLIAMSON, M.A., 1995. Overpressures and hydrocarbon generation in the Sable Basin offshore Nova Scotia. *Basin Research.* **7.** 7-21.

WILSON, M.S., GUNNESON, B.G., PETERSON, K., HONORE, R., & LAUGHLAND, M.M., 1998. Abnormal pressures encountered in a deep wildcat well, southern Piceance Basin Colorado. *In:* LAW. B.E., ULMISHEK, G.F., & SLAVIN, V.I., (eds.). *Abnormal pressures in hydrocarbon environments.* The American Association of Petroleum Geologists Memoir. **70.** 195-214.

WRIGHT, W.F., 1979. *Petroleum geology of the Permian Basin.* Midland West Texas Geological Society. pp 98.

WUELLNER, D.E., LEHTONEN, L.R., & JAMES, W.C., 1986. Sedimentary-tectonic development of the Marathon and Val Verde basins, West Texas, USA.: a Permo-Carboniferous migrating foredeep. *In:* ALLEN, P.A., & HOMEWOOD, P., (eds). *Foreland Basins.* Special Publication Number 8 of the International Association of Sedimentologists.

YANG, K., & DOROBEK, S.L., 1995*a*. The Permian Basin of West Texas and New Mexico:Flexural modeling and evidence for lithospheric herterogeneity across the Marathon foreland. *In:* DOROBEK., S.L., & ROSS, G.M., (eds). *Stratigraphic Evolution of Foreland Basins.* Society for Sedimentary Geology. Special Publication. **52.**

YANG, K., & DOROBEK, S.L., 1995*b*. The Permian Basin of West Texas and New Mexico: Tectonic history of a "composite" foreland basin and its effects on stratigraphic development. *In:* DOROBEK, S.L., & ROSS, G.M., (eds). *Stratigraphic Evolution of Foreland Basins.* Society for Sedimentary Geology. Special Publication. **52.**

YANG, W., & KOMINZ, M.A., 2002. Characteristics, stratigraphic architecture, and time framework of multi-order mixed siliciclastic and carbonate depositional sequences, outcropping Cisco Group (Late Pennsylvanian and Early Permian), Eastern Shelf, north-central Texas, USA. *Sedimentary Geology.* **154.** 53-87.

YANG, Y., & APLIN, A.C., 1998. Influence of lithology and effective stress on the pore size distribution and modelled permeability of some mudstones from the Norwegian Margin. *Marine and Petroleum Geology.* **15.** 163-175.

YANG, Y., APLIN, A.C., & LARTER, S.R., 2002. Quantification, Permeability and Compaction of Mudstones: Some Applications to Basin Modelling and Pore Pressure Estimation. *The Ammerican Association of Petroleum Geologists.* Annual Meeting. March 10th-13th. 2002. Houston Texas.

YARDLEY, G.S., 1998. Can lateral transfer explain the high pressures in the Central North Sea? – Overpressures in petroleum exploration; Proc. Workshop, Pau April 1998-Bull. Centre Rech. Elf Explor. Prod., Mem. 22 201-206.

YARDLEY, G.S., & SWARBRICK, R.E., 2000. Lateral transfer: a source of additional overpressure? *Marine and Petroleum Geology.* **17.** 523-537.

YASSIR, N.A., & BELL, J.S., 1996. Abnormally high fluid pressures and associated stress regimes in sedimentary basins. . *SPE.* **48.** 5-10.

YE, H., ROYDEN, L., BURCHFIELD, C., & SCHUEPBACH, M., 1996. Late Paleozoic deformation of Interior North America: the greater ancestral Rocky Mountains. *The American Association of Petroleum Geologists Bulletin.* **80 (9).** 1397-1432.

YUCKLER, M.A., & DAHL, B., 1993. Future potential of basin modelling techniques. *In:* DORE, A.G., (ed.). *Baisn Modelling: Advances and Application.* Elsevier. Amsterdam. p71-84.